

New record of *Nausithoe werner* (Scyphozoa, Coronatae, Nausithoidae) from the Brazilian coast and a new synonymy for *Nausithoe maculata*

Clarissa Garbi Molinari¹, Maximiliano Manuel Maronna¹,
André Carrara Morandini^{1,2}

1 Departamento de Zoologia, Instituto de Biociências, Universidade de São Paulo, Rua do Matão, travessa 14, n. 101, Cidade Universitária, São Paulo, SP, 05508-090, Brazil **2** Centro de Biologia Marinha, Universidade de São Paulo, Rodovia Manuel Hypólito do Rego km 131.5, São Sebastião, SP, 11600-000, Brazil

Corresponding author: Clarissa G. Molinari (clarissamolinari@gmail.com)

Academic editor: B.W. Hoeksema | Received 10 July 2020 | Accepted 20 September 2020 | Published 4 November 2020

<http://zoobank.org/22EB0B21-7A27-43FB-B902-58061BA59B73>

Citation: Molinari CG, Maronna MM, Morandini AC (2020) New record of *Nausithoe werner* (Scyphozoa, Coronatae, Nausithoidae) from the Brazilian coast and a new synonymy for *Nausithoe maculata*. ZooKeys 984: 1–21. <https://doi.org/10.3897/zookeys.984.56380>

Abstract

The order Coronatae (Scyphozoa) includes six families, of which Nausithoidae Haeckel, 1880 is the most diverse with 26 species. Along the Brazilian coast, three species of the genus *Nausithoe* Kölliker, 1853 have been recorded: *Nausithoe atlantica* Broch, 1914, *Nausithoe punctata* Kölliker, 1853, and *Nausithoe aurea* Silveira & Morandini, 1997. Living polyps ($n = 9$) of an unidentified nausithoid were collected in September 2002 off Arraial do Cabo (Rio de Janeiro, southeastern Brazil) at a depth of 227 m, and have been kept in culture since then. We compared these specimens with three species cultured in our laboratory: *Nausithoe aurea* (from Ilhabela, São Paulo, Brazil), *Nausithoe maculata* Jarms, 1990 (from Cuba and Puerto Rico), and *Nausithoe werner* Jarms, 1990 (from the Atlantic Ocean off Morocco and from the Mediterranean Sea). The criteria used for comparison were: main aspects of the morphology, life cycle, and DNA sequences (18S, 28S, and COI). The results indicate that the unidentified polyps belong to *N. werner*. Furthermore, *N. aurea* is considered a junior synonym of *N. maculata*.

Keywords

Coronamedusae, jellyfish, life cycle, periderm, polyp, scyphomedusae, systematics

Introduction

The class Scyphozoa Goette, 1887 (true jellyfishes) comprises two main clades: Coronamedusae Calder, 2009 and Discomedusae Haeckel, 1880 (Jarms and Morandini 2019). The Coronamedusae have a single class, Coronatae Vanhöffen, 1892, which is mostly known from the deep-sea medusae of the genera *Atolla* Haeckel, 1880, *Periphylla* Müller, 1861, and *Paraphyllina* Maas, 1903. In addition, the group also includes several shallow-water species in the genera *Nausithoe* Kölliker, 1853 and *Linuche* Eschscholtz, 1829 (Jarms and Morandini 2019). Coronate species are distinguished from other scyphomedusae by the presence of a coronal furrow (groove) on the exumbrella (Mayer 1910; Russell 1970). Of the 59 species of coronates, the life cycles of 16 have been described (Jarms 2010). All of these have a metagenetic life cycle, with the holoplanktonic *Periphylla periphylla* (Péron & Lesueur, 1810) as an exception (Jarms et al. 1999). An additional feature of coronates is the presence of a periderm tube in species that have a known polyp stage (Russell 1970; Jarms 1991).

The high morphological similarity among polyps in this order and the difficulty in relating the polyp to the medusa (as they are usually not collected together) have led to two classification systems. Polyps were historically identified only as “Coronatae polyps” or were classified as belonging to the genus *Stephanoscyphus* Allman, 1874 (later changed to *Stephanoscyphistoma* Jarms, 1990, to accommodate these specimens). Studying the life cycle has been essential for advancing the systematics and understand the evolution of the group (Jarms 1990, 2010). Such an approach allows integration of the two classification systems, ensuring more precise recognition, diagnosis, and eventual identification of species and specimens.

Recent studies have advanced our taxonomic understanding of the group, using morphological characters of the periderm tube to differentiate species relying only on the polyp stage (Morandini and Jarms 2005, 2010, 2012). These characters consist of several tube measurements (total length, opening diameter, and diameter at different heights along the tube, following Jarms 1990, 1991), the number of internal cusps, and differentiation of the tube’s external ornamentation (number of rings). Although useful to distinguish genera and some species, this analysis is not as effective in differentiating all species, especially in the genus *Nausithoe* (Molinari and Morandini 2019). These limitations are even more evident in the sister clade Discomedusae, in which species cannot be identified solely on the polyp stage (van Walraven et al. 2020). Thus, it is important to state that genetic information, together with morphological data, has been fundamental in differentiating and identifying cnidarian species (Dawson 2005; Gómez Daglio and Dawson 2017).

The order Coronatae is composed of six families (13 genera and 59 species), of which Nausithoidae Haeckel, 1880, is the most speciose, with three genera and 26 species (Jarms and Morandini 2019). The most diverse genus, *Nausithoe*, contains 22 accepted species, which are distributed worldwide in shallow to deep waters, and from the tropics to polar regions (Jarms and Morandini 2019). Along the coast and in offshore territorial waters of Brazil, three species of the family have

been described or recorded: the medusae of *Nausithoe atlantica* Broch, 1913 and *Nausithoe punctata* K lliker, 1853, and the polyp of *Nausithoe aurea* Silveira & Morandini, 1997 (Oliveira et al. 2016).

The purpose of this study was to identify coronate polyps from the Brazilian continental slope off Arraial do Cabo (southeastern Brazil, western South Atlantic) and to compare them with the other known species from the Atlantic Ocean and the Brazilian coast, and thus, to improve our knowledge of coronate biodiversity and distribution.

Materials and methods

Deep-sea specimens from Brazil were collected during a cruise of the *Navio Oceanogr fico Prof. Wladimir Besnard* off the coast of Arraial do Cabo (Rio de Janeiro state, southeastern Brazil, 23 45.80'S, 41 44.40'W) on 15 September 2002, at a depth of 227 m. Calcareous substrates were collected using a box-corer, and the polyps were found on these. The collected polyps were provisionally named *Nausithoe* sp. and numbered as follows: AC01, AC02, AC08, AC10, AC17, AC18, and AC20 (Table 2). They were kept alive in small dishes for a few days aboard ship (under room temperature 20–23  C) and brought to the laboratory on 18 September 2002. Since their establishment in culture, three polyps (AC01, AC02, and AC10) reproduced asexually by forming tissue balls from the ephyrae (Fig. 1A, B), consistent with the observations of Silveira et al. (2003).

The study was conducted at the Laborat rio de Cultivo e Estudos de Cnidaria, in the Zoology Department of the Biosciences Institute, University of S o Paulo (IB-USP). For comparison, we used living polyps of several species: nine *Nausithoe* sp., nine *Nausithoe weneri* Jarms, 1990, 14 *Nausithoe maculata* Jarms, 1990, and three *Nausithoe aurea* (Table 1). They were selected due to their availability in culture at our laboratory and for their distribution in the Atlantic Ocean, which we considered important for comparison.

Table 1. Data from studied species of *Nausithoe* (*Nausithoe* sp., *N. weneri*, *N. maculata*, and *N. maculata* (= *N. aurea*)).

	Locality	# of polyps	Depth (m)	Culture temperature (�C)	Sampling date	Culture codes	# of ephyrae cultivated	# of mature medusae
<i>Nausithoe</i> sp.	off Arraial do Cabo, Brazil	9	227	15	15.09.2002	AC01, AC02, AC08, AC10, AC17, AC18, and AC20	850	25
<i>Nausithoe weneri</i>	Atlantic off Morocco	4	800–3,000	15	Original culture clones (1980)	ACM156	69	4
<i>Nausithoe weneri</i>	Mediterranean	5	200	15	2008	ACM157	70	9
<i>Nausithoe maculata</i> (= <i>N. aurea</i>)	Ilhabela, Brazil	3	3–9	20–22	02.2018	ACM120	85	0
<i>Nausithoe maculata</i>	Gir�n, Cuba	8	5–10	20–22	02.2004	ACM026, ACM027	50	8
<i>Nausithoe maculata</i>	Puerto Rico	6	5–10	20–22	Original culture clones (1971)	ACM025	160	33

Table 2. Measurements of the polyps according to Jarms (1990) and Jarms et al. (2002). Specimens of *Nausithoe* sp. were measured twice, in 2002 and 2018 (except for tissue balls, measured only in 2018). Da = diameter at aperture, Dbd = diameter of basal disc, Db = diameter just above basal disc, $D_{2\text{ mm}}$ = diameter at 2 mm height, $D_{5\text{ mm}}$ = diameter at 5 mm height, L_{tot} = total length, Nwt = number of whorls of internal cusps, Nw = number of cusps per whorl, – = not measured.

Polyp ID	L_{tot} (mm)	Da (mm)	Ddb (mm)	Db (mm)	$D_{2\text{ mm}}$	$D_{5\text{ mm}}$	Da/ L_{tot}	Nwt	Nw
AC01 (2002)	6.60	0.70	–	–	0.35	0.45	0.1061	7	8 / 16
AC01 (2018)	13.46	1.29	–	–	–	–	0.0958		
AC02 (2002)	11.15	0.90	–	0.15	0.30	0.50	0.0807	8	8 / 16
AC02 (2018)	17.74	1.09	–	–	–	–	0.0614		
AC02 (tissue ball 2018)	15.71	1.17	–	0.14	0.09	0.44	0.0746	6	8 / 16
AC08 (2002)	9.10	–	–	–	0.30	0.50	0.0769	9	8 / 16
AC08 (2018)	16.44	1.00	–	–	–	–	0.0608		
AC10 (2002)	14.25	1.15	–	0.15	0.20	0.40	0.0807	12	8 / 16
AC10 (2018)	15.33	1.15	–	–	–	–	0.0753		
AC10 (tissue ball 2018)	11.79	0.92	0.66	0.15	0.09	0.46	0.0782	6	8 / 16
AC17 (2002)	5.05	0.55	–	0.40	0.45	0.55	0.1089	9	8 / 16
AC17 (2018)	20.20	1.65	–	–	–	–	0.0818		
AC18 (2002)	10.50	0.95	–	0.15	0.35	0.5	0.0905	5	8 / 16
AC18 (2018)	12.27	1.02	–	–	–	–	0.0830		
AC20 (2002)	5.15	0.35	–	0.20	0.30	0.35	0.0680	10	8 / 16
AC20 (2018)	20.13	1.47	–	–	–	–	0.0733		
Mean \pm SD (2002)	8.83 \pm 3.17	0.77 \pm 0.27	–	0.21 \pm 0.10	0.32 \pm 0.07	0.46 \pm 0.06	0.09 \pm 0.01	8 \pm 3	8 / 16
Mean \pm SD (2018)	15.90 \pm 2.91	1.20 \pm 0.22	0.66 \pm 0	0.15 \pm 0	0.09 \pm 0	0.45 \pm 0	0.08 \pm 0.01		
<i>N. werner</i> 1	11.35	1.29	0.53	0.11	0.12	0.15	0.1139	6	8
<i>N. werner</i> 2	15.27	0.95	–	0.23	0.11	0.17	0.0620	6	8
<i>N. werner</i> 3	31.43	0.93	0.24	0.07	0.07	0.07	0.0297	7	8
<i>N. werner</i> 4	19.37	1.28	0.40	0.08	0.08	0.11	0.0660	13	8
<i>N. werner</i> 5	13.70	1.02	0.29	0.09	0.09	0.13	0.0744	8	8
<i>N. werner</i> 6	5.24	0.55	–	0.10	0.10	0.11	0.1048	8	8
<i>N. werner</i> 7	13.49	0.68	0.35	0.08	0.09	0.13	0.0502	14	8
<i>N. werner</i> 8	6.47	0.65	0.34	0.08	0.12	0.15	0.1003	8	8
<i>N. werner</i> 9	2.56	0.33	0.30	0.10	–	0.13	0.1293	7	8
Mean \pm SD	13.21 \pm 8.17	0.85 \pm 0.31	0.35 \pm 0.09	0.10 \pm 0.05	0.10 \pm 0.02	0.13 \pm 0.03	0.08 \pm 0.03	8.56 \pm 2.75	8
<i>N. maculata</i> 1	13.58	0.88	0.42	0.15	0.12	0.14	0.0646	3	16
<i>N. maculata</i> 2	14.41	1.21	–	–	–	–	0.0843	–	16
<i>N. maculata</i> 3	15.01	1.18	–	–	–	–	0.0785	–	–
<i>N. maculata</i> 4	18.64	1.08	–	–	–	–	0.0578	–	–
<i>N. maculata</i> 5	14.60	1.58	–	0.20	0.12	0.19	0.1083	4	16
<i>N. maculata</i> 6	15.82	1.29	–	–	–	–	0.0817	–	16
<i>N. maculata</i> 7	16.42	0.66	–	0.17	0.09	0.20	0.0405	6	16
<i>N. maculata</i> 8	12.85	0.74	0.51	0.10	0.10	0.18	0.0580	–	–
<i>N. maculata</i> 9	8.75	0.83	0.41	0.10	0.16	0.19	0.0955	5	16
<i>N. maculata</i> 10	3.79	0.39	0.38	0.13	–	0.16	0.1041	4	16
<i>N. maculata</i> 11	7.23	0.69	0.30	0.10	0.12	0.19	0.0949	4	16
<i>N. maculata</i> 12	12.72	0.64	0.41	0.13	0.12	0.16	0.0504	8	16
<i>N. maculata</i> 13	4.91	0.77	–	–	0.14	0.21	0.1576	5	16
<i>N. maculata</i> 14	8.01	1.19	–	0.11	0.11	0.17	0.1382	3	16
Mean \pm SD	11.91 \pm 4.39	0.94 \pm 0.06	0.41 \pm 0.06	0.13 \pm 0.03	0.12 \pm 0.02	0.18 \pm 0.02	0.09 \pm 0.03	4.67 \pm 1.49	16
<i>N. maculata</i> (= <i>N. aurea</i>) 1	3.93	0.38	0.17	0.08	–	0.17	0.0979	6	16
<i>N. maculata</i> (= <i>N. aurea</i>) 2	3.86	0.53	0.36	0.11	–	0.16	0.1388	5	16
<i>N. maculata</i> (= <i>N. aurea</i>) 3	5.47	0.60	0.60	0.13	0.11	0.19	0.1091	6	16
Mean \pm SD	4.42 \pm 0.74	0.50 \pm 0.09	0.38 \pm 0.18	0.11 \pm 0.02	0.11 \pm 0	0.17 \pm 0.01	0.12 \pm 0.02	5.67 \pm 0.47	16

Voucher specimens of *Nausithoe* sp. were deposited in the Museu de Zoologia da Universidade de São Paulo as: MZUSP8502 (one medusa), MZUSP8503 (two polyps), MZUSP8504 (50+ ephyrae).

Cultivation

All polyps were fed with 1–2-day-old nauplii of *Artemia* sp. once a week. Strobilation usually produced hundreds of ephyrae (Fig. 1E), and excessive feeding to increase the number of jellyfish was not necessary. Polyps and ephyrae were kept separately in 200-mL acrylic containers (maximum of 20 ephyrae per dish) in incubation chambers at the appropriate temperature for each species (*N. weneri* and *Nausithoe* sp. at 15 °C; *N. maculata* and *N. aurea* at 20 °C). Once ephyrae were released, they were fed daily with macerated mussel gonads (*Perna perna*). As soon as they grew large enough to catch *Artemia*, we began to vary their diet, adding 1-day-old nauplii. Food was provided in abundance. The water in the polyp dishes was changed 1 day after feeding, and in the medusae and ephyrae containers, it was changed 1 hour after feeding (as these stages are more responsive to variations in water quality). Measurements and photographs of all stages were taken for comparison using a Nikon SMZ800 stereomicroscope and a Nikon Eclipse 80i microscope.

Morphological analyses

Measurements followed the protocols established by Jarms (1990, 1991) and Jarms et al. (2002). The main measurements were: i) total tube length, ii) tube diameter at 2 mm above the base, iii) tube diameter at 5 mm above the base, iv) diameter of the basal disc, v) diameter just above the basal disc, and vi) aperture diameter. The type of external ornamentation (number of transverse rings per 4-mm length) and whether these rings were more or less prominent with respect to an imaginary line tangential to the tube contour was noted for possible comparison (according to Morandini and Jarms 2005). For the more translucent tubes, we were able to observe the number of whorls of the cusps and the number of cusps per whorl. We also took scanning electron microscope (SEM) photographs of the internal cusps of some polyps (*Nausithoe* sp. and *N. weneri*) in order to observe their shape and ornamentation (with special attention to whether they had additional cusps on the margin and surface). Characters and measurements of the ephyrae and medusae are shown in Fig. 2. The SEM observations were conducted at the Laboratório de Biologia Celular e Microscopia of the IB-USP, and the method of preparing the specimens followed the protocols of Morandini and Jarms (2005, 2010, 2012).

Cnidome analyses

Capsule types and sizes of nematocysts in the different life-cycle stages (polyp, ephyra, medusa) were measured (Mariscal 1974; Östman 2000) using a Nikon Eclipse 80i light microscope. A total of 60 measurements were performed on each type per life-cycle stage of *Nausithoe* sp. and on the medusa tentacles of *N. weneri* and *N. maculata*.

Table 3. List of primers used to amplify each gene. *LEM = Laboratório de Evolução Molecular (IB–USP).

Gene	Primer	Primer sequence 5'–3'	F/R	Temp. – base pairs	Source
COI	COXI-F2	TCGACTAATCATAAAGATATCGGCAC	F	52 °C – 26 bp	Ward et al. 2005
	MEDCOXR	TGGTNGCYCANACNATRAANCC	R	52 °C – 23 bp	Lawley et al. 2016
	LCO1490JJ4	CIACIAAYCAYAARGAYATYGG	F	55 °C+45 °C – 22 bp	Astrin et al. 2016
	HCO2198JJ4	ANACTTCNGGRTGNCCAAARAATC	R	55 °C+45 °C – 25 bp	Astrin et al. 2016
	LCO1490JJ2	CHACWAAYCAYAARGAYATYGG	F	60 °C+45 °C – 22 bp	Astrin et al. 2016
	HCO2198JJ2	ANACTTCNGGRTGNCCAAARAATCA	R	60 °C+45 °C – 25 bp	Astrin et al. 2016
28S	F15	CTAACAAAGGATCCCCTAGTAACGGCGAG	F	55.5 °C – 30 bp	LEM *
	R798	GGTCCGTGTTCAAGACGG	R	55.5 °C – 19 bp	Medina et al. 2001
	F798	CCGTCTTGAACACGGACC	F	55.5 °C – 19 bp	Medina et al. 2001
	R1446	GTTGTACACACTCCTTAGCGG	R	55.5 °C – 22 bp	Medina et al. 2001
	18S	18S – A	AACCTGGTTGATCCTGCCAGT	F	54 °C – 21 bp
	18S – L	CCAACCTACGAGCTTTTAACTG	R	54 °C – 22 bp	Apakupakul et al. 1999
	18S – C	CGTAATTCAGCTCCAATAG	F	54 °C – 21 bp	Apakupakul et al. 1999
	18S – Y	CAGACAAATCGTCCACCAAC	R	54 °C – 21 bp	Apakupakul et al. 1999
	18S – O	AAGGGCACCACAGGAGTGGAG	F	54 °C – 22 bp	Apakupakul et al. 1999
	18S – B	TGATCCTTCCGACAGTTCACCT	R	54 °C – 22 bp	Medlin et al. 1988

DNA analyses

Because hundreds of ephyrae were produced, most of the molecular tissue for DNA extractions came from them (and some from mature medusae). We extracted DNA from specimens representing all the putative species in this study: *Nausithoe* sp., *Nausithoe aurea*, *Nausithoe maculata*, and *Nausithoe wernerii*. DNA was extracted using an ammonium acetate-based protocol adapted from Fetzner (1999). Preliminary tests established that the minimum number of ephyrae for a satisfactory extraction was around 30, considering their size. Three partial genes were amplified by polymerase chain reaction (PCR): mitochondrial protein coding cytochrome oxidase subunit I (COI), and nuclear ribosomal markers 18S and 28S, using published primers and PCR conditions (Table 3). PCR products were purified with the Agencourt AMPure kit (#A63881). The BigDye reaction was conducted using the same primers and annealing temperature in each case. These steps were performed in the Laboratório de Evolução Molecular of the Zoology Department (IB–USP). Finally, the precipitated DNA were sequenced at the Laboratório de Sinalização de Redes Regulatórias de Plantas at the Botanical Department, IB–USP, with a Hitachi 3730xl DNA Analyzer. Chromatograms (.abi files) and consensus sequences were created and checked to identify potential sequencing errors and/or contamination, using Geneious software 9.1 (Kearse et al. 2012; all COI sequences were translated to check potential mitochondrial pseudogenes (NUMTs) or indel artifacts – genetic code: Invertebrate Mitochondrial). Sequence alignments were performed with the Geneious 9.1 MAFFT module for 18S and 28S markers (auto-mode; Katoh and Standley 2013), and Translation Align module for COI marker (genetic code: Invertebrate Mitochondrial; MAFFT alignment: E-INS-i); this way, we avoid inserting any spurious gap in the COI alignment. To avoid any difference (artifact) on COI distances (the most relevant dataset to discuss species delimitation), we edited ends of COI alignment. Doing so, all sequences present the same basic

information (sequence length). Corrected distance values from each molecular marker alignment were obtained using MEGA X – Kimura 2 Parameters (Kumar et al. 2018).

Results

All the morphological features observed on the available specimens are summarized in Tables 2, 4. The time periods until medusae developed distinct morphological characters are listed in Table 5.

Systematics section

Class Scyphozoa Goette, 1887

Subclass Coronamedusae Calder, 2009

Order Coronatae Vanhöffen, 1892

Family Nausithoidae Haeckel, 1880

Genus *Nausithoe* Kölliker, 1853

Nausithoe sp.

Figs 1, 3, 4

Metagenetic species. Solitary polyp with typical periderm tube, dark to light brown (Fig. 1C, D), conical, with transverse rings on the surface with longitudinal striations (5 rings every 0.4 mm at 2 mm above base). Polyps 5.05–20.2 mm long; basal disk 0.63–0.66 mm in diameter; diameter just above the basal disk 0.14–0.4 mm; tube diameter at 2-mm height 0.09–0.45 mm, and at 5-mm height 0.35–0.45 mm; tube aperture diameter 1.28 mm. Tubes with 3–10 whorls of internal cusps (Fig. 1C); closer to base, number of internal cusps per whorl is 16: 4 large (perradius) with additional cusps on the surface, 4 intermediate (interradius), and 8 small (adradius) (Fig. 3A). Upper whorls with only 8 cusps: 4 large (perradius) with no additional cusps, and 4 intermediate (interradius) (Fig. 3B, C). Polyps with 26–37 filiform tentacles (Fig. 1D). Polydisc strobilation, with more than 100 ephyrae at a time. Medusa (Figs 2A, B, 4) entirely translucent, with slightly flattened smooth umbrella; 16 slightly elongated lappets with rounded margins; 8 rhopalia with statocyst and red ocelli. Live specimens measuring up to: 9.5 mm total diameter; 7.74 mm diameter between opposite rhopalia; 2.83 mm coronal groove diameter; gastric cirri approximately 0.9 mm in length; and tentacle length up to half the total diameter of the medusa. Stomach with 4 gastric septa, each with 2 gastric filaments (8 in total) (Figs 2A, 4D, E). Gonads, 8, but not fully developed (Fig. 4A–C); in fact, only a single individual had them and they were malformed (Fig. 4B, C), so complete data about their morphology are lacking. Cnidome composed of only two nematocyst types: holotrichous isorhiza and heterotrichous microbasic eurytele (Fig. 5; Table 6).

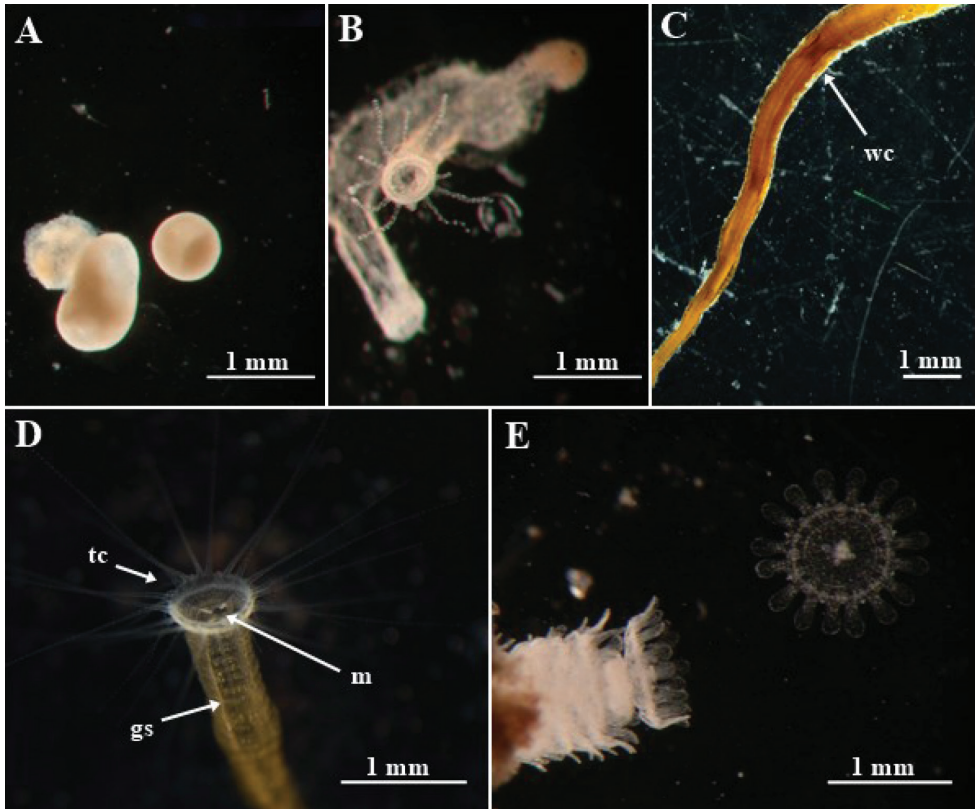


Figure 1. *Nausithoe* sp. from Brazil. **A** tissue balls originated from polyp AC02 ephyrae **B** emerged polyps from same tissue balls in A after 22 weeks, showing the polyp opening; note that the basal parts are fused **C** external view of part of polyp AC18, showing by transparency the internal whorls of cusps (**wc**) **D** oral disc of polyp AC01, showing the tentacle crown (**tc**) and the mouth opening (**m**) with the gastric longitudinal septa (**gs**) **E** polyp AC02 releasing ephyrae.

Nausithoe maculata Jarms, 1990

Fig. 6

Nausithoe maculata Jarms 1990: 21–24, figs 15–17, pl. V. Type locality: Puerto Rico. Holotype: ZMH C11534.

Nausithoe aurea Silveira and Morandini 1997: 236–239, figs 1–7, pls I, II. Type locality: Ilhabela (23°51'S, 45°25'W), Brazil. Holotype: MNRJ 2899. (syn. nov.)

Metagenetic species. Solitary polyp with typical periderm tube, dark to light brown, conical, with transverse rings on the surface with longitudinal striations (3–5 rings every 0.4 mm at 2 mm above base). Polyps 3.79–18.64 mm long. Basal disk 0.17–0.6 mm in diameter. Diameter of aperture 0.39–1.58 mm. Diameter just above the basal disc 0.08–0.2 mm. Diameter at 2-mm height 0.09–0.16 mm, and at 5-mm height 0.14–0.21 mm. Three to 8 whorls of 16 internal smooth cusps: 4 large (perradius),

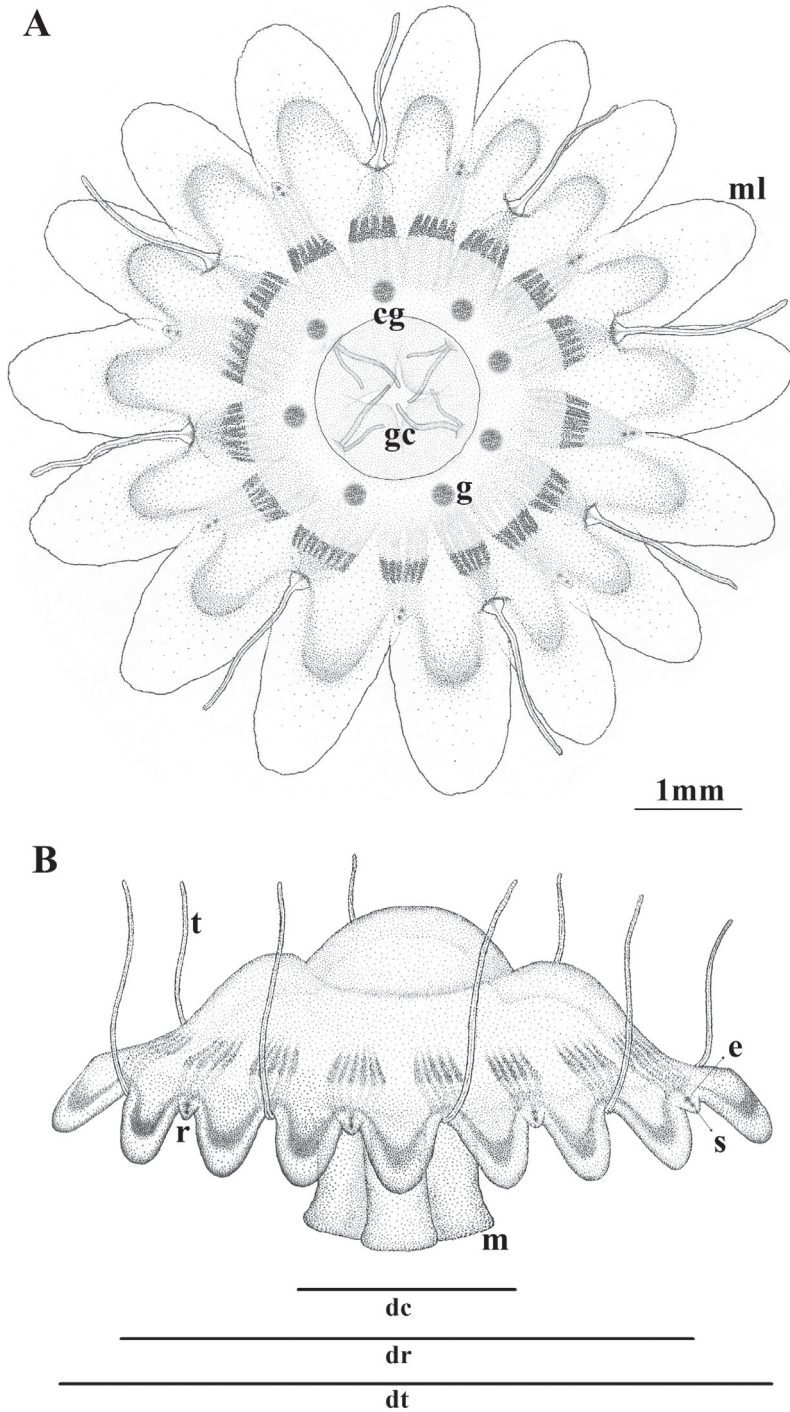


Figure 2. Schematic view of a typical *Nausithoe* sp. adult medusa, illustrating the main characters. **A** aboral view **B** lateral view. **dc** diameter of coronal furrow **dr** diameter between rhopalia **dt** total diameter **cg** coronal groove **gc** gastric cirri **m** manubrium **ml** marginal lappets **r** rhopodium **t** tentacle **e** eyespot **g** gonad **s** statolith.

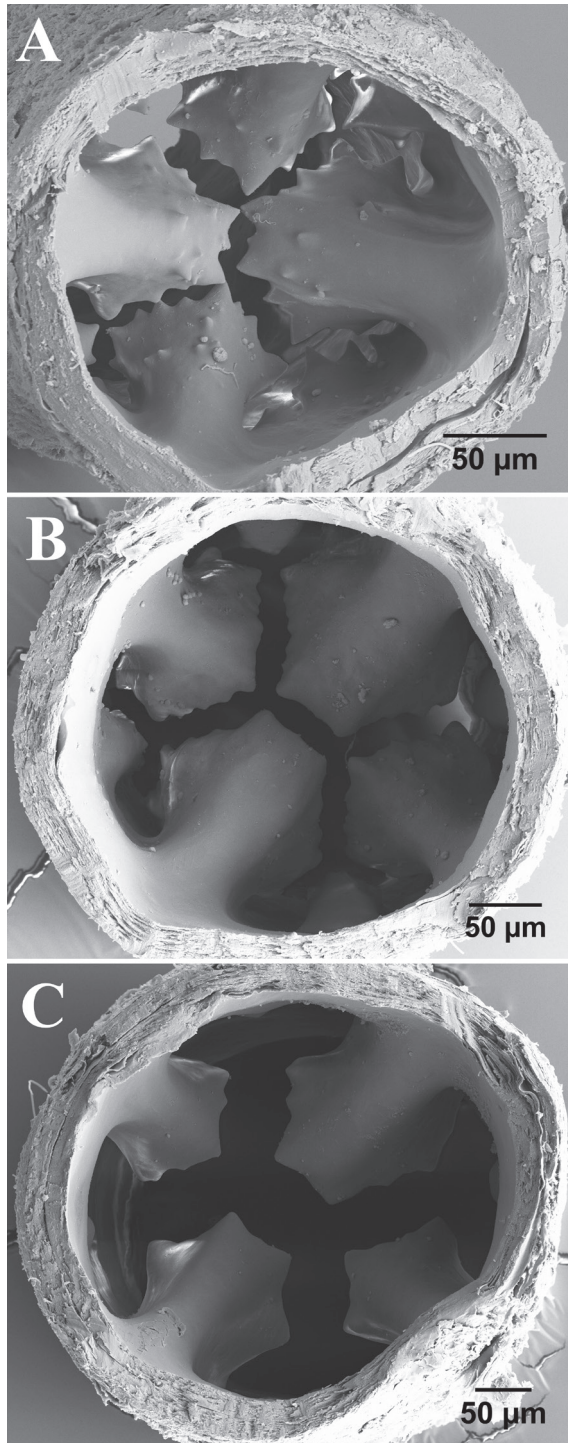


Figure 3. SEM of cross-sections of the tube of the polyp of *Nausithoe* sp. AC02 at different heights. **A** more-basal series, with 16 cusps and additional cusps over 4 larger periradial cusps **B** and **C** two more-distal series (**C** being the highest along the tube), each with 8 cusps.

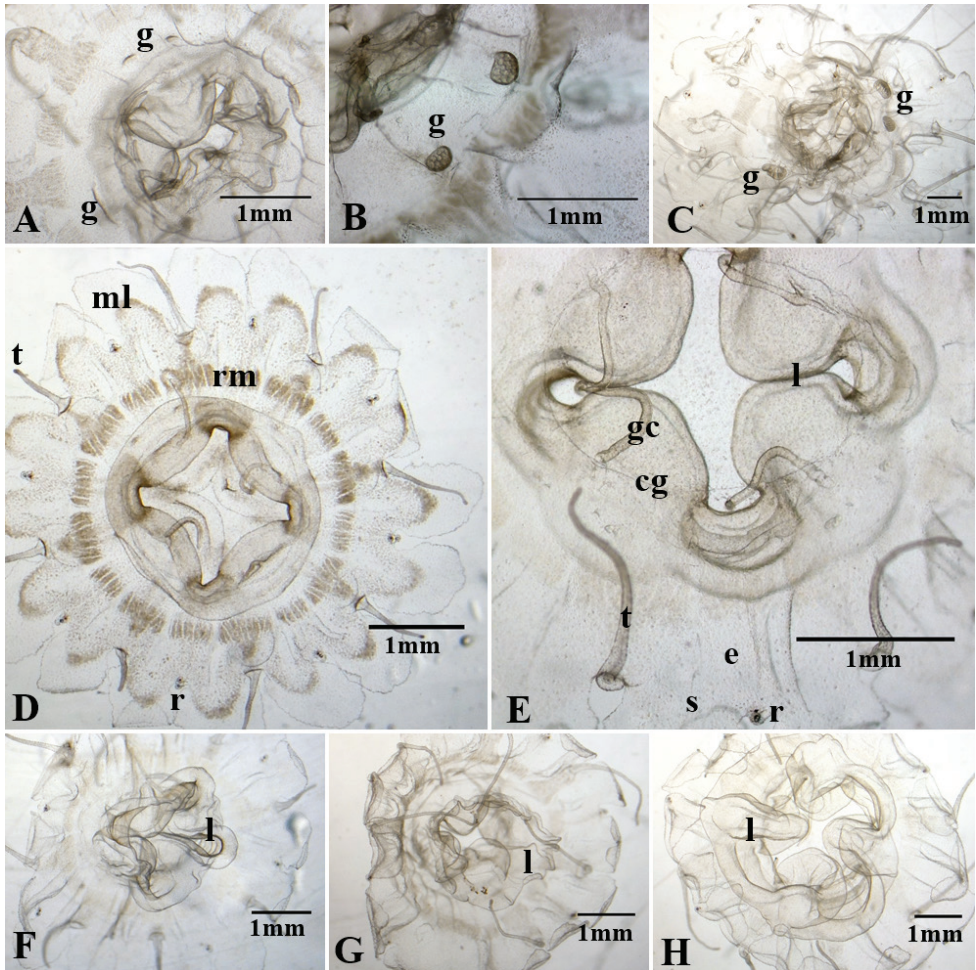


Figure 4. Adult medusae from polyps of *Nausithoe* sp. AC10 (**A–C**) and AC20 (**D–H**) **A** beginning of gonad (**g**) development **B** two gonads with gametic cells still differentiating **C** general view of a medusa that we managed to maintain until the gonads emerged (note degree of irregularities in this specimen, due to the long period in cultivation) **D** aboral view of 3-month-old medusa, showing the radial muscle (**rm**), marginal lappets (**ml**), rhopalium (**r**), and tentacles (**t**) **E** detail of 6-month-old medusa, showing gastric filaments (**gf**), rhopalium with ocelli (**e**), and statocyst (**s**), and coronal groove (**cg**); note, no trace of gonad development **F**, **G** and **H** Oral view of medusae, showing lips (**l**) and projection of the manubrium, from less projected (**F**) to more projected (**H**).

4 intermediate (interradius), and 8 small (adradius). Polydisc strobilation, with more than 100 ephyrae at a time. Medusa translucent, with yellow pigment spot in center of each lappet (Fig. 6A, B). Umbrella flattened, with 16 slightly elongated lappets with rounded margins and 8 rhopalia with statocyst and red ocelli. Live specimens measuring up to: 3.9 mm total diameter; 2.7 mm between opposite rhopalia; 1.5 mm coronal-groove diameter; gastric cirri approximately 0.5 mm in length; and tentacle length up to 1.5 mm. Stomach with 4 gastric septa, each with 3–7 gastric filaments.

Table 4. Morphological data for studied species of *Nausithoe*. Data combined from literature and observations on specimens. Brazilian state abbreviations: BA, Bahia; RJ, Rio de Janeiro; SP, São Paulo.

		<i>N. sp.</i>	<i>N. maculata</i> (= <i>N. auvea</i>)	<i>N. maculata</i>	<i>N. weneri</i>
Medusae	Number / shape of lappets	16, slightly elongate with rounded margins	16, slightly elongate with rounded margins	16, slightly elongate with rounded margins	16, slightly elongate with rounded margins
	Rhopalium with ocellus	yes	yes	yes	yes
	Number of gastric filaments	8 (2 × 4)	12–24 (3–6 × 4)	28 (7 × 4)	4–12 (1–3 × 4)
	Gonad shape	round	round	round	round
	Central disc shape	central dome slightly elevated	flattened	flattened	central dome elevated
	Total diameter (mm) / Central disc diameter (mm)	9.5 / 2.83	5 / 1.9	4 / 1.5	12 / 4.5
	General coloration	transparent	transparent with yellow pigment spot on lappets	transparent with yellow pigment spot on lappets	transparent
	Gonad color	dark brown	yellow to brown	yellow to brown	dark brown
Tentacle length (mm)	5	1.5	2	3	
Polyp	Habitus	solitary	solitary	solitary	solitary
	Occurrence	off Cabo Frio, RJ (Brazil)	Brazil (SP to BA)	Puerto Rico; Cuba	Atlantic off Morocco; Greenland
	Depth (m)	227	3–9	5–10	200–3000
	Length (mm)	5.05–20.2	1.35–9.18	3.79–18.64	2.56–31.46
	Number of cusps/whorls	8 + 16	16	16	8
	Number of whorls of cusps	3–10	2–7	3–8	6–14

***Nausithoe weneri* Jarms, 1990**

Fig. 7

Nausithoe weneri Jarms 1990: 12–17, figs 1–7, pls I, III. Type locality: Morocco coast (25°20.4'N, 16°08.4'W, 415–420 m depth). Holotype: ZMH C11530.

Metagenetic species. Solitary polyp with typical periderm tube, dark to light brown, conical, with transverse rings on surface with longitudinal striations (4–5 rings every 0.4 mm at 2 mm above the base). Polyps 2.56–31.46 mm long. Basal disk 0.24–0.53 mm in diameter. Diameter of aperture 0.33–1.29 mm. Diameter just above basal disc 0.07–0.23 mm. Diameter at 2-mm height 0.07–0.12 mm, and at 5-mm height 0.07–0.17 mm. Six to 14 whorls of 8 internal cusps: 4 large (perradius) and 4 intermediate (interradius), with additional cusps. Polyp with up to 40 filiform tentacles. Polydisc strobilation, with more than 100 ephyrae at a time. Medusa with smooth umbrella (Fig. 7) with high central dome; 16 slightly elongated lappets with rounded margins, and 8 rhopalia with statocyst and red ocelli. Live specimens measuring up to: 6.8 mm total diameter; 5 mm between opposite rhopalia; 2.5 mm coronal groove diameter; gastric cirri approximately 1.9 mm in length; and tentacle length up to 3 mm. Stomach with 4 gastric septa, each with 1 gastric filament (4 in total).

Sequences from all species studied are available on GenBank (Table 7). DNA comparisons of the sequenced markers of the species are summarized in Tables 8 and 9. We were not able to amplify the three proposed markers for all polyps. Therefore, *Nausithoe* sp. specimens AC01 (no 28S data), AC17 (no COI data), and AC18 (no COI data) were not included in the molecular analyses. Polyps with all three genes

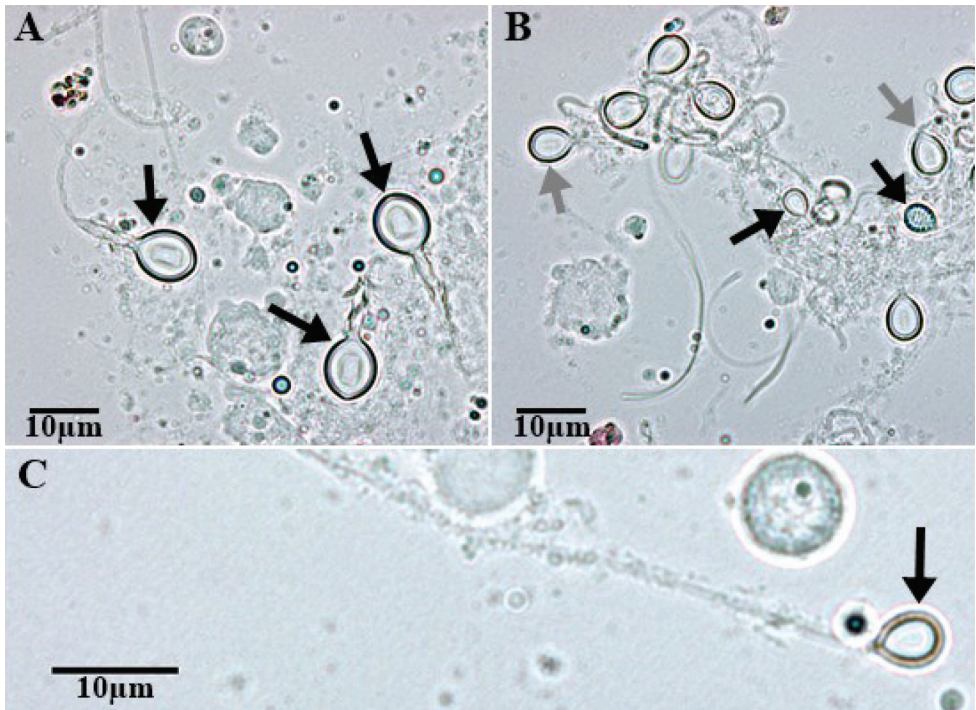


Figure 5. Photomicrographs of the two nematocyst types found in *Nausithoe* sp. **A** three heterotrichous microbasic euryteles discharged **B** holotrichous isorhiza capsules of two different sizes (large, grey arrow; small, black arrow) **C** a small discharged holotrichous isorhiza.

sequenced were compared with each other and with *N. maculata* (= *N. aurea* from Brazil), *N. maculata* (Cuba), and *N. weneri*. Using only the COI marker, *Nausithoe* sp. (specimens AC02, AC08, AC10, AC20) and *N. weneri* had less than 6% genetic difference from each other and almost 20% genetic difference from *N. maculata* (Cuba) and *N. maculata* (= *N. aurea* from Brazil). *Nausithoe maculata* from Cuba had less than 7% difference from *N. maculata* (= *N. aurea*) from Brazil. The remaining DNA extractions from cultures are also considered as vouchers (Table 7).

Discussion

The objective of this study was to identify the polyps of *Nausithoe* sp. from deep waters off southeastern Brazil by comparing them with previous records along the Brazilian coast. We used two approaches: morphology combined with life-cycle observations, and molecular data. Also, we present previously unpublished data on nematocysts for *N. weneri* and *N. maculata* from Cuba.

So far, only three species of *Nausithoe* have been recorded from the Brazilian coast: *N. aurea*, *N. atlantica*, and *N. punctata* (Oliveira et al. 2016). *Nausithoe aurea* is endemic

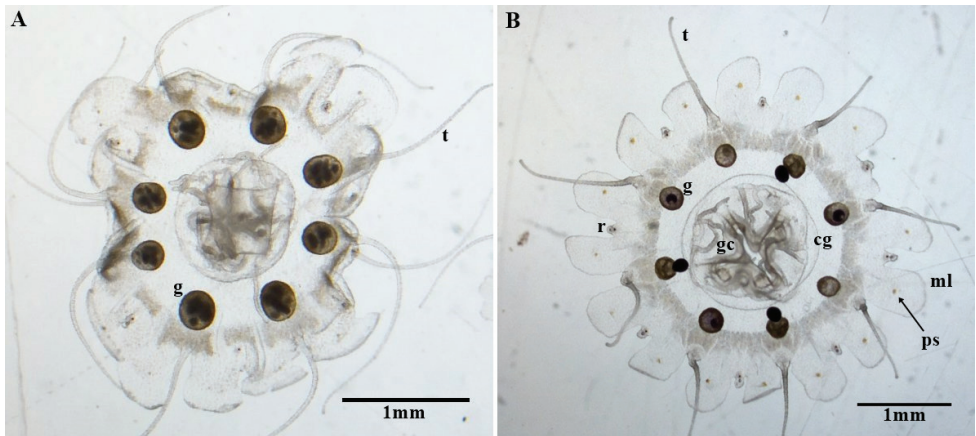


Figure 6. Aboral view of *Nausithoe maculata* medusae from Cuba's polyp culture. **A** four-month-old medusa with mature male gonads (**g**), long tentacles (**t**), and malformations in the lappets and central disc. **B** three-month-old medusa with mature female gonads (**g**), showing the rhopalium (**r**), coronal groove (**cg**), marginal lappets (**ml**) with pigment spot (**ps**), gastric cirri (**gc**), and tentacles (**t**).

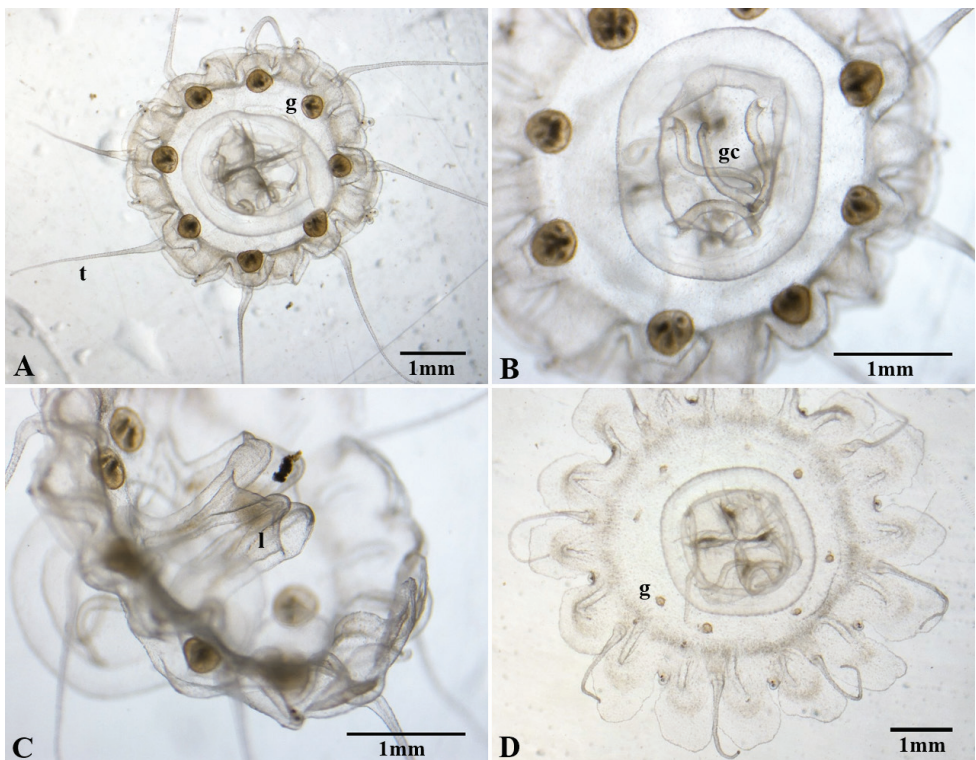


Figure 7. *Nausithoe weneri* male medusae from Mediterranean's polyp culture (**A–C** 5 months old **D** 3 months old) **A** aboral view of an adult medusa with mature gonads (**g**), contracted lappets, and extended tentacles (**t**) **B** detail of gastrovascular cavity, focusing on the gastric cirri (**gc**) **C** lateral view, focusing on the lips (**l**) and the extension of the manubrium **D** beginning of gonad (**g**) development (aboral view).

Table 5. Development times (in weeks, under laboratory conditions) of several structures in the species studied.

	<i>N. wernerii</i>	<i>N. maculata</i> (= <i>N. aurea</i>)	<i>N. maculata</i>	<i>N. sp.</i>
Ocelli	4	2	3	3
First gastric filament	3	1	2	2
Second gastric filament	–	–	8	13
Tentacle buds	7	3	3	2
Lappets, pigment spot	–	2	2	–
Gonads	9	3	4	24

Table 6. Cnidome of studied species of *Nausithoe*. The range was obtained from 60 nematocysts of each type at each stage. *Data from Silveira and Morandini (1997; from 20 nematocysts of each type at each stage).

		Holotrichous isorhiza		Heterotrichous microbasic eurytele	
		Width (µm)	Length (µm)	Width (µm)	Length (µm)
<i>Nausithoe</i> sp.	medusa (tentacle)	4.41–6.49	5.65–8.65	7.28–10.96	8.47–12.99
	ephyra (whole)	4.11–7.33	5.29–8.98	7.1–12.59	8.19–14.27
	polyp (tentacle)	5.86–7.58	8.24–9.67	9.58–11.54	11.28–13.53
	medusa (tentacle)	3.0–4.2	4.2–6.0	5.4–7.2	6.6–9.0
<i>N. maculata</i> (= <i>N. aurea</i>)*	ephyra (whole)	3.6–6.0	5.4–7.2	9.0–11.4	10.2–12.6
	polyp (tentacle)	3.6–5.4	6.0–7.8	3.0–4.8	9.0–15.0
<i>N. maculata</i>	medusa (tentacle)	3.52–5.08	4.5–5.83	6.49–8.17	7.49–9.21
<i>N. wernerii</i>	medusa (tentacle)	4.33–6.69	5.47–7.45	7.06–9.27	8.67–10.92

to the Brazilian coast and can be found in shallow waters (Silveira and Morandini 1997; Morandini and Silveira 2001). The polyps are solitary with 16 smooth cusps per series; and the medusae have a characteristic single yellow spot in the center of each marginal lappet (Silveira and Morandini 1997). These features show that this species is not identical to *Nausithoe* sp.

Nausithoe punctata is a cosmopolitan species that lives in shallow waters (Jarms and Morandini 2019); in Brazil it was reported by Goy (1979) and Neumann-Leitão et al. (2008). The polyp stage is colonial and inhabits sponges (Werner 1979; Uriz et al. 1992). Medusae are transparent with a pale-pink disc and yellowish lappets; the umbrella is flattened and reaches up to 15 mm in diameter (Kölliker 1853; Kramp 1961; Werner 1970). With these features, we can also discard this species as identical to *Nausithoe* sp. As pointed out by Jarms and Morandini (2019), there is extensive confusion in the taxonomy and identification of *N. punctata*, and many records around the world might be erroneous.

Nausithoe atlantica is known only from the medusa stage (Jarms and Morandini 2019). Although records from the Pacific Ocean exist (Oliveira et al. 2016), the only confirmed identifications are from the North Atlantic, near the type locality (Broch 1913; Russell 1956). The adult medusa is dark yellowish-brown, up to 35 mm in diameter, and has rhopalia without ocelli, oblong gonads, and more than 160 gastric filaments (Russell 1970). The Brazilian record provided by Oliveira et al. (2016) derives from a thesis in which the specimens were collected off Santa Catarina state. The description provided is identical to Russell (1970), and no voucher material is available for comparison. Considering the divergent features and doubtful record, we discard this species as identical to *Nausithoe* sp.

Table 7. Sequence accession numbers in GenBank and their respective DNA extraction vouchers.

	COI	18S	28S	DNA Voucher
<i>Nausithoe</i> sp. AC02	MT603856 (717 bp)	MT603629 (1765 bp)	MT621557 (1304 bp)	N02
<i>Nausithoe</i> sp. AC08	MT603855 (735 bp)	MT603631 (1767 bp)	MT621552 (1309 bp)	N08
<i>Nausithoe</i> sp. AC10	MT603857 (708 bp)	MT603630 (1765 bp)	MT621553 (1319 bp)	N10
<i>Nausithoe</i> sp. AC20	MT603854 (609 bp)	MT603628 (1772 bp)	MT621555 (1344 bp)	N20
<i>N. weneri</i> (Mediterranean)	MT603858 (610 bp)	MT603627 (1767 bp)	MT621554 (1337 bp)	NW (Med)
<i>N. maculata</i> (= <i>N. aurea</i>) (Brazil)	MT603859 (579 bp)	MT603632 (1777 bp)	MT621558 (1305 bp)	NA
<i>N. maculata</i> (Cuba)	MT603860 (591 bp)	MT603633 (1780 bp)	MT621559 (1310 bp)	NM (Cuba)

Table 8. Genetic similarity (percent) between each *Nausithoe* sp. polyp (AC02, AC08, AC10, AC20), *Nausithoe maculata* (= *N. aurea* from Brazil), *Nausithoe maculata* (from Cuba), and *Nausithoe weneri*. 18S in white and 28S in *italic*.

	AC02	AC08	AC10	AC20	<i>N. weneri</i>	<i>N. maculata</i> (Brazil)	<i>N. maculata</i> (Cuba)
AC02		100	100	99.94	99.94	99.86	99.86
AC08	<i>94.86</i>		100	99.94	99.94	99.86	99.86
AC10	<i>97.04</i>	<i>94.63</i>		99.94	99.94	99.86	99.86
AC20	<i>97.41</i>	<i>95</i>	<i>97.18</i>		99.89	99.80	99.80
<i>N. weneri</i>	<i>97.22</i>	<i>94.69</i>	<i>96.91</i>	<i>97.28</i>		99.80	99.80
<i>N. maculata</i> (Brazil)	<i>96.64</i>	<i>94.22</i>	<i>96.62</i>	<i>96.76</i>	<i>96.51</i>		99.94
<i>N. maculata</i> (Cuba)	<i>96.66</i>	<i>94.18</i>	<i>96.37</i>	<i>96.74</i>	<i>96.47</i>	<i>97.36</i>	

The two types of nematocysts found in *Nausithoe* sp. (heterotranchous microbasal euryteles and holotranchous isorhizas) are the same as in *N. aurea* (Silveira and Morandini 1997) and in *N. planulophora* (Werner 1971). These are the most common types in scyphozoans (Östman 2000), which indicate that this information might not be useful in differentiating species of the group. There is an overlap of the measurements obtained from *Nausithoe* sp. and *N. weneri*, and polyp nematocysts are slightly larger than ephyrae and medusae ones. For now, much more work on the scyphozoan cnidome is needed to improve understanding of the types of cnidae in the group's evolutionary history.

As do most of the solitary Nausithoidea polyps, those of *Nausithoe* sp. and *N. weneri* resemble each other. As stated by several authors, the most useful features to distinguish *Nausithoe* polyps are the number and shape of the internal cusps of the tube (e.g., Jarms 1991; Morandini and Jarms 2012). Although these features are used widely in the systematics of the group, the variation among specimens has not been thoroughly studied, in part because of the relatively few samples that can be used for scanning electron microscopy. It is also unknown how laboratory conditions might affect the growth of the animals and the shape of the cusps. SEM observations of the cusps of *Nausithoe* sp. showed 16 internal cusps per whorl close to the base and eight cusps in the upper whorls of the tube (Fig. 3), whereas in *N. weneri*, only eight cusps are found per whorl, both in the literature (Jarms 1990) and in our observations.

Both the ephyrae and medusae of the Brazilian deep-sea *Nausithoe* sp. are morphologically similar to *N. weneri*: translucent body, rhopalium with statocyst and red ocelli, lappets slightly elongated with rounded margins, and total diameter (Table 4). The only differences we noted were the shape and size of the manubrium, the shape

Table 9. Genetic similarity (percent) between each *Nausithoe* sp. polyp (AC02, AC08, AC10, AC20), *N. maculata* (= *N. aurea* from Brazil), *N. maculata* (from Cuba), and *N. weneri*. COI in italic; all three markers combined in white. Boldface indicates higher similarity that we are considering to be the same species.

	AC02	AC08	AC10	AC20	<i>N. weneri</i>	<i>N. maculata</i> (Brazil)	<i>N. maculata</i> (Cuba)
AC02		96.28	97.33	94.60	95.35	91.74	92.08
AC08	97.35		96.11	94.1	94.28	90.99	91.39
AC10	100	97.32		94.73	95.32	91.77	92.11
AC20	94.25	95.40	94.25		94.73	92.00	92.18
<i>N. weneri</i>	100	97.21	100	94.06		91.72	92.05
<i>N. maculata</i> (Brazil)	<i>80.83</i>	<i>80.83</i>	<i>80.83</i>	<i>81.35</i>	<i>80.83</i>		94.06
<i>N. maculata</i> (Cuba)	<i>81.89</i>	<i>82.40</i>	<i>81.89</i>	<i>82.29</i>	<i>81.89</i>	93.06	

of the central disc, and the number of gastric cirri. In *Nausithoe* sp., the manubrium is wider (Fig. 4F–H) than in *N. weneri* (Fig. 6D). The elevated central dome of *N. weneri* is also not present in *Nausithoe* sp. Although Jarms (1990) described *N. weneri* with two or three gastric cirri per quadrant, our cultivated specimens (derived from Jarms's culture) had only one gastric cirrus per quadrant (Fig. 6B); *Nausithoe* sp. has eight filaments in the stomach. These variations in morphological features might be related to plasticity in the response of the species under different environmental conditions and food supply. Certainly, the food provided in our laboratory differs from that used by Jarms (1990). Although our specimens were kept in the same conditions, there might be some individual variation. To ascertain the utility of these morphological features it would be necessary to examine many specimens from a broad population.

An interesting feature is the difference in the time taken to develop gonads between *Nausithoe* sp. and our specimens of *N. weneri* (Table 5). *Nausithoe* sp. took more than 20 weeks to begin the differentiation and development of the reproductive organs, while *N. weneri* required only nine weeks. These times are comparable because all species were kept in the same kind of container and temperature, with similar population densities, and fed equally.

Genetic divergence related to species delimitation is difficult to discern, especially for clades with limited molecular markers and specimens. For Discomedusae, the sister clade of Coronamedusae, Gómez Daglio and Dawson (2017) proposed that the mean intraspecific pairwise genetic distance ($x \pm$ s.d.) is 0.006 ± 0.005 and the mean interspecific distance between congeneric species ($x \pm$ s.d.) is 0.12 ± 0.04 . Our molecular data showed that specimens of *Nausithoe* sp. and *N. weneri* had less than 6% of genetic difference for the COI gene (Table 8) and each of them differed by ~20% from *N. maculata* (from Cuba) and *N. maculata* (= *N. aurea* from Brazil). Together with the morphological similarities, we state they are the same species, according to the criteria of Gómez Daglio and Dawson (2017). Following the same rationale, we found less than 7% of genetic difference in the COI gene between *N. maculata* (from Cuba) and *N. maculata* (= *N. aurea* from Brazil). In these two species, the morphological resemblance is obvious, and the only difference is the formation of planuloids inside the periderm tube of *N. aurea* (Silveira and Morandini 1997), which was considered one of the distinguishing features of this species, not observed in *N. maculata*. Considering that

coronamedusae species were mostly defined by a few specimens, we propose that this feature represents possible genetic plasticity not previously recorded for *N. maculata*.

Comparing the life cycle and morphology of scyphomedusae is extremely important to help in identifying and describing species. However, the simple structure of these animals, as evidenced by the traditional use of certain uninformative characters in the description of specimens (e.g., Kramp 1961; Russell 1970), can yield insufficient information for a precise analysis (Dawson 2005). Future approaches, including additional genetic data from other species of Coronatae, will add detail to the systematics of this clade. A broader sampling of molecular markers, individuals, populations, species, and clades in general will allow for novel insights to be applied to Coronamedusae, the proposal of a more refined “genetic gap” for the delimitation of species, and specific genetic diagnoses (DeSalle and Goldstein 2019). Nevertheless, the use of genetic data must be combined with information on morphology and life cycles to confirm or reject the validity of species and to identify new taxa.

To conclude, based on both the morphological and molecular data obtained, we identify the deep-sea *Nausithoe* sp. specimens from off the Brazilian coast as *Nausithoe wernerii*, thus expanding the distribution of this species to the western South Atlantic. Additionally and also based on molecular and morphological data, we consider the species *Nausithoe aurea* as a junior synonym of *Nausithoe maculata*.

Acknowledgements

We thank Drs Sergio A. Vanin for collecting the specimens on shipboard and Fábio L. da Silveira for keeping them for so many years. We also thank Dr Alberto A. F. Ribeiro (IB-USP) for allowing the use of the scanning electron microscope, Enio Mattos and Phillip Lenktaitis for helping with SEM observations, and Beatriz Vieira Freire, Manuel Antunes Júnior, and Sabrina Baroni for assistance with molecular protocols. Resources used in this project were provided by FAPESP (2010/50174-7, 2015/21007-9). CGM received support from a FAPESP MSc scholarship (2017/04954-0, 2018/11523-8) and CAPES/PROEX; MMM was awarded a FAPESP post-doctoral grant (2016/04560-9); ACM received support from a CNPq grant (309440/2019-0). We thank Dr Janet Reid for correcting the English and Dr Allen Collins and an anonymous referee for comments and suggestions to improve the text. This is a contribution of NPBioMar, USP.

References

- Allman GJ (1874) Report on the Hydroida collected during the Expeditions of H.M.S. ‘Porcupine’. Transactions of the Zoological Society of London 8(8): 469–481. [pls 65–68] <https://doi.org/10.1111/j.1096-3642.1874.tb00566.x>
- Broch H (1913) Scyphomedusae from the “Michael Sars” North Atlantic Deep-Sea Expedition 1910. Report on the Scientific Results of the “Michael Sars” North Atlantic Deep-Sea Expedition 3(4): 1–20. [pl. I]

- Calder DR (2009) Cubozoan and scyphozoan jellyfishes of the Carolinian biogeographic province, southeastern USA. *Royal Ontario Museum Contributions in Science* 3: 1–58.
- Collins AG (2009) Recent insights into cnidarian phylogeny. *Smithsonian Contributions to the Marine Sciences* 38: 139–149.
- Dawson MN (2005) Renaissance taxonomy: integrative evolutionary analyses in the classification of Scyphozoa. *Journal of the Marine Biological Association of the UK* 85(3): 733–739. <https://doi.org/10.1017/S0025315405011641>
- Dawson MN, Jacobs DK (2001) Molecular evidence for cryptic species of *Aurelia aurita* (Cnidaria, Scyphozoa). *The Biological Bulletin* 200(1): 92–96. <https://doi.org/10.2307/1543089>
- DeSalle R, Paul Goldstein P (2019) Review and interpretation of trends in DNA barcoding. *Frontiers in Ecology and Evolution* 7: 1–11. <https://doi.org/10.3389/fevo.2019.00302>
- Eschscholtz F (1829) *System der Acalephen. Eine ausführliche Beschreibung aller Medusenartigen Strahlthiere.* Ferdinand Dümmler, Berlin, 190 pp. [16 plates] <https://doi.org/10.5962/bhl.title.10139>
- Fetzner JW (1999) Extracting high-quality DNA from shed reptile skins: a simplified method. *Biotechniques* 26(6): 1052–1054. <https://doi.org/10.2144/992666bm09>
- Goette A (1886) Verzeichnis der Medusen, welche von Dr Sander, Stabsarzt auf S.M.S. “Prinz Adalbert” gesammelt wurden. *Sitzungsberichte der Königlich Preussischen Akademie der Wissenschaften zu Berlin* 39: 831–837.
- Gómez Daglio L, Dawson MN (2017) Species richness of jellyfishes (Scyphozoa: Discomedusae) in the Tropical Eastern Pacific: missed taxa, molecules, and morphology match in a biodiversity hotspot. *Invertebrate Systematics* 31: 635–663. <https://doi.org/10.1071/IS16055>
- Goy J (1979) Campagne de la Calypso au large des côtes atlantiques de l’Amérique du Sud (1961–1962) – 35. Méduses. *Annales de l’Institut Océanographique, Paris* 55 (Suppl.): 263–296.
- Haeckel E (1880) *Das System der Medusen. I, 2: System der Acraspeden.* Gustav Fischer, Jena, 361–672.
- Holland BS, Dawson MN, Crow GL, Hofmann DK (2004) Global phylogeography of *Cassiopea* (Scyphozoa: Rhizostomeae): molecular evidence for cryptic species and multiple invasions of the Hawaiian Islands. *Marine Biology* 145: 1119–1128. <https://doi.org/10.1007/s00227-004-1409-4>
- Holst S, Laakmann S (2014) Morphological and molecular discrimination of two closely related jellyfish species, *Cyanea capillata* and *C. lamarckii* (Cnidaria, Scyphozoa), from the northeast Atlantic. *Journal of Plankton Research* 36(1): 48–63. <https://doi.org/10.1093/plankt/fbt093>
- Jarms G (1990) Neubeschreibung dreier Arten der Gattung *Nausithoe* (Coronatae, Scyphozoa) sowie Wiederbeschreibung der Art *Nausithoe marginata* Kölliker, 1853. *Mitteilungen aus dem Hamburgischen Zoologischen Museum und Institut* 87: 7–39.
- Jarms G (1991) Taxonomic characters from the polyp tubes of coronate medusae (Scyphozoa, Coronatae). *Hydrobiologia* 216: 463–470. <https://doi.org/10.1007/BF00026500>
- Jarms G (2010) The early life history of Scyphozoa with emphasis on Coronatae. A review with a list of described life cycles. *Verhandlungen des Naturwissenschaftlichen Vereins in Hamburg* 45: 17–31.
- Jarms G, Morandini AC (2019) Coronamedusae In: Jarms G, Morandini AC (Eds) *World Atlas of Jellyfish.* *Abhandlungen des Naturwissenschaftlichen Vereins, Hamburg*, 112–259.

- Jarms G, Båmstedt U, Tiemann H, Martinussen MB, Fosså JH (1999) The holopelagic life cycle of the deep-sea medusa *Periphylla periphylla* (Scyphozoa, Coronatae). *Sarsia* 84(1): 55–65. <https://doi.org/10.1080/00364827.1999.10420451>
- Jarms G, Morandini AC, Silveira FL (2002) Cultivation of polyps and medusae of Coronatae (Cnidaria, Scyphozoa) with a brief review of important characters. *Helgoland Marine Research* 56(3): 203–210. <https://doi.org/10.1007/s10152-002-0113-3>
- Katoh K, Standley DM (2013) MAFFT Multiple Sequence Alignment Software version 7: improvements in performance and usability. *Molecular Biology and Evolution* 30(4): 772–780. <https://doi.org/10.1093/molbev/mst010>
- Kearse M, Moir R, Wilson A, Stones-Havas S, Cheung M, Sturrock S, Buxton S, Cooper A, Markowitz S, Duran C, Thierer T, Ashton B, Meintjes P, Drummond A (2012) Geneious Basic: an integrated and extendable desktop software platform for the organization and analysis of sequence data. *Bioinformatics* 28(12): 1647–1649. <https://doi.org/10.1093/bioinformatics/bts199>
- Kölliker A (1853) Bericht über einige im Herbst 1852 in Messina angestellte vergleichend-anatomische Untersuchungen. 11. *Zeitschrift für wissenschaftliche Zoologie* 4: 299–370.
- Kramp PL (1961) Synopsis of the Medusae of the world. *Journal of the Marine Biological Association of the UK* 40: 7–469. <https://doi.org/10.1017/S0025315400007347>
- Kumar S, Stecher G, Li M, Knyaz C, Tamura K (2018) MEGA X: Molecular Evolutionary Genetics Analysis across Computing Platforms. *Molecular Biology and Evolution* 35(6): 1547–1549. <https://doi.org/10.1093/molbev/msy096>
- Maas O (1903) Die Scyphomedusen der Siboga-Expedition. *Siboga-Expeditie* 11. Buchhandlung und Druckerei vormals E. J. Brill, Leiden, 18–23.
- Mariscal RN (1974) Nematocysts. In: Muscatine L, Lenhoff HM (Eds) *Coelenterate Biology: Reviews and New Perspectives*. Academic Press, New York, 129–178. <https://doi.org/10.1016/B978-0-12-512150-7.50008-6>
- Molinari CG, Morandini AC (2019) Update on benthic scyphozoans from the Brazilian coast (Cnidaria: Scyphozoa: Coronatae). *Revista Brasileira de Zoociências* 20(2): 1–14. <https://doi.org/10.34019/2596-3325.2019.v20.27610>
- Morandini AC, Jarms G (2005) New combinations for two coronate polyp species (Atorellidae and Nausithoidae, Coronatae, Scyphozoa, Cnidaria). *Contributions to Zoology* 74(1–2): 117–123. <https://doi.org/10.1163/18759866-0740102008>
- Morandini AC, Jarms G (2010) Identification of coronate polyps from the Arctic Ocean: *Nausithoe wernerii* Jarms, 1990 (Cnidaria, Scyphozoa, Coronatae), with notes on its biology. *Steenstrupia* 32(1): 69–77.
- Morandini AC, Jarms G (2012) Discovery and redescription of type material of *Nausithoe simplex* (Kirkpatrick, 1890), comb. nov. (Cnidaria: Scyphozoa: Coronatae: Nausithoidae) from the North Atlantic. *Zootaxa* 3320: 61–68. <https://doi.org/10.11646/zootaxa.3320.1.5>
- Morandini AC, Silveira FL (2001a). New observations and new record of *Nausithoe aurea* (Scyphozoa, Coronatae). *Papéis Avulsos de Zoologia* 41(27): 519–527.
- Morandini AC, Silveira FL (2001b) Sexual reproduction of *Nausithoe aurea* (Scyphozoa, Coronatae). Gametogenesis, egg release, embryonic development, and gastrulation. *Scientia Marina* 65(2): 139–149. <https://doi.org/10.3989/scimar.2001.65n2139>

- Müller F (1861) Ueber die systematische Stellung der Charybdeiden. Archiv für Naturgeschichte 27(1): 302–311.
- Neumann-Leitão S, Sant’anna EME, Gusmão LMO, Do Nascimento-Vieira DA, Paranaguá MN, Schwaborn R (2008) Diversity and distribution of the mesozooplankton in the tropical Southwestern Atlantic. Journal of Plankton Research 30(7): 795–805. <https://doi.org/10.1093/plankt/fbn040>
- Östman C (2000) A guideline to nematocyst nomenclature and classification, and some notes on the systematic value of nematocysts. Scientia Marina 64(1): 31–46. <https://doi.org/10.3989/scimar.2000.64s131>
- Russell FS (1956) On the Scyphomedusae *Nausithoë atlantica* Broch and *Nausithoë globifera* Broch. Journal of the Marine Biological Association of the UK 35(2): 363–370. <https://doi.org/10.1017/S0025315400010195>
- Russell FS (1970) Nausithoëidae. In: Russell FS (Ed.) The Medusae of the British Isles II. Pelagic Scyphozoa with a Supplement to the First Volume on Hydromedusae. Cambridge University Press, London, 29–37.
- Silveira FL, Morandini AC (1997) *Nausithoe aurea* n. sp. (Scyphozoa, Coronatae, Nausithoëidae), a species with two pathways of reproduction after strobilation: sexual and asexual. Contributions to Zoology 66(4): 235–246. <https://doi.org/10.1163/26660644-06604004>
- Silveira FL, Jarms G, Morandini AC (2003) Experiments in nature and laboratory observations with *Nausithoe aurea* (Scyphozoa: Coronatae) support the concept of perennation by tissue saving and confirm dormancy. Biota Neotropica 2(2): 1–25. <https://doi.org/10.1590/S1676-06032002000200009>
- Uriz MJ, Rosell D, Maldonado M (1992) Parasitism, commensalism or mutualism? The case of Scyphozoa (Coronatae) and horny sponges. Marine Ecology Progress Series 81: 247–255. <https://doi.org/10.3354/meps081247>
- Vanhöffen E (1892). Die Akalephen der Plankton-Expedition. Ergebnisse der Plankton-Expedition der Humboldt-Stiftung 2: 3–28.
- van Walraven L, van Bleijswijk J, van der Veer HW (2020). Here are the polyps: *in situ* observations of jellyfish polyps and podocysts on bivalve shells. PeerJ 8: e9260. <https://doi.org/10.7717/peerj.9260>
- Werner B (1970) Contribution to the evolution in the genus *Stephanoscyphus* (Scyphozoa Coronatae) and ecology and regeneration qualities of *Stephanoscyphus racemosus* Komai. Publications of the Seto Marine Biological Laboratory 18(1): 1–20. <https://doi.org/10.5134/175623>
- Werner B (1971) *Stephanoscyphus planulophorus* n. spec., ein neuer Scyphopolyp mit einem neuen Entwicklungsmodus. Helgoländer wissenschaftliche Meeresuntersuchungen 22: 120–140. <https://doi.org/10.1007/BF01611366>
- Werner B (1979) Coloniality in the Scyphozoa: Cnidaria. In: Larwood G, Rosen BR (Eds) Biology and Systematics of Colonial Organisms. Academic Press, London, 81–103.

A new genus and species of Nannopodidae (Crustacea, Copepoda, Harpacticoida) from the Yellow Sea of South Korea

Jong Guk Kim¹, Jimin Lee¹

¹ Marine Ecosystem Research Center, Korea Institute of Ocean Science & Technology, Busan 49111, South Korea

Corresponding author: Jimin Lee (jmlee@kiost.ac.kr)

Academic editor: D. Defaye | Received 23 March 2020 | Accepted 27 September 2020 | Published 4 November 2020

<http://zoobank.org/3BD22689-146D-4E3B-9CFE-6ACFB58F2778>

Citation: Kim JG, Lee J (2020) A new genus and species of Nannopodidae (Crustacea, Copepoda, Harpacticoida) from the Yellow Sea of South Korea. *ZooKeys* 984: 23–47. <https://doi.org/10.3897/zookeys.984.52252>

Abstract

A new monospecific genus of the family Nannopodidae Brady, 1880 is proposed, based on specimens of both sexes of *Concilicoxa hispida* **gen. et sp. nov.** collected from subtidal sandy sediments in the Yellow Sea of South Korea. The presence of a coxal outer projection on the first to fourth legs and reduction of both rami of the second to fourth legs in this new genus show a clear relationship with a clade, which is characterised by the modified thoracopods for burrowing ability, comprising *Huntemannia* Poppe, 1884, *Rosacletodes* Wells, 1985, *Laophontisochra* George, 2002, *Acuticoxa* Huys & Kihara, 2010 and *Talpacoxa* Corgosinho, 2012 in Nannopodidae. Within this clade, *C. hispida* **gen. et sp. nov.** is most closely related to *L. maryamae* George, 2002 in having the prehensile endopod in the first leg, broad intercoxal sclerite on the second to fourth legs and the female fifth leg being composed of separate exopod and baseopod, but is distinguished by the absence of mandibular exopod, two-segmented mandibular endopod, presence of four setae on the distal exopodal segment of the first leg, and fusion of the intercoxal sclerite to the coxae in the third and fourth legs. These four features are considered as autapomorphies of the new genus. The possible relationship amongst members of the nannopodid clade is further discussed. Additionally, some comments on the taxonomic position of *L. terueae* Björnberg, 2014 are given, resulting in the transfer of the species to *Acuticoxa* as *A. terueae* **comb. nov.**

Keywords

benthic copepod, *Concilicoxa hispida* gen. et sp. nov., East Asia, meiofauna, taxonomy

Introduction

Por (1986) proposed the family Huntemanniidae Por, 1986 to accommodate six cleto-did genera, *Nannopus* Brady, 1880, *Huntemannia* Poppe, 1884, *Pontopolites* T. Scott, 1894, *Metahuntemannia* Smirnov, 1946, *Beckeria* Por, 1986 (= a junior subjective synonym of *Metahuntemannia*) and *Pseudocletodes* T. Scott & A. Scott, 1893—the latter three genera with some reserves. Since its proposal, two genera, *Rosacletodes* Wells, 1985 [= *Echinocletodes* Pallares, 1982 *nec* Lang (1936)] and *Dahmsopottekina* Özdikmen, 2009 [= *Talpina* Dahms & Pottek, 1992 *nec* Hagenow (1840)], have been added to the family (Dahms and Pottek 1992; Huys et al. 1996; Wells 2007; Huys 2009). The family-group name Huntemanniidae was initially universally accepted (Huys et al. 1996; Boxshall and Halsey 2004; Wells 2007; Huys 2009); however, Huys (2009) recognised that Brady (1880) had assigned the new genus *Nannopus* to the new subfamily Nannopinae within Harpacticidae and that this genus could be considered the type genus of the latter subfamily. Therefore, Huys (2009) formally synonymised the family Huntemanniidae with Nannopodidae (adjusted name), considering the huntemanniid genera proposed by Por (1986) as valid members of the latter family. Subsequent studies questioned the monophyly of Nannopodidae and excluded three genera: Kihara and Huys (2009) transferred *Pseudocletodes* to the family Normanellidae Lang, 1944 and Huys and Kihara (2010) re-assigned both *Metahuntemannia* and *Dahmsopottekina* to the subfamily Hemimesochrinae Por, 1986.

Huys and Kihara (2010) also noted that *Laophontisochra* George, 2002, *Acuticoxa* Huys & Kihara, 2010, *Huntemannia* and *Rosacletodes* share the coxal modifications of the first leg and proposed the inclusion of two former genera into the family Nannopodidae. Subsequently, the nannopodid genus *Talpacoxa* Corgosinho, 2012 was established for an intriguing species, *T. brandini* Corgosinho, 2012, which is characterised by hypertrophied coxae of the first leg. According to Corgosinho (2012), these five nannopodid genera constitute a clade supported by the presence of an outer coxal projection on the first leg and reduction of both rami on the second to fourth legs as a morphological adaptation for a burrowing lifestyle.

Recently, Kim et al. (2017) proposed the revival of the genus *Ilyophilus* Lilljeborg, 1902, which had been considered a junior synonym of *Nannopus*, based on a morphological difference in the segmentation of endopod in the third leg, i.e. *Nannopus* could accommodate only two species, *N. palustris sensu stricto* Brady (1880) and *N. parvipilis* Kim, Choi & Yoon, 2017, having a one-segmented endopod and the other *Nannopus* species with a two-segmented endopod should be transferred into *Ilyophilus*. However, Vakati et al. (2019: 376) questioned the validity of re-instating *Ilyophilus*, based on morphological and molecular affinities between both genera. More recently, Lee (2020) proposed the new genus *Doolia* Lee, 2020 as a valid genus of the family Nannopodidae from off Jeju Island of South Korea. To date, the family Nannopodidae is composed of 30 valid species distributed in eight genera, *Nannopus*, *Huntemannia*, *Pontopolites*, *Rosacletodes*, *Laophontisochra*, *Acuticoxa*, *Talpacoxa* and *Doolia* (Kim et al. 2017; Vakati and Lee 2017; Karanovic and Cho 2018; Lee 2020).

In the present study, a new genus, attributed here to the family Nannopodidae, is proposed to accommodate a new harpacticoid collected from subtidal sandy sediments around the Socheongcho Ocean Research Station (SORS), which is a platform-type observation tower in the Yellow Sea of South Korea. SORS plays an important role in monitoring ocean and meteorological changes related to global climate change. Herein, we describe this new taxon and clarify its taxonomic relationship within Nannopodidae. Additionally, we also discuss the taxonomic position of *L. teruae* Björnberg, 2014.

Materials and methods

Sampling for meiofauna was carried out from off SORS in the Yellow Sea of South Korea (Fig. 1). Sediment sample was taken at a depth of 68 m using a Smith-McIntyre Grab sediment sampler (0.1 m²). To anaesthetise meiofaunal organisms, the sample was immediately bottled with a 7.5% MgCl₂ solution for 1 h and fixed with a 10% formalin solution. In the laboratory, this sample was rinsed and sieved with tap water using a 50 µm sieve. Harpacticoid copepods were sorted out from sediments under a stereomicroscope (M165 C; Leica, Germany) and stored in 95% ethanol. Specimens of a new taxon were cleared in lactic acid. Whole specimens were mounted separately on temporary slides for habitus drawing and measurement of the total body length and the latter was measured from the anterior tip of the rostrum to the posterior end of the caudal rami in lateral view. Specimens were dissected on a reverse slide (Humes and Gooding 1964) using tungsten needles and the dissected parts were examined. All drawings were made with a microscope (DM2500; Leica, Germany) equipped with differential interference contrast (DIC) and a drawing tube. Drawings of the habitus and appendages were prepared at a magnification of 400× and 1000×, respectively. After morphological examination, each dissected part was mounted in lactophenol or fluoromount-G (SouthernBiotech, USA) mounting medium on an H-S slide (Shirayama et al. 1993) and sealed with Hoyer's solution. Scale bars in figures are given in µm.

We adopted the descriptive terminology of Huys and Boxshall (1991). The following abbreviations were used in the text and figures:

- ae** aesthetasc;
P1–P6 first to sixth thoracopod;
exp(enp)-1(-2, -3) to denote the proximal (middle, distal) segment of exopod (endopod).

Prior to scanning electron micrography (SEM), specimens were pre-fixed with 2.5% glutaraldehyde for 4 h, post-fixed with 2% osmium tetroxide for 2 h and then stored in 0.1 M phosphate buffer (pH 7.4) overnight. At each step, the samples were washed with phosphate buffer solution three times for 10 min each. The materials were dehydrated through a graded series of ethanol dilutions (50%, 60%, 70%, 80%, 90%, 100%) for 30 min each, dried in a freeze dryer (Hitachi ES-2030; Japan), coated with

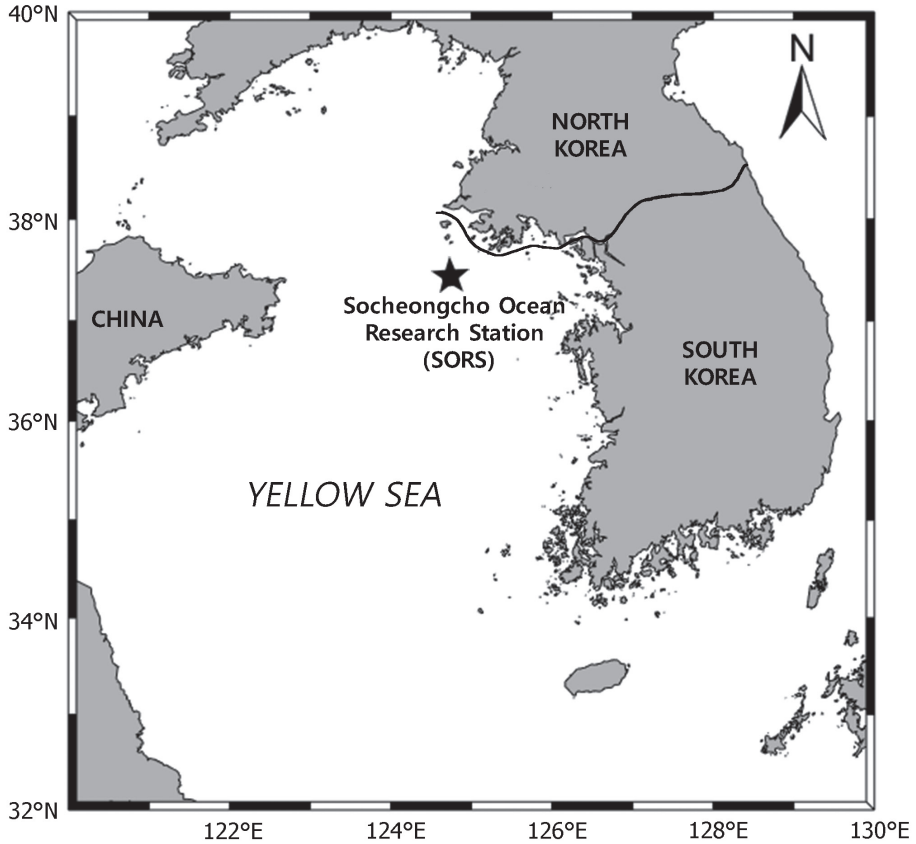


Figure 1. Map of the sampling location.

gold in an evaporator (Hitachi E-1045; Japan) and then examined via SEM (Hitachi S-4300; Japan).

Type materials were deposited in the Marine Interstitial fauna Resources Bank (MIInRB) of the Korea Institute of Ocean Science and Technology (KIOST), Busan, South Korea.

Systematics

Family Nannopodidae Brady, 1880

Genus *Concilioxa* gen. nov.

<http://zoobank.org/76CAD23D-83AE-4ADD-BA77-D21CB3E66CE5>

Diagnosis. Nannopodidae. Body subcylindrical, slightly depressed dorsoventrally, without distinct constriction between prosome and urosome; hyaline frills of somites weak,

ornamented with long setules. Rostrum well-developed, triangular, with 1 pair of sensilla. Genital slit ♀ reverse U-shaped, covered by 1 pair of large opercula. Caudal rami elongate, oval in ♀, rectangular in ♂, with 7 setae; principal seta V as long as caudal rami in ♀, slightly shorter than urosome in ♂. Antennule 4-segmented, with elongate first segment in ♀; chirocerate and 6-segmented in ♂. Antennary allobasis without abexopodal seta; exopod represented by single seta. Mandibular palp uniramous, with 1 seta on basis; exopod absent and endopod 2-segmented. Maxillular praecoxal arthritis with 1 surface seta; exopod 1-segmented and endopod absorbed into basis. Maxillary syncoxa with 2 endites; endopod absorbed into basis. Maxilliped with elongate basis; endopod drawn out into long geniculate claw. P1 coxa with 1 coarsely serrate outer projection; inner element on basis displaced onto anterior surface; exopod 2-segmented, with 4 setae on exp-2; endopod arising from well-developed inner pedestal of basis, prehensile, 2-segmented; enp-1 elongate, unarmed; enp-2 with 1 stout claw and 1 long seta. P2–P4 with 1 coarsely serrate outer projection on coxa; intercoxal sclerite hugely broad, separated in P2 and laterally fused to coxae in P3 and P4; outer setophore on basis articulated in P3 and P4; exopod 1-segmented; proximal outer spine on exopod with serrate outer margin, with inner and outer longitudinal rows of setules; endopod absent in P2, represented by 1 small distinct protuberance in P3, 1-segmented in P4; male P3 endopod 1-segmented and armed with 1 stout spine. Setal armature formulae of P1–P4 as follows:

	Exopod	Endopod
P1	0.022	0.011
P2	022	absent
P3	112	000 [010 in ♂]
P4	112	010

P5 baseoendopod broad; endopodal lobe weakly developed, with 1 seta; exopod 1-segmented, with 4 setae.

P6 represented by 2 setae in ♀; slightly asymmetrical and represented by 3 setae in ♂.

Type species. *Concilicoxa hispida* gen. et sp. nov., by monotypy.

Etymology. The generic epithet is a combination of the Latin verb *concilio* meaning 'unite separate parts into a whole' and the Latin noun *coxa*, meaning 'hip' and alludes to the fusion of the coxae and the intercoxal sclerite in P3 and P4. It is a noun in the feminine singular.

***Concilicoxa hispida* gen. et sp. nov.**

<http://zoobank.org/06ABD568-8291-43BC-8AC7-0A6FE8F9BECC>

Figs 2–8

Type locality. Off the Socheongcho Ocean Research Station (SORS) (37°25'57.16"N, 124°44'56.4"E) in the Yellow Sea of South Korea, sandy sediments, 68 m depth.

Material examined. Holotype: SOUTH KOREA•♀ dissected and mounted on 11 slides; the Yellow Sea, off SORS; 37°25'57.16"N, 124°44'56.4"E; 68 m depth; 23 Mar 2018; Kim, J.G. leg.; sandy sediments; cat. MInRB-Hr59-S001.

Allotype: SOUTH KOREA•♂ dissected and mounted on 11 slides; same data as for holotype; cat. MInRB-Hr59-S002.

Paratypes: SOUTH KOREA•3♀♀2♂♂ dissected and mounted on 11 or 12 slides each; same data as for holotype; cat. MInRB-Hr59-S003–MInRB-Hr59-S007•3♀♀2♂♂ preserved together in 95% ethanol; same data as for holotype; cat. MInRB-Hr59-L001.

Other material for SEM. SOUTH KOREA•2♀♀1♂ on a stub for SEM; same data as for holotype.

Description of holotype female (MInRB-Hr59-S001). Total body length 617 µm (measurement based on holotype and six paratypes: range = 530–626 µm; mean = 588 µm; $n = 7$); maximum width 86 µm measured at the middle of cephalothorax. Body (Figs 2A, B, 8A) subcylindrical, slightly depressed, without distinct constriction between prosome and urosome; prosome slightly longer than urosome. Rostrum (Fig. 2C) well-developed, triangular, reaching distal fourth of first antennular segment, defined from cephalothorax basally, with 1 pair of sensilla laterally and 1 median anterior pore ventrally; lateral margins convex proximally. Cephalothorax nearly square in dorsal aspect, slightly wider than long; integument covered with paired sensilla, several round depressions and irregular wrinkles (visible at high magnification, 1,000×; see insert in Fig. 2A); posterior margin ornamented with short and fine setules; arthrodistal membrane of first pedigerous somite visible dorsally and laterally. Tergites of somites with surface ornamentation composed of 1–3 transverse furrows, with 1 mid pore (absent in penultimate and anal somites) and 1 pair of lateral pores (absent in penultimate somite); posterior margins with several paired sensilla (absent in penultimate somite); hyaline frills weak, with 1 row of long setules posteriorly except for anal somite. Genital somite and first abdominal somite fused ventrally forming genital double-somite, but original segmentation indicated by internal chitinous rib dorsally and laterally; genital field (Fig. 3A, D) with 1 large copulatory pore on midventral depression posterior to genital slit; genital slit reverse U-shaped, covered by 1 pair of large opercula derived from P6 on both sides; P6 represented by 1 long and 1 small seta, with 1 row of spinules subdistally; single midventral egg sac carrying 6 large eggs, as long as 1/4 of total body length. Anal somite (Figs 2A, B, 3A, B) with 1 pair of dorsal sensilla near base of operculum, 1 row of long setules on both ventrolateral margins; operculum semicircular, with smooth distal margin; anal opening with lateral row of small posterior spinules on each side; anal opening with 3 fringes of fine setules (Fig. 3B).

Caudal rami (Figs 2A, B, 3A–C) elongate, oval, about 2.4 times as long as largest width, twice as long as anal somite; with a notch in mid-outer margin below caudal setae I and II; anterior half with a row of outer setules ventrolaterally; distal half with non-chitinous lateral margin; with 7 setae: seta I small naked, inserted in mid-length of outer margin ventrolaterally; seta II dorsal to and closely set to seta I, naked, longer than seta I; seta III naked, as long as seta II, arising from subdistal peduncle with

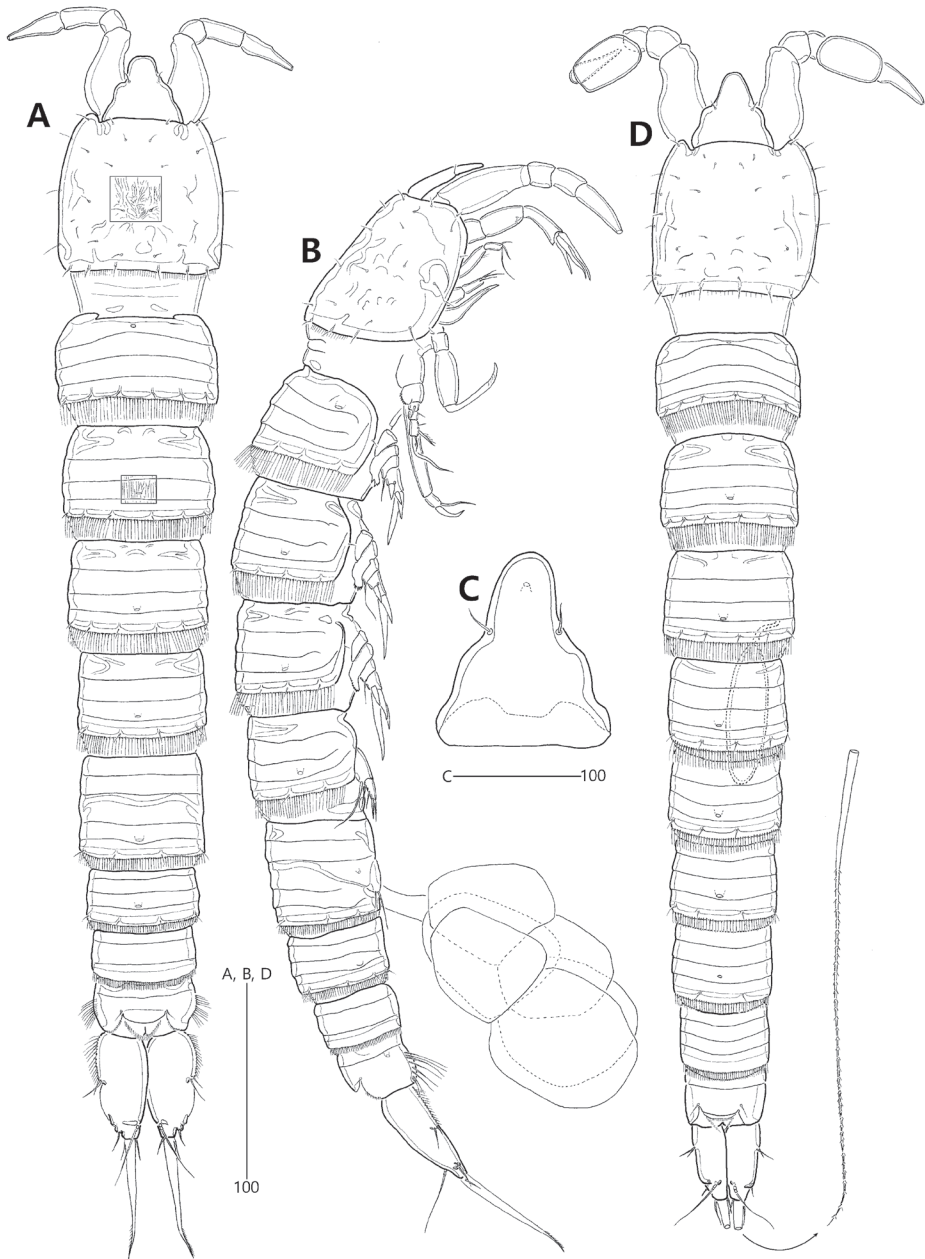


Figure 2. *Concilicoxa hispida* gen. et sp. nov., female holotype (**A–C**) **A** habitus, dorsal **B** habitus, lateral **C** rostrum, dorsal. Male allotype (**D**) **D** habitus, dorsal.

1 tube pore basally (Fig. 3C); seta IV small, naked, slightly longer than setae II and III, fused to principal seta V basally; principal seta V well-developed, slightly longer than caudal ramus, ornamented with outer spinules distally; seta VI naked, as long as seta

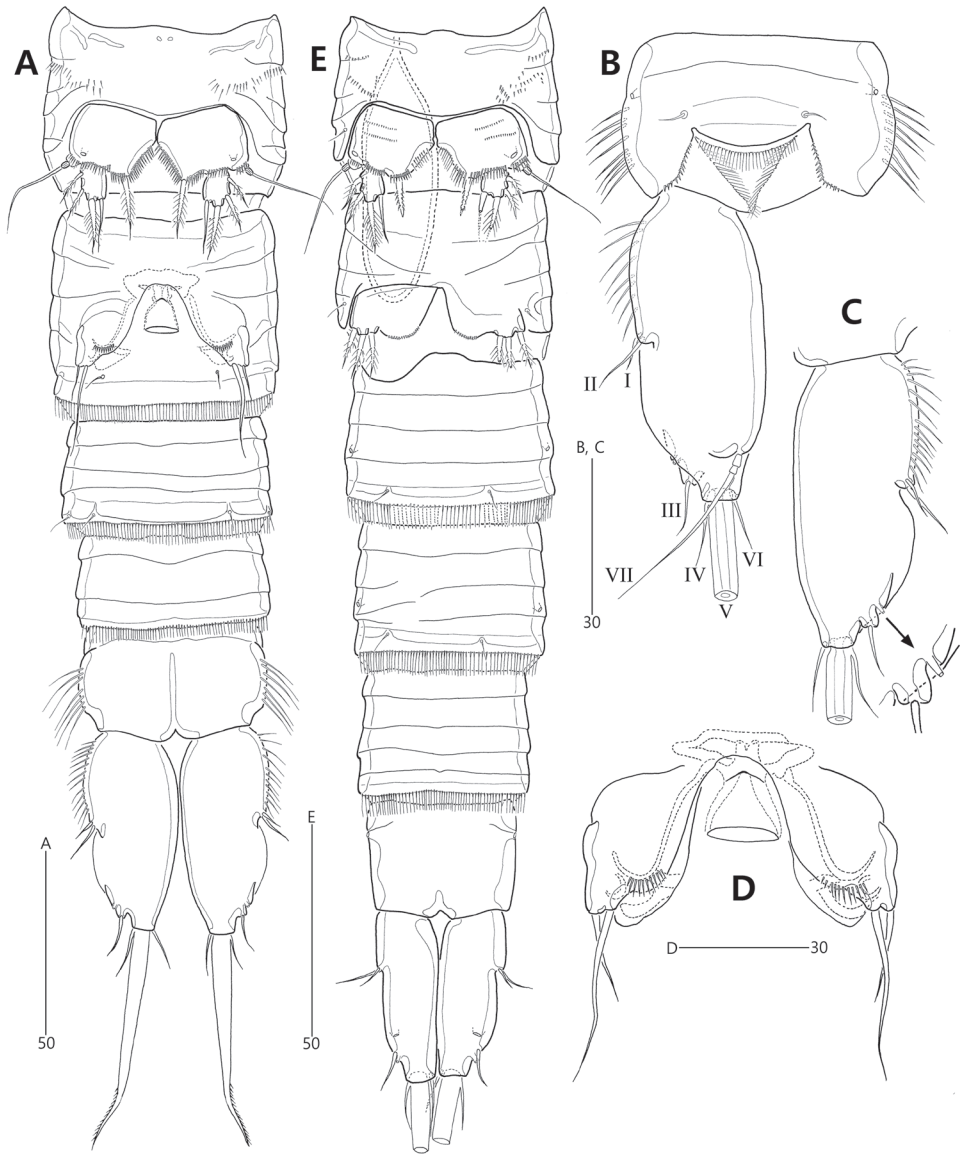


Figure 3. *Concilicoxa hispida* gen. et sp. nov., female holotype (**A–D**) **A** urosome, ventral **B** anal somite and caudal ramus, dorsal **C** caudal ramus, ventral **D** genital field, ventral. Male allotype (**E**) **E** urosome, ventral.

IV, inserted in outer distal corner; dorsal seta VII naked, tri-articulate at base, arising subdistally close to inner margin.

Antennule (Fig. 4A) short, 4-segmented. First segment largest, elongate, as long as distal two segments combined, with 1 small naked seta subdistally; inner margin with short row of spinules subdistally; outer margin convex, with longitudinal row

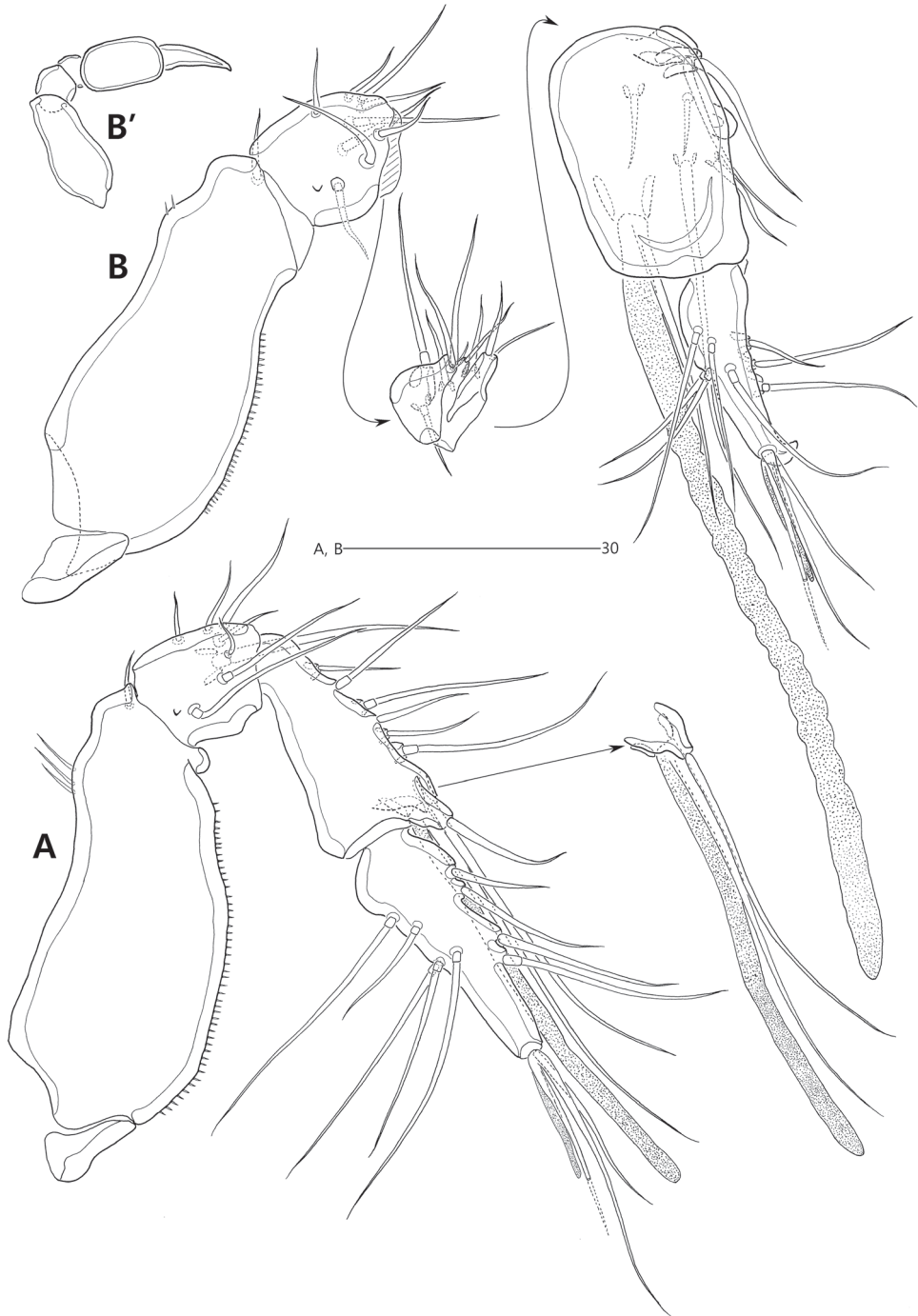


Figure 4. *Concilicoxa hispida* gen. et sp. nov., female holotype (**A**) **A** antennule. Male allotype (**B**) **B** antennule.

of minute spinules. Second segment smallest, with 3 bi-articulate and 5 naked setae; outer margin with 1 weak protuberance. Third segment about twice as long as second one, gradually widening distally; lateral margin with 3 bi-articulate and 3 naked setae; inner distal corner with 3 peduncles, of which two with 1 apical seta each, and one bearing 1 apical seta fused to basally to 1 ae. Distal segment as long as preceding one, tapering distally; lateral margins with 6 bi-articulate and 3 naked setae; distal margin with 1 naked seta and 1 acrothek composed of 1 ae and 2 bare setae. Setal armature as follows: 1-[1], 2-[8], 3-[8+ (1 + ae)], 4-[10 + acrothek].

Antenna (Fig. 5A) with small, unornamented coxa (not shown). Allobasis elongate, 2.8 times as long as wide, exopod represented by 1 naked seta issuing at proximal third; abexopodal seta absent. Free endopodal segment with 1 short row of spinules subdistally and 1 surface frill distally; lateral armature composed of 2 weakly-serrate setae; distal armature comprising 1 small and 1 stout spine, 3 geniculate setae, innermost one of which fused basally to 1 small naked seta.

Mandibular coxa (Fig. 5B) slender, with 1 bulge and 1 row of spinules proximally; gnathobase well-developed, with 1 bicuspid and 3 unicuspid teeth, 1 small spinule and 1 unipinnate seta. Palp well-developed, uniramous; basis elongate, covered with rows of spinules, with 1 plumose seta distally; endopod 2-segmented, with 1 long plumose seta on proximal segment and 1 subapical and 2 apical setae on distal segment.

Maxillule (Fig. 5C). Praecoxa with 1 row of outer spinules; arthrite with 1 naked seta on anterior surface and 7 spines on distal margin and ornamented with few long spinules on distal margin, 1 row of small spinules on dorsal margin and several spinules on posterior surface. Coxa armed with 1 row of outer spinules; endite elongate, with 2 elements distally and 1 row of small spinules laterally. Basis broad, with 2 endites: distal endite with 1 subapical and 3 apical setae; proximal endite incorporated into basis, represented by 2 long naked setae. Endopod incorporated into basis, represented by 3 long naked setae. Exopod 1-segmented, small, with 1 short and 1 long naked seta.

Maxilla (Fig. 5D). Syncoxa armed with 1 row of stout spinules and 1 row of setules along outer margin, 1 row of minute spinules on surface and 1 patch of spinules near inner margin; with 2 coxal endites: proximal endite with 1 long naked seta and 1 short unipinnate seta (fused to endite basally); distal endite with 2 long naked setae and 1 unipinnate seta (fused to endite basally). Allobasis drawn out into strong claw with 2 accompanying naked setae and few spinules. Endopod incorporated into basis, represented by 2 long naked setae fused basally.

Maxilliped (Fig. 5E) enlarged. Syncoxa elongate, ornamented with 1 group of spinules proximally. Basis elongate, about 3.4 times as long as maximum width, with 1 row of outer spinules proximally. Endopod drawn out into long and geniculate claw bearing 1 small accessory seta proximally.

P1 (Fig. 6A). Praecoxa large, triangular, unornamented. Intercoxal sclerite broad, unornamented. Coxa wide, with outer margin forming 1 large and coarsely-serrated projection. Basis with 1 anterior pore and few spinules proximally; inner pedestal well-developed, with serrate distal margin; outer seta plumose, bi-articulated basally, arising from setophore ornamented with 1 row of small spinules at its base; inner

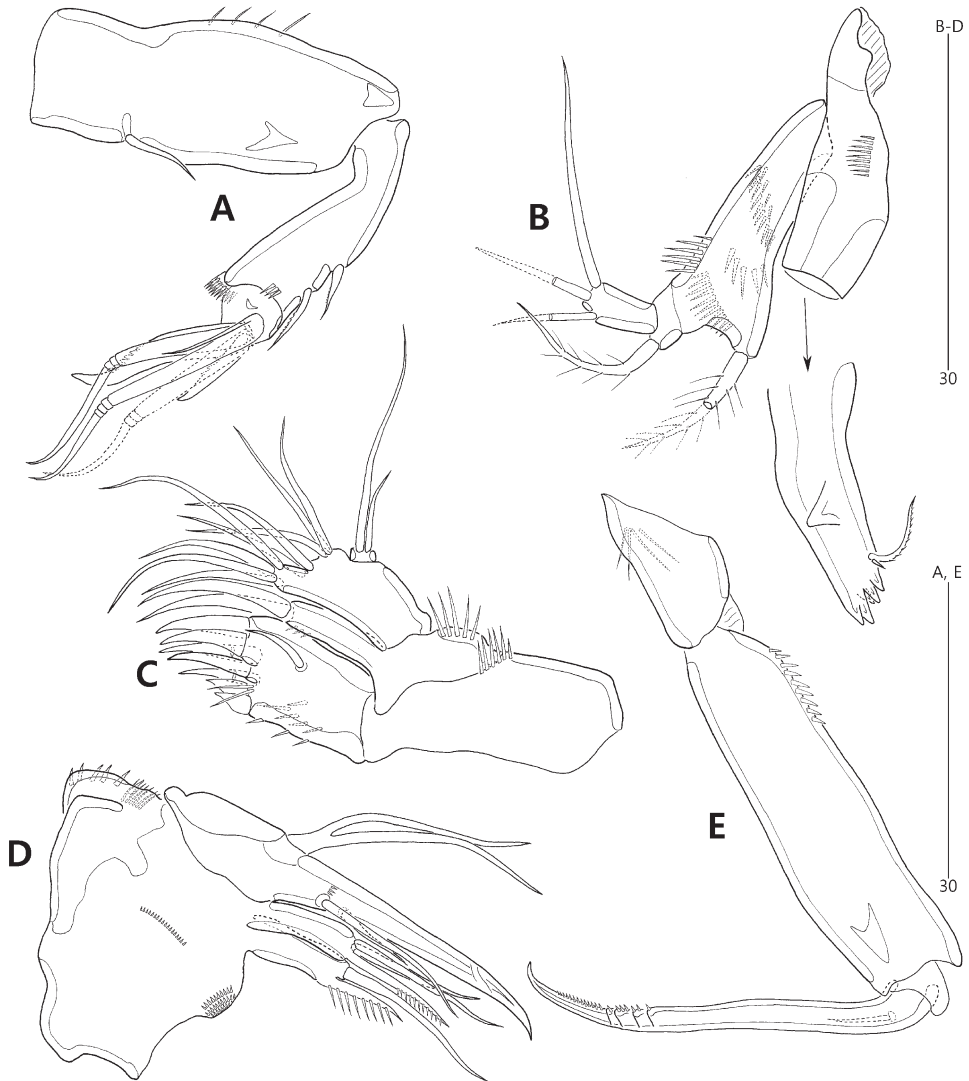


Figure 5. *Concilicoxa hispida* gen. et sp. nov., female holotype. **A** antenna (lacking coxa) **B** mandible **C** maxillule **D** maxilla **E** maxilliped.

seta naked, arising anteriorly, with 1 group of small spinules at its base. Exopod 2-segmented, short, about 0.3 times as long as enp-1; exp-1 with 1 naked outer seta and 1 row of stout outer spinules; exp-2 with 1 small naked seta and 1 stout unispinulose seta on outer margin and 1 short naked and 1 long geniculate seta on distal margin; anterior surface with 1 small pore. Endopod prehensile, 2-segmented; enp-1 elongate, 3.7 times as long as largest width, ornamented with 1 row of small spinules along outer margin and few long inner spinules; enp-2 short, slightly longer than wide, ornamented with few inner spinules and armed with 1 stout, recurved

distal claw and 1 long flexible outer seta, of which distal half with very thin cuticular inner lines.

P2–P4 (Figs 7A–F, 8B, C). Protopods composed of praecoxa, coxa and basis. Praecoxae small, ornamented with 2 rows of spinules. Intercoxal sclerites large, broad, separate in P2, fused to coxae laterally in P3 and P4 (see arrowheads in Fig. 8B, C). Coxae wide, with 1, 3 and 2 groups of spinules on anterior surface in P2–P4, respectively; outer margin drawn out into an elongate and coarsely-serrated projection. Bases wide, with 1 pore on anterior surface; outer setophore elongate, ornamented with 1 row of spinules basally, non-articulated in P2 with 1 plumose seta, bi-articulated in P3 and P4, with 1 naked seta; inner distal corner (near base of inner ramus) with 1 group of spinules. Exopod 1-segmented, ornamented with rows of spinules along outer and distal margins; with 4 stout outer spines, of which proximal one uniserrate and ornamented with 2 rows of setules, others pinnate; distal outer spines of P4 strongly pinnate. Endopod absent in P2, represented by 1 small unarmed protuberance in P3 and 1-segmented, ornamented with distal spinules and armed with 1 stout pinnate distal spine in P4.

P5 (Fig. 6B). Baseoendopod broad, with 1 anterior pore, ornamented with rows of spinules along distal and inner margins; endopodal lobe weak, with 1 plumose distal seta; outer setophore articulate, with 1 long naked seta. Exopod small, with 3 pinnate setae and 1 naked seta.

Male (allotype MInRB-Hr59-S002). Total body length slightly shorter than in female, 525 μm (measurement based on allotype and 4 paratypes: range = 485–556 μm ; mean = 512 μm , $n = 5$); body (Fig. 2D) slightly more slender than in female, maximum width 74 μm measured at the middle of cephalothorax; urosome 6-segmented, comprising P5-bearing somite, genital somite, 3 abdominal somites and anal somite; penultimate somite slightly shorter than its width, without lateral ornamentation. Caudal rami (Figs 2D, 3E) parallel, rectangular, more slender than in female; inner margin straight, outer margin slightly convex; outer margins unornamented, with clear cuticular inner line; additional large pore present on ventral surface; seta III issuing from subdistal lateral margin ventrally; set of setae I and II issuing from proximal third of outer margin; seta V slightly shorter than urosome (Fig. 2D).

Antennule (Fig. 4B) chirocerate, 5-segmented. First segment elongate, with 1 short naked seta subdistally; inner margin with few small spinules; outer margin convex, with 1 row of minute spinules. Second segment slightly longer than wide, with 2 bi-articulate and 7 naked setae and 1 minute protuberance. Third segment partially separated into two parts; proximal one with 2 bi-articulate and 6 naked setae; distal part with 2 setae. Fourth segment swollen, with 1 medial protuberance, 4 naked surface setae and 3 well-developed posterior peduncles: one proximal and one medial peduncle with 1 long naked apical seta each; subdistal peduncle with 1 long naked seta fused to 1 long ae basally. Distal segment elongate, slightly recurved distally, hook-shaped, with 2 naked and 6 bi-articulate setae laterally, 1 long naked seta distally and 1 acrothek composed of 1 ae and 2 naked setae fused basally. Setal armature as follows: 1-[1], 2-[9], 3-[10], 4-[6 + (1 + ae)], 5-[10 + acrothek].

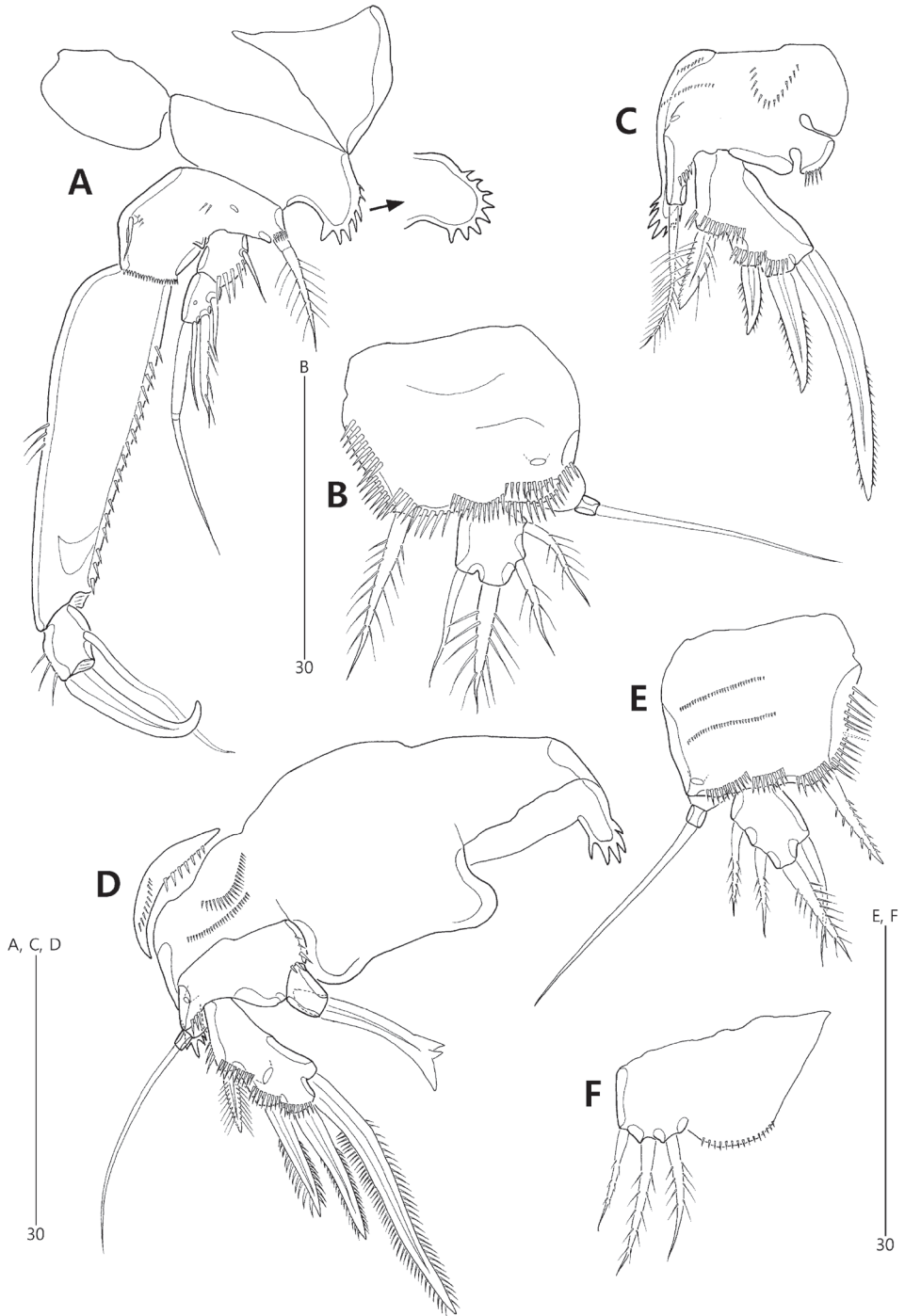


Figure 6. *Concilicoxa hispida* gen. et sp. nov., female holotype (**A–B**) **A** P1, anterior **B** P5, anterior. Female paratype (**C**) **C** abnormality of P2, anterior. Male allotype (**D–F**) **D** P3, anterior **E** P5, anterior **F** P6, anterior.

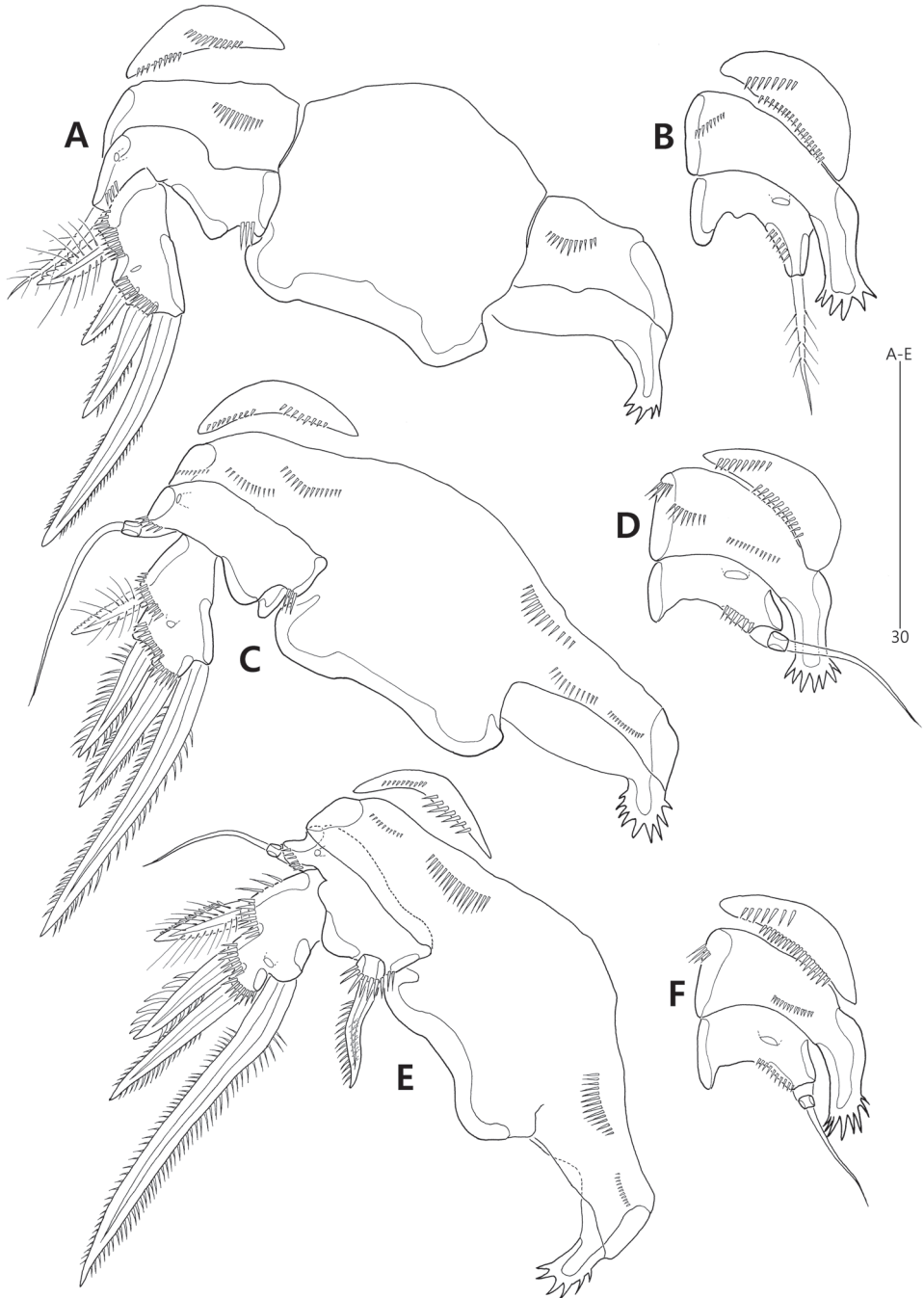


Figure 7. *Concilicoxa hispida* gen. et sp. nov., female holotype **A** P2, anterior **B** protopod of P2, lateral **C** P3, anterior **D** protopod of P3, lateral **E** P4, anterior **F** protopod of P4, lateral.

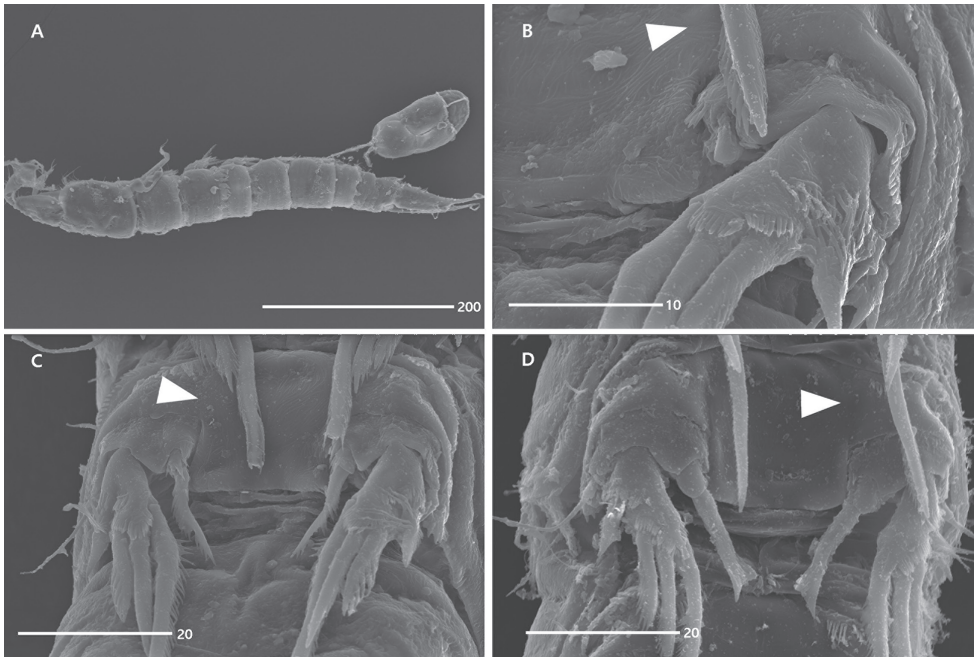


Figure 8. *Concilicoxa hispida* gen. et sp. nov., scanning electron micrograph, female (**A–C**) **A** habitus, lateral **B** P3, anterior **C** P4, anterior. Male (**D**) **D** P3, anterior. Arrowheads indicate fusion of coxa and intercoxal sclerite.

P3 (Fig. 6D) as in female, except for 1-segmented endopod with 1 stout distal spine bearing 2 pointed lateral processes.

P5 (Figs 3E, 6E) as in female except for anterior ornamentation with 2 rows of minute spinules.

P6 (Figs 3E, 6F) asymmetrical (one side completely fused to genital somite basally, other side articulated at base), each represented by a plate bearing 3 plumose setae and 1 row of minute spinules distally on inner extension.

Spermatophore as long as 4/5 length of P5-bearing and genital somites combined (Figs 2D, 3E).

Etymology. The species epithet “*hispida*” is derived from the Latin adjective *hispidus*, which means ‘hairy’ and refers to the setulose lateral ornamentation of the anal somite and caudal rami in the female. It is a noun in the feminine singular.

Variability and abnormality. The investigated individuals of *Concilicoxa hispida* gen. et sp. nov. show intraspecific differences in appendage ornamentation. Dense spinular ornamentation was observed on the mandibular basis in one female paratype (MInRB-Hr-59-S003). This paratype also displays fusion of the coxa and basis of the P2 symmetrically (Fig. 6C).

Remarks. George (2002) established the genus *Laophontisochra* to accommodate *L. maryamae* from the Patagonian continental slope (Chile) and *Laophontisochra* sp. from the Magellan Straits (Chile). He allocated this genus into the family Cristacoxidae Huys, 1990, based on the presence of an outward growth on the coxa of P1, an enlarged maxilliped and atrophy of the antennary exopod and abexopodal seta despite the discrepancies with the following characters of the family Cristacoxidae, which were defined by Huys (1990): the first antennular segment with an outer spinous process, the absence of the exopod and an abexopodal seta in the antenna, the presence of modified seta on the middle endite of maxillary syncoxa and the single plate P5 with the same setae/spines in both sexes, which is considered as a neotenous origin. George (2002) suggested that the Cristacoxidae could be divided into two lineages: a plesiomorphic group comprising only *Laophontisochra* and a derived group composed of *Noodtorthopsyllus* Lang, 1965, *Cubanocleta* Petkovski, 1977 and *Cristacoxa* Huys, 1990 [the latter was considered as a junior synonym of *Noodtorthopsyllus* by Huys and Kihara (2010)]. However, Huys and Kihara (2010) transferred the genus *Laophontisochra* to the family Nannopodidae, based on a re-evaluation of the three fundamental morphological differences between the two groups suggested by George, with their newly-erected genus *Acuticoxa* within the family Nannopodidae for *Laophontisochra* sp. *sensu* George, 2002 (= *A. biarticulata* Huys & Kihara, 2010) and *A. ubatubaensis* Huys & Kihara, 2010 from the Brazilian coast. They assumed that both genera differ from the Cristacoxidae with the following evidence: (1) P1 coxa with a pair of serrated cristae (outer projections) in *Noodtorthopsyllus* and *Cubanocleta* vs. a single non-serrate, lobate or spinulose outgrowth in *Laophontisochra* and *Acuticoxa*; (2) maxillipedal endopod represented by a geniculated claw in *Laophontisochra* and *Acuticoxa* vs. non-geniculated in *Noodtorthopsyllus* and *Cubanocleta*; (3) antennary exopod consistently absent in *Noodtorthopsyllus* and *Cubanocleta* vs. atrophied in *Laophontisochra* and *Acuticoxa* (see Huys and Kihara 2010: 34). In addition, Huys and Kihara (2010) suggested that *Laophontisochra* and *Acuticoxa* are more closely related to both *Huntemannia* and *Rosacletodes* than to the cristacoxid genera, in that they share the presence of a coxal projection on the P1–P4 (vs. the plesiomorphic state of this character expressed in *Laophontisochra*, which lacks the coxal processes in the P2–P4). Corgosinho (2012) created the genus *Talpacoxa*, which was first mentioned as “Genus X” by Huys and Kihara (2010) and revealed close relationships amongst the genera of the nannopodid clade—*Huntemannia*, *Rosacletodes*, *Laophontisochra*, *Acuticoxa* and *Talpacoxa*—supported by three synapomorphies that are likely morphological adaptations to a burrowing lifestyle: (1) P1 coxa with an outer projection; (2) the P2–P4 exopods one- or two-segmented; and (3) the P2–P4 endopods one-segmented or vestigial.

The new genus *Concilicoxa* gen. nov. is assigned to the Nannopodidae because, as a member of the nannopodid clade, it exhibits the burrowing adaptation of the thoracopods. *Concilicoxa* gen. nov. appears to be closely related to both *Laophontisochra* and *Acuticoxa* in that they share four-segmented female antennules with elongate first segments, the prehensile P1 endopod, the presence of coxal outer projection on the P1, large and broad intercoxal sclerites on the P2–P4, the general shape of the female geni-

tal field (with a large copulatory pore and a well-developed operculum derived from P6) and elongate caudal rami. However, the novel genus is easily distinguishable from *Laophontisochra* by the distal armature of the antennary endopod with three geniculate and three non-geniculate elements (vs. four geniculate and two non-geniculate elements in *Laophontisochra*), the presence of coxal outer projections in the P2–P4 (vs. absent in *Laophontisochra*) and one-segmented exopods in the P2–P4 (vs. two-segmented in *Laophontisochra*). The new genus is also different from *Acuticoxa* in the absence of the P2 endopod (vs. one-segmented in *Acuticoxa*), a serrate coxal outer projection in the P1–P4 (vs. acute in *Acuticoxa*) and the female P5 exopod and baseendopod separate (vs. fused into a single plate in *Acuticoxa*).

In contrast to a close resemblance with both genera in habitus and thoracopod morphology, *Concilicoxa* gen. nov. displays unambiguous autapomorphies that require the formation of a new genus: (1) the loss of the mandibular exopod, as observed in *Huntemannia*, is more derived than the exopod represented by a single seta; (2) the mandibular endopod is two-segmented, which seems to be secondarily divided, comparing to other related genera with only one-segmented endopod; (3) the P1 exp-2 comprises a total of only four elements, but five or six setae in *Laophontisochra* and *Acuticoxa*, respectively (in the original description of *L. terueae*, this segment was described as having one lateral and three terminal setae, but was depicted as having three outer and three terminal elements; see Björnberg 2014: fig. 11A); and (4) the intercoxal sclerites of P3 and P4 are laterally fused with the coxae in *Concilicoxa* gen. nov. (Figs 6D, 7C, E, 8B–D), but this fusion has rarely been reported in harpacticoid copepods (i.e. *Orthopsyllus* sp. of the family Orthopsyllidae Huys, 1990; cf. Huys and Boxshall 1991). By contrast, the presence of the maxillular exopod, as observed in *Talpacoixa* demonstrates a more plesiomorphic state than the lack of endopod.

The males of *Concilicoxa* gen. nov. exhibit distinctive potential autapomorphies for the genus as follows: (1) the P3 endopod has a sexual dimorphic distal element that is a robust spine; (2) the shape of P5 is nearly similar to that of the female; and (3) the caudal rami show sexual dimorphisms in the length of caudal seta V, the issuing position of setae I and II and the number of tube pores. However, we could not compare these characters with other related genera, because males of *L. maryamae* and *A. ubatubaensis* remain unknown. The sexual dimorphism of thoracopods is one of the most robust characters used to assess the phylogenetic relationships between genera and between families because it facilitates comparison of the positions of homologue elements (such as setae or apophyses) of rami in females and males (Huys 1990; Huys and Kihara 2010). In this nannopodid clade, the known males tend to exhibit differences in morphology of the P3 endopod: (1) the male of *Rosacletodes* has a two-segmented P3 endopod with an elongate inner apophysis on enp-2, instead of a single seta as in the female (Pallares 1982); (2) all known males of the species of *Huntemannia* have an additional armature element on the P3 endopod, with no differences in segmentation as in *Nannopus* and *Pontopolites* (Song et al. 2007; Karanovic and Cho 2018); (3) the male of *T. brandini* exhibits a distal small apophysis on the one-segmented P3 endopod; and (4) although the male of *L. maryamae* has yet to be discovered, there

is no sexual dimorphism on the P3 in *L. terueae*, whose taxonomic position seems to be problematic (see below). The male P3 endopod of the new genus presented herein is one-segmented with a stout spine (Figs 6D, 8D), whereas the female P3 endopod is represented by an unarmed protrusion. Such diverse sexual dimorphism of the P3 endopod prevents deeper insight into the systematic position of this clade within the Nannopodidae. We hypothesise that the lack of original outer element on the female P3 endopod in *L. maryamae* and *C. hispida* gen. et sp. nov. leads to the absence of the sexual dimorphic apophysis in the male. In contrast, the presence of a small apophysis on the corresponding ramus in *T. brandini* seems to be derived from a rudimental apical seta in the female.

Harpacticoids generally display sexual dimorphism in the size, shape and setae of the male P5. However, no sexual dimorphism has been observed in the male P5 of Arenopontiidae Martínez Arbizu & Moura, 1994 (Martínez Arbizu and Moura 1994). Additionally, both sexes bear the same number of setae/spines on the P5 of some taxa, such as Metidae Boeck, 1873, Rotundiclipeidae Huys, 1988, Ectinosomatidae Sars, 1903 and Cristacoxidae Huys, 1990 (Huys 1988; Fiers 1992; Clément and Moore 1995; Huys and Kihara 2010). Except for Ectinosomatidae, the P5 of these families is remarkably reduced or represented by a single plate in both sexes. Although this sexual dimorphism is observed in other nannopodid genera, the structure of this leg in our new taxon is very similar in both sexes, except for micro-ornamentation, such as cuticular spinules and pores (Fig. 6B, E). In addition, the male of *Concilicoxa* gen. nov. expresses rare sexual dimorphisms in the shape of the caudal rami (oval in the female, but rectangular in the male), the length of caudal seta V (slightly longer than the caudal ramus in the female, but slightly shorter than the urosome in the male), the number of pores on the surface (one pore in the female vs. two pores in the male) and the lateral ornamentation (the presence of a row of long setules proximally in the female vs. absent in the male). These sexual dimorphisms could support the erection of a new genus *Concilicoxa* gen. nov.

Discussion

Taxonomic position of *Laophontisochra terueae* Björnberg, 2014

Björnberg (2014) described the second species of *Laophontisochra* (*L. terueae*) from the south-eastern coast of Brazil, but provided insufficient description and illustrations. She argued that *L. terueae* fits the generic diagnosis of the genus as amended by Huys and Kihara (2010), despite obvious differences in the presence of endopods in P2 and P3 and in the structure of the female P5. Huys and Kihara (2010) suggested that two species of *Acuticoxa*, *A. biarticulata* and *A. ubatubaensis*, share five synapomorphies: (1) body somites with dense setular surface ornamentation; (2) distal armature of antennary endopod composed of three geniculate and three non-geniculate elements; (3) P2–P4 coxae with outer spinous process; (4) P4 exopod one-segmented; and (5) female

P5 exopod and baseoendopod fused into a single plate, with eight elements in total. *Laophontisochra terueae* expresses these characters except for character 3, i.e. the outer spinous process on the coxae of P2–P4 is absent in *L. terueae*. Based on the absence of this character alone, Björnberg (2014) assigned this species, not to *Acuticoxa*, but to *Laophontisochra*. This species also shares the biarticulated condition of the caudal seta V comprising swollen proximal part and setular distal part with all *Acuticoxa* species (cf. Huys and Kihara 2010), indicating a probable close affinity between these taxa. Thus, we propose to tentatively re-allocate *L. terueae* into *Acuticoxa* as *A. terueae* (Björnberg, 2014) comb. nov.

Relationships amongst clade members with coxal outer projections on the thoracopods

The monophyly of the family Nannopodidae has been questioned by several researchers (e.g. Boxshall and Halsey 2004; Kihara and Huys 2009; Huys and Kihara 2010; Karanovic and Cho 2018). Por (1986) proposed the family Huntemanniidae and presented a brief diagnosis combining *Metahuntemania*, *Huntemania*, *Beckeria*, *Nannopus*, *Pontopolites* and *Pseudocletodes*, being unaware of the previous composition of Nannopodidae, which included *Nannopus*. Huys (2009) thereafter synonymised Huntemanniidae with Nannopodidae. Although the taxonomy, conceptualised by Por's (1986), remains available for nannopodid copepods (Huys and Kihara 2010), this old familial diagnosis cannot satisfactorily accommodate the morphological range of nannopodid copepods because it is neither specific nor accurate. Since Por's (1986) proposal, some nannopodid genera have been included and some excluded (see Dahms and Pottek 1992; Huys et al. 1996; Kihara and Huys 2009; Huys and Kihara 2010; Corgosinho 2012). Only three genera, *Huntemania*, *Nannopus* and *Pontopolites* have remained in the family Nannopodidae, amongst which the genus *Pontopolites* remains questionable in that it differs from the familial diagnosis in having two-segmented antennary exopods and a natatorial P1 exopod. Based on its affinity with *Huntemania*, which shares the presence of coxal processes on the P1, Huys and Kihara (2010) and Corgosinho (2012) included four genera, *Rosacletodes*, *Laophontisochra*, *Acuticoxa* and *Talpacoxa* in this family; however, both *Laophontisochra* and *Acuticoxa* show significant deviations from Por's (1986) diagnosis, including female antennules with four segments, prehensile P1 and elongate caudal rami. These deviations imply that either the familial diagnosis should be extended or the phylogenetic relationship of the family members should be re-assessed.

Corgosinho (2012) suggested that *Huntemania*, *Rosacletodes*, *Laophontisochra*, *Acuticoxa* and *Talpacoxa* form a clade within the family Nannopodidae; this relationship is supported by the presence of an outer coxal projection on the P1 and reduced P2–P4. However, there are morphological differences in the rostrum, male antennules, antennary endopod and exopod, both rami of the P1 and sexual dimorphism in the P3. It raises questions about the validity of this relationship amongst the five genera. George (2002) suggested that *L. maryamae* and *A. biarticulata* belong to a plesiomor-

phic lineage of the family Cristacoxidae. This argument was subsequently rejected by Huys and Kihara (2010) who provided contrary evidence showing a close relationship between *L. maryamae* and *A. biarticulata* and the nannopodid genus *Huntemannia*, rather than between those two species and any cristacoxid genera. These authors suggested that the presence of coxal projections on the P1–P4 is a significant synapomorphy between *Huntemannia* and *Laophontisochra*. However, a closer relationship between *Huntemannia* and *Nannopus* is evident. These two genera share the presence of anterior setules on the rostrum, the absence of geniculate distal elements on the antennary endopod, the uniramous mandibular palp, the non-prehensile P1 endopod, the short caudal rami and the shape of the sexually-dimorphic male P3. Karanovic and Cho (2018) noted that some species of both genera show different endopodal complements on the P3 between females and males, without any differences in segmentation. By contrast, the species of *Nannopus* display certain primitive characters, such as the presence of two abexopodal setae on the antennary allobasis (e.g. Fiers and Kotwicki 2013; Kim et al. 2017; Vakati and Lee 2017).

As reported by Huys and Kihara (2010), the prehensile P1 endopod is a significant synapomorphy for *Laophontisochra* and *Acuticoxa*. The new nannopodid genus, *Concilicoxa* gen. nov., described from the Yellow Sea of South Korea, also shares this character, as well as additional synapomorphies that provide evidence of affinity amongst these three genera: (1) the four-segmented female antennule and its elongate first segment (vs. five-segmented in other congeners); (2) antennary exopod and abexopodal seta rudimentary or missing (vs. a one-segmented exopod and presence of a developed abexopodal seta in other congeners); (3) the enlarged maxilliped with a geniculate claw-like endopod (vs. non-geniculate endopod in other congeners); (4) both coxae of the P2–P4 are connected by a large, broad intercoxal sclerite (vs. a small and narrow plate in other congeners); and (5) the female genital complex with a typical structure comprising a large copulatory pore and reverse ‘V’- or ‘U’-shaped genital slit (vs. small copulatory pore and transverse genital slit in other congeners).

Although the male of *Laophontisochra* remains unknown, a derived condition may be expressed in the male antennules—with a single compound segment distal to geniculation in *A. terueae* comb. nov. and *C. hispida* gen. et sp. nov. The male antennule of *T. brandini* possesses two segments distal to geniculation and the male antennule of *R. kuehnemanni* (Pallares, 1982) remains undescribed.

Huys and Kihara (2010) assumed that the P1 endopods in *Rosacletodes* and *Talpacoxa* are structurally identical with those of *Laophontisochra* and *Acuticoxa* in the segmentation and setal armature, even though there is a remarkable difference in the length of the first endopodal segment. However, a fundamental difference in exopods of *Rosacletodes* and *Talpacoxa* from those of *Laophontisochra* and *Acuticoxa*, as well as *Concilicoxa* gen. nov., is also readily recognised: the exopodal elements on the P1 are strong and enlarged in *Rosacletodes* and *Talpacoxa*, except for a single delicate one, but *Laophontisochra*, *Acuticoxa* and *Concilicoxa* gen. nov. have setiform or geniculate elements instead. Except for *A. ubatubaensis*, the setal pattern of the P1 exp-2 is identical

in *Laophontisochra*, *Acuticoxa* and *Concilicoxa* gen. nov., with one to three small outer setae, one stout and uniplumose outer seta, one delicate distal seta and one geniculate distal seta.

Given these characteristics, the clade with outer coxal projections on the P1–P4 can be subdivided into three groups: (1) *Huntemannia*, which is characterised by the presence of a setular group on the rostrum, a five-segmented female antennule, the absence of geniculate setae on the distal armature of the antennary endopod, a one-segmented antennary exopod with four setae, a one-segmented mandibular palp, non-prehensile P1 endopod, sexual dimorphism expressed in the number of elements on the distal segment of the male P3 endopod; (2) *Rosacletodes* and *Talpacoxa*, which are characterised by the absence of a setular group on the rostrum, a five-segmented female antennule, the presence of geniculate setae on the distal armature of the antennary endopod, a one-segmented antennary exopod with three setae, a two-segmented mandibular palp, prehensile short P1 endopod, P1 exopod with stout spines and presence of a sexually-dimorphic apophysis on the distal endopodal segment of the male P3; and (3) *Laophontisochra*, *Acuticoxa* and *Concilicoxa* gen. nov., which are characterised by the absence of a setular group on the rostrum, a four-segmented female antennule with elongation of the first segment, the presence of geniculate setae on the distal armature of the antennary endopod, the atrophied condition of the antennary exopod (represented by a single seta or absent), a two-segmented mandibular endopod, prehensile long P1 endopod, setiform elements on the P1 exopod and absence of sexual dimorphism in the male P3 (*A. terueae* comb. nov.) or development of a stout spine in the male P3 endopod (*C. hispida* gen. et sp. nov.) (Table 1).

Corgosinho (2012) suggested that the development of the coxal outer process and the reduction of both rami in P2–P4, along with the strengthening of the outer exopodal elements in *Huntemannia*, *Rosacletodes*, *Laophontisochra*, *Acuticoxa* and *Talpacoxa* are the results of adaptation to a burrowing interstitial lifestyle. He also suggested that the burrowing ability of *Talpacoxa* was conferred by the remarkably-developed process of the P1 coxa and both compact and well-ornamented rami of the P1. It is likely that the specialised morphology of the intercoxal sclerite of P1, which is broad, elongate and bearing a transversal groove, can facilitate the burrowing activity (Corgosinho 2012: figs 4A, 6A). However, the morphology of the P2–P4 is relatively unsuitable for burrowing activity due to its weak outer elements and absence of the intercoxal sclerite. By contrast, three genera, *Laophontisochra*, *Acuticoxa* and *Concilicoxa* gen. nov., exhibit prehensile P1 endopods, with a small coxal projection, which is distinctly smaller than coxa, does not seem designed for burrowing. Instead, these three genera may have acquired a burrowing lifestyle by the development of stout and well-developed exopodal elements and large, broad intercoxal sclerites in P2–P4. Our comparison of the detailed morphology of thoracopods indicates that the P1 may play a role in the burrowing activity in *Talpacoxa*, whereas the P2–P4 confers this ability in *Laophontisochra*, *Acuticoxa* and *Concilicoxa* gen. nov. This hypothesis supports the subdivision of the nannopodid clade into three groups.

Table 1. Comparison of morphological characters among nannopodid copepods with modified thoracopods for burrowing ability (female only).

	A1		A2		Md		Mxl		P1		P2		P3		P4		P5		References				
	seg	exp	seg	exp	seg	exp	seg	exp	exp	enp	exp	enp	exp	enp	exp	enp	exp	enp					
<i>Hantemannahia</i>																							
<i>H. jaldensis</i>	5	1/4	ab	fu/2	re/2	0.0.022	0.023	0.023	0.023	0.023	0.023	0.023	0.023	0.023	0.023	0.123	0.10	0.123	0.10	4–5	4	Sars 1909; Kornev and Chertoprud 2008	
<i>H. micropus</i>	5	1/4	uk	uk	uk	0.023	0.021	0.021	0.021	0.021	0.021	0.021	0.021	0.021	0.021	0.022	0.10	0.022	0.10	4	4	Monard 1935	
<i>H. lacustris</i>	uk	uk	uk	uk	uk	2–3 seg ¹	0.5 [*]	1(2) [*]	0.5(6) [*]	1(2) [*]	0.6 [*]	1 [*]	5	4	4	4	4	4	4	4	4	Wilson 1958	
<i>H. biarticulatus</i>	5	1/4	uk	uk	uk	0.0.023	0.022	0.022	0.022	0.022	0.022	0.022	0.022	0.022	0.022	0.10	0.222	0.10	0.222	0.10	5	4	Shen and Tai 1973
<i>H. dobooni</i>	5	1/4	ab	fu/2	re/1	0.0.022	0.20	0.20 ²	0.10	0.11 ²	0.10	0.11 ²	0.10	0.11 ²	0.10	0.11 ²	0.10	0.11 ²	0.10	5	4	Song et al. 2007	
<i>Rosactetodes</i>																							
<i>R. kuehneimanni</i>	6	1/3	fu/1	1/3	1/2	0.021	0.020	0.022	0.10	1.21	0.10	1.21	0.10	1.21	0.10	1.21	0.10	1.21	0.10	5	6	Pallares 1982	
<i>Laophonitsochbra</i>																							
<i>L. maryanae</i>	4	re/1	re/1	1/3	ab	0.023	0.011	0.022	ab	0.022	ab	0.022	ab	0.022	0.10	0.4	1	1	1	1	1	George 2002	
<i>Acuticoxa</i>																							
<i>A. biarticulata</i>	4	1/1	uk	uk	uk	0.023	0.011	0.022	0.10	0.022	0.10	0.022	0.10	0.022	0.10	1.22	0.10	1.22	0.10	4	3	George 2002	
<i>A. abatanbaensis</i>	4	ab	re/1	1/3	ab	0.023	0.011	0.23	0.10	0.23	0.10	0.23	0.10	0.23	0.10	0.23	0.10	0.23	0.10	4	2	Huys and Kihara 2010	
<i>A. revueae</i> comb. nov.	4	ab ³	re/2	1/2 ³	ab	0.033 ⁴	0.020	0.011(2)	0.10	0.022	0.10	0.022	0.10	0.022 ⁵	0.10	0.4	3	3	3	3	3	Björnberg 2014	
<i>Talpacoxa</i>																							
<i>T. brandini</i>	5	1/3	1/1	1/3	1/2	0.23	0.020	0.020	0.10	0.121	0.10	0.121	0.10	0.121	0.10	0.121	0.10	0.121	0.10	5	3	Corgosinho 2012	
<i>Conciliocoxa</i> gen. nov.																							
<i>C. hispida</i> gen. et sp. nov.	4	re/1	ab	2/1.3	1/2	0.022	0.011	0.22	ab	1.12	0.00	1.12	0.00	1.12	0.10	0.4	1	1	1	1	1	the present study	

Abbreviations: A1, antennule; A2, antenna; ab, absent; enp, endopod; exp, exopod; fu, fused to basis, Md, mandible; Mxl, maxillule; re, endopod or exopod represented by setae; seg, segmentation; uk, unknown.

¹Total number of setae.

²The original description by Wilson (1958) provided only its segmentation.

³Exopods of the P2–P4 are one-segmented, but with a vestigial suture line between the two segments.

⁴Segmentation and armature of the male antenna and mandible were referred because those of females were damaged.

⁵Björnberg (2014) described the exopod bearing one seta on the first segment, and one lateral and three terminal setae on the second segment. However, the illustration of Björnberg (2014, fig. 11A) indicates an armature of 0.033.

⁶The male has a one-segmented exopod.

Acknowledgements

The authors thank Prof. Rony Huys (the National History Museum, London) for his great help in early identification and useful comments. We also gratefully thank Prof. S. Gómez and two anonymous reviewers for their critical and valuable advice to improve our initial manuscript. This research was supported by the Basic Science Research Program through the National Research Foundation of Korea (NRF) funded by the Ministry of Education (2018R1A6A3A01012703) to JG Kim and by the Marine Biotechnology Program of the Korea Institute of Marine Science and Technology Promotion (KIMST) funded by the Ministry of Oceans and Fisheries (MOF) (No. 20170431). This work was also conducted with the support offered through the research programme of KIOST (Contract No. PE99813).

References

- Björnberg T (2014) Three new species of benthonic Harpacticoida (Copepoda, Crustacea) from São Sebastião Channel. *Nauplius* 22: 75–90. <https://doi.org/10.1590/S0104-64972014000-200002>
- Boxshall GA, Halsey SH (2004) *An Introduction to Copepod Diversity*. The Ray Society, London, 966 pp.
- Brady GS (1880) *A Monograph of the Free and Semi-parasitic Copepoda of the British Islands*. The Ray Society, London, 182 pp.
- Clément M, Moore CG (1995) A revision of the genus *Halectinosoma* (Harpacticoida, Ectinosomatidae): a reappraisal of *H. sarsi* (Boeck) and related species. *Zoological Journal of the Linnean Society* 114: 247–306. <https://doi.org/10.1111/j.1096-3642.1995.tb00118.x>
- Corgosinho PHC (2012) *Talpacoxa brandini* gen. et sp. nov. a new Nannopodidae Brady, 1880 (Copepoda: Harpacticoida) from submersed sands of Pontal do Sul (Paraná, Brazil). *Journal of Natural History* 46: 2865–2879. <https://doi.org/10.1080/00222933.2012.725138>
- Dahms HU, Pottek M (1992) *Metahuntemannia* Smirnov, 1946 and *Talpina* gen. nov. (Copepoda, Harpacticoida) from the deep-sea of the high Antarctic Weddell-Sea with a description of eight new species. *Microfauna Marina* 7: 7–78.
- Fiers F (1992) *Metis reducta* n. sp. and *Laubiera tercera* n. sp. (Harpacticoida, Metidae) from the southern coast of Papua New Guinea. *Belgian Journal of Zoology* 122: 37–51.
- George KH (2002) New phylogenetic aspects of the Cristacoxidae Huys (Copepoda, Harpacticoida), including the description of a new genus from the Magellan region. *Vie et Milieu* 52: 31–41.
- Hagenow F von (1840) *Monographie der Rügen'schen Kreide-Versteinerungen, II. Abtheilung: Radiarien und Annulaten, nebst Nachträgen zur ersten Abtheilung*. *Neues Jahrbuch für Mineralogie, Geognosie, Geologie und Petrefakten-Kunde*, 1840: 631–672.
- Humes AG, Gooding RU (1964) A method for studying the external anatomy of copepods. *Crustaceana* 6: 238–240. <https://doi.org/10.1163/156854064X00650>

- Huys R (1988) Rotundiclepidae fam. nov. (Copepoda, Harpacticoida) from an anchihaline cave on Tenerife, Canary Islands. *Stygologia* 4: 42–63.
- Huys R (1990) A new family of harpacticoid copepods and an analysis of the phylogenetic relationships within the Laophontoidea Scott, T. *Bijdragen tot de Dierkunde* 60: 79–120. <https://doi.org/10.1163/26660644-06002002>
- Huys R (2009) Unresolved cases of type fixation, synonymy and homonymy in harpacticoid copepod nomenclature (Crustacea: Copepoda). *Zootaxa* 2183: 1–99. <https://doi.org/10.11646/zootaxa.2183.1.1>
- Huys R, Boxshall GA (1991) *Copepod Evolution*. The Ray Society, London, 468 pp.
- Huys R, Gee JM, Moore CG, Hamond R (1996) *Marine and Brackish Water Harpacticoid Copepods. Part 1. Keys and notes for identification of the species*. Field Studies Council, Shrewsbury, 352 pp.
- Huys R, Kihara TC (2010) Systematics and phylogeny of Cristacoxidae (Copepoda, Harpacticoida): a review. *Zootaxa* 2568: 1–38. <https://doi.org/10.11646/zootaxa.2568.1.1>
- Karanovic T, Cho J-L (2018) Second members of the harpacticoid genera *Pontopolites* and *Pseudoleptomesochra* (Crustacea, Copepoda) are new species from Korean marine interstitial. *Marine Biodiversity* 48: 367–393. <https://doi.org/10.1007/s12526-017-0731-2>
- Kihara TC, Huys R (2009) Contributions to the taxonomy of the Normanellidae (Copepoda, Harpacticoida): description of a new genus from the Brazilian continental shelf and re-assignment of *Pseudocletodes vararensis* Scott & Scott, 1893 (*ex* Nannopodidae). *Zootaxa* 2233: 1–38. <https://doi.org/10.11646/zootaxa.2233.1.1>
- Kim JG, Choi HK, Yoon SM (2017) A reappraisal of the genera *Nannopus* Brady, 1880 and *Ilyophilus* Lilljeborg, 1902 (Copepoda, Harpacticoida, Nannopodidae) with a description of *N. parvipilis* sp. nov. from South Korea. *Crustaceana* 90: 1351–1365. <https://doi.org/10.1163/15685403-00003700>
- Kornev PN, Chertoprud ES (2008) *Harpacticoid Copepods of the White Sea: Morphology, Systematics, Ecology*. KMK Scientific Press Ltd, Moscow, 379 pp. [In Russian]
- Lang K (1936) Die Familie der Cletodidae Sars, 1909. *Zoologische Jahrbücher für Systematik*, 68: 445–480.
- Lee W (2020) *Doolia*, a new genus of Nannopodidae (Crustacea: Copepoda: Harpacticoida) from off Jeju Island, Korea. *Diversity* 12: 3. <https://doi.org/10.3390/d12010003>
- Martínez Arbizu P, Moura G (1994) The phylogenetic position of the Cyliindropsyllinae Sars (Copepoda, Harpacticoida) and the systematic status of the Leptopontiinae Lang. *Zoologische Beiträge, Neue Folge* 35: 55–77.
- Monard A (1935) Étude sur la faune des harpacticoides marins de Roscoff. *Travaux de la Station biologique de Roscoff* 13: 5–88.
- Pallares RE (1982) Copépodos harpacticoides marinos de Tierra del Fuego (Argentina). IV. Bahía Thetis. *Contribuciones Científicas del Centro de Investigación de Biología Marina (CIBIMA)*, Buenos Aires 186: 3–39. [fig. 1, pls. 1–12]
- Por FD (1986) A re-evaluation of the family Cletodidae Sars, Lang (Copepoda, Harpacticoida). In: Schriever G, Schminke HK, Shih C-t (Eds) *Proceedings of the Second International Conference on Copepoda*, Ottawa (Canada), August 1984. National Museums of Canada, Ottawa, *Syllogeus* 58: 420–425.

- Sars GO (1909) Copepoda Harpacticoida. Parts XXVII & XXVIII. Cletodidae (concluded), Anchorabolidae, Cylandropsyllidae, Tachidiidae (part). An account of the Crustacea of Norway, with short descriptions and figures of all the species 5: 305–336. [pls. 209–224]
- Shen CJ, Tai AY (1973) Preliminary analysis of the characteristics of the harpacticoid copepod fauna of China and description of some new species. *Acta Zoologica Sinica* 19: 365–384. [In Chinese with English translation of diagnoses of new taxa]
- Shirayama Y, Kaku T, Higgins RP (1993) Double-sided microscopic observation of meiofauna using an HS-Slide. *Benthos Research* 1993: 41–44. https://doi.org/10.5179/benthos1990.1993.44_41
- Song SJ, Rho HS, Kim W (2007) A new species of *Huntemannia* (Copepoda : Harpacticoid : Huntemanniidae) from the Yellow Sea, Korea. *Zootaxa* 1616: 37–48. <https://doi.org/10.11646/zootaxa.1616.1.3>
- Vakati V, Eyun SI, Lee W (2019) Unraveling the intricate biodiversity of the benthic harpacticoid genus *Nannopus* (Copepoda, Harpacticoida, Nannopodidae) in Korean waters. *Molecular Phylogenetics and Evolution* 130: 366–379. <https://doi.org/10.1016/j.ympev.2018.10.004>
- Vakati V, Lee W (2017) Five new species of the genus *Nannopus* (Copepoda: Harpacticoida: Nannopodidae) from intertidal mudflats of the Korean West Coast (Yellow Sea). *Zootaxa* 4360: 1–66. <https://doi.org/10.11646/zootaxa.4360.1.1>
- Wells JBJ (2007) An annotated checklist and keys to the species of Copepoda Harpacticoida (Crustacea). *Zootaxa* 1568: 1–872. <https://doi.org/10.11646/zootaxa.1568.1.1>
- Wilson MS (1958) North American harpacticoid copepods 4. Diagnoses of new species of freshwater Canthocamptidae and Cletodidae (genus *Huntemannia*). *Proceedings of the Biological Society of Washington* 71: 43–48.

A new wood-inhabiting mite species of the genus *Dendroseius* Karg, 1965 (Acari, Mesostigmata, Rhodacaridae) from Central Europe (Slovakia)

Peter Mašán¹

¹ Institute of Zoology, Slovak Academy of Sciences, Dúbravská cesta 9, 845-06 Bratislava, Slovakia

Corresponding author: Peter Mašán (peter.masan@savba.sk; uzaepema@savba.sk)

Academic editor: F. Faraji | Received 5 August 2020 | Accepted 24 September 2020 | Published 4 November 2020

<http://zoobank.org/5EEF002A-6019-4449-B613-8A20A4F682C1>

Citation: Mašán P (2020) A new wood-inhabiting mite species of the genus *Dendroseius* Karg, 1965 (Acari, Mesostigmata, Rhodacaridae) from Central Europe (Slovakia). ZooKeys 984: 49–57. <https://doi.org/10.3897/zookeys.984.57256>

Abstract

A new rhodacarid mite of the genus *Dendroseius* Karg, 1965, *D. reductus* **sp. nov.**, was described based on females found in wood detritus and under bark of dead and dying poplar trees in a flood-plain forest in South Slovakia. The new species is unusual among the known congeners in the specifically formed triramous epistome of which the central projection is reduced in length, truncate, and markedly shorter than lateral ones. In other congeneric species, the anterior margin of the epistome possesses three pointed projections of similar size. A dichotomous key for identification of females of the world species classified in the genus *Dendroseius* is provided.

Keywords

Description, morphology, poplar tree, saproxylic habitat, systematics

Introduction

Dendroseius was originally described as a subgenus of *Dendrolaelaps* Halbert, 1915 by Karg in 1965, and treated at the generic level by Hirschmann (1974), Lindquist (1975), Evans and Till (1979), Shcherbak (1980), Karg (1993), and other acarologists. The

modern concept of *Dendroseius* is largely based on above cited authors who separated the genus from other “*Dendrolaelaps*-like” genera primarily by the following diagnostic character states: (1) dorsal setae j2 with more posterior position, situated between setae j1 and j3, not in a transverse setal row between j1 and z1; (2) gnathosomal groove on deutosternum with seven transverse furrows of which none is reaching beyond the lateral borders of the groove; (3) movable digit of chelicera with three teeth in addition to the apical hook; (4) straight anterior margin of opisthonotal shield; (5) sperm induction system associated with coxae IV.

Dendroseius is a small group of rhodacarid mites, currently includes only six known species, namely *D. reticulatus* Sheals, 1956 (= *D. scotarius* Sheals, 1958) distributed mainly in Western Europe (with sporadic findings in North Africa and Central Europe), *D. badenhorsti* (Ryke, 1962) from South Africa, *D. gujarati* Wiśniewski & Hirschmann, 1989 from India, *D. congoensis* Wiśniewski & Hirschmann, 1992 from under bark of a tree imported to Poland from Africa, *D. amoliensis* Faraji, Sakenin-Chelav & Karg, 2006 from Iran, and *D. vulgaris* Ma, Ho & Wang, 2014 from China. Further species initially described under the subgeneric name *Dendroseius*, namely *Dendrolaelaps* (*Dendroseius*) *fimetarius* Karg, 1965 distributed in Central Europe, is now regarded as a member of the genus *Oligodentatus* Shcherbak, 1980 (see Shcherbak 1980).

Dendroseius species display a relatively wide spectrum of habitat specialization. Most original descriptions and subsequent reports are based on specimens found in heterogeneous soil detritus (*D. amoliensis*, *D. reticulatus*, *D. vulgaris*), wood substrates (*D. congoensis*, *D. vulgaris*), and manure or cow dung (*D. badenhorsti*, *D. vulgaris*) (Sheals 1956, 1958; Ryke 1962; Wiśniewski and Hirschmann 1992; Karg 1993; Faraji et al. 2006; Ma et al. 2014). Some species may show a phoretic interaction with insects because the deutonymphs of *D. gujarati* was found on an unidentified scarabaeid beetle (Wiśniewski and Hirschmann 1989).

The purpose of this study is to describe a distinct new species of *Dendroseius* from Slovakia contributing thus to knowledge of Rhodacaridae European fauna. Our finding represents also a first record of the genus *Dendroseius* for Slovakia. An introduction of a new key to the identification of the world species based on females is a supplementary aim of this paper.

Materials and methods

The mites were extracted from decomposing wood detritus by means of a modified Berlese-Tullgren funnel equipped with a 40-Watt bulb, and preserved in ethyl alcohol. Some specimens were collected by wet pincette from under loosen bark. Before identification, the mites were mounted onto permanent microscope slides, using Swan's chloral hydrate mounting medium. A Leica DM 1000 light microscope equipped with a Leica EC3 digital camera was used to obtain measurements and photos. Measurements were made from slide-mounted specimens. Lengths of idiosoma and shields

were measured along their midlines, and widths at their widest point (if not otherwise specified in the description), legs I–IV from coxal base but without the pretarsal ambulacrum. Idiosomal setae were measured from the bases of their insertions to their tips. Measurements are mostly presented as ranges (minimum to maximum). The terminology of dorsal and ventral chaetotaxy follows Lindquist and Evans (1965), and that for leg and gnathosomal setae follows that of Evans (1963a, 1963b).

Results

Dendroseius reductus sp. nov.

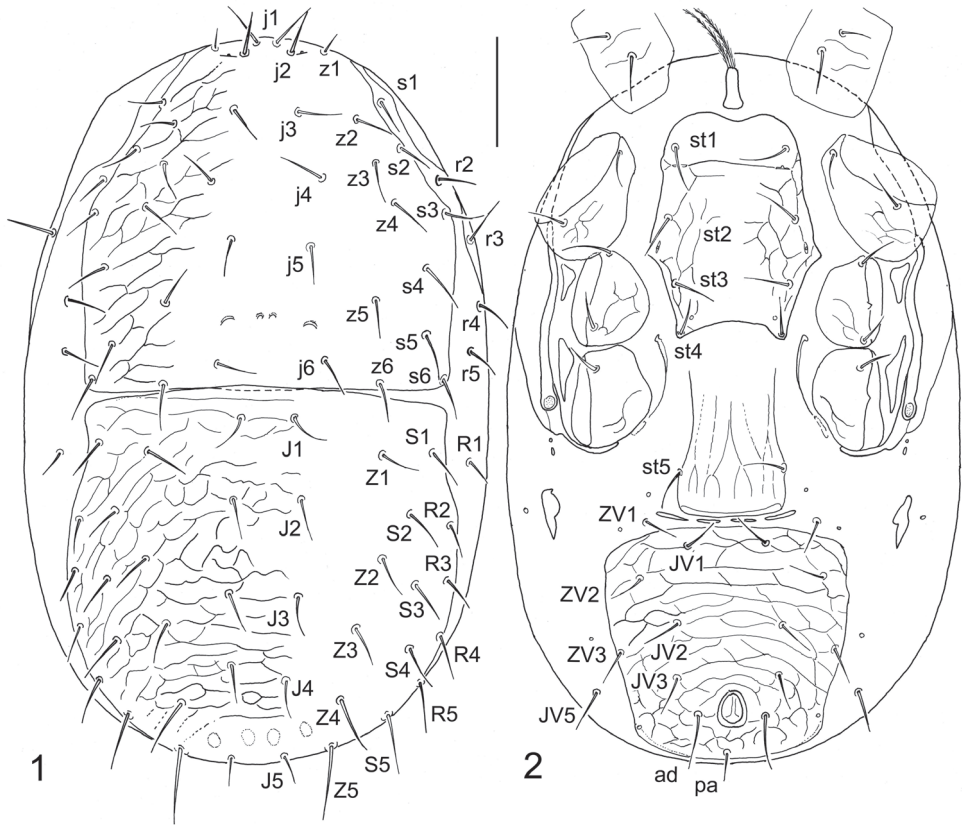
<http://zoobank.org/8C144F00-0FF6-4D7C-84AB-11A865AE85E1>

Figs 1–10

Type material examined. *Holotype* female: SW Slovakia, Podunajská Rovina Flatland, Bratislava Capital, Rusovce Settlement, hard-wood flood-plain forest (*Fraxino-Ulmetum carpinetosum*) with poplar (*Populus* sp.), 135 m a.s.l., March 7, 2020, detritus from a hollow of old and dying poplar tree. *Paratype* females: one specimen, with the same data as for holotype; three specimens, the same locality as in holotype, May 19, 2004, under bark of dead poplar tree. The type material is deposited at the Institute of Zoology, Slovak Academy of Sciences, Bratislava, Slovakia.

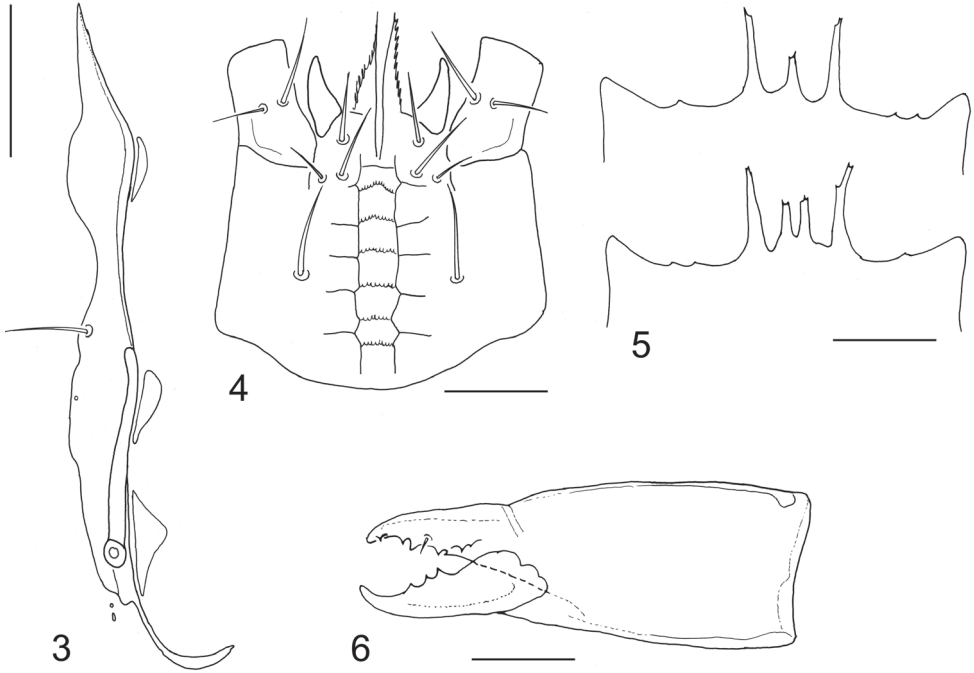
Description (Female). *Dorsal idiosoma* (Figs 1, 7). Idiosoma oblong, regularly oval, widest at medial portion, 315–345 µm long and 195–220 µm wide ($N = 5$). Dorsal shield completely divided to podonotal and opisthonotal parts, not completely covering dorsal surface, exposing narrow strips of lateral soft integument. Podonotal shield 157–170 µm long and 170–175 µm wide, with smooth medial surface, delicate lateral reticulation, 17–18 pairs of setae (j1–j6, z1–z6, s2–s6, s1 symmetrically or asymmetrically situated on the shield and soft integument, respectively), and two pairs of scleronoduli between setae j5 and j6; outer scleronoduli larger and more conspicuous. Marginal setae r2, r4, r5 and R1 inserted in lateral soft integument, apparently outside the dorsal shields, and humeral setae r3 placed on peritrematal shields. Opisthonotal shield 165–180 µm long and 175–190 µm wide, finely reticulate on whole surface, and bearing 19 pairs of setae (J1–J5, Z1–Z5, S1–S5, R2–R5). All dorsal setae smooth and needle-shaped, mostly similar in their lengths; setae z1 shortest (10–11 µm) and Z5 longest (35–40 µm); the lengths of some selected dorsal setae as follows: j1 16–19 µm, j3 21–23 µm, j5 17–21 µm, r5 24–28 µm, J1–J4 and Z1–Z3 18–23 µm, J5 17–19 µm, Z4 25–29 µm, S1–S4 21–25 µm, S5 27–30 µm, R2–R4 18–20 µm.

Ventral idiosoma (Figs 2, 9). Tritosternum with long columnar base and two long and distinctly pilose laciniae. Presternal area lacking separate scutal elements. Sternal shield oblong, 90–100 µm long, 66–73 µm wide at level of constriction between coxae II, with smooth and weakly sclerotized but well-defined anteriormost portion possessing first pair of sternal setae and reaching level of first pair of lyrifissures (iv1);



Figures 1, 2. *Dendroseius reductus* sp. nov., female, with setal notation of idiosomal setae **1** dorsal idiosoma **2** ventral idiosoma. Scale bar: 50 μ m.

posterior margin regularly convex and produced to relatively acute angles each bearing a metasternal seta (st4); the shield with fine reticulate pattern on lateral parts, four pairs of sternal setae (st1–st4) and three pairs of lyrifissures, iv1–iv3 (opening of iv1 and iv2 slit-like while iv3 suboval, iv1 with transverse position to the body axis while iv2 oriented longitudinally). Epigynal shield oblong, 50–60 μ m wide, hyaline anteriorly (anterior margin obscure and not distinguishable), almost straight or widely rounded posteriorly, bearing one pair of setae (st5) and a pattern of longitudinal lines; genital lyrifissures (iv5) situated on soft integument behind st5, outside the shield. Four slit-like postgenital sclerites close to posterior margin of epigynal shield present. Peritremes shortened, 66–80 μ m long, with anterior end reaching slightly beyond posterior margin of coxa II; peritrematal shields well-developed, free from podonotal shield, markedly narrowed behind coxae IV, bearing humeral setae (r3), and adjacent to anterior margin of podonotal shield close to paraverticral setae z1 (Fig. 3). Three subtriangular exopodal platelets between peritrematal shields and coxae present. Metapodal soft integument with a pair of small irregular platelets having longitudinal position. Ventrianal shield subquadrate, only slightly wider than long (105–115 μ m long and 112–130 μ m wide),

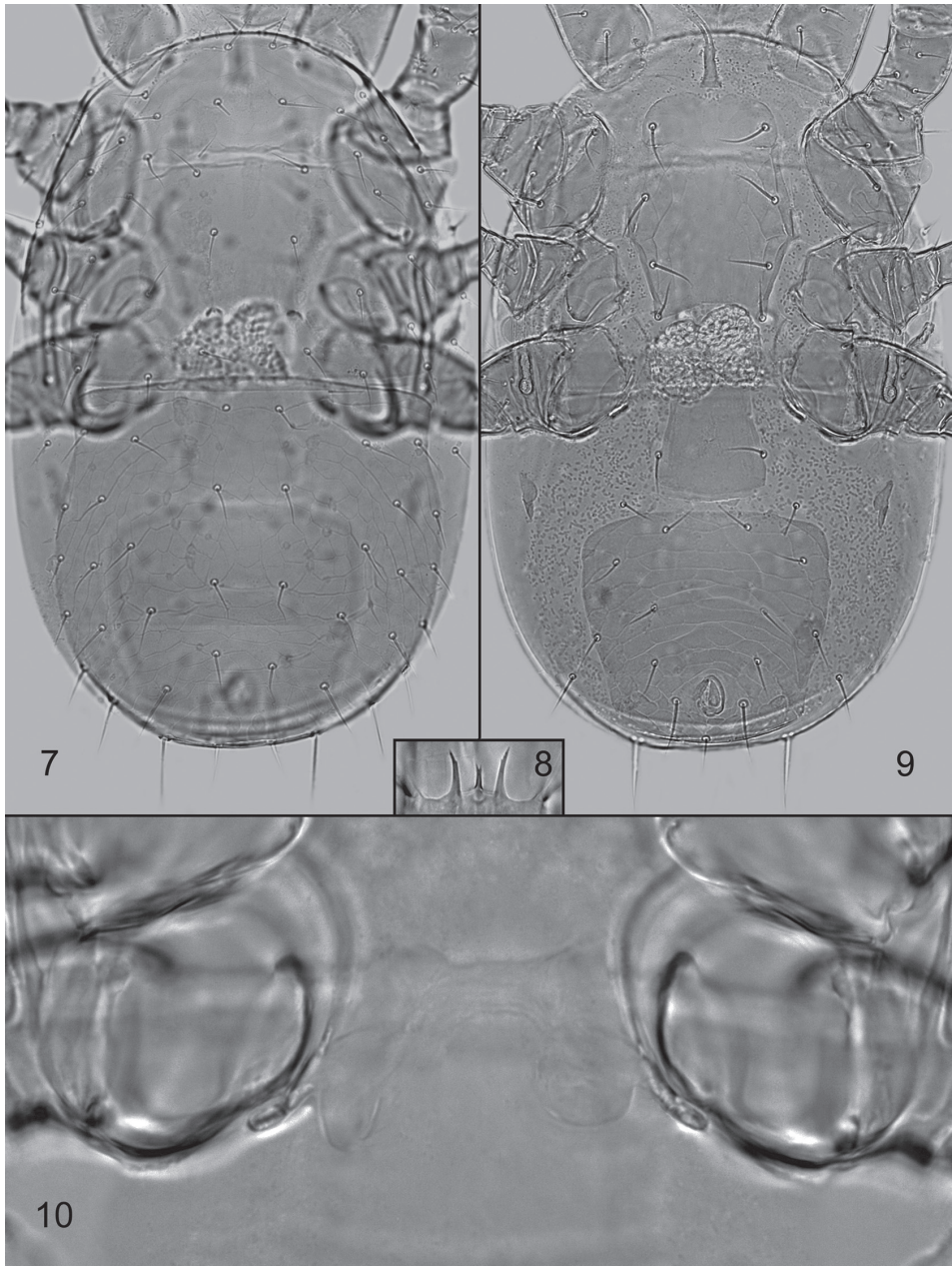


Figures 3–6. *Dendroseius reductus* sp. nov., female **3** peritrematal shield and adjacent exopodal platelets **4** ventral gnathosoma **5** epistomes, normal form and an aberration having two central prongs **6** chelicera, lateral view. Scale bars: 50 μm (**3**), 25 μm (**4**), 20 μm (**5, 6**).

delicately reticulate on whole surface, bearing five pairs of pre-anal setae (JV1–JV3, ZV2, ZV3) in addition to three circum-anal setae, and a pair of marginal gland pores (gv3) more or less aligned with posterior margin of anal opening; adanal setae (ad) apparently longer than postanal seta (ad 27–30 μm , pa 15–17 μm). Soft opisthogastric integument bearing two pairs of setae (ZV1, JV5). Ventrally situated setae similarly formed as those on dorsal side of idiosoma. The lengths of some selected setae on ventrum as follows: st1 25–28 μm , st2 24–27 μm , st3 22–26 μm , st4 21–24 μm , st5 21–23 μm , JV1 and JV2 18–23 μm , JV5 22–27 μm .

Sperm induction system (Fig. 10). Each gonoporus associated with inner posterior margin of coxa IV, together with relatively short and broad duct formed as a club-shaped structure; the duct opening into small hyaline sacculus. Sperm system of both coxae mutually connected with membranous structure (Fig. 10).

Gnathosomal structures (Figs 4–6, 8). Deutosternal groove with seven transverse sculptural furrows, six posterior ones with tiny denticles; corniculi horn-like, divergent; internal malae with median projections contiguous and with serrate margins (Fig. 4). The lengths of hypostomal setae as follows: h1 17–22 μm , h2 11–14 μm , h3 19–22 μm , pc 21–25 μm ; the setae smooth and needle-like. Palp apotele 2-tined. Epistome triramous, with short central and longer lateral branches, each terminally with one to three points; one specimen abnormally with two central branches



Figures 7–10. *Dendroseius reductus* sp. nov., photographs of female **7** dorsal idiosoma **8** epistome **9** ventral idiosoma **10** sperm induction system. Not to scale.

(Figs 5, 8). Cheliceral digits of similar size, dentate; movable digit with three closely set teeth in addition to distal hook; fixed digit with about seven teeth in addition to apical hook and minute setiform *pilus dentilis* (Fig. 6); a coronet-like fringe, dorsal cheliceral seta and antiaxial lyrifissure not discerned.

Legs. All legs with well-developed pretarsus and ambulacral apparatus (including pulvillus and two claws), shorter than idiosoma: legs I 290–310 µm, legs II 210–230 µm, legs III 180–200 µm, and legs IV 260–285 µm long. Leg segments not spurred ventrally, with normal chaetotactic pattern for the genus: leg I – coxa 0-0/1, 0/1-0 (2), trochanter 1-1/1, 0/2-1 (6), femur 2-3/2, 2/2-2 (13), genu 2-3/2, 2/1-2 (12), tibia 2-3/2, 2/1-2 (12); leg II – coxa 0-0/1, 0/1-0 (2), trochanter 1-0/1, 0/2-1 (5), femur 2-3/1, 2/2-1 (11), genu 2-3/1, 2/1-2 (11), tibia 2-2/1, 2/1-2 (10); leg III – coxa 0-0/1, 0/1-0 (2), trochanter 1-1/1, 0/2-0 (5), femur 1-2/1, 1/0-1 (6), genu 2-2/1, 2/1-1 (9), tibia 2-1/1, 2/1-1 (8); leg IV – coxa 0-0/1, 0/0-0 (1), trochanter 1-1/1, 0/2-0 (5), femur 1-2/1, 1/0-1 (6), genu 1-2/1, 2/0-1 (7), tibia 1-1/1, 2/1-1 (7); tarsi II–IV – 18 setae each. Leg setae uniform and similar in length, smooth and needle-like.

Etymology. The specific name is derived from the Latin word *reductus* (reduced) and expresses an important feature of the species – an unusual shape of epistome, a fine flat structure situated on upper surface of gnathosoma, with partly reduced central projection on its anterior margin.

Taxonomic notes. The triramous epistome of the new species, with remarkably shortened central projection, is unique and quite unlike any other known species in the genus *Dendroseius*. In other congeners, this central projection is much longer and more acuminate in the terminal part, reaching to (in *D. amoliensis*) or slightly beyond the level of the adjacent lateral apices (in all other congeners, including two species exclusively based on deutonymphs and not included in the key below). Nevertheless, the new species is most similar to *D. vulgaris* distributed in China (Ma, Ho and Wang 2014), and it can be distinguished from *D. vulgaris* and other species by the character states presented in the identification key below. Some metric data for *D. reticulatus* provided in the key are derived from specimens in author's personal collection from Wales, UK (Anglesey, Newborough Beach, found in decomposing plant substrate in a sandy coastal area). The morphological data used for other *Dendroseius* species were based only on the original descriptions.

Key to world species of *Dendroseius* (females)

- 1 Ventrianal shield subtriangular in shape, with posterior margin convex, and four pairs of pre-anal setae (JV1–JV3, ZV2; ZV3 situated outside the shield); peritremes relatively shorter, reaching about the middle of coxae III; length of idiosoma: 367 µm [Iran] *Dendroseius amoliensis* Faraji, Sakenin-Chelav & Karg, 2006
- Ventrianal shield subquadrate or subrectangular in shape, with posterior margin only moderately curved, and five pairs of pre-anal setae (JV1–JV3, ZV2, ZV3); peritremes relatively longer, reaching coxae II **2**
- 2 Podonotal soft integument with at most two pairs of setae (r4, r5; r2 situated on dorsal shield); length of idiosoma: 364 µm [South Africa] *Dendroseius badenhorsti* (Ryke, 1962)
- Podonotal soft integument with at least three pairs of setae (r2, r4, r5; sometimes s1) **3**

- 3 Dorsal shield setae shorter (J1–J4 normally less than 15 µm in length); setae r5 and Z5 similar in length (26–32 µm); ventrianal shield wider than long (L 95–100 µm; W 120–135 µm), dish-shaped; smaller species, length of idiosoma: 260–290 µm [Europe, North Africa] *Dendroseius reticulatus* (Sheals, 1956)
- Dorsal shield setae longer (J1–J4 normally more than 18 µm in length); setae r5 1.5–2 times shorter than Z5 (r5 23–28 µm, Z5 35–55 µm); ventrianal shield similar in width and length (L 105–143 µm; W 112–135 µm), cup-shaped; larger species, length of idiosoma: 315–375 µm 4
- 4 Central process of epistome shortened, about two times shorter than those on lateral margins; dorsal shield setae generally shorter: J4≈1/2×J4–J5, S1≈1/2×S1–R2, S2≈1/2×S2–S3, S3≈1/2×S3–S4 (j5 17–20 µm, J1–J4 19–23 µm, J5 17–19 µm, Z5 35–40 µm); ventrianal shield slightly wider than long (L 105–115 µm; W 112–130 µm); length of idiosoma: 315–345 µm [Slovakia]..... *Dendroseius reductus* sp. nov.
- Epistome with three well-developed prongs, central process slightly longer than lateral ones; dorsal shield setae generally longer: J4≈J4–J5, S1≈S1–R2, S2≈S2–S3, S3≈S3–S4 (j5 25–30 µm, J1–J4 23–42 µm, J5 26–38 µm, Z5 48–55 µm); ventrianal shield slightly longer than wide (L 131–143 µm; W 128–135 µm); length of idiosoma: 353–375 µm [Taiwan]..... *Dendroseius vulgaris* Ma, Ho & Wang, 2014

Acknowledgements

This study was fully supported by the Scientific Grant Agency of the Ministry of Education of Slovak Republic and the Academy of Sciences [VEGA Grant No. 2/0036/18: Systematics, ecological requirements and chorology of saproxylic mites (Acari: Mesostigmata) phoretically associated with woodboring insects in Europe].

References

- Evans GO (1963a) Observations on the chaetotaxy of the legs in the free-living Gamasina (Acari: Mesostigmata). Bulletin of the British Museum (Natural History), Zoology 10: 275–303. <https://doi.org/10.5962/bhl.part.20528>
- Evans GO (1963b) Some observations on the chaetotaxy of the pedipalps in the Mesostigmata (Acari). Annals and Magazine of Natural History, Series 13, 6: 513–527. <https://doi.org/10.1080/00222936308651393>
- Evans GO, Till WM (1979) Mesostigmatic mites of Britain and Ireland (Chelicerata: Acari – Parasitiformes). An introduction to their external morphology and classification. Transactions of the Zoological Society of London 35: 145–270. <https://doi.org/10.1111/j.1096-3642.1979.tb00059.x>

- Faraji F, Sakenin-Chelav H, Karg W (2006) A new species of *Dendroseius* Karg from Iran (Acari: Rhodacaridae), with a key to the known species. *Zootaxa* 1221: 63–68. <https://doi.org/10.11646/zootaxa.1221.1.2>
- Hirschmann W (1974) Gangsystematik der Parasitiformes. Teil 190. Die Gattung *Dendrolaelaps* Halbert, 1915, Hirschmann nov. comb. Nova Subgenera *Multidendrolaelaps*, *Tridendrolaelaps* Hirschmann. Stadien von 4 neuen *Dendrolaelaps*-Arten. *Acarologie, Schriftenreihe für Vergleichende Milbenkunde* 20: 50–70.
- Karg W (1965) Larvalsystematische und phylogenetische Untersuchung sowie Revision des Systems der Gamasina Leach, 1915 (Acarina, Parasitiformes). *Mitteilungen aus dem Museum für Naturkunde in Berlin, Zoologische Reihe* 41: 193–340. <https://doi.org/10.1002/mmz.19650410207>
- Karg W (1993) Acari (Acarina), Milben. Parasitiformes (Anactinochaeta). Cohors Gamasina Leach. Raubmilben. 2. Überarbeitete Auflage. *Die Tierwelt Deutschlands* 59: 1–523.
- Lindquist EE (1975) *Digamasellus* Berlese, 1905, and *Dendrolaelaps* Halbert, 1915, with description of new taxa of Digamasellidae (Acarina: Mesostigmata). *The Canadian Entomologist* 107: 1–43. <https://doi.org/10.4039/Ent1071-1>
- Lindquist EE, Evans GO (1965) Taxonomic concept in the Ascidae, with a modified setae nomenclature for the idiosoma of the Gamasina (Acarina: Mesostigmata). *Memoirs of the Entomological Society of Canada* 47: 1–64. <https://doi.org/10.4039/entm9747fv>
- Ma LM, Ho CC, Wang SC (2014) Two new species of Digamasellidae from Taiwan (Acari: Mesostigmata). *Zootaxa* 3768: 43–58. <https://doi.org/10.11646/zootaxa.3768.1.3>
- Ryke PAJ (1962) The subgenera *Digamasellus* Berl. and *Euryparasitus* Oudemans of the genus *Cyrtolaelaps* Berlese (Acarina: Rhodacaridae). *Journal of the Entomological Society of Southern Africa* 25: 88–115.
- Shcherbak GI (1980) The Palearctic mites of the family Rhodacaridae. Kiev, Naukova Dumka, 216 pp. [In Russian with English abstract]
- Sheals JG (1956) Notes on a collection of soil Acari. *Entomologist's Monthly Magazine* 92: 99–103.
- Sheals JG (1958) A revision of the British species of *Rhodacarus* Oudemans and *Rhodacarellus* Willmann (Acarina, Rhodacaridae). *Annals and Magazine of Natural History* 1: 298–304. <https://doi.org/10.1080/00222935808650949>
- Wiśniewski J, Hirschmann W (1989) Neue *Dendroseius*- und *Dendrolaelaps*-Arten (Acarina, Trichopygidiina) aus Indien, Java, Peru und Bulgarien. *Polskie Pismo Entomologiczne* 59: 319–333.
- Wiśniewski J, Hirschmann W (1992) *Dendroseius congoensis* nov. spec. (Acarina, Mesostigmata) auf importierten Holz in Polen. *Bulletin de la Société des Amis des Sciences et des Lettres de Poznań, Serie D* 29: 63–67.

***Bombus (Pyrobombus) johanseni* Sladen, 1919, a valid North American bumble bee species, with a new synonymy and comparisons to other “red-banded” bumble bee species in North America (Hymenoptera, Apidae, Bombini)**

Cory S. Sheffield¹, Ryan Oram¹, Jennifer M. Heron²

¹ Royal Saskatchewan Museum, 2340 Albert Street, Regina, Saskatchewan, Canada S4P 2V7 ² British Columbia Ministry of Environment and Climate Change Strategy, Vancouver, British Columbia, Canada V6T 1Z1

Corresponding author: Cory S. Sheffield (Cory.Sheffield@gov.sk.ca)

Academic editor: Michael S. Engel | Received 25 June 2020 | Accepted 29 September 2020 | Published 4 November 2020

<http://zoobank.org/12323F95-59D6-41EC-B57F-F6C47318B27D>

Citation: Sheffield CS, Oram R, Heron JM (2020) *Bombus (Pyrobombus) johanseni* Sladen, 1919, a valid North American bumble bee species, with a new synonymy and comparisons to other “red-banded” bumble bee species in North America (Hymenoptera, Apidae, Bombini). ZooKeys 984: 59–81. <https://doi.org/10.3897/zookeys.984.55816>

Abstract

The bumble bee (Hymenoptera, Apidae, Bombini, *Bombus* Latreille) fauna of the Nearctic and Palearctic regions are considered well known, with a few species occurring in both regions (i.e., with a Holarctic distribution), but much of the Arctic, especially in North America, remains undersampled or unsurveyed. Several bumble bee taxa have been described from northern North America, these considered either valid species or placed into synonymy with other taxa. However, some of these synonymies were made under the assumption of variable hair colour only, without detailed examination of other morphological characters (e.g., male genitalia, hidden sterna), and without the aid of molecular data. Recently, *Bombus interacti* Martinet, Brasero & Rasmont, 2019 was described from Alaska where it is considered endemic; based on both morphological and molecular data, it was considered a taxon distinct from *B. lapponicus* (Fabricius, 1793). *Bombus interacti* was also considered distinct from *B. gelidus* Cresson, 1878, a taxon from Alaska surmised to be a melanistic form of *B. lapponicus sylvicola* Kirby, 1837, the North American subspecies (Martinet et al. 2019). Unfortunately, Martinet et al. (2019) did not have DNA barcode sequences (COI) for females of *B. interacti*, but molecular data for a melanistic female specimen matching the DNA

barcode sequence of the holotype of *B. interacti* have been available in the Barcodes of Life Data System (BOLD) since 2011. Since then, additional specimens have been obtained from across northern North America. Also unfortunate was that *B. sylvicola* var. *johanseni* Sladen, 1919, another melanistic taxon described from far northern Canada, was not considered.

Bombus johanseni is here recognized as a distinct taxon from *B. lapponicus sylvicola* Kirby, 1837 (*sensu* Martinet et al. 2019) in the Nearctic region, showing the closest affinity to *B. glacialis* Friese, 1902 of the Old World. As the holotype male of *B. interacti* is genetically identical to material identified here as *B. johanseni*, it is placed into synonymy. Thus, we consider *B. johanseni* a widespread species occurring across arctic and subarctic North America in which most females are dark, with rarer pale forms (i.e., “*interacti*”) occurring in and seemingly restricted to Alaska. In addition to *B. johanseni* showing molecular affinities to *B. glacialis* of the Old World, both taxa also inhabit similar habitats in the arctic areas of both Nearctic and Palearctic, respectively. It is also likely that many of the specimens identified as *B. lapponicus sylvicola* from far northern Canada and Alaska might actually be *B. johanseni*, so that should be considered for future studies of taxonomy, distribution, and conservation assessment of North American bumble bees.

Keywords

Arctic, bumble bee, DNA barcode, Holarctic species, melanism, morphology, synonymy

Introduction

The bumble bees, *Bombus* Latreille, 1802 (Hymenoptera: Apoidea, Apidae) are one of the most thoroughly studied groups of bees, and extensive taxonomic coverage has existed for the North American fauna since Cresson (1863) first reviewed the species, with many subsequent taxonomic works (e.g., Franklin 1912; Frison 1923; Frison 1929; Lutz 1916; Lutz and Cockerell 1920; Stephen 1957; Thorp et al. 1983; Lavery and Harder 1988). In the most recent taxonomic treatment of bumble bees in North American north of Mexico, Williams et al. (2014) recognized 46 species, with two species of the subgenus *Psithyrus* Lepeletier, 1833 previously recognized as Nearctic, *B. fernaldae* (Franklin, 1911) and *B. ashtoni* (Cresson, 1864) considered synonyms of *B. flavidus* Eversmann, 1852 and *B. bohemicus* (Seidl, 1838), respectively; the latter two species thus treated as Holarctic. Since Williams et al. (2014), other taxonomic works have been published on the North American bumble bee fauna: in the subgenus *Bombus*, a subspecies of *B. occidentalis* Greene, 1858 was recognized, *B. occidentalis mckayi* Ashmead, 1902 (Williams et al. 2012; Sheffield et al. 2016); a new species of *Alpinobombus* Skorikov, 1914, *B. kluanensis* Williams & Cannings, 2016 was described from the Yukon and Alaska (Williams et al. 2016); and two additional species of *Alpinobombus*, *B. natvigi* Richards, 1931 and *B. kirbiellus* Curtis, 1835 were considered distinct from their Old World conspecifics, *B. hyperboreus* Schönherr, 1809 and *B. balteatus* Dahlbom, 1832, respectively (Williams et al. 2019). Within the subgenus *Pyrobombus* Dalla Torre, 1880, two taxa, *B. vancouverensis vancouverensis* Cresson, 1878 and *B. vancouverensis nearcticus* Handlirsch, 1888 were recognized as molecularly dis-

tinct from *B. bifarius* Cresson, 1878 (Ghisbain et al. 2020); *B. sylvicola* Kirby, 1837 was recognized as a subspecies of the Holarctic *B. lapponicus* (Fabricius, 1793); and a new species of *Pyrobombus* with close affinities to *B. lapponicus*, *B. interacti* Martinet, Brasero & Rasmont, 2019 was described from Alaska (Martinet et al. 2019). At this point, 48 species of bumble bee are now recognized in North America north of Mexico, though the taxonomic status of some species is still unresolved (e.g., Yanega 2013; Koch et al. 2018).

One common trend exists for most of these recently treated bumble bee species in North America – they are taxa with ranges that extend into, or are restricted to, northern regions of the globe. In North America and elsewhere, northern latitudes have been one of the most poorly studied and sampled regions for bumble bees (Popatov et al. 2019). Though the bee fauna of this region is typically considered much less speciose than others (for Canada, see Sheffield et al. 2014), it is of interest because of the obvious connection to the Old World via Beringia (Williams 1985; Hines et al. 2006; Williams et al. 2019).

Recent research contributing to the overall creation of a DNA barcode library for bees in Canada (Sheffield et al. 2017) was built on previous studies on the taxonomy and distribution of species in that country. For instance, Sheffield et al. (2011) recognized two *Megachile* species as Holarctic for the first time, and associated sexes for other species with the aid of DNA barcoding. In addition, DNA barcoding facilitated synonymies of taxa that were determined to be melanistic forms of other species (Sheffield et al. 2011), and the recognition of distinct taxa among cryptic species groups (e.g., Rehan and Sheffield 2011; Vickruck et al. 2012; Williams et al. 2012; Sheffield et al. 2016). Our main purpose here is to clarify the taxonomic status of a melanistic northern bumble bee taxon with close molecular and morphological affinities to an Old World taxon. A second objective is to provide diagnoses with accompanying photographs to facilitate identification of “red-banded” bumble bee species (i.e., Figure 5 “O” in Williams 2007; “Mimicry Pattern 5” of Williams et al. 2014) of North America in the field and from pinned specimens.

Materials and methods

Bumble bee specimens from northern Canada contained the Royal Saskatchewan Museum (**RSKM**) were subject to DNA barcoding (Hebert et al. 2003) following procedures previously published for bees in Canada (Sheffield et al. 2009, 2017); all sequences used or created here and their associated specimen data are accessible through the Barcodes of Life Data System (BOLD) (Ratnasingham and Hebert 2007); Process IDs and Barcode Index Numbers (BINs; Ratnasingham and Hebert 2013) of specimens are provided in Table 1. Mitochondrial cytochrome oxidase subunit 1 (COI) gene sequences were obtained from samples of these and other pinned bumble bees of the subgenus *Pyrobombus*, and sequences from *B. (Bombus) terricola*

Kirby, 1837 were selected as an outgroup; protocols for DNA extraction, polymerase chain reaction and sequencing follow those described elsewhere (Sheffield et al. 2009, 2017). Additional COI sequences were downloaded directly from GenBank (from Martinet et al. 2019) or from GenBank via BOLD (from Gjershaug et al. 2013, and Potapov et al. 2017) corresponding to *B. interacti* (male holotype only), *B. monticola* Smith, 1849, *B. lapponicus lapponicus*, and *B. glacialis* Friese, 1902, respectively (Table 2). These COI sequences were aligned with sequences in BOLD (MUSCLE) to provide confirmation of identification, and the reported genetic distances were analyzed using various sequence analysis tools on BOLD, including the Taxon ID Tree, Distance Summary, Barcode Gap Analysis, and Diagnostic Characters tools. Sequences were then downloaded as fasta (.fas) files and uploaded into MEGA X (Kumar et al. 2018) for phylogenetic analysis. All sequences were aligned using ClustalW, and the best DNA model using maximum likelihood was found based on the BIC value; the General Time Reversible with Gamma Variation (GTR+G) model was selected and a maximum likelihood tree was constructed with 500 bootstraps. Based on results of the tree, each taxon was collapsed and distance values within each (Tables 1, 2) were calculated to support species group delineation. Distances among taxa were also calculated, and diagnostic nucleotides for species of interest were determined (Table 3).

To document the geographic range of the taxon of interest, localities from literature (i.e., Cresson 1878; Ashmead 1902; Franklin 1912; Sladen 1919; Bequaert 1920; Lutz and Cockerell 1920; Frison 1927a; Martinet et al. 2019) and from specimens at the RSKM were mapped using SimpleMappr (Shorthouse 2010) based on original taxon name and colour pattern. In addition, records from iNaturalist (www.inaturalist.org) were first verified, with data subsequently mined. The full dataset for the specimens used in this study is archived with Canadensys (<http://community.canadensys.net/>) under resource title “*Bombus johanseni*, a valid North American bumble bee species” and can be accessed using the following: <https://doi.org/10.5886/3ex36t>.

Photomicrography was undertaken with a Canon EOS 5D Mark II digital camera with an MP-E 65 mm 1:2.8 1–5× macro lens. Measurements were made with an ocular micrometer on a Nikon SMZ1000 stereomicroscope.

Results

Phylogenetic analysis and genetic distance of COI sequences support the close affinity of *B. johanseni* to *B. glacialis* (1.98% genetic distance) and *B. monticola* (2.74% genetic distance), both Old World taxa (Fig. 1), and support that *B. johanseni* should not be considered conspecific with *B. lapponicus sylvicola* (3.49% distance). In addition, the COI sequence from the holotype male of *B. interacti* shows no differences from specimens matching the type material and descriptions *B. johanseni* (Fig. 1), all belonging to BIN ABA8452, with <0.001% genetic distance among specimens (Table 1), supporting the synonymy below.

Table 1. Species and specimens of bumble bees with COI sequences in BOLD used for genetic analyses in this study, including BOLD Process IDs (when available) for each specimen, the Barcode Index Number (BIN) to which the specimens have been assigned, and the genetic distance observed within each species.

Species	BOLD Process ID	BIN	Genetic distance (%)
<i>Bombus johanseni</i>	ACHAR117-18, CCHAR061-19, CCHAR062-19, ACHAR3482-19, DCHAR2640-19, MOBIL1097-15, BEECF718-11, WASPS1609-20, WASPS1607-20, WASPS1603-20, WASPS1604-20, WASPS1605-20, FCHAR3225-19, FCHAR4872-19, FCHAR4878-19	BOLD:ABA8452	0.0009
<i>B. bimaculatus</i>	UPOLB204-09, UPOLB218-09, BOWGF1488-10, BEECD873-10, BOWGF1653-10	BOLD:AAB4829	0
<i>B. sylvicola</i> s. str.	BEECA042-06, BEECA296-06, BEECA297-06, JSYKA168-10, JSYKA176-10, BWTWO1164-10	BOLD:AAA8078	0
<i>B. melanopygus</i>	TTHYW305-08, TTHYW340-08, TTHYW341-08, TTHYW479-08, BCLRB862-10, BEECD829-10, BCII522-10, BCII742-10, BCII743-10	BOLD:AAB5223	0.0004
<i>B. ternarius</i>	BEECD864-10, BEECD865-10, BEECD867-10, BBHYL228-10, OPPFC190-17, OPPFE004-17	BOLD:AAB5221	0.0022
<i>B. perplexus</i>	TTHYW593-08, TTHYW595-08, TTHYW616-08, BBHEC177-09, BEECD417-09, BEECD419-09, BEECD422-09, BEECD423-09, BEECD424-09, BEECD436-09, BEECD878-10, BEECD879-10	BOLD:AAB2150	0.0012
<i>B. sitkensis</i>	TTHYW283-08, BCII485-10, BCII486-10, BBHYL258-10, BCIII001-11	BOLD:AAI4757	0.003
<i>B. mixtus</i>	BCLRB866-10, BCLRB920-10	BOLD:AAB1091	0
<i>B. jonellus</i>	BEECF862-12, BEECF863-12, BEECF873-12, BEECF887-12, BOWGF2140-12, UAMIC749-13	BOLD:AAD4941	0.0135
<i>B. frigidus</i>	MHBEE033-07, MHBEE034-07, TTHYW237-08, BWTWO1201-10, BEECE682-10, BEECE715-10, BBHYL221-10	BOLD:AAB1090	0.001
<i>B. flavifrons</i>	BEECA039-06, BEECA040-06, HMBCH001-07, TTHYW207-08, TTHYW234-08, TTHYW313-08, TTHYW488-08, BOWGF787-09, JSYKA173-10, JSYKA174-10, BBHYL273-10	BOLD:ACE3465	0.0011
<i>B. terricola</i>	TTHYW654-08, TTHYW807-08, BEECD330-09, BEECD331-09, BBHEC139-09, BBHEC143-09, BBHEC144-09, BWTWO706-09, BWTWO707-09, BEECD383-09, BEECD410-09, BEECD735-09, BCLRB868-10	BOLD:AAA8658	0.0001

Table 2. List of *Bombus* species for which sequences were obtained from GenBank, with GenBank accession numbers, Barcode Index Number (BIN) and the genetic distance observed within each species. Published source of the data are Gjershaug et al. 2013 (*Bombus monticola*, *B. lapponicus*); Potapov et al. 2017 (*B. glacialis*); Martinet et al. 2019 (*B. interacti*). *see *B. johanseni* in Table 1.

Species	GenBank Acc. No.	BIN	Genetic distance (%)
<i>B. glacialis</i>	KY202838, KY202839, KY202840, KY202841, KY202842, KY202843	BOLD:ADU5113	0
<i>B. interacti</i>	MG280603	BOLD:ABA8452	*
<i>B. monticola</i>	GU705913, KJ838349, KJ838456, KJ837131, KF434337, KF434338, KF434339	BOLD:AAD8242	0.0011
<i>B. lapponicus</i>	KF434329, KF434330, KF434331, KF434332	BOLD:AAA8078	0.0011

Table 3. Diagnostic nucleotides and their position within the COI mitochondrial gene (i.e., DNA barcode) for *Bombus glacialis* (ADU5113), *B. johanseni* (ABA8452, includes *B. interacti*), *B. lapponicus* (ssp. *lapponicus* – AAA8078), *B. monticola* (AAD8242) and *B. lapponicus* (ssp. *sylvicola* – AAA8078).

Species	Nucleotide position																							
	48	105	195	207	241	259	270	318	333	334	349	387	402	411	433	447	504	537	540	555	603	607	648	
<i>B. glacialis</i>		C	C				A										C						C	
<i>B. johanseni</i>				A	C			C						C				C	C			G		
<i>B. lapponicus</i>	C					C																		
<i>B. monticola</i>								A		C	A	G	C			C								C
<i>B. sylvicola</i>									G						G						C			

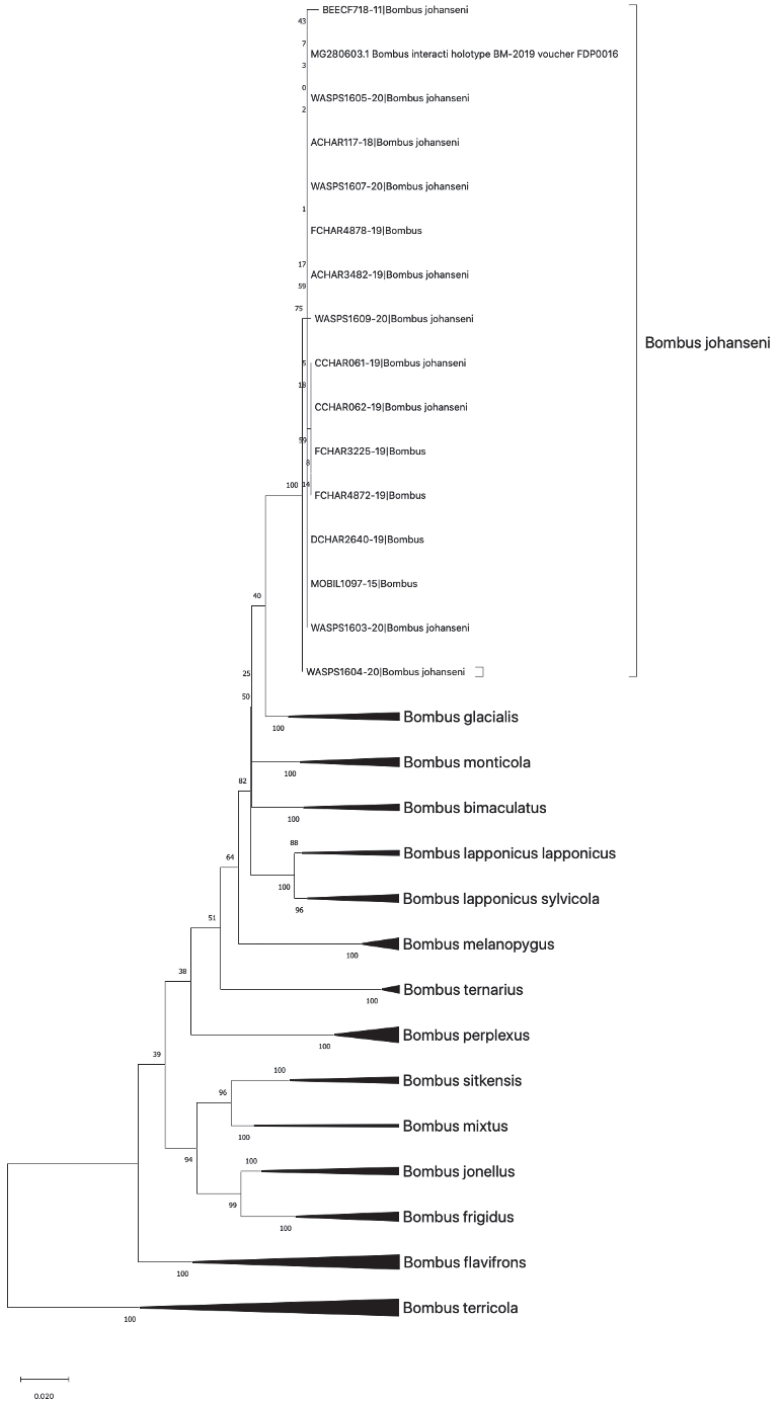


Figure 1. Maximum likelihood tree constructed with 500 bootstraps for selected taxa of *Pyrobombus*, with *B. (Bombus) terricola* as an outgroup. The taxon *Bombus johanseni* consists of specimens identified in BOLD as *Bombus* sp. and *B. johanseni*, in addition to the holotype male of *B. interacti*.

Taxonomic accounts

Bombus (Pyrobombus) johanseni Sladen, 1919, comb. nov.

Bombus sylvicola var. *johanseni* Sladen, 1919: 30g [♀].

Holotype ♀. CANADA, Northwest Territories, Bernard Harbour, 3 July 1916 [3 July 1915], Canadian Arctic Expedition, by F. Johansen [Canadian National Collection of Insects, Arachnids, and Nematodes, CNC no. 2029]. [photographs of holotype examined, see Fig. 2].

Bombus (Pyrobombus) interacti Martinet, Brasero, & Rasmont, 2019: 611 [♀, ♂]. syn. nov.

Holotype ♂. USA, Alaska, Toolik field station, 68°37'32.9"N 149°35'48.8"W, 725m, 28 July 2015, by Martinet and Rasmont, on *Epilobium angustifolium* [Royal Belgian Institute of Natural Sciences]. Photographs of holotype (as per Martinet et al. 2019) examined.

Diagnosis. Among the members of the *Bombus lapponicus* – complex, and other *Pyrobombus* considered here, *B. johanseni* is genetically most similar to the northern Palearctic *B. glacialis* (and see Martinet et al. 2019). In northern North America, the melanistic females of *B. johanseni* (Figs 2, 3, 4a, b) are most similar to darker forms of *B. melanopygus* (Fig. 4c) and atypical dark forms of *B. ternarius* Say, 1837 from Newfoundland and Labrador (Fig. 7c, d), while paler forms (i.e., “*interacti*”) are most similar to *B. lapponicus sylvicola* (Fig. 4d); all these taxa have the characteristic “red-banded” metasomal colour pattern of tergum 1 primarily yellow, terga 2 and 3 primarily red or orange, and tergum 4 primarily yellow at least laterally (Fig. 5a); with T5 yellow, at least laterally. *Bombus johanseni* females differ from these other taxa by the colour of the pubescence on the face, being entirely dark in *B. johanseni* (Figs 2a, 3a, 4a, b, 6a, b; but see Martinet et al. 2019), but primarily yellow in *B. lapponicus sylvicola* (Figs 4d, 6e) or strongly intermixed in *B. melanopygus* (Figs 4c, 6c). The dark forms of *B. johanseni* also have extensive dark pubescence on much of the mesosoma, including the pleura (Figs 2, 3, 4a, b), with the dark pubescence extending laterally

* The type locality of *B. johanseni* is in northern Nunavut; Northwest Territories was originally indicated by Sladen (1919) (Fig. 2c), and subsequently by Sarazin (1986), but Nunavut officially separated from the Northwest Territories on 1 April 1999 via the Nunavut Act. Though the specimen is labelled as a “Lectotype” designated by H.E. Milliron 1960 (Fig. 2c), we cannot find any published account of this designation, though it was not required as Sladen (1919: 30g) clearly indicate the “type” by original designation as a single queen collected on 3 July 1916 [1915 in Sladen 1919], the only specimen with that collection information. Though Sladen (1919) originally described and treated his taxon as a variety of *B. sylvicola* s. str., which was done so by subsequent authors (e.g., Frison 1927a, 1927b; Hurd 1979) we consider this name valid as according to Article, 45.6.4.1 of the ICZN Code (International Commission on Zoological Nomenclature 1999), an infrasubspecific name (i.e., under Article 45.6.4) is considered subspecific from its original publication use if, before 1985, it was either adopted as the valid name of a species or subspecies, which was done so by Lutz and Cockerell (1920) who treated it as a subspecies of *B. sylvicola*.

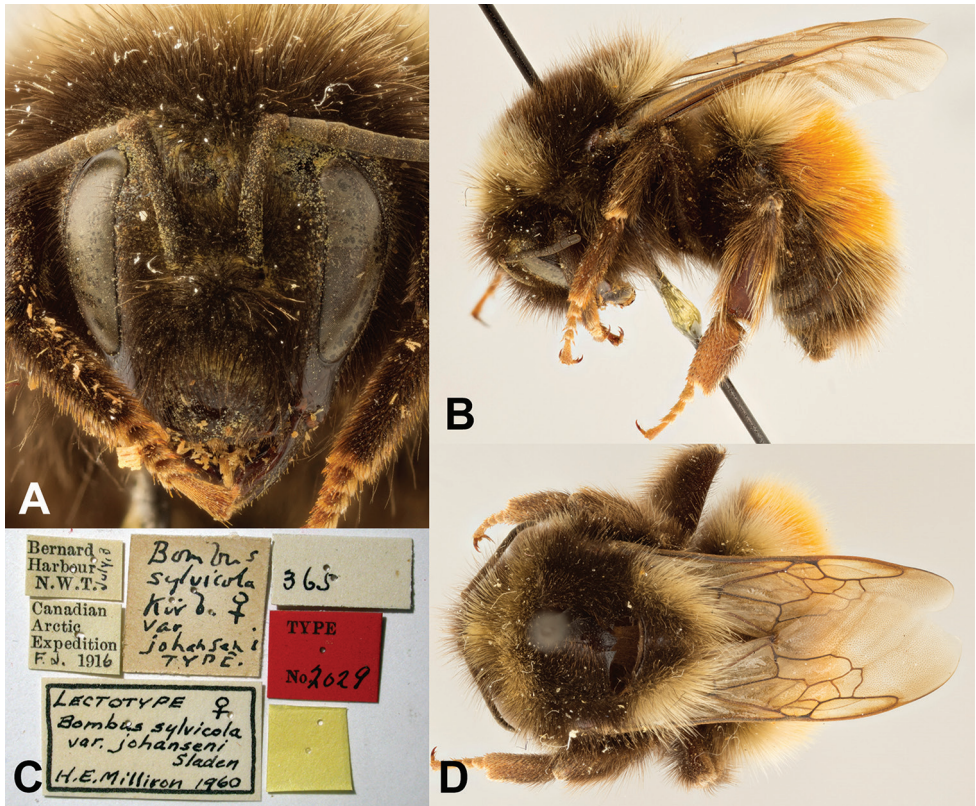


Figure 2. Holotype female of *Bombus sylvicola* var. *johanseni* **A** face **B** lateral view **C** associated specimen labels **D** dorsal view. Photographs by Joel Kits, Ottawa Research and Development Centre.

on the dorsal anterior surface (Figs 2, 3a, 4a, 6a), the latter characteristic shared only with dark specimens of *B. melanopygus*, though in the latter species the hair is usually intermixed (Figs 4c, 6c, d), not a solid colour (Figs 2, 3, 4a, 6a, b). Other specimens of *B. johanseni* have dark hairs on the pleura, with hairs becoming paler on the dorsal surface (Fig. 4b), while others (i.e., *interacti*) are almost entirely pale haired on the pleura (but becoming somewhat darker below) and dorsal surface (see Martinet et al. 2019) and more closely resemble *B. lapponicus sylvicola* (Figs 4d, 6e, f). Morphologically, the females of *B. johanseni* and *B. lapponicus sylvicola* are very similar (Martinet et al. 2019), as are the Old World taxa *B. glacialis* and *B. lapponicus lapponicus* (Potapov et al. 2017).

The “red-banded” pattern (Fig. 5a) of these northern taxa is also shared with other, typically more southern species, including *B. ternarius*, *B. huntii* Greene, 1860, some *B. vancouverensis*, and some *B. rufocinctus* Cresson, 1863 (Fig. 7, and see Mimicry Pattern 5 in Williams et al. 2014), though these latter species generally tend to have females with either T5 entirely black (*B. huntii*, *B. ternarius*, Fig. 7a, d), or with tergum 2 black (*B. vancouverensis*, Fig. 7e) or yellow (*B. rufocinctus*, Fig. 7f) basiomedially.



Figure 3. *Bombus johanseni* female from Sachs Harbour, Banks Island, Northwest Territories, Canada. **A** Left arrow shows the characteristic black pubescence of the face, right arrow shows the solid area of darker pubescence on the anterior part of thorax **B** left arrow shows the solid area of darker pubescence on the anterior part of thorax, right arrow shows the typical “red-banding” of the abdomen. Photographs by JMH.

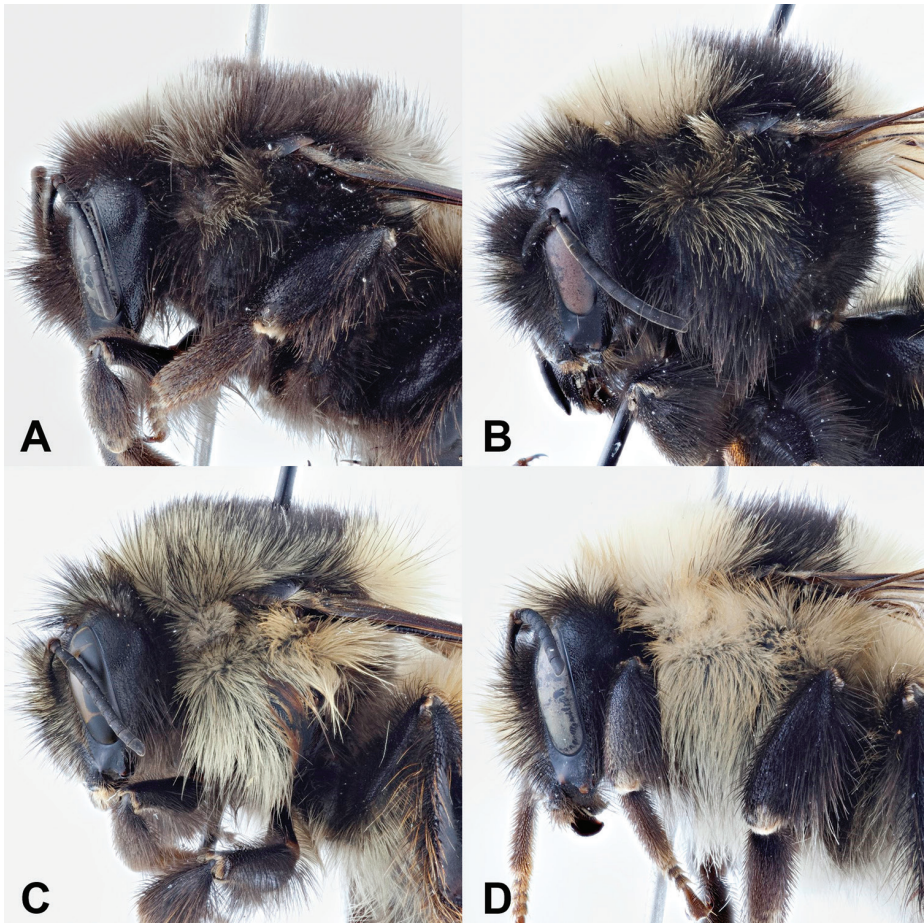


Figure 4. Lateral view of the thorax of female *Bombus* species. **A, B** *Bombus johanseni* **C** *B. melanopygus* **D** *B. lapponicus sylvicola*.

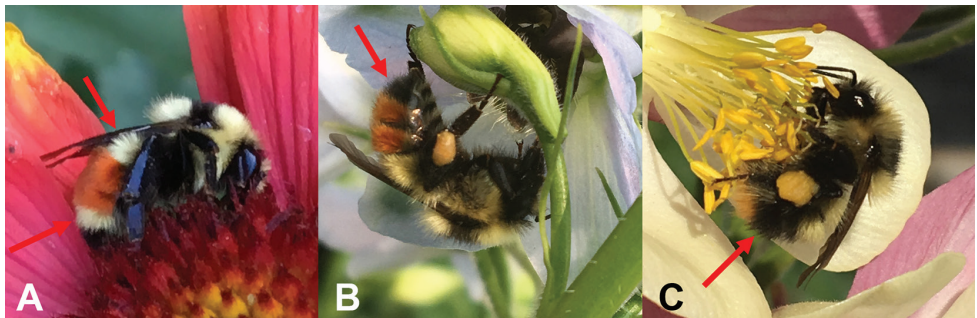


Figure 5. **A** A typical “red-banded” bumble bee, *Bombus huntii*, showing the two red bands (terga 2 and 3) with yellow bands on either side (arrows, terga 1 and 4), and “red-tailed” bumble bees **B** *B. centralis*, with red band (terga 3 and 4) preceded by a yellow band (terga 1 and 2) with black apically (arrow) **C** *B. mixtus*, with a black band (arrow) separating the basal yellow and apical red bands. Photographs by CSS.

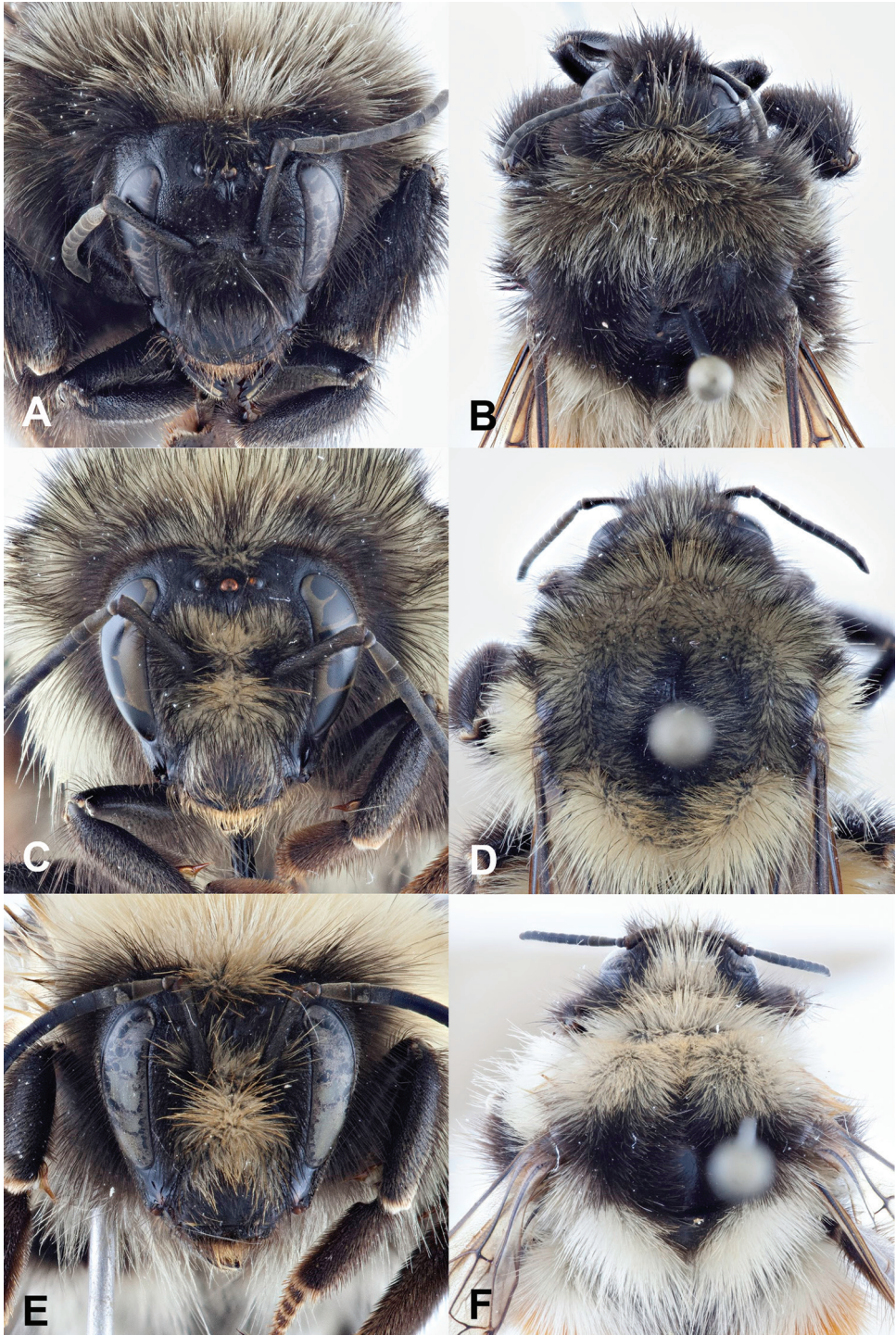


Figure 6. Faces (A, C, E) and thorax in dorsal view (B, D, F) in female bumble bees A, B *Bombus johanseni* C, D *B. melanopygus* E, F *B. lapponicus sylvicola*.

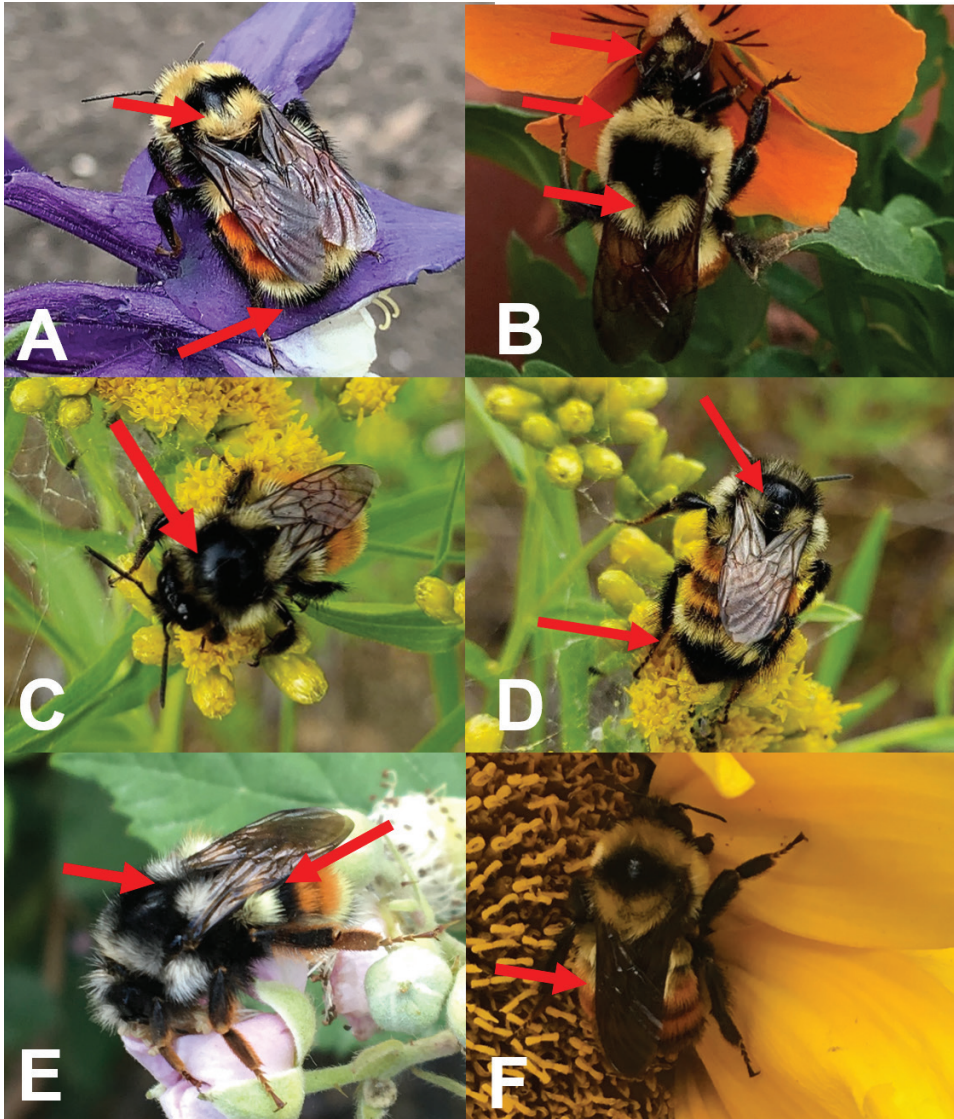


Figure 7. Examples of “red-banded” bumble bees. **A** *Bombus huntii* female. Top arrow shows the complete yellow hair patch on the rear of the thorax (scutellum), bottom arrow shows the completely black tergum 5 **B** *B. ternarius* female. Top arrow shows the face with both yellow and black hairs, middle arrow shows the entirely yellow anterior area of the thorax, bottom arrow shows the yellow hair patch on the rear of the thorax (scutellum) divided in two by a wedge of black hairs. Photographs by CSS **C**, **D** *B. ternarius* female, from Newfoundland. Arrow in **C** shows the atypical intermixed black hair on the anterior area of the thorax. Top arrow in **D** shows the yellow hair patch on the rear of the thorax (scutellum) divided in two by a wedge of black hairs, bottom arrow shows all black tergum 5. Photographs by Carolyn Parsons **E** *B. vancouverensis* female (red form). Left arrow shows the pale hair patch on the rear of the thorax (scutellum) divided in two by a wedge of black hairs, right arrow shows the incomplete red band of tergum 2, with black hairs in basal half **F** *B. rufocinctus* female (red form). Arrow shows the incomplete red band of tergum 2, being yellow medially in the basal half. Photographs by CSS.



Figure 8. Penis-valve head of male **A** *Bombus johanseni*, and **B** *B. lapponicus sylvicola*.

In North America, the males of *B. johanseni* resemble *B. lapponicus sylvicola*, *B. ternarius*, *B. huntii*, some *B. vancouverensis*, and pale individuals of *B. melanopygus*. The males of *B. johanseni* and *B. lapponicus sylvicola* can be distinguished from all other *Pyrobombus* in North America by the bulbous tip of the penis valve (Stephen 1957; Thorp et al. 1983; Williams et al. 2014) (Fig. 8), though in the former, the tip of the penis valve (Fig. 8a) is not quite as bulbous as in *B. lapponicus sylvicola* (Fig. 8b). In *B. johanseni*,

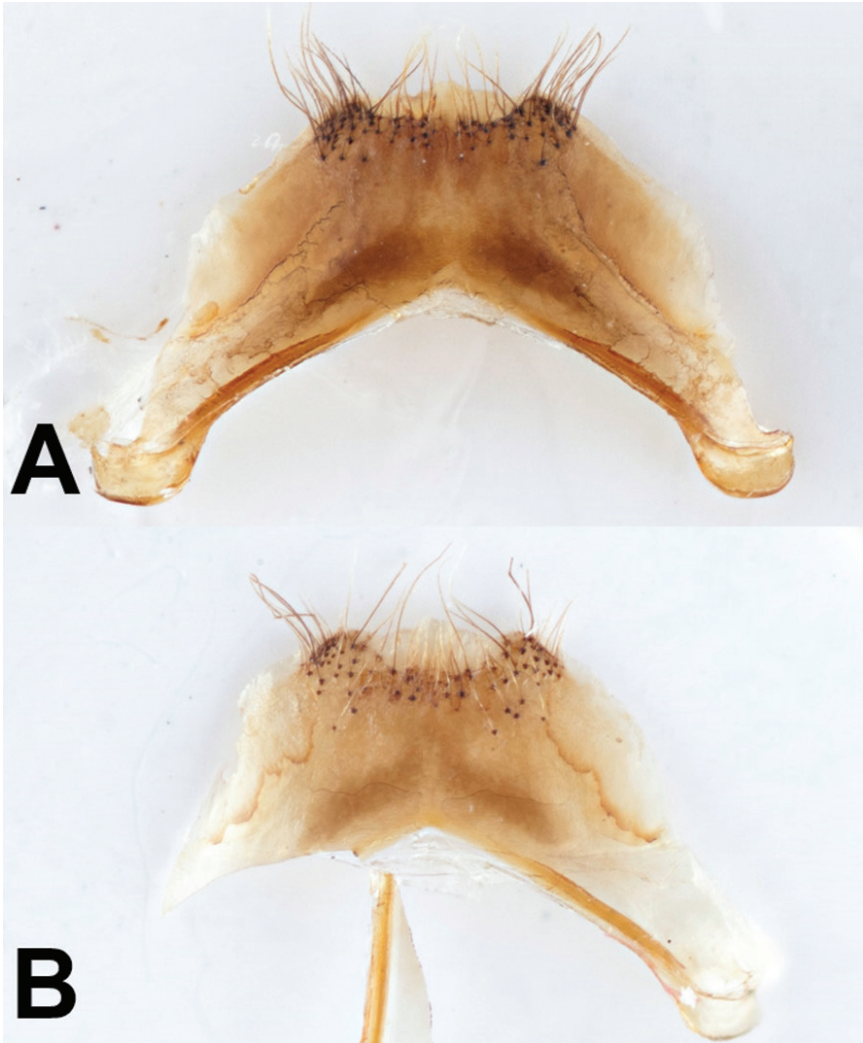


Figure 9. Sternum 7 of male **A** *Bombus johanseni*, and **B** *B. lapponicus sylvicola*.

sternum 7 has more elongate hairs on the apicolateral edges, with a shallower apicomedial depression somewhat rectangular, approximately $1/4$ as deep as wide (Fig. 9a), but broadly U-shaped in *B. lapponicus sylvicola*, and $1/3$ as deep as wide (Fig. 9b).

Discussion

The *Bombus lapponicus* – complex (Williams et al. 2014) has been of interest to many researchers in the Old World for some time, with many taxa recognized at subspecific rank (e.g., Pittioni 1942, 1943), but also as distinct species in the past (Svensson 1979;

Pekkarinen 1982; Martinet et al. 2018) and more recently (Gjershaug et al. 2013; Potapov et al. 2017, 2019). In a recent treatment of the North American members, Martinet et al. (2019) recognized *B. lapponicus sylvicola* as a Nearctic subspecies, with the typical taxon occurring in the Palearctic, supporting previous speculation on the status of this species (e.g., Pittioni 1943, Thorp 1962; Thorp et al. 1983; Williams et al. 2014). Hines et al. (2006) indicated that this species group originated in the New World, with dispersal to the Old World occurring within the last 4 million years. Though colour variation in *B. lapponicus* in the Old World is substantial (see Gjershaug et al. 2013), resulting in the past recognition of many subspecific taxa (i.e., Pittioni 1943), it mostly retains the colour pattern typical of the Western Nearctic taxon in parts of its Old World range (Hines et al. 2006; Williams 2007; Martinet et al. 2019). Exceptions include the specimens originally described as *B. gelidus* Cresson, 1878 described from Alaska (Cresson 1878) and *Bremus sylvicola* var. *lutzi* Frison, 1923 described from Arizona (Frison 1923), both of which have the pleura with dark hairs in the lower half, and the face with hairs mostly black, with slight intermixtures of pale hair (Cresson 1878; Franklin 1912; Frison 1923, 1927a). In North America, the typical form of *B. lapponicus sylvicola* is widespread in boreal-alpine areas, including throughout most of the north and in western mountain regions, though another dark form with the red hairs of terga 2 and 3 of the typical form replaced by black hairs is found in the Sierra Mountains of California (Williams et al. 2014). The nature and ecological significance of melanism in bumble bees has been the subject of several studies (e.g., Williams 2007; Rapti et al. 2014; Polidori et al. 2017), and significant variation is common within and among species (Stephen 1957; Williams et al. 2014; Huang et al. 2015).

Martinet et al. (2019) also described another member of this species complex sharing this colour pattern, *B. interacti*, a species almost identical to *B. lapponicus sylvicola*, with mostly pale pleura in both sexes, and presumably with identical male genitalia; only slight morphological differences in pubescence colour and density were noted, in addition to the molecular and semio-chemical differences (Martinet et al. 2019). The differences in males of these two taxa, as diagnosed by Martinet et al. (2019), were based on the pubescence of the [hind] tibia, being “very hairy” in *B. lapponicus sylvicola* but presumably not so in the holotype male of *B. interacti*, the latter thus matching Franklin’s description of the male of *B. gelidus* (Franklin 1912); we now assume that what Franklin (1912) was describing was likely the male of *B. johanseni*/*B. interacti*. As reported by Sikes and Rykken (2020), *B. interacti* is considered very rare, representing one of almost 34,000 bumble bee records in that study; the type series contained ten males and four queens from Alaska (Martinet et al. 2019). Also, in that work, Martinet et al. (2019) supported the opinion of some earlier works (e.g., Franklin 1912; Frison 1927a, 1927b; Stephen 1957; Hurd 1979; Williams et al. 2014), but not all (Ashmead 1902; Lutz 1916; Lutz and Cockerell 1920) on the affinity of *B. gelidus* to *B. lapponicus sylvicola*, treating it as a synonym (i.e., as forma *gelidus*) and indicating that it was just a melanistic form. Williams et al. (2014) also mentioned *B. gelidus* as a dark form of *B. lapponicus sylvicola* (with dark hairs on the face and sides of the thorax) found most

frequently in Alaska, but did not include a representative colour pattern to account for the variation in this species. *Bombus gelidus* was described from the Aleutian Islands of Alaska (Cresson 1878), albeit only from the single female (queen) type specimen that was examined by Martinet et al. (2019). Other materials identified as *B. gelidus* by T.D.A. Cockerell and incorrectly labelled as co-types by Franklin (1912) were typical *B. lapponicus sylvicola* according to Martinet et al. (2019); among this material was one additional queen, 14 workers, and a male. Like the holotype, these specimens were also from Alaska, including the Shumagin Islands group (Popoff Island), the Aleutian Islands (Nualaska, presumably Unalaska), and from the southern mainland (Koyukuk River, Kukak Bay) and collected by Trevor Kincaid during the Harriman Alaska Expedition in 1899. Ashmead (1902) originally published on the Hymenoptera collected during the Harriman Alaska Expedition, and in addition to identifying *B. gelidus* (after examining the holotype) from the Pribilof Islands, an island group much more isolated than the Aleutian Islands, he also (and incorrectly) synonymized *B. kincaidii* Cockerell, 1898 (= *Bombus (Alpinobombus) polaris* Curtis, 1835) under that species. Bequaert (1920) also identified *B. gelidus* from Alaska, from Kodiak, Katmai, and Valdez. An additional, albeit aberrant worker of *B. gelidus* was mentioned but not described by Franklin (1912) from Signuia, Baffin Island (Nunavut) (Fig. 10), which if correct would suggest that the melanistic form was more widespread than just Alaska (Williams et al. 2014; Martinet et al. 2019); an alternative and more likely explanation is that this aberrant specimen was what Sladen (1919) later named *B. sylvicola* var. *johanseni*. Similarly, Lutz (1916) recorded five additional specimens of *B. gelidus* from Battle Harbor, Labrador collected by C.W. Leng, but Lutz and Cockerell (1920) later determined these to be *B. ternarius*, typically a southern species in the east (Lavery and Harder 1988) though more recently found in Nunavut (Gibson et al. 2018). However, Packard (1891) recorded *Bombus lacustris* Cresson, 1863 (= *B. melanopygus*) as common on the northern coast of Labrador, though Frison (1926) suggested that these were likely *B. lapponicus sylvicola*, a species much more common in northern Labrador than *B. melanopygus* (Williams et al. 2014). As Cresson (1863) described *B. lacustris* as a taxon with much black hair intermixed with the yellow on the head and thorax, it is possible Packard (1891) observed *B. johanseni*, not *B. lapponicus sylvicola*, thus supporting its presence in Labrador. Another possibility is that these were atypical *B. ternarius*, as specimens from Labrador and insular Newfoundland typically have large intermixtures of black and yellow hair on the anterior thorax (Fig. 7c, d), thus resembling *B. melanopygus*.

Stephen (1957) also examined material identified as *B. gelidus* from Alaska, but indicated that the male genitalia and sterna 7 and 8 were similar to that of *B. melanopygus*, though he also felt that *B. lapponicus sylvicola* and *B. melanopygus* were virtually indistinguishable in parts of their ranges, so these specimens may have been misidentified. The male of *B. gelidus* was apparently known by Franklin (1912) and Bequaert (1920), the former offering a brief description, but was described in more detail by Martinet et al. (2019). The morphological characteristics used to distinguish *B. gelidus*/*B. lapponicus sylvicola* from *B. interacti* were subtle (Martinet et al. 2019).

Unfortunately, Sladen's taxon *B. sylvicola* var. *johanseni* has received little attention, and until this time it was still considered conspecific with *B. lapponicus sylvicola*

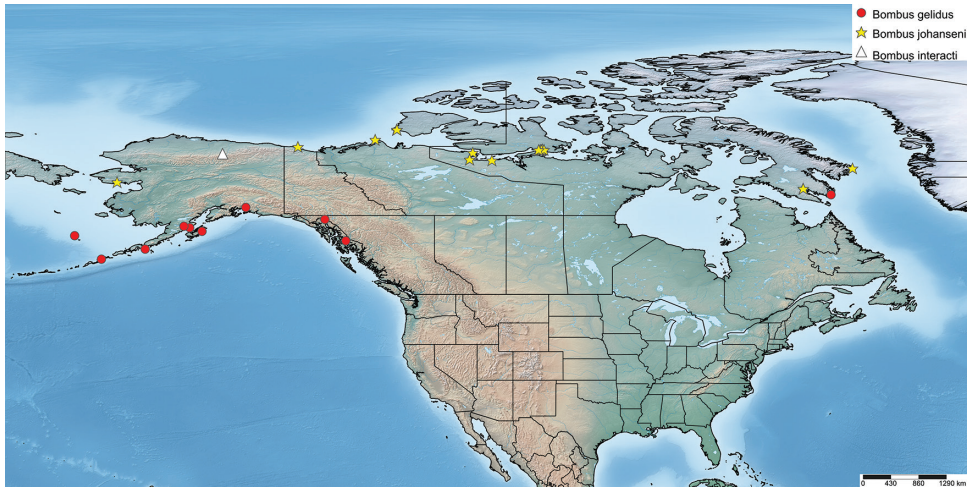


Figure 10. Distribution map of known specimens of *B. johanseni*, including *B. interacti*. Specimens identified in the literature as *B. gelidus* are also included as it is likely that some of these, especially the eastern record, are actually *B. johanseni*, and not dark specimens of *B. sylvicola*.

(Lutz and Cockerell 1920; Pittioni 1943; Hurd 1979), nor was it included in the treatments of Stephen (1957) and Thorp et al. (1983) for western North America, nor Lavery and Harder (1988) in the east. Though clearly described as a melanistic variety of *B. lapponicus sylvicola* (Sladen 1919), seemingly even much more so than *B. gelidus* (Figs 2, 4a, b; Martinet et al. 2019: fig. 7), with a distribution now known to range far into Canada's eastern arctic region westward to Alaska (Fig. 10), Sladen's taxon has largely been ignored. Genetic (Fig. 1) and morphological evidence provided here allies *B. johanseni* most closely with *B. glacialis*, a species with a similar northern distribution in the Old World (Potapov et al. 2017, 2019) and considered a valid species in the phylogenetic analysis of Martinet et al. (2019); both *B. johanseni* and *B. glacialis* are clearly genetically distinct (3.5% and 2.8%, respectively) from *B. lapponicus s. l.* (Fig. 1, and see Potapov et al. 2017 and Martinet et al. 2019). Molecular data (Fig. 1), the distinct colour patterning (Figs 2, 4, 6), male genitalia (Fig. 8) and sternum 7 (Fig. 9) provide evidence that *B. johanseni* is not a melanistic form of *B. lapponicus sylvicola*, but rather a distinct taxon with a northern Nearctic distribution. Additionally, *B. johanseni* males are seemingly morphologically similar to those of *B. interacti*, and also do not differ genetically (Fig. 1), supporting the synonymy above. Females of *B. johanseni* are also morphologically similar to dark females of *B. lapponicus sylvicola* (i.e., *B. gelidus*), though the latter taxon almost always has some pale hairs on the face and seems more common in southern Alaska (Fig. 10), though more sampling is required to determine the extent of this form. As *B. johanseni* is the oldest name available for this taxon, we here consider it a valid species, and as COI sequences from these darker taxa match the male holotype of *B. interacti*, we synonymize that species under *B. johanseni*, considering it a rarer (Fig. 10; and see Sikes and Rykken 2020) paler form. As shown by Huang et al. (2015) and Williams et al. (2019), species with wide variance in colour pattern may show little

covariation in COI. At present, the darker forms of *B. johanseni* seem widespread across northern North America (Fig. 10), while the females of the pale form are seeming only observed, albeit rarely, in Alaska (Martinet et al. 2019; Sikes and Rykken 2020).

Future phylogenetic analysis that includes all New and Old World *Pyrobombus* may clarify the relationships between *B. johanseni* and *B. glacialis*, though it would be very useful to obtain additional material, including males, from the Aleutian Islands for additional molecular and morphological analyses. This island chain has proven an interesting link to the Old World bumble bee fauna (Williams and Thomas 2005, Sheffield and Williams 2011). Until a globally comprehensive phylogeny of *Pyrobombus* that includes molecular data and males from all taxa (including those treated as synonymies and known from one sex) occurs, the relationships of the taxa, and between the fauna of the Nearctic and Palearctic faunas will hold some unresolved issues. In the meantime, much work will be required to reassess collections to verify the identity of material presently identified as *B. lapponicus sylvicola*, and *B. melanopygus* from northern North America to facilitate conservation assessments (e.g., Hatfield et al. 2014; Canadian Endangered Species Conservation Council 2016) and studies of distribution (e.g., Williams et al. 2014; Sikes and Rykken 2020).

Acknowledgements

Thanks to Andy Bennett and Sophie Cardinal (Canadian National Collection of Insects (CNC), Ottawa) and Joel Kits (Joel Kits, Ottawa Research and Development Centre, Ottawa) for providing photographs of the holotype of *B. sylvicola* var. *johanseni*, and Jason Weintraub and Jon Gelhaus (Department of Entomology, Academy of Natural Sciences, Philadelphia) for photographs of the holotype of *B. gelidus* during a difficult time of museum closure due to COVID-19. We thank the Government of the Northwest Territories, Wildlife Division, Environment and Natural Resources who provided some of the funding for inventory in that territory, with sincere thanks to Suzanne Carriere (Government of the Northwest Territories, Yellowknife) and Allison Thompson (Wildlife Management Advisory Council [Northwest Territories], Inuvik) for advice, facilitation, local knowledge and genuine support for work in that territory. We received kind help from Rosemin Nathoo (Wildlife Management Advisory Council), John and Samantha Lucas, Kyle Wolki, the Hunters and Trappers Committee, staff at the Sachs Harbour Parks Canada office and many others in the community of Sachs Harbour, Northwest Territories. Funding from NatureServe Canada contributed to the processing of specimens collected in Northwest Territories and Yukon. Additional thanks to Paul Williams (Natural History Museum, London) for encouraging continued research on bumble bee taxonomy, and to Paul and Pierre Rasmont (Université de Mons, Mons, Belgium) for constructive comments and critique of the manuscript. Thanks also to Doug Yanega (University of California, Riverside, Riverside) for continued discussions of the ICZN code – it is always much appreciated.

This work is dedicated to Dr. Ken W. Richards (1946–2019) for his work on Canadian bees, including arctic bumble bees.

References

- Ashmead WH (1902) Papers from the Harriman Alaska Expedition. XXVIII. Hymenoptera. Proceedings of the Washington Academy of Sciences 4: 117–274. <https://doi.org/10.5962/bhl.part.18572>
- Bequaert J (1920) Scientific results of the Katmai Expeditions of the National Geographic Society. XIII. Bees and wasps. The Ohio Journal of Science 20(7): 292–297.
- Canadian Endangered Species Conservation Council (2016) Wild Species 2015: The General Status of Species in Canada. National General Status Working Group, 128 pp. http://www.registrelep-sararegistry.gc.ca/virtual_sara/files/reports/Wild%20Species%202015.pdf
- Cresson ET (1863) List of the North American species of *Bombus* and *Apathus*. Proceedings of the Entomological Society of Philadelphia 2: 83–116.
- Cresson ET (1878) Descriptions of new species of North American bees. Proceedings of the Academy of Natural Sciences of Philadelphia 30: 181–221.
- Franklin HJ (1912) The Bombidae of the New World. Transactions of the American Entomological Society 38 (3/4): 177–486. <http://www.jstor.org/stable/25076901>
- Frison TH (1923) Systematic and biological notes on bumblebees (Bremidae; Hymenoptera). Transactions of the American Entomological Society 48(4): 307–326. <http://www.jstor.org/stable/25077076>
- Frison TH (1927a) Records and descriptions of western bumblebees (Bremidae). Proceedings of the California Academy of Sciences, Fourth Series 16(12): 365–380.
- Frison TH (1927b) A contribution to our knowledge of the relationships of the Bremidae of America North of Mexico (Hymenoptera). Transactions of the American Entomological Society 53(2): 51–78. <http://www.jstor.org/stable/25077174>
- Frison TH (1929) Additional descriptions, synonymy and records of North America bumblebees (Hymenoptera: Bremidae). Transactions of the American Entomological Society 55(2): 103–117. <http://www.jstor.org/stable/25077215>
- Ghisbain G, Lozier JD, Rahman SR, Ezray BD, Tian L, Ulmer JM, Heraghty SD, Strange JP, Rasmont P, Hines HM (2020) Substantial genetic divergence and lack of recent gene flow support cryptic speciation in a colour polymorphic bumble bee (*Bombus bifarius*) species complex. Systematic Entomology 45(3): 635–652. <https://doi.org/10.1111/syen.12419>
- Gibson SD, Bennet K, Brooks RW, Langer SV, MacPhail VJ, Beresford DV (2018) New records and range extensions of bumble bees (*Bombus* spp.) in a previously undersampled region of North America's Boreal Forest. Journal of the Entomological Society of Ontario 149: 1–14.
- Gjershaug JO, Staverløll A, Kleven O, Ødegaard F (2013) Species status of *Bombus monticola* Smith (Hymenoptera: Apidae) supported by DNA barcoding. Zootaxa 3716(3): 431–440. <https://doi.org/10.11646/zootaxa.3716.3.6>
- Hatfield R, Colla S, Jepsen S, Richardson L, Thorp R, Foltz Jordan S (2014). IUCN Assessments for North American *Bombus* spp. Xerces Society for Invertebrate Conservation, Portland, Or. 56 pp. <https://xerces.org/sites/default/files/publications/14-065.pdf>
- Hebert PDN, Cywinska A, Ball S, deWaard J (2003) Biological identifications through DNA barcodes. Proceedings of the Royal Society of London. Series B: Biological Sciences 270(1512): 313–321. <https://doi.org/10.1098/rspb.2002.2218>

- Hines HM, Cameron SA, Williams PH (2006) Molecular phylogeny of the bumble bee subgenus *Pyrobombus* (Hymenoptera: Apidae: Bombus) with insights into gene utility for lower-level analysis. *Invertebrate Systematics* 20(3): 289–303. <https://doi.org/10.1071/IS05028>
- Huang J, Wu J, An J, Williams PH (2015) Newly discovered colour-pattern polymorphism of *Bombus koreanus* females (Hymenoptera: Apidae) demonstrated by DNA barcoding. *Apidologie* 46: 250–261. <https://doi.org/10.1007/s13592-014-0319-9>
- Hurd PD (1979) Superfamily Apoidea. In: Krombein KV, Hurd PD, Smith DR, Burks BD (Eds) *Catalog of Hymenoptera in America North of Mexico. Volume 2. Apocrita (Aculeata)*. Smithsonian Institution Press, Washington, 2209 pp.
- International Commission on Zoological Nomenclature (1999) *International Code of Zoological Nomenclature*. Fourth edition. International Trust for Zoological Nomenclature, London, xxix + 306 pp.
- Koch J, Rodriguez J, Pitts J, Strange J (2018) Phylogeny and population genetic analyses reveals cryptic speciation in the *Bombus fervidus* species complex (Hymenoptera: Apidae). *PLOS ONE* 13(11): e0207080. <https://doi.org/10.1371/journal.pone.0207080>
- Kumar S, Stecher G, Li M, Knyaz C, Tamura K (2018) MEGA X: Molecular Evolutionary Genetics Analysis across computing platforms. *Molecular Biology and Evolution* 35(6): 1547–1549. <https://doi.org/10.1093/molbev/msy096>
- Laverty T, Harder L (1988) The bumble bees of eastern Canada. *The Canadian Entomologist* 120(11): 965–987. <https://doi.org/10.4039/Ent120965-11>
- Lutz FE (1916) The geographic distribution of Bombidae (Hymenoptera), with notes on certain species of Boreal America. *Bulletin of the American Museum of Natural History* 35(26): 501–521. <http://hdl.handle.net/2246/1387>
- Lutz FE, Cockerell TDA (1920) Notes on the distribution and bibliography of North American bees of the families Apidae, Meliponidae, Bombidae, Euglossidae and Anthophoridae. *Bulletin of the American Museum of Natural History* 42(15): 491–641. <https://doi.org/10.5962/bhl.title.17909>
- Martinet B, Lecocq T, Brasero N, Biella P, Urbanová K, Valterová I, Cornalba M, Gjershaug JO, Michez D, Rasmont P (2018) Following the cold: geographical differentiation between interglacial refugia and speciation in the arcto-alpine species complex *Bombus monticola* (Hymenoptera: Apidae). *Systematic Entomology* 43(1): 200–217. <https://doi.org/10.1111/syen.12268>
- Martinet B, Lecocq T, Brasero N, Gerard M, Urbanová K, Valterová I, Gjershaug JO, Michez D, Rasmont P (2019) Integrative taxonomy of an arctic bumblebee species complex highlights a new cryptic species (Apidae: *Bombus*). *Zoological Journal of the Linnean Society* 187(3): 599–621. <https://doi.org/10.1093/zoolinnean/zlz041>
- Packard AS (1891) *The Labrador coast*. N. D. C. Hodges, New York, 513 pp. <https://doi.org/10.5962/bhl.title.48506>
- Pekkarinen A (1982) Morphology and specific status of *Bombus lapponicus* (Fabricius) and *B. monticola* Smith (Hymenoptera: Apidae). *Insect Systematics & Evolution* 13(1): 41–46. <https://doi.org/10.1163/187631282X00525>
- Pittioni B (1942) Die borealpinen Hummeln und Schmarotzerhummeln (Hymen., Apidae, Bombinae). I. Teil. Mitteilungen aus den Königlichen Naturwissenschaftlichen Instituten in Sofia 15: 155–218.

- Pittioni B (1943) Die borealpinen Hummeln und Schmarotzerhummeln (Hymen., Apidae, Bombinae). II. Teil. Mitteilungen aus den Königlichen Naturwissenschaftlichen Instituten in Sofia 16: 1–77.
- Polidori C, Jorge A, Ornos C (2017) Eumelanin and pheomelanin are predominant pigments in bumblebee (Apidae: *Bombus*) pubescence. PeerJ 5: e3300. <https://doi.org/10.7717/peerj.3300>
- Potapov GS, Kondakov AV, Filippov BY, Gofarov MY, Kolosova YS, Spitsyn VM, Tomilova AA, Zubrii NA, Bolotov IN (2019) Pollinators on the polar edge of the Ecumene: taxonomy, phylogeography, and ecology of bumble bees from Novaya Zemlya. ZooKeys 866: 85–115. <https://doi.org/10.3897/zookeys.866.35084>
- Potapov GS, Kondakov AV, Spitsyn VM, Filippov BY, Kolosova YS, Zubrii NA, Bolotov IN (2017) An integrative taxonomic approach confirms the valid status of *Bombus glacialis*, an endemic bumblebee species of the High Arctic. Polar Biology 41(4): 629–642. <https://doi.org/10.1007/s00300-017-2224-y>
- Rapti Z, Duennes MA, Cameron SA (2014) Defining the colour pattern phenotype in bumble bees (*Bombus*): a new model for evo devo. Biological Journal of the Linnean Society 113(2): 384–404. <https://doi.org/10.1111/bij.12356>
- Ratnasingham S, Hebert PDN (2007) BOLD: The Barcode of Life Data System (<http://www.barcodinglife.org>). Molecular Ecology Notes 7(3): 355–364. <https://doi.org/10.1111/j.1471-8286.2007.01678.x>
- Ratnasingham S, Hebert PDN (2013) A DNA-Based Registry for All Animal Species: The Barcode Index Number (BIN) System. PLOS ONE 8(7): e66213. <https://doi.org/10.1371/journal.pone.0066213>
- Rehan SM, Sheffield CS (2011) Morphological and molecular delineation of a new species in the *Ceratina dupla* species-group (Hymenoptera: Apidae: Xylocopinae) of eastern North America. Zootaxa 2873: 35–50. <https://doi.org/10.11646/zootaxa.2873.1.3>
- Sarazin M (1986) Primary types of Aculeata (Hymenoptera) in the Canadian National Collection. The Canadian Entomologist 118(4): 287–318. <https://doi.org/10.4039/Ent118287-4>
- Sheffield CS, Williams PH (2011) Discover of *Bombus distinguendus* (Hymenoptera: Apidae) in continental North America. Journal of the Entomological Society of Ontario 142: 53–56.
- Sheffield CS, Hebert PDN, Kevan PG, Packer L (2009) DNA barcoding a regional bee (Hymenoptera: Apoidea) fauna and its potential for ecological studies. Molecular Ecology Resources 9: 196–207. <https://doi.org/10.1111/j.1755-0998.2009.02645.x>
- Sheffield CS, Ratti C, Packer L, Griswold T (2011) Leafcutter and mason bees of the genus *Megachile* Latreille (Hymenoptera: Megachilidae) in Canada and Alaska. Canadian Journal of Arthropod Identification 18: 1–107.
- Sheffield CS, Frier SD, Dumesh S (2014) The bees (Hymenoptera: Apoidea, Apiformes) of the Prairies Ecozone, with comparisons to other grasslands of Canada. In: Giberson DJ, Cárcamo HA (Eds) Arthropods of Canadian Grasslands: Biodiversity and Systematics Part 2. 4. Biological Survey of Canada, Ottawa, 479 pp.
- Sheffield CS, Richardson L, Cannings S, Ngo H, Heron J, Williams PH (2016) Biogeography and designatable units of *Bombus occidentalis* Greene and *B. terricola* Kirby (Hymenoptera: Apidae) with implications for conservation status assessments. Journal of Insect Conservation 20(2): 189–199. <https://doi.org/10.1007/s10841-016-9853-2>

- Sheffield CS, Heron J, Gibbs J, Onuferko TM, Oram R, Best L, deSilva N, Dumesh S, Pindar A, Rowe G (2017) Contribution of DNA barcoding to the study of the bees (Hymenoptera: Apoidea) of Canada: progress to date. *The Canadian Entomologist* 149(6): 736–754. <https://doi.org/10.4039/tce.2017.49>
- Shorthouse DP (2010) SimpleMappr, an online tool to produce publication-quality point maps. <https://www.simplemappr.net> [accessed 22 June 2020]
- Sikes DS, Rykken JJ (2020) Update to the identification guide to female Alaskan bumble bees and a summary of recent changes to the Alaskan bumble bee fauna. *Newsletter of the Alaska Entomological Society* 13(1): 31–38.
- Sladen FWL (1919) The wasps and bees collected by the Canadian Arctic Expedition, 1913–1918. *Report of the Canadian Arctic Expedition 1913–18* 3: 25–35.
- Stephen WP (1957) Bumble bees of western North America (Hymenoptera: Apoidea). Oregon State College Agricultural Experiment Station Technical Bulletin 40: 1–163.
- Svensson BG (1979) *Pyrobombus lapponicus* auct., in Europe recognized as two species: *P. lapponicus* (Fabricius, 1793) and *P. monticola* (Smith, 1849) (Hymenoptera, Apoidea, Bombinae). *Insect Systematics & Evolution* 10(4): 275–296. <https://doi.org/10.1163/187631279X00178>
- Thorp RW (1962) Notes on the distributions of some bumblebees of western North America (Hymenoptera: Apidae). *The Pan-Pacific Entomologist* 38: 21–28.
- Thorp RW, Horning DS, Dunning LL (1983) Bumble bees and cuckoo bumble bees of California (Hymenoptera: Apidae). *Bulletin of the California Insect Survey* 23: 1–79.
- Vickruck JL, Rehan SM, Sheffield CS, Richards MH (2012) Nesting biology and DNA barcode analysis of *Ceratina dupla* and *C. mikmaqi*, and comparisons with *C. calcarata* (Hymenoptera: Apidae: Xylocopinae). *The Canadian Entomologist* 143(3): 254–262. <https://doi.org/10.4039/n11-006>
- Williams PH (1985) A preliminary cladistic investigation of relationships among the bumble bees (Hymenoptera, Apidae). *Systematic Entomology* 10: 239–255. <https://doi.org/10.1111/j.1365-3113.1985.tb00529.x>
- Williams PH (2007) The distribution of bumblebee colour patterns worldwide: possible significance for thermoregulation, crypsis, and warning mimicry. *Biological Journal of the Linnean Society* 92(1): 97–118. <https://doi.org/10.1111/j.1095-8312.2007.00878.x>
- Williams PH, Thomas J (2005) A bumblebee new to the New World: *Bombus distinguendus* (Hymenoptera: Apidae). *The Canadian Entomologist* 137(2): 158–162. <https://doi.org/10.4039/n04-056>
- Williams PH, Brown MJF, Carolan JC, An J, Goulson D, Aytekin AM, Best LR, Byvaltsev AM, Cederberg B, Dawson R, Huang J, Ito M, Monfared A, Raina RH, Schmid-Hempel P, Sheffield CS, Šima P, Xie Z (2012) Unveiling cryptic species of the bumblebee subgenus *Bombus s. str.* worldwide with COI barcodes (Hymenoptera: Apidae). *Systematics and Biodiversity* 10(1): 21–56. <https://doi.org/10.1080/14772000.2012.664574>
- Williams PH, Cannings SG, Sheffield CS (2016) Cryptic subarctic diversity: a new bumblebee species from the Yukon and Alaska (Hymenoptera: Apidae). *Journal of Natural History* 50: 2881–2893. <https://doi.org/10.1080/00222933.2016.1214294>
- Williams PH, Thorp RW, Richardson LL, Colla SC (2014) *Bumble Bees of North America*. Princeton University Press, Princeton, 208 pp.

- Williams PH, Berezin MV, Cannings SG, Cederberg B, Ødegaard F, Rasmussen C, Richardson LL, Rykken J, Sheffield CS, Thanooosing C, Byvaltsev AM (2019) The arctic and alpine bumblebees of the subgenus *Alpinobombus* revised from integrative assessment of species' gene coalescents and morphology (Hymenoptera, Apidae, *Bombus*). *Zootaxa* 4625(1): 1–68. <https://doi.org/10.11646/zootaxa.4625.1.1>
- Yanega D (2013) The status of Cockerell's Bumblebee, *Bombus (Pyrobombus) cockerelli* Franklin, 1913 (Hymenoptera: Apidae). *Southwestern Entomologist* 38(3): 517–522. <https://doi.org/10.3958/059.038.0313>

New stiletto flies from New Caledonia (Therevidae, Agapophytinae)

Michael E. Irwin^{1,2}, Shaun L. Winterton³, Mark A. Metz⁴

1 Emeritus, University of Illinois, Urbana-Champaign, Illinois, USA **2** University of Arizona, Tucson, USA
3 California State Collection of Arthropods, California Department of Food & Agriculture, Sacramento, California, USA **4** USDA, ARS, Systematic Entomology Laboratory, Beltsville, Maryland, USA

Corresponding author: Shaun L. Winterton (wintertonshaun@gmail.com)

Academic editor: M. Hauser | Received 23 April 2020 | Accepted 16 September 2020 | Published 4 November 2020

<http://zoobank.org/D8B945AE-6209-4957-8BB1-D96DDBB5AA44>

Citation: Irwin ME, Winterton SL, Metz MA (2020) New stiletto flies from New Caledonia (Therevidae, Agapophytinae). ZooKeys 984: 83–132. <https://doi.org/10.3897/zookeys.984.53587>

Abstract

Stiletto-flies (Diptera: Therevidae) are highly diverse and species-rich in Australia and New Zealand, yet relatively few species have been recorded from neighbouring Papua New Guinea, Indonesia and throughout the remainder of Oceania. Indeed, in New Caledonia only a single species of the widely distributed Australasian genus *Anabarhynchus* Macquart (Therevinae) is previously known. Herein we describe two new agapophytine genera (i.e., *Jeanchazeauia* **gen. nov.**, *Calophytus* **gen. nov.**), together comprising nine charismatic new species; this represents a first record of the subfamily from New Caledonia. The new genera and species are described and figured.

Keywords

Asiloidea, Australasia, Diptera, Oceania

Introduction

Stiletto flies (Diptera: Therevidae) comprise more than 1200 species in ca. 130 genera worldwide, with the family divided into four subfamilies: Therevinae, Xestomyzinae, Phycusinae, and Agapophytinae (Winterton et al. 2016). They are present in all major

biogeographical regions and are particularly common and diverse in mesic to xeric habitats. The greatest species-level diversity is in the subfamily Therevinae, followed by Agapophytinae, with the other two smaller subfamilies much less species-rich. Individuals of Agapophytinae can be distinguished from other therevids by the following characteristics: 1) absence of adpressed scale-like setae on the femora; 2) female genitalia internally with three spermathecae and a spermathecal sac; and 3) male genitalia always have an articulated inner gonocoxal process and an aedeagus with a strongly forked ventral apodeme (Winterton et al. 2001, 2016). The presence of adpressed scale-like setae on the femora is a unique characteristic found only in Therevinae and is the main external feature used to differentiate Therevinae from other subfamilies; all other important characters used to separate subfamilies are internal and genitalic. Caution should be used though in the Australasian and Neotropical regions as one group of therevine genera (the *Anabarhynchus* genus-group: *Anabarhynchus* Macquart, 1848; *Megathereva*, Lyneborg, 2001; *Microthereva* Malloch, 1932; *Peralia* Malloch, 1932) typically lack adpressed setae on the femora, although they exhibit all other therevine characteristics.

While Therevinae are cosmopolitan in their distribution, Agapophytinae are a distinctively southern hemisphere radiation found in Australia, Indonesia, New Zealand, Papua New Guinea and South America. The bulk of the agapophytine generic diversity occurs in Australasia, although four genera have been described from South America (Webb et al. 2013; Irwin and Winterton 2020). Relatively few species are known from Papua New Guinea and Indonesia. Here we describe two new genera of Agapophytinae from near-by New Caledonia, an archipelago in the South Pacific comprised of Grande Terre, the Loyalty Islands, and a series of smaller islands. It is located in the Coral Sea southeast of Vanuatu, 1200 km to the east of Australia and 2400 km north of New Zealand. One subspecies of the aforementioned genus *Anabarhynchus* (i.e., *A. hyalipennis varicineta* (Bigot, 1860)) is distributed widely in New Caledonia and Vanuatu; the other subspecies (*A. hyalipennis hyalipennis* (Macquart, 1846)) is distributed widely throughout Australia, including Lord Howe and Norfolk Islands (Lyneborg 2001). The remaining stiletto fly fauna newly described here comprises two new genera containing nine new species endemic to New Caledonia. *Calophytus* gen. nov. and *Jeanchazeauia* gen. nov. were previously included in a phylogenetic study of Therevidae by Winterton et al. (2016) (as undescribed genus 'NC'), who recovered them as members of the *Taenogera* genus-group (Agapophytinae) (Fig. 4). The New Caledonia genera were recovered as sister to the remaining *Taenogera* genus-group, which includes the genera *Collessiama* Lambkin, 2013, *Ectinorhynchus* Macquart, 1850, *Evansomyia* Mann, 1928, *Taenogera* Kröber, 1912 and *Taenogarella* Winterton & Irwin, 1999b (see Winterton et al. 1999b; Winterton et al. 2016). It also includes the genus *Squamopygia* Kröber, 1928, and while this genus was not included in their molecular phylogenetic study by Winterton et al. (2016) it was included in the morphological phylogeny by Winterton et al. (1999b), where it was placed as sister to *Ectinorhynchus* and *Evansomyia*. Winterton

et al. (2016) hypothesised that the common ancestor of the New Caledonia genera and the Australasian genera of the *Taenogera* genus-group diverged during the end of the Palaeogene or the start of the Neogene (12–23 MYA). This suggests that this New Caledonia stiletto-fly fauna is a relative recent radiation of closely related taxa whose common ancestor arrived via dispersal from Papua New Guinea, New Zealand or Australia.

Materials and methods

Adult morphological terminology follows Cumming and Wood (2017) with additional therevoid-specific genitalic morphology according Winterton et al. (1999a, b, c) and Winterton (2006). Genitalia were macerated in 10% KOH or lactic acid to remove soft tissue, then rinsed in dilute glacial acetic acid or distilled water, respectively, and dissected in 80% ethanol or glycerine. Genitalia preparations were placed in glycerine in a genitalia vial mounted on the pin beneath the specimen. Specimen images were taken at different focal points using a digital camera and subsequently combined into a serial montage image. Specimens have a unique number attached to them usually on a separate yellow label with ME Irwin Therevidae Specimen Number “MEI99999”. These are contained in a specimen database ‘Mandala’ (Kampmeier and Irwin 2009). All new nomenclatural acts are registered in ZooBank (Pyle and Michel 2008). Specimens are deposited in the following institutions:

- BPBM** Bishop Museum, Honolulu, Hawai’i, USA;
- CSCA** California Food and Agricultural Department, Sacramento, California, USA;
- CNC** Canadian National Collection of Insects, Arachnids & Nematodes, Agriculture & Agri-Food Canada, Ottawa, Ontario, Canada;
- FSCA** Florida State Collection of Arthropods, Gainesville, Florida, USA;
- MNHN** Muséum national d’Histoire naturelle, Paris, Île-de-France, France;
- NHRS** Naturhistoriska Riksmuseet, Stockholm, Uppland, Sweden;
- QM** Queensland Museum, Brisbane, Queensland, Australia;
- UMSP** University of Minnesota, Saint Paul, Minnesota, USA.

Taxonomy

A key to genera of stiletto flies of New Caledonia is presented. While *Anabarhynchus hyalipennis varicineta* is a widely distributed species in both New Caledonia and Vanuatu, *Calophytus* gen. nov. and *Jeanchazeauia* gen. nov. are entirely endemic to Grande Terre. No other Therevidae have been recorded from New Caledonia. A revised key to Australasian genera is needed but is beyond the scope of this study.

Key to genera of New Caledonian Therevidae

- 1 Antennae much shorter than head length, flagellum strongly conical; wing markings largely absent; 2 pairs of scutellar macrosetae; fore- and midfemora with anteroventral and posteroventral macrosetae present; female sternite VIII with subapical, forked process projecting ventrally; two spermathecae present *Anabarhynchus* (i.e., *A. hyalipennis varicineta*)
- Antennae slightly to much longer than head, flagellum elongate and tapered apically; wing markings distinct, derived from infuscation of wing membrane and dark microtrichia; single pair of scutellar macrosetae; fore- and midfemora without macrosetae; female sternite VIII without projecting process; three spermathecae present **2**
- 2 Anepisternum glabrous, lacking silver pubescence (e.g., Fig. 9); wing with basal radial cell (br) bisected along its length by a stripe of microtrichia along wing fold (Fig. 8); scutellum polished or with sparse pubescence; hind femur lacking subapical anteroventral setae; single posteroventral macroseta midway along hind femur; female tergite VIII quadrangular-shaped (Fig. 23A) *Calophytus* gen. nov. (6 spp.) (Figs 9, 11, 13, 15, 16, 19)
- Anepisternum with silver pubescence (e.g., Fig. 28); wing with cell *br* not bisected by stripe of microtrichia, when microtrichia present then irregular and not arranged as a single stripe along wing fold (Fig. 7G, H); scutellum often with dense, matte pubescence; hind femur with one or more distinct subapical anteroventral macrosetae; posteroventral macrosetae present as series along hind femur but very small and sometimes barely evident; female tergite VIII short, ‘T’-shaped with anteromedial projection elongate, often with robust, up-curved setae laterally (Fig. 23B–D) *Jeanchazeauia* gen. nov. (3 spp.) (Figs 24, 25, 28, 29)

***Calophytus* gen. nov.**

<http://zoobank.org/CB02979A-20AF-4C4E-BFB1-B8D05668523C>

Type species. *Calophytus chazeauui* sp. nov., here designated.

Diagnosis. Antennae elongate, longer than head, narrow cylindrical; frons wider than ocellar tubercle at narrowest point with only slight sexual dimorphism; dorsocentral macrosetae absent; velutum patches absent on femora; single posteroventral macroseta present midway along hind femur; wing with hyaline areas often free of microtrichia; distinct stripe of dark microtrichia bisecting cell *br* along wing fold; male genitalia with gonocoxites without velutum patch and medial atrium (gonocoxites proximal medially).

Description. Antenna longer than head; flagellum cylindrical, slightly tapered distally, shorter than combined scape and pedicel length, rarely longer (in *C. webbi* sp. nov.); scape cylindrical, usually elongate; head shape in profile with length and height subequal; frons glossy, slightly protruding anterior to eye around base of antennae; frons wider than ocellar tubercle at narrowest point, only slight sexual dimorphism

in frons width with space between eyes slightly narrower in male; parafacial without setae, postocular macrosetae in both sexes arranged in a single row dorsally, rarely scattered dorsomedially on occiput (in *C. grandiosus* sp. nov.); prosternum without setae; fore and hind femoral velutum patches absent; femoral macrosetae absent except for single posteroventral macroseta present midway along hind femur; posterior surface of mid coxa without setae; hind femur and tibia relatively longer than that of fore and mid legs; post-spiracular setae absent; scutal chaetotaxy (pairs): notopleural (np), 1–2; supra alar (sa), 1; post alar (pa), 1; dorsocentral (dc), 0; scutellar (sc), 1; wing cell m_3 open to margin; wing vein R_{2+3} smoothly curved or straight to wing margin, wing with markings faint to strongly banded, hyaline areas often free of microtrichia; distinct stripe of dark microtrichia bisecting cell br along wing fold; abdominal tergite II with all setae uniform and regular in length. Male genitalia with dorsal apodeme of aedeagus ‘T’-shaped, distiphallus narrow, straight, ventral apodeme forked; gonocoxite with velutum patch absent, posteromedial margins proximal to each other; inner gonocoxal process (igp) present and articulated; ventral lobe small, rounded apically. Female genitalia with tergite VIII elongate, quadrangular, anteromedial process narrow; tergite VII lacking anteromedial process; acanthophorite setae as two sets (A1 & A2), A1 enlarged and rounded apically, A2 series prominent; sternite VIII emarginate posteromedially, flattened; spermathecal sac present, not lobed; three sac-like spermathecae present, joined to spermathecal sac duct near junction with bursa copulatrix.

Etymology. Derived from the Greek *kallos*, beauty; and *phyton*, plant, and relating to the charismatic appearance of the flies and the natural areas where they are collected in New Caledonia. The name also associates this genus with New Caledonia via the Proto-Celtic root of *kal*, hard, pertaining to the Roman name for the original provenance of Caledones in Britannia. Gender is masculine.

Comments. All species of *Calophytus* gen. nov. are medium to large stiletto flies, with heads mostly glossy with striking patches of silver pubescence on the parafacial and pleuron, banded wings and antennae longer than the head. Distinctive to members of *Calophytus* gen. nov. is the presence of a single posteroventral macroseta midway along the hind femur and a stripe of microtrichia along the wing fold bisecting an otherwise glabrous wing cell br. These two characteristics are also found in the genus *Squamopygia* from Australia and Papua New Guinea and appear unique to these two genera amongst all Therevidae; they are notably absent in *Jeanchazeauia* gen. nov. While Winterton et al. (2016) recovered a clear sister-group relationship between *Calophytus* gen. nov. and *Jeanchazeauia* gen. nov. (included in their study as undescribed genus ‘NC’) (Fig. 4), they did not include the rarely collected *Squamopygia*. The two aforementioned characters found only in *Squamopygia* and *Calophytus* gen. nov. also support a likely sister-group relationship between these two genera. *Squamopygia* is a monotypic genus with a single species from Northern Australia; two undescribed species are known from southern Australia and Papua New Guinea. *Calophytus* gen. nov. can be separated from *Squamopygia* by the absence of subapical anteroventral macrosetae on the hind femur (present in *Squamopygia*), absence of dorsocentral macrosetae (present in *Squamopygia*) and by the width of the male frons. The sexual dimorphism in male frons width is more pronounced in *Squamopygia* with the eyes being contiguous. In *Calophytus* gen. nov. (and *Jeanchazeauia*

gen. nov.) the male frons is only slightly narrower than that of the female, with the frons wider than the ocellar tubercle in both sexes. *Squamopygia* also has banded wings similar to *Calophytus* gen. nov., but the hyaline areas of the wing membrane retain extensive pale microtrichia. The male and female genitalia of *Squamopygia* and *Calophytus* are very similar. *Calophytus grandiosus* sp. nov. is rather distinct from all other *Calophytus* species, differing in the arrangement of postocular macrosetae, wing banding pattern and body size, supporting its position as sister to the rest of the genus (Fig. 4). *Calophytus* species have been collected in all of the main habitat types throughout New Caledonia, including rainforest, maquis scrub and dry sclerophyll forest (Figs 22, 31, 32).

Included species. *Calophytus chazeau* sp. nov., *C. grandiosus* sp. nov., *C. matilei* sp. nov., *C. monteithi* sp. nov., *C. schlingeri* sp. nov., *C. webbi* sp. nov.

Key to species of *Calophytus* gen. nov.

- 1 Postocular macrosetae densely scattered over entire occiput; maxillary palpi large, dark brown, bulbous; labellum brown; large, showy, banded-winged species, infuscation well demarcated (Figs 2, 11) ***C. grandiosus* sp. nov.**
- Postocular macrosetae concentrated as a single row along postocular ridge; maxillary palpi small, thin with base yellow and apical third light to dark brown; labellum yellowish apically; smaller, yellow to brown species, wing markings typically irregular or fenestrate, sometimes with diffuse margins, not distinctly banded **2**
- 2 Scutum predominantly black, sometimes orange laterally along notopleuron (e.g., Fig. 6C); scutellum black; abdomen ground colour dark brown, male abdomen with extensive silver velutum pubescence (e.g., Fig. 16B) **3**
- Scutum predominantly dark yellow orange, with dark dorsocentral stripes merging posteriorly (Fig. 6D); scutellum dark yellow, sometimes with brown suffusion (tint) medially; abdomen predominantly dark yellow, male (where known) abdomen lacking silver pubescence (Fig. 9B) **4**
- 3 Parafacial with silvery pubescence as an acute wedge-shaped patch along eye margin below antennal insertion, replaced by matte black pubescence ventrally along margin of buccal area; mid- and hind coxae extensively orange, midcoxa almost completely orange (Fig. 13) ***C. matilei* sp. nov.**
- Parafacial with silvery pubescence as an elongate wedge-shaped patch along eye margin below antennal insertion and extending ventrally along margin of buccal area; mid- and hind coxae extensively dark brown to black, often only apices orange (Fig. 16) ***C. schlingeri* sp. nov.**
- 4 Antennal flagellum longer than scape (Figs 5E, 20); costal cell of wing only with slight yellowish infuscation (Fig. 7E); scutellum with sparse silver pubescence; relatively small, diminutive individuals (body length: ca. 5.5–8.0 mm) (Fig. 19) ***C. webbi* sp. nov.**
- Antennal flagellum shorter than scape (Fig. 5A–D); costal cell of wing with distinct yellow infuscation (Fig. 7A, F); scutellum lacking silver pubescence; relatively larger individuals (body length: ca. 7.0–10.0 mm) **5**

- 5 Postocular macrosetae orange to brown; pleuron orange; frons around base of antenna, face, and parafacial yellow orange (Fig. 15).....*C. monteithi* sp. nov.
- Postocular macrosetae black; dorsal half of pleuron dark brown, orange in ventral half; frons, face and parafacial brown to black (Fig. 9).....*C. chazeaui* sp. nov.

***Calophytus chazeaui* sp. nov.**

<http://zoobank.org/F8FF4B02-80A9-4E0C-A5AA-8D52A274221A>

Figs 1, 5A, 7A, 8A, 9, 10, 22, 31A

Diagnosis. Scutum with large areas of orange; wing with dark infuscation over discal cell and parts of adjoining cells, as well most of apical third of wing; costal cell with yellow infuscation; male abdomen without silver velutum pubescence; occipital macrosetae black, arranged in single row dorsally in both sexes; legs yellow; flagellum shorter than scape.

Description. Length 7.8–10.6 mm. *Head.* Glossy black, smooth. Frons smooth, raised around base of antennae. Eyes separated at narrowest point by 3× width of median ocellus in both sexes. Parafacial with silver pubescence laterally along eye margin. Occiput silver pubescent laterally and ventrally onto gena, with fine white setae



Figure 1. *Calophytus chazeaui* sp. nov., male habitus (specimen: MEI123497) (artistic rendering by J. Marie Metz).

ventrally. Postocular macrosetae black, arranged in a single row dorsally. Scape equal to head length; mostly brown-black, dark yellow basally with numerous short, brown filiform setae along entire length. Basal flagellomere $\frac{1}{2}\times$ length of scape; with short, black, filiform setae on basal $\frac{1}{2}$. Second flagellomere apical, cylindrical, $\frac{1}{7}\times$ length of basal flagellomere. Third flagellomere $\frac{1}{2}\times$ length of second. Style subequal in length to third flagellomere, spiculate. Palpus widened subapically; apex slightly acuminate; yellow basally, black at apex; yellow pubescent basally, black pubescent at apex, black setose at apex. Mouthparts yellowish; brown setose. *Thorax*. Dark yellow to orange, except scutum with dark brown dorsocentral stripes, narrow anteriorly, widening and converging posteriorly; dorsal pleuron dark brown; posterodorsal katepisternum, metanepisternum, metepimeron, meron and metakatepisternum silver pubescent; scutellum brown; macrosetae black (np: 2, sa: 1, pa: 1, dc: 0, sc: 1); scutum with short black setae; katatergite, lateral postpronotum, cervical sclerite, proepisternum, and lateral prosternum with pale setae. *Legs*. Yellow except with small black spot ventrally at union of femur and trochanter, tarsi brownish; coxae with pale filiform setae anteriorly. *Wing*. Membrane mostly hyaline; costal cell hyaline with pale yellow infuscation; subcostal and radial cells adjacent to pterostigma and entire wing apex with light brown infuscation with dark microtrichia; membrane with extensive areas bare of microtrichia; pterostigma brown. Venation brown, cell m_3 widely open at wing margin. Haltere completely yellow. *Abdomen*. Dark yellow and brown, proportions highly variable. Tergites II and III yellow with brown medial stripe, brown laterally; tergites IV–VII dark brown; sternites I–VI yellow, sternite VII brown; sparse short, black, fine setae on all segments, longer laterally. *Genitalia*. Male: tergite VIII emarginated posteriorly; setose laterally. Sternite VIII ovate; posterior margin setose. Epandrium with posterolateral corners extending posteriorly level with end of cerci; setae uniformly short and dark. Cercus subtriangular, rounded apically. Subepandrial sclerite narrow, half width of epandrium; partially sclerotised, lateral margins more strongly so. Gonocoxites elongate, rounded with large subtriangular outer gonocoxal process, dark setae erect and sparse, longer ventrally; inner gonocoxal process very narrow, curved medially; gonostylus robust, spatulate, forked as pair of tooth-like lobes apically. Aedeagus with distiphallus relatively straight, fine spines apically; dorsal apodeme forked, 'T'-shaped; ventral apodeme forked, arms narrow and divergent; lateral ejaculatory apodemes narrow and band-like around anterior of basiphallus; ejaculatory apodeme relatively small, roughly cylindrical, basiphallus subcordate. Female: acanthophorite spines light brown. Sternite X triangular, truncate posteriorly. Furca rounded anteriorly, elongated and acuminate posteriorly. Spermathecal duct equal to four furcal lengths. Spermathecal sac duct two furcal lengths; spermathecal sac ovoid, longer than wide; $2.0\times$ length of spermathecal sac duct. *Variation*. Some individuals with apical $\frac{2}{3}$ of scape brown; notum dark with dorsocentral stripes evident; amount of dark brown colour on pleuron varying with most of pleuron dark; wing infuscation variable from slightly tinged to intensely dark; abdominal colouration variable, tergites III–VII from completely brown to lighter; sternite VII brown on posterior margin.

Etymology. This species is named after Dr Jean Chazeau, for his gracious hospitality during the visits to New Caledonia by MEI.

Comments. *Calophytus chazeaui* sp. nov. is known only from the southern province. It is often found associated with sclerophyll and maquis scrub habitats (e.g., Fig. 31A). Based on collecting records it is a more commonly encountered species relative to other members of the genus. GenBank sequences for this species (see Winterton et al. 2016: table S1): KT290077 (16S rDNA), KM884999 (28S rDNA), KM879116 (EF1a).

Specimens examined. *Holotype* male, NEW CALEDONIA: Province Sud: Chutes de Madeleine, Malaise trap (-22.226, 166.854), 28.XI.2000, J.H. Skevington (MEI123120, MNHN).

Paratypes. NEW CALEDONIA: Province Sud: 1 males, 2 females, Parc Territorial de la Rivière, 23.5 km NNW Plum, Malaise trap [-22.049, 166.654], 213 m, 28.X–21.XI.2000, D.W. Webb, E.I. Schlinger, M.E. Irwin (MEI125567–69, CSCA); 1 male, Parc Territorial de la Rivière, 23.5 km NNW Plum, hand collected [-22.049, 166.654], 213 m, 28.XI.2000, D.W. Webb, E.I. Schlinger, M.E. Irwin, (MEI125566, CSCA); 14 males, Chutes de Madeleine, malaise trap (-22.226, 166.854), 28.XI.2000, J.H. Skevington (MEI123114–23, 123349, 123493–96, CNC); 5 males, Parc Territorial de la Rivière Bleue, Malaise trap (-22.100, 166.66), 28.XI.2000, J.H. Skevington (MEI123497–501, CSCA); 5 males, Plaine des Lacs, S of Grand Lac, hand netted, high shrub [-22.275, 166.900], 280 m, 14.X.1985, P. Bouchet (MEI028279–80, 30098, 30100–02, MNHN); 6 males, Rivière Bleue National Park, Malaise trap, (-22.251, 166.872), 20.IX–11.IX.2000, J. & A. Skevington (MEI125623–28, CNC); 1 male, 5 females, Rivière Bleue Provincial Park, 30 km NW Yate, Malaise trap, scrub on ridge [-22.117, 166.658], 310 m, 13.X–28.X.1986, L.B. de Larbogne, J. Chazeau, A. & S. Tillier (MEI030097, 030125–30, MNHN); 18 males, 16 females, Rivière Bleue Provincial Park, 25.8 km Rivière Bleue Road, Malaise trap across forest path [-22.11, 166.65], 213 m, various dates: 30.X–28.XI.1992, D.W. Webb, E.I. & M. Schlinger (MEI030103–17, 030122–23, 030138–9, 030141–54, CSCA); 5 males, 1 female, Rivière Bleue Provincial Park, Rivière Bleue, trail to Vallée de Pourina, Malaise trap across forest path, [-22.017, 166.733], 850 m, 19–28.XI.1992, D.W. Webb, E.I. & M. Schlinger, (MEI030118–21, 030133, 030132, CSCA); 3 males, 1 female, Upper Boulari River [La Coulee] [-22.180, 166.593], 17.XI.1968, C.R. Joyce, (MEI129018, 030096, 030099, 030127, BPBM); 1 female, Rivière Bleue Provincial Park, Rivière Bleue, Rivière Bleue Road, Malaise trap across forest path [-22.11, 166.65], 290 m, 16–19.XI.1992, D.W. Webb (MEI030156, CSCA); 3 females, Rivière Bleue Provincial Park, Rivière Bleue, 25.8 km Rivière Bleue Road, Malaise trap in maquis (scrub) [-22.117, 166.658], 290 m, various dates: 30.X–3.XI.1992, D.W. Webb, E.I. & M. Schlinger (MEI030134–6, CSCA); 9 females, Rivière Bleue Provincial Park, Rivière Bleue, 25.8 km Rivière Bleue Road Malaise trap across forest path, [-22.11, 166.65], 213 m, various dates: 5–28.XI.1992, D.W. Webb, E.I. & M. Schlinger, (MEI030131, 030137, 030140, 030148, 030150–54, CASC); 3 females, Rivière Bleue Malaise trap, scrub near ridge (maquis sur crête) [-22.098, 166.630], 310 m, 12–25.XI.1986, L.B. de Larbogne, J. Chazeau, A. & S. Tillier (MEI028277–8, 030124, MNHN).

***Calophytus grandiosus* sp. nov.**

<http://zoobank.org/1D84D7A3-0E7B-430A-9A05-C36101CB9AC8>

Figs 2, 5B, 6B, 7C, 11, 12, 22, 31A, 32C

Diagnosis. Black postocular setae scattered over occiput in both sexes; flagellum shorter than scape; scutum dark; wing infuscation as two bands, apex with white infuscation; costal cell hyaline except for brown infuscation distally; legs dark with white on dorsal surface of tibia; male abdomen lacking silver pubescence.

Description. Length 10.0–12.5 mm. *Head.* Glossy black, smooth. Frons slightly verrucous, raised around base of antennae. Eyes separated by 4× width of median ocellus in both sexes. Parafacial silver pubescent, face glabrous medially. Occiput sparse silver pubescent, denser laterally and ventrally onto gena, admixed with scattered, black setae; posterior oral margin black, sparsely pubescent. Postocular macrosetae black scattered on occiput, not in distinct rows. Scape 1.3× head length, brown basally, black on apical 3/4, sparsely pubescent. Pedicel black, 1/10× length of scape, densely covered with short, black setae. Basal flagellomere 1/2× length of scape, short, black setae covering entire length. Second flagellomere subequal in length to third flagellomere, extremely short. Style minute. Palpus cylindrical basally, apex spatulate with a truncate tip; cream-coloured basally and medially towards apex, otherwise black. Mouthparts black except labellum, which is grey-brown; brown setose. *Thorax.* Dark brown. Matte black anteromedially on scutum. Silver pubescence on dorsal part of proepimeron, posterior katapisternum, lateral and extreme posterior part of scutum, scutellum, posterior anepimeron, metanepisternum, metepimeron, meron, and metakatepisternum; macrosetae black (np: 2, sa: 1, pa: 1, dc: 0, sc: 1); notum and katatergite with short, white setae. *Legs.* Black except white on dorsal surface of tibiae and basal 3/4 of mid- and hind basal tarsomere; sparsely silver pubescent, admixed with short, black setae. Fore- and midcoxa with four black anteroventral, marginal macrosetae. Hind coxa with anteroventral margin truncated with a single black, anteroventral, marginal macroseta. *Wing.* Strongly banded, dark areas infuscated with dark microtrichia; broad subapical band and a narrow band at mid length; apex with white infuscation; hyaline areas mostly lacking microtrichia. Pterostigma brown. Venation brown except anterior costal margin, basal Sc, and all veins at wing apex cream-coloured; cell m_3 widely open at wing margin. Haltere stalk brownish, knob white. *Abdomen.* Segments mostly black, white laterally on tergite I and with a broad white band on segment II; shiny, lacking pubescence, sparsely covered with short, black setae; tergites I and II with long, white setae laterally. *Genitalia.* Male: tergite VIII with anterior margin slightly emarginated. Sternite VIII quadrate, wider posteriorly. Epandrium dark, quadrangular with posterolateral processes. Cercus broad, rounded posteriorly. Subepandrial sclerite wide, 2/3 width of epandrium; partially sclerotised, lateral margins more strongly so. Gonocoxites dark brown with dark, elongate, setae laterally, inner gonocoxal process curved medially along length, rounded apically; outer gonocoxal process angular. Aedeagus with dorsal apodeme of parameral sheath 'T'-shaped, laterally forked apically; ventral apodeme divergently forked, arms broad; distiphallus robust, straight with numerous sinuous processes apically. Ejacula-

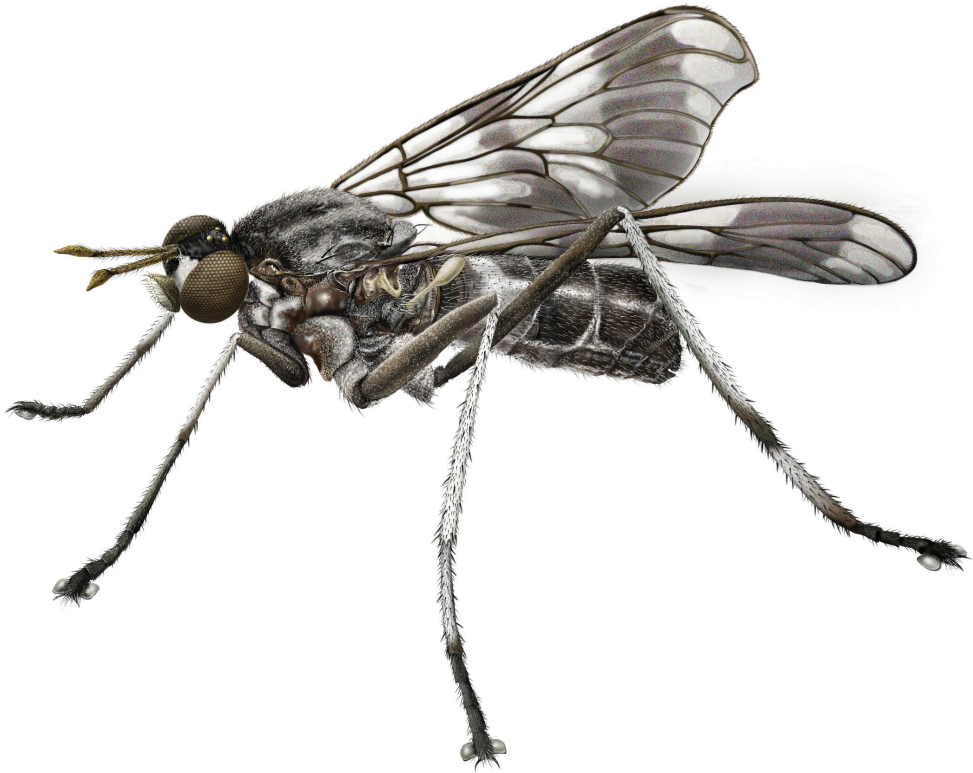


Figure 2. *Calophytus grandiosus* sp. nov., male habitus (MEI030208) (artistic rendering by J. Marie Metz).

tory apodeme robust, roughly cylindrical, with a dorsal carina and anterior end with a blunt cap; lateral ejaculatory apodemes arc-like around basiphallus. Female: tergite VIII wider than long, narrower posteriorly, with a narrow anteromedial projection. Acanthophorite and acanthophorite spines dark brown. Sternite X triangular, anterior margin truncate. Spermathecal duct equal to $4 \times$ length of furca. Spermathecal sac duct equal to $3.5 \times$ furcal lengths; sac ovoid, longer than wide; $0.5 \times$ length of spermathecal sac duct.

Etymology. The species epithet is derived from the Latin *grandis*, great, large, magnificent, and *-osus*, fullness, abundance; referring to the distinctive size and striking wing patterning of this species. Gender is masculine.

Comments. *Calophytus grandiosus* sp. nov. is a relatively large species with distinctive wing banding and black and white legs. It is distinct from other *Calophytus* species and is rather isolated in the genus as sister to the rest of the genus (Fig. 4). This species is found in the mid- to upper-elevation forests (Figs 31, 32). GenBank sequences for this species (see Winterton et al. 2016: table S1): KT290078 (16S rDNA), KM885004 (28S rDNA), KM879121 (EF1a).

Specimens examined. *Holotype* male, NEW CALEDONIA: Province Sud: Sarraméa, Malaise trap in forest [-21.641, 165.846], 780 m, 2–5.XII.2001, T. Pape, B. Viklund (MEI135021, MNHN).

Paratypes. NEW CALEDONIA: Province Sud: female, 17 km NNE Nouméa, Mount Koghis, Malaise trap across path in rainforest [-22.176, 166.505], 425 m, 26.I.1996, M.E. Irwin, D.W. Webb, E.I. Schlinger (MEI071889, CSCA); female, 17 km NNE Nouméa, Mt. Koghis, Malaise trap [-22.167, 166.533], 500 m, 23–26.XII.1991, M.E. Irwin, D.W. Webb, (MEI030209, CSCA); 2 females, Rivière Bleue Provincial Park, 30 km NW Yaté, Station Parc 5, Malaise trap [-22.117, 166.658], 19.XI–4.XII.1985 & 20.XII.1985–8.I.1986, L.B. de Larbogne, J. Chazeau (MEI030210–11, MNHN); female, Mt. Koghis, Malaise trap in forest [-22.167, 166.533], 600 m, 2–5.XII.2001, T. Pape, B. Viklund (MEI135022, NHRS); female, Rivière Bleue Provincial Park, 30 km NW Yaté, Malaise trap across forest path [-22.117, 166.658], 27–28.XII.1991, M.E. Irwin, D.W. Webb (MEI030208, CSCA); female, 9.3 km NW Sararaméa, Malaise trap [-21.581, 165.787], 497 m, 17–24.XI.1998, M.E. Irwin, E.I. & M.B. Schlinger (MEI011284, CSCA); female, Rivière Bleue Provincial Park, trail to Upper Rivière Bleue, Malaise trap across forest path [-22.117, 166.658], 290 m, 19–28.XI.1992, D.W. Webb (MEI030212, CSCA). Province Nord: female, 5 km WSW Puébo [Pouébo], Mount Mandjélia, Malaise trap [-20.397, 164.528], 720 m, 27.VI–8.VII.2000, M.E. Irwin, E.I. Schlinger, D.W. Webb (MEI131366, CSCA).

***Calophytus matilei* sp. nov.**

<http://zoobank.org/3C325DB8-82AC-4230-80C4-60D0583837D3>

Figs 5D, 6C, 7D, 13, 14, 22

Diagnosis. Black postocular setae as single row dorsally; flagellum shorter than scape; scutum dark with yellow along notopleural callus; legs yellow, mid- and hind coxae extensively yellow; wing with extensive infuscation, fenestrate in apical half; abdomen dark, male with silver velutum pubescence.

Description. Length 7.8–10.6 mm. *Head.* Glossy black. Frons smooth, raised around base of antenna, sometimes with patch of silver pubescence lateral to and above base of antennae. Eyes separated by slightly more than 2× width of median ocellus. Occiput black with silver or gold pubescence laterally, extending ventrally onto gena, admixed laterally and ventrally with light brown to white, fine setae; parafacial silver pubescent dorsally, black pubescent ventrally; posterior buccal cavity brown, sparsely pubescent. Postocular macrosetae on occiput few in number, arranged dorsally in single row in both sexes, typically black, sometimes with orange suffusion. Scape 0.8× head length; yellow basally, black apically. Pedicel short, 1/8 length of scape, black, sparsely yellow pubescent, with numerous short, brown setae. Basal flagellomere ½× length of scape; elongate, gradually tapering to a blunt point apically with short, black setae covering entire length. Second flagellomere cylindrical. Third flagellomere subequal in length of second. Style subequal in length to third flagellomere, spiculate. Palpus more or less cylindrical, slightly capitate at apex; yellow basally, black at apex; yellow pubescent basally, black pubescent at apex; yellow setose basally, black setose at apex. Mouthparts yellow. *Thorax.* Dark brown, except prothorax, postpronotal lobe, and

notopleuron yellow; prosternum, ventral proepimeron, posterodorsal katepisternum, posterior scutum, scutellum, subscutellum, metanepisternum, metepimeron, meron and metakatepisternum with silver pubescence; pronotum, anatergite, and dorsal proepimeron gold-yellow pubescent; macrosetae black (np: 2; sa: 1; pa: 1, dc: 0, sc: 1); scutum with relatively short setae. *Legs*. Yellow, except for black suffusion on foretarsus and hind coxa, legs with pale setae except dark setae apically on femora and on all tarsi; coxae silver pubescent, especially on hind coxa; hind femur with posteroventral macroseta yellow; hind basitarsomere with admix of white and gold setae ventrally and medially. Coxae with yellow setae anteriorly, hind coxa with two black setae laterally. Forecoxa with four marginal and one submarginal anteroventral, black and yellow macrosetae. Midcoxa with two marginal and three submarginal, anteroventral, black and yellow macrosetae. Hind coxa with anteroventral margin extended ventrally in a short point with three marginal, black or yellow macrosetae. *Wing*. Strongly marked, slightly variable and irregular amongst individuals. Costal cell with slight yellow infuscation; darker brown in cells sc, r adjacent to pterostigma, basal portions of r_1 and r_{2+3} , and r_{4+5} , d, bm, basal portions of m_3 and cua_1 , cup, and entire wing apex; infuscated areas also with dark microtrichia, hyaline areas of membrane largely void of microtrichia; pterostigma brown. Venation brown, except costa and R at base of wing gold; m_3 widely open at wing margin. Haltere yellow. *Abdomen*. Segments mostly dark brown, males with tergites I–III and sternites II–V with portion of medial area lighter, light brown to dark yellow; female usually uniform dark brown although sometimes with lighter brown to dark yellow areas laterally on tergite II; male with tergites II–VI with silver velutum pubescence; tergites I–III with sparse short, pale, fine setae, longer laterally; tergite IV admixed with gold and black setae; remaining tergites with black setae. *Genitalia*. Male: epandrium narrowed posteriorly, with uniform scattered, dark setae. Cercus broad, truncate posteriorly. Subepandrial sclerite narrow, 1/3 width of epandrium; partially sclerotised, lateral margins more strongly so. Gonocoxites with scattered elongate brown setae; slightly denser ventrally; outer gonocoxal process subtriangular in profile; inner gonocoxal process uniformly narrow, curved medially. Parameral sheath of aedeagus with ‘T’-shaped dorsal apodeme, arms slightly bifurcated; ventral apodeme fork relatively short, lobes rounded, distiphallus straight; basiphallus bulbous, lateral ejaculatory apodeme narrow, band-like with lateral process; Ejaculatory apodeme robust. Female: tergite VIII wider than long; anteromedial, projection long and narrow, 1/3× length of tergite VIII; posterior margin emarginated. Acanthophorite brown; acanthophorite spines brown admixed with short, brown setae. Sternite X sharply acute posteriorly. Spermathecal duct equal to four furcal lengths. Spermathecal sac duct equal to two furcal lengths; spermathecal sac ovoid, longer than wide; 1.5× length of spermathecal sac duct.

Etymology. *Calophytus matilei* sp. nov. is named in honour of the late Dr Loïc Matile, former curator of Diptera, Muséum national d’Histoire naturelle, Paris, France, who was extremely helpful to this project by providing loans of New Caledonian Therevidae.

Comments. *Calophytus matilei* sp. nov. is very similar to *C. schlingeri* sp. nov. but can be differentiated based on the pattern of silver pubescence on the face, pattern of wing

infuscation and whether the mid- and hind coxae are largely dark yellow or brown. These are the only known species in the genus with silver velutum pubescence on the male abdomen. *Calophytus matilei* sp. nov. is known from forest habitats in the northern parts of the South Province. GenBank sequences for this species (see Winterton et al. 2016: table S1): KT290079 (16S rDNA), KM885000 (28S rDNA), KM879118 (EF1a).

Specimens examined. *Holotype* male, NEW CALEDONIA: Province Sud: Sarraméa, Malaise trap in forest [-21.641, 165.846], 780 m, 2–5.XII.2001, T. Pape, B. Viklund (MEI135020, MNHN).

Paratypes. NEW CALEDONIA: Province Sud: 6 males, 1 female, Sarraméa, Malaise trap in forest [-21.641, 165.846], 780 m, 2–5.XII.2001, T. Pape, B. Viklund (MEI135015–19, 135054–5, NHRS, CSCA); 5 females, Reserve Col d'Amieu, 7.5 km NW Sarraméa, Malaise trap [-21.585, 165.819], 300 m, 4–9.XI.2000, M.E. Irwin, E.I. Schlinger, D.W. Webb, (MEI123351–5, NHRS, CSCA); 4 females, Pointe du Cagou, base de Naemeni, humid forest on peridotite [-21.681, 166.335], 30 m, 5–8.XI.1984, Tillier, Bouchet (MEI030190–2, MNHN).

***Calophytus monteithi* sp. nov.**

<http://zoobank.org/5801CAFA-7A24-4293-BF56-FE445D34F1F6>

Figs 7F, 15, 22, 32A

Diagnosis. Body mostly dark yellow to orange; single row of orange postocular setae dorsally; flagellum shorter than scape; wing with pale yellowish infuscation, darker apically with hyaline fenestrations in most cells; head yellow except for black on upper frons and dorsolaterally on occiput; legs yellow except for dark tarsi apically.

Description. Length: 10.3 mm. *Head.* Glossy dark yellow, upper frons and dorso-lateral portion of occiput dull black. Frons smooth, raised around base of antenna, eyes separated by $3\times$ width of median ocellus. Lateral occiput, lower frons, face, parafacial, and gena dull orange, sparsely pubescent; lateral and ventral occiput silver pubescent with scattered yellow setae ventrally; posterior oral margin orange, not pubescent. Postocular macrosetae yellow-orange, single row with a few scattered macrosetae ventral to the dorsal row. Scape $\frac{3}{4}\times$ head length; orange basally, dark brown on apical $\frac{1}{4}$ sparsely yellow pubescent. Pedicel dark brown, sparsely yellow pubescent, with one whorl of short, black, setae with a few additional setae. Basal flagellomere $0.7\times$ length of scape; gradually tapering to a blunt point apically; short, fine, black setae dorsally at base. Second flagellomere slightly conical, apex narrower than base; $< \frac{1}{10}\times$ length of basal flagellomere. Third flagellomere $\frac{1}{3}\times$ length of second flagellomere. Style small, spiculate. Palpus cylindrical, apex slightly capitate; orange; yellow pubescent admixed with yellow setae. Mouth parts orange with yellow setae. *Thorax.* Thorax dark yellow-orange; posterodorsal katapisternum, posterior metepimeron, anteroventral portion of meron, and posterodorsal metakatepisternum silver pubescent; macrosetae black (np: 2, sa: 1, pa: 1, dc: 0, sc: 1); scutum with short, black setae; katatergite, lateral postpronotum, postpronotal lobe, cervical sclerite, proepisternum, and lateral prosternum

with short, yellow-white setae. Scutum with dark brown, dorsocentral stripes, narrow anteriorly, widening and merging into a single broad stripe posteriorly. *Legs*. Yellow except with small black spot ventrally at junction of femora and trochanters; base of hind femur and tibia and all tarsomeres with brown suffusion; legs sparsely yellow pubescent, admixed with short pale setae; dorsal 1/4 of hind coxa silver pubescent; all coxae with short, yellow setae. Forecoxa with two, midcoxa with four, and hind coxa with two yellow, anteroventral, marginal macrosetae. *Wing*. Membrane mostly hyaline with extensive pale yellow infuscation, most cells with central hyaline fenestration, wing apex with darker infuscation; membrane mostly lacking dark microtrichia, present as apical band, patch at apex of cell d, as elongate narrow stripe in cell br, and along all veins; pterostigma light brown. Cell m_3 widely open at wing margin. Haltere stalk yellow, knob brown. *Abdomen*. Uniform dark yellow to orange, overlain with yellow-gold pubescence and fine pale setae, longer laterally; tergites I–IV with at least some short, black, setae medially. *Genitalia*. Not dissected.

Etymology. This species is named in honour of Dr Geoffrey Monteith, Emeritus Senior Curator, Queensland Museum, Brisbane, who was one of the collectors of one of the two known female specimens of this species.

Comments. *Calophytus monteithi* sp. nov. is known only from two female specimens but can readily be distinguished from other species of *Calophytus* by the body being mostly orange except for the dark dorsocentral stripe posteriorly, dark tarsi distally, and the mostly hyaline wing with faint yellowish infuscation. This species is known from misty rainforest habitats at higher elevations (430–850 m) (Fig. 32A). The male is unknown.

Specimens examined. *Holotype* female, NEW CALEDONIA: Province Sud: Col d'Amieu, humid forest, 430 m, 7.X.1984, 21°36'00"S, 165°48'08"E [-21.6, 165.802], Tillier & Bouchet, Collection #116a (MEI030193, MNHN).

Paratype. NEW CALEDONIA: Province Nord: 1 female, 8711, 21°11'S, 165°18'E [-21.183, 165.3], 850 m, Aoupinie, top camp, 3–23.X.2001, C. Burwell & G. Monteith, Malaise, rainforest (MEI138464, QM).

***Calophytus schlingeri* sp. nov.**

<http://zoobank.org/76F032BE-4F50-46B1-908E-146A0BB5E1EE>

Figs 5C, 6A, 7B, 16–18, 22, 23A, 31A

Diagnosis. Flagellum shorter than scape; single row of postocular setae dorsally; scutum dark except for orange suffusion on notopleural callus; legs yellow except for tarsi dark apically; wing with dark infuscation, fenestrate apically; male abdomen with silver velutum pubescence.

Description. Length 8.5–10.7 mm. *Head*. Glossy black. Frons smooth, raised around base of antenna. Eyes separated by slightly more than 2× width of median ocellus. Occiput black with silver or gold pubescence laterally, extending ventrally onto gena, admixed laterally and ventrally with light brown to white, fine setae; parafacial silver pubescent as elongate wedge shape, extending ventrally along margin of buccal

area. Postocular macrosetae on occiput few in number, arranged dorsally in single row in both sexes, typically black, sometimes with orange suffusion. Scape $0.8\times$ head length; yellow basally, black apically. Pedicel short, $1/8$ length of scape, black, sparsely yellow pubescent, with numerous short, brown setae. Basal flagellomere $1/2\times$ length of scape; elongate, gradually tapering to a blunt point apically with short, black setae covering entire length. Second flagellomere cylindrical. Third flagellomere subequal in length of second. Style subequal in length to third flagellomere, spiculate. Palpus more or less cylindrical, slightly capitate at apex; yellow basally, black at apex; yellow pubescent basally, black pubescent at apex; yellow setose basally, black setose at apex. Mouthparts yellow. *Thorax*. Dark brown to black, except prothorax, postpronotal lobe, and notopleuron yellow; prosternum, ventral proepimeron, posterodorsal katapisternum, posterior scutum, scutellum, subscutellum, metanepisternum, metepimeron, meron and metakatepisternum overlain with silver pubescence; pronotum, anatergite, and dorsal proepimeron gold-yellow pubescent; scutum with faint dorsocentral silver pubescent stripes; macrosetae black (np: 2; sa: 1; pa: 1, dc: 0, sc: 1); scutum with relatively short setae. *Legs*. Yellow, except for black suffusion on foretarsus and hind coxa, legs with pale setae except dark setae apically on femora and on all tarsi; coxae silver pubescent, especially on hind coxa; hind femur with posteroventral macroseta yellow; hind basal tarsomere with admix of white and gold setae ventrally and medially. Coxae with yellow setae anteriorly, hind coxa with two black lateral setae. Forecoxa with four marginal and one submarginal anteroventral, black and yellow macrosetae. Midcoxa with two marginal and three submarginal, anteroventral, black and yellow macrosetae. Hind coxa with anteroventral margin extended ventrally in a short point with three marginal, black or yellow macrosetae. *Wing*. Strongly marked, variable in shape, irregular. Costal cell with pale yellow infuscation; brown infuscation in cells sc, r adjacent to pterostigma, basal portions of r_1 and r_{2+3} , and r_{4+5} , d, bm, basal portions of m_3 and cua_1 , cup, and entire wing apex; infuscated areas also with dark microtrichia, hyaline areas of membrane largely void of microtrichia; pterostigma brown. Venation brown, except costa and R at base of wing gold; cell m_3 widely open at wing margin. Haltere yellow. *Abdomen*. Segments mostly dark brown, males with tergites I–III and sternites II–V with portion of medial area lighter, light brown to dark yellow; female usually uniform dark brown although sometimes with lighter brown to dark yellow areas laterally on tergite II; male with tergites II–VI with silver velutum pubescence; tergites I–III with sparse short, pale, fine setae, longer laterally; tergite IV admixed with gold and black setae; remaining tergites with black setae. *Genitalia*. Male: epandrium narrowed posteriorly, with uniform scattered, dark setae. Cercus relatively narrow, rounded posteriorly. Subepandrial sclerite narrow, $1/3$ width of epandrium; partially sclerotised, lateral margins more strongly so. Gonocoxites with scattered elongate brown setae; slightly denser ventrally; outer gonocoxal process sub-triangular in profile; inner gonocoxal process uniformly narrow, curved medially, spatulate apically. Parameral sheath of aedeagus with ‘T’-shaped dorsal apodeme, arms slightly bifurcated, ventral apodeme fork relatively short, lobes rounded, distiphallus straight; basiphallus bulbous, lateral ejaculatory apodeme narrow, band-like with lateral process; Ejaculatory

apodeme robust. Female: tergite VIII wider than long; anteromedial, projection long and narrow, $1/3 \times$ length of tergite VIII; posterior margin emarginated. Acanthophorite brown; acanthophorite spines brown admixed with short, brown setae. Sternite X sharply acute posteriorly. Spermathecal duct equal to four furcal lengths. Spermathecal sac duct equal to two furcal lengths; spermathecal sac ovoid, longer than wide; $1.5 \times$ length of spermathecal sac duct. *Variation.* Some paratypes with frons sparsely pubescent; ventral parafacial variably silver and/or gold pubescent; all postocular macrosetae black; additional postocular macrosetae ventral to single dorsal row; apical $3/4$ scape brown; basal flagellomere with covering of short, black, filiform setae variable from basal $1/4$ to entire; notopleuron variably coloured light to dark brown; midcoxae variably gold to brown; coxae with anteroventral, marginal macrosetae number variable from 3–5 and variably coloured gold to black; hind coxa lateral macrosetae number variable, 0–2; wing infuscation variable in intensity and distribution.

Etymology. Named in honour of the late Dr Evert I. Schlinger, who participated in the New Caledonian expeditions, from which much of the material for this paper was collected.

Comments. *Calophytus schlingeri* sp. nov. is very similar to *C. matilei* sp. nov. and can be distinguished based on the pattern of silver pubescence on the face, pattern of wing infuscation and whether the mid- and hind coxae are largely dark yellow or brown. These are the only known species in the genus with silver velutum pubescence on the male abdomen. Specimens of *Calophytus schlingeri* sp. nov. were collected in a variety of habitats including dry sclerophyll forest, rainforest and maquis scrub (Fig. 31A). GenBank sequences for this species (see Winterton et al. 2016: table S1): KM885001 (28S rDNA), KM879117 (EF1a).

Specimens examined. *Holotype* male, NEW CALEDONIA: Province Sud: Plaine des Lacs, 5 km E of Grand Lac, hand netted [-22.267, 166.967], 300 m, 22–25.I.1984, M. Pogue, M. Epstein (MEI030164, MNHN).

Paratypes. NEW CALEDONIA: Province Sud: 1 male, 2 females, Plaine des Lacs, 5 km E of Grand Lac, black light (UV) [-22.267, 166.967], 300 m, 22–25.I.1984, M. Pogue, M. Epstein (MEI030165, 03173–4, UMSP); 4 males, 3 females, Plaine des Lacs, 5 km E of Grand Lac, hand netted [-22.267, 166.967], 300 m, 22–25.I.1984, M. Pogue, M. Epstein, male, (MEI030161–3, 030166, 030175–7, FSCA, CASC); 1 female, Mt. Koghis, Malaise trap in forest [-22.167, 166.533], 600 m, 2–5.XII.2001, T. Pape, B. Viklund (MEI135023, NHRS); 1 male, Rivière des Pirogues black light (UV) [approximated as -22.275, 166.687], 7–9.II.1984, M. Pogue, M. Epstein (MEI030167, UMSP); 2 males, 4 females, Rivière Bleue Provincial Park, 25.8 km Rivière Bleue Road, Malaise trap across forest path [-22.117, 166.658], 213 m, various dates: 5–28.XI.1992, D.W. Webb, E.I. & M. Schlinger (MEI030158–9, 030170–2, CSCA); 1 male, Rivière Bleue Provincial Park, Rivière Bleue Road, Malaise trap across forest path [-22.117, 166.658], 290 m, 5–16.XI.1992, D.W. Webb, male, (MEI030160, CSCA); 1 female, 17 km NNE Nouméa, Mt. Koghis, [Koghis stream waterfall] Malaise trap in tropical forest [-22.171, 166.512], 500 m, 21–29.XI.1992, D.W. Webb, (MEI030169, CSCA).

***Calophytus webbi* sp. nov.**

<http://zoobank.org/9CD4647C-D573-4A06-B7A2-DB2E3EED144C>

Figs 5E, 6D, 7E, 8B, 19–22, 31B

Diagnosis. Flagellum longer than scape; single row of black postocular macrosetae dorsally; body predominantly yellow; wing mostly hyaline, dark apically; scutellum overlain with sparse silver pubescence; abdomen yellow, tergites brown posteriorly; legs yellow, tarsi brownish; male abdomen lacking silver pubescence.

Description. Length 5.5–8.1 mm. *Head.* Glossy black, yellow around base of antenna. Frons glossy, smooth, slightly raised around base of antennae; eyes separated by 3× width of median ocellus in both sexes. Occiput black with silver pubescence laterally and ventrally, admixed with pale setae laterally and onto gena; single row of black to orange postocular macrosetae in both sexes. Parafacial dark, yellowish laterally, overlain with silver pubescence along eye margin; posterior oral margin yellow, not pubescent. Scape 3/4 of head length, dark yellow, brown suffusion apically. Basal flagellomere 2.5× length of scape, cylindrical, abruptly tapering to a blunt point apically, densely covered with brown pubescence. Second flagellomere subapical, subequal in length to third flagellomere; style small, spiculate. Palpus cylindrical, apex slightly capitate. Mouthparts yellow with pale setal pile, yellow on labium, black on labellum. *Thorax.* Yellow; scutum with dark dorso-central stripes, narrow anteriorly, thickening posteriorly and merging medially into a single stripe before posterior margin, brownish suffusion sometimes posteriorly on scutum; scutellum brown dorsally; posterodorsal katepisternum, metanepisternum, metepimeron, and metakatepisternum overlain with silver pubescence; sparse silver pubescent on posterior scutum and scutellum; macrosetae black (np: 1, sa: 1, pa: 1, dc: 0, sc: 1); scutum, katatergite, lateral postpronotum, postpronotal lobe, cervical sclerite, proepisternum, and lateral prosternum with short, yellow setae. *Legs.* Yellow except with small black spot ventrally at union of femora and trochanters; foretarsus light brown; sparsely pubescent, dorsal part of hind coxa silver pubescent; legs with short, yellowish, setae, except foretarsus with brown setae. Forecoxa with some longer, gold, filiform setae anteriorly. Forecoxa with two macrosetae; mid- and hind coxae with three anteroventral macrosetae. *Wing.* Membrane mostly hyaline; costal, subcostal, pterostigma and adjacent r cells, and entire wing apex light brown infuscation; membrane with extensive areas bare of microtrichia. Venation brown with dark microtrichia along veins, m_3 widely open at wing margin. Haltere stalk yellow, knob light brown. *Abdomen.* Yellow, posterior and lateral margins of tergites II–VII brown, terminal segments darker; glossy, not pubescent and male lacking silver pubescence; sparse fine pale setae; medial setae darker, especially on terminal segments. *Genitalia.* Male: tergite VIII anterior margin slightly emarginate; laterally with brown setae. Cercus relatively narrow, rounded posteriorly. Sternite VIII quadrate, wider posteriorly; posterior 1/6 with brown setae. Epandrium yellow basolaterally and at extreme posterolateral margin, otherwise brown; brown setae sparsely distributed; subepandrial sclerite narrow, 1/3 width of epandrium, partially sclerotised, lateral margins more strongly so. Gonocoxites yellow-brown, elongate dark setae sparsely distributed, except lacking setae ventromedially; outer gonocoxal process sub-triangular; aedeagus with ejaculatory apodeme sub-cylindrical; inner gonocoxal process narrow; dorsal apodeme of parameral sheath ‘T’-shaped, ventral

apodeme forked; lateral ejaculatory apodeme band-like with small outer process. Female: acanthophorite and acanthophorite spines yellow-brown. Tergite VIII wider than long, with a narrow anteromedial projection, posterior margin slightly emarginated. Sternite VIII gold; long, brown, setae sparsely distributed, bare laterally and more dense on posterior lobes. Median lobe of tergite IX reduced, very short. Sternite X quadrangular with short, brown setae. Spermathecal duct 5× furcal length. Spermathecal sac duct 3.5× furcal length; spermathecal sac ovoid, longer than wide; 0.5× length of spermathecal sac duct.

Etymology. This species is named after the late Dr Donald W. Webb, who was a member of several of the expeditions to New Caledonia and was one of the collectors of this species.

Comments. *Calophytus webbi* sp. nov. is a relatively diminutive, bright yellow species with distinctive antennae that readily distinguishes it from all other *Calophytus* species (Figs 5E, 19, 20). This species appears endemic to the tropical dry forest of the Pindai Peninsula (Fig. 31B) on the west coast of the Northern Province (Fig. 22); it is only known from a series of specimens collected from two localities on this peninsula. Genbank sequences for this species (see Winterton et al. 2016: table S1): KT290080 (16S rDNA), KM885002 (28S rDNA), KM879120 (EF1a); KT306930 (CAD) (not KT306928 as reported in Winterton et al. 2016).

Specimens examined. *Holotype* male, NEW CALEDONIA: Province Nord: 45 m, Presqu'île de Pindai, 2.5 km WSW Népouï, Malaise, "21.383°S, 164.974°E" [GPS coordinates apparently erroneous; approximated instead as -21.33, 164.96], 26.XI–4.XII.2000, M.E. Irwin, E.I. Schlinger, D.W. Webb (MEI123356, MNHN).

Paratypes. NEW CALEDONIA: Province Nord: 1 female, Presqu'île de Pindai, 2.5 km WSW Népouï, Malaise, "21.383°S, 164.974°E" [GPS coordinates apparently erroneous; approximated instead as -21.33, 164.96], 10–17.XI.2000, M.E. Irwin, E.I. Schlinger, D.W. Webb (MEI108224, CSCA); 8 males, [Presqu'île de Pindai], 3 km SW Népouï, Pindai Forest, Malaise trap in costal forest [-21.35, 164.964], 13–23.XI.1992, D.W. Webb, E.I. & M. Schlinger (MEI030180–7, CSCA); 3 males, [Presqu'île de Pindai] 3 km SW Népouï, Pindai Forest, Malaise trap in coastal forest [-21.35, 164.964], 7–13.XI.1992, D.W. Webb, E.I. Schlinger, M. Schlinger (MEI030178-9, 030188, CSCA).

Jeanchazeauia gen. nov.

<http://zoobank.org/599FD78A-C5E9-417E-A18B-18937C798CF1>

Type species. *Jeanchazeauia nubilosus* sp. nov., here designated.

Diagnosis. Frons width slightly wider than ocellar tubercle with little sexual dimorphism; postocular macrosetae arranged in one row in both sexes; femoral velutum patches absent; hind femur with anteroventral macroseta(e) subapically, frequently as a row; hind femur with series of posteroventral macrosetae; cell *br* with scattered microtrichia; male gonocoxite lacking medial atrium and velutum patch; female tergite VII with broad anteromedial process; tergite VIII narrowly band-like and 'T'-shaped.

Description. Antennal length variable, longer than head to equal to head length; flagellum cylindrical, slightly tapered distally, length subequal to combined length of

scape and pedicel; scape narrow, elongate ($> 3\times$ pedicel length); upper frons flat, slightly raised around base of antennae; head shape in profile higher than long; male frons width at narrowest point slightly wider than ocellar tubercle, little sexual dimorphism in frons width; parafacial without setae; postocular macrosetae arranged in one row immediately lateral of ocellar tubercle in both sexes; prosternum without setae; abdominal tergite II all setae uniform and regular in length; fore- and hind femoral velutum patches absent; fore- and midfemoral macrosetae absent; hind femur with anteroventral macroseta(e) subapically, frequently as a row; hind femur with posteroventral macrosetae short, present as series around middle of segment; posterior surface of midcoxa without setae; hind femur and tibia relatively long compared to other legs; post-spiracular setae absent. Scutal chaetotaxy (pairs): np, 1–2; sa, 1; pa, 1; dc, 0 or 1–2 (minute); sc, 1; wing cell m_3 open, cell br with scattered microtrichia, not restricted to wing fold; uniform wing dark infuscation to strongly banded. Male genitalia with dorsal apodeme of aedeagus ‘T’-shaped, distiphallus narrow, ventral apodeme with forked arms divergent; gonocoxite with posteromedial margins proximal to each other, velutum pubescence absent, inner gonocoxal process present, ventral lobe small, usually rounded apically; female genitalia with tergite VII with broad anteromedial process; tergite VIII narrowly band-like and ‘T’-shaped, with narrow anteromedial process; female acanthophorite setae with two sets present (A1 & A2); A1 slender, elongate acuminate apically, A2 series slightly reduced in size; sternite VIII cup-like, extensively pilose, greatly emarginate posteromedially; spermathecal sac elongate and rounded apically, not lobed; three spermathecae joining to spermathecal duct near junction of bursa copulatrix.

Etymology. This new genus is named in honour of Dr Jean Chazeau, who extended unbridled hospitality and assistance to the members of our expeditions during our stays in New Caledonia. Gender is masculine.

Comments. Of the three species in this genus, the male is known only for *J. nubilosus* sp. nov., which exhibits distinct sexual dimorphism in wing patterning. The modification of both tergite VII and tergite VIII in the female appears unique to this genus amongst all Therevidae. Although members of some Xestomyzinae (e.g., *Lynborgia ammodyta* Irwin, 1973), Agapophytinae (e.g., *Agapophytus bicolor* (Kröber, 1928)) and Therevinae (e.g., *Apenniverpa venezuelensis* Webb, 2005) have a modified ‘T’-shaped female tergite VIII remarkably similar in shape to members of *Jeanchazeauia* gen. nov., in all cases tergite VII is not modified at all. Species in this genus are relatively rare compared to the more widely encountered *Calophytus* gen. nov. and appear to be more restricted to montane rainforest habitats (Figs 31, 32).

Included species. *Jeanchazeauia amoa* sp. nov., *J. nubilosus* sp. nov., and *J. rufinatus* sp. nov.

Key to species of *Jeanchazeauia* gen. nov.

- 1 Legs with white macrosetae (male unknown) (Fig. 24).....***J. amoa* sp. nov.**
- Legs with dark macrosetae (Figs 25, 28)..... **2**

- 2 Frons densely silver pubescent; abdomen with broad silver pubescent band anteriorly on tergite II; posterior margin of tergite III and all of tergites IV and V reddish-orange; scutum with broad, silver, dorsocentral stripes (male unknown) (Figs 28, 29) *J. rufinatus* sp. nov.
- Frons with mostly dull black or brownish pubescence; abdomen entirely brown-black, silver velutum pubescence on tergites II–IV in male, present only along posterior margin of tergites I–IV in female; scutum sparsely pubescent, lacking dorsocentral stripes (Figs 25, 26) *J. nubilosus* sp. nov.

***Jeanchazeauia amoa* sp. nov.**

<http://zoobank.org/8A0B7D2E-0B4D-4AF4-A816-EE746682CDF7>

Figs 7G, 23B, 24, 30

Diagnosis. White macrosetae on tibiae, in two rows on hind tibia; frons dark; abdomen mostly dark brown; wing banded, apex hyaline.

Description. Length 7.8–9.8 mm. *Head.* Dark brown; mostly silver pubescent, upper frons slightly bronze pubescent, frons with short, black, setae on dorsal half; eyes separated by width of ocellar tubercle. Occiput flat, overlain with silver pubescence, matte black pubescence dorsally along postocular ridge; white, elongate setae ventrolaterally and onto gena; postocular macrosetae black, in a single row dorsally. Scape 0.3× head length; dark brown, silver pubescence admixed with short, black setae except on medial surface. Basal flagellomere 1.3× length of scape; elongate, tapering to a blunt point apically; sparsely silver pubescent with short, fine, black setae dorsally at base. Second flagellomere apical; slightly conical, apex narrower than base; < 1/10× length of basal flagellomere. Third flagellomere minute. Style small, spiculate. Palpus one segmented; cylindrical, apex slightly capitate; brown; silver pubescent admixed with white setae. Mouthparts brown with brown setae. *Thorax.* Dark brown, mostly sparsely silver pubescent; scutum with very faint grey pubescent dorsocentral stripes; scutellum black, matte pubescent dorsally, bronze and silver pubescent on posterior margin; anterior anepisternum and katepisternum and posterior anepimeron glossy, glabrous; macrosetae black (np: 1, sa: 1, pa: 1, dc: 0, sc: 1); scutum with short, black, setae medially, white laterally; postpronotum, postpronotal lobe, cervical sclerite, proepisternum, and lateral prosternum with short, white setae; katatergite admixed with erect white and black setae. *Legs.* Brown except for apical 1/2 of foretibia and base of all basitarsi white; sparsely silver pubescent; short, black setae where cuticle is brown, white setae where cuticle is white; all macrosetae white. Coxae admixed with long, black and white, filiform setae. Forecoxa with two, midcoxa with three, and hind coxa with four black or white, anteroventral, marginal macrosetae. Hind coxa with one black, lateral macroseta. Hind femur with two white subapical anteroventral macroseta; short series of minute, dark, posteroventral macrosetae barely evident along middle of femur. White macrosetae on mid and hind tibia; midtibia with few macrosetae; hind tibia with white macrosetae arranged in two dorsal rows, another

row of 3–5 five macrosetae present anteroventrally. *Wing*. Membrane hyaline with two broad dark bands; basal band originating at pterostigma and covering membrane to posterior wing margin; apical band covering wing tip except apical 1/6 of wing; membrane completely covered with microtrichia. Pterostigma dark. Veins dark; cell m_3 wide open at wing margin. Haltere stalk and base of knob dark brown, knob white apically. *Abdomen*. Dark brown, sparsely silver pubescent, sparsely brown pubescent medially on tergites I–III; covered with short, black, setae, apical segments with longer setae laterally; tergites I and II with long, white, setae laterally. *Genitalia*. Female: tergites VI–VIII modified with anterior margin with medial process, broad and barely evident in tergite VI, to greatly elongate and narrow in tergite VIII, tergite VII representing an intermediate between the two; tergite VIII much wider than long; dark elongate setae present laterally on tergites VI–VIII. Sternite VIII slightly longer than wide, convex ventrally, posterior lobes tapering sharply posteriorly, separated by distance $3/4$ width of one lobe, with a medial aedeagal guide; extensive elongate, setae over much of surface, bare at extreme lateral margin. Acanthophorite dark brown; acanthophorite spines dark, six tapered spines in A1 series, A2 series spines indistinguishable in size and thickness from rest of acanthophorite setae. Sternite X quadrate, with posterolateral edges expanded laterally; posterior margin widely rounded; dark brown; short, brown setae. Furca longer than wide, semicircular anteriorly, tapered to a point posteriorly; spermathecal sac relatively small and elongate, spermathecal sac duct and spermathecal sac indistinguishable; spermathecal ducts origination on spermathecal sac duct immediately adjacent to furcal membrane.

Etymology. Named for the mountain peak, Pic d’Amoa, the type locality for this species and is a noun in apposition.

Comments. *Jeanchazeauia amoa* sp. nov. is the only species in the genus *Jeanchazeauia* that has white macrosetae on the legs. It is otherwise a comparatively drab coloured species, being mostly dark brown. It is one of the few species of New Caledonia stiletto flies known only from the Northern Province. The male is unknown.

Specimens examined. *Holotype* female, NEW CALEDONIA: Province Nord: “8905” 20°58’S, 165°17’E, Malaise [approximated as -20.963, 165.277], 500 m, Pic d’ Amoa, N slopes, 24.XI.01–31.I.2002, Burwell, Monteith (MEI138463, MNHN).

Paratype. NEW CALEDONIA: 1 female, Province Nord: “Mt. Mandjanie”, 5.3 km WSW P[o]uebo [approximated as -20.402, 164.525], 9–26.XI.1992, D.W. Webb, 550 m, Malaise trap in tropical forest (MEI030205, CSCA).

Jeanchazeauia nubilosus sp. nov.

<http://zoobank.org/F826CA19-F56D-4391-A6CC-EAA198ECE40C>

Figs 3, 6E, 7H, 23C, 25–27A–F, 30, 31A, C, 32B

Diagnosis. Black macrosetae on legs; frons dark, sparsely pubescent; female abdomen dark with white bands; female wing with strong banding, irregular basally, wing apex dark; male wing with uniform infuscation.

Description. Length 8.3–9.6 mm. *Head*. Black to brown; mostly silver pubescent, upper frons sparsely pubescent, admixed with black setae, longer in male, a few setae

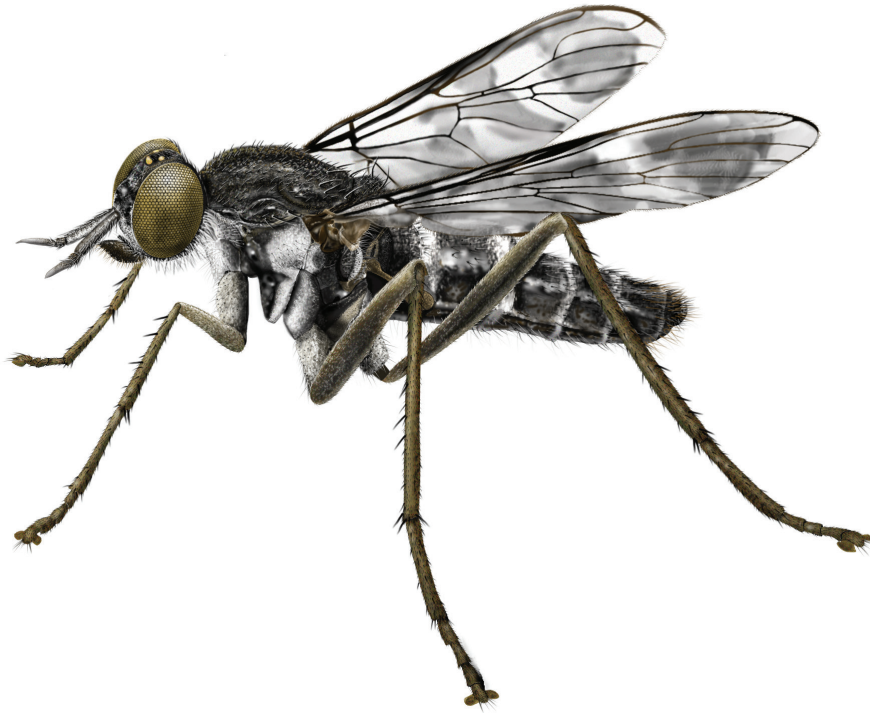


Figure 3. *Jeanchazeauia nubilosus* sp. nov., female habitus (MEI030203) (artistic rendering by J. Marie Metz).

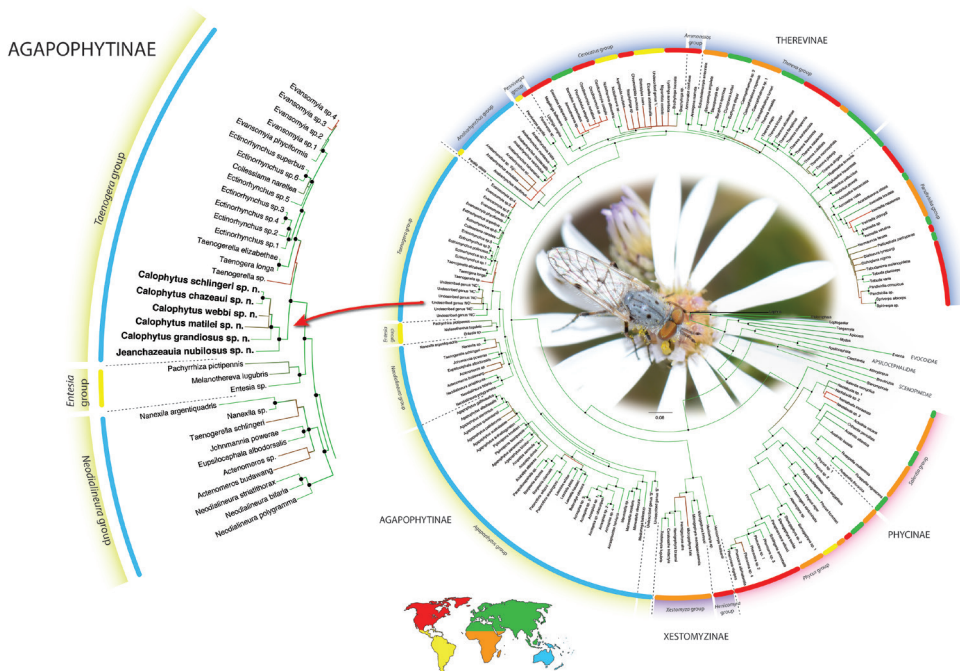


Figure 4. Phylogenetic placement of *Calophytus* gen. nov. and *Jeanchazeauia* gen. nov. in Agapophytinae based on supermatrix analysis of DNA sequence data. Figure modified after Winterton et al. (2016: fig. 3).

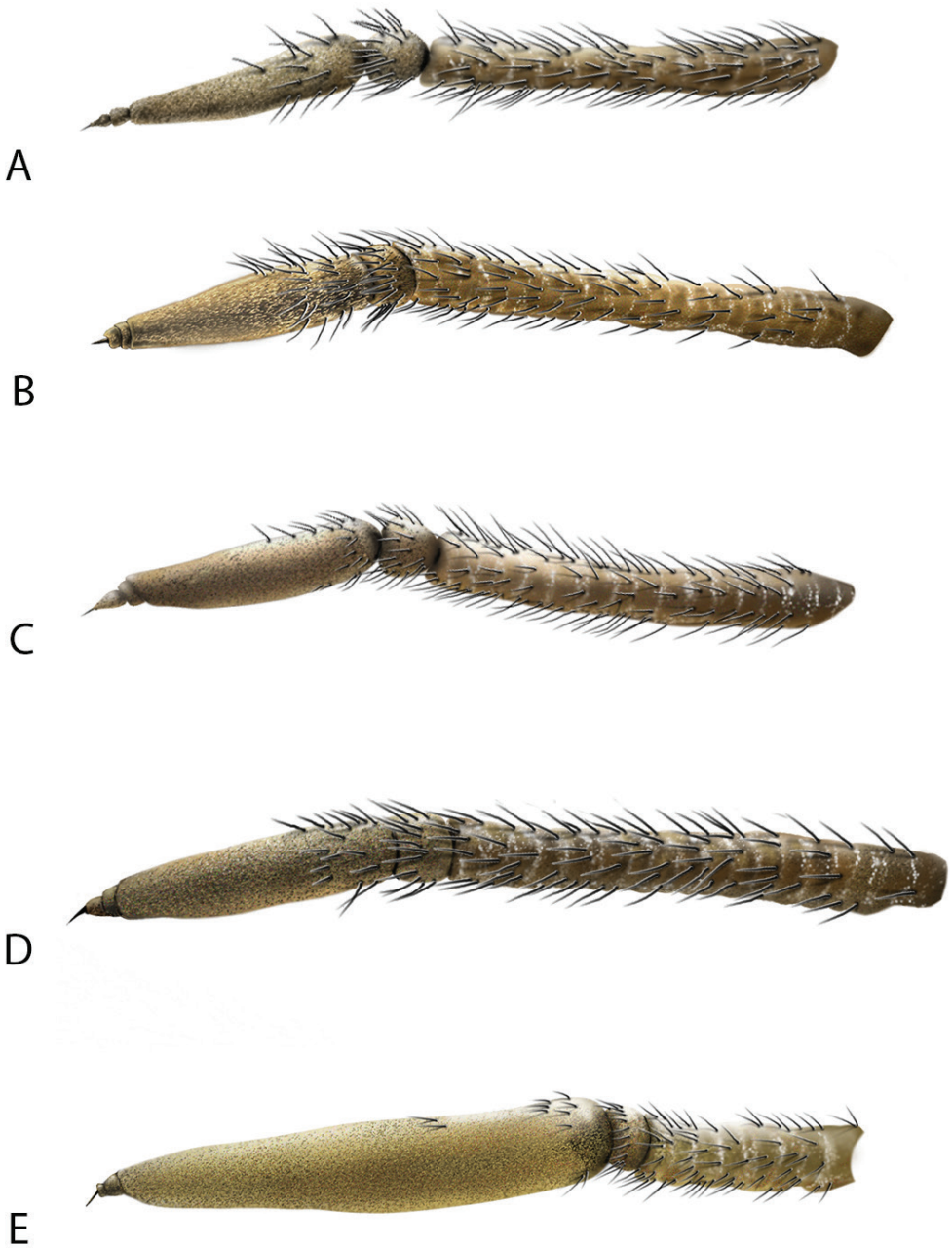


Figure 5. Lateral view of antennae of *Calophytus* gen. nov. **A** *C. chazeauui* sp. nov. **B** *C. grandiosus* sp. nov. **C** *C. schlingeri* sp. nov. **D** *C. matilei* sp. nov. **E** *C. webbi* sp. nov. (figures not to scale) (drawings by J. Marie Metz).

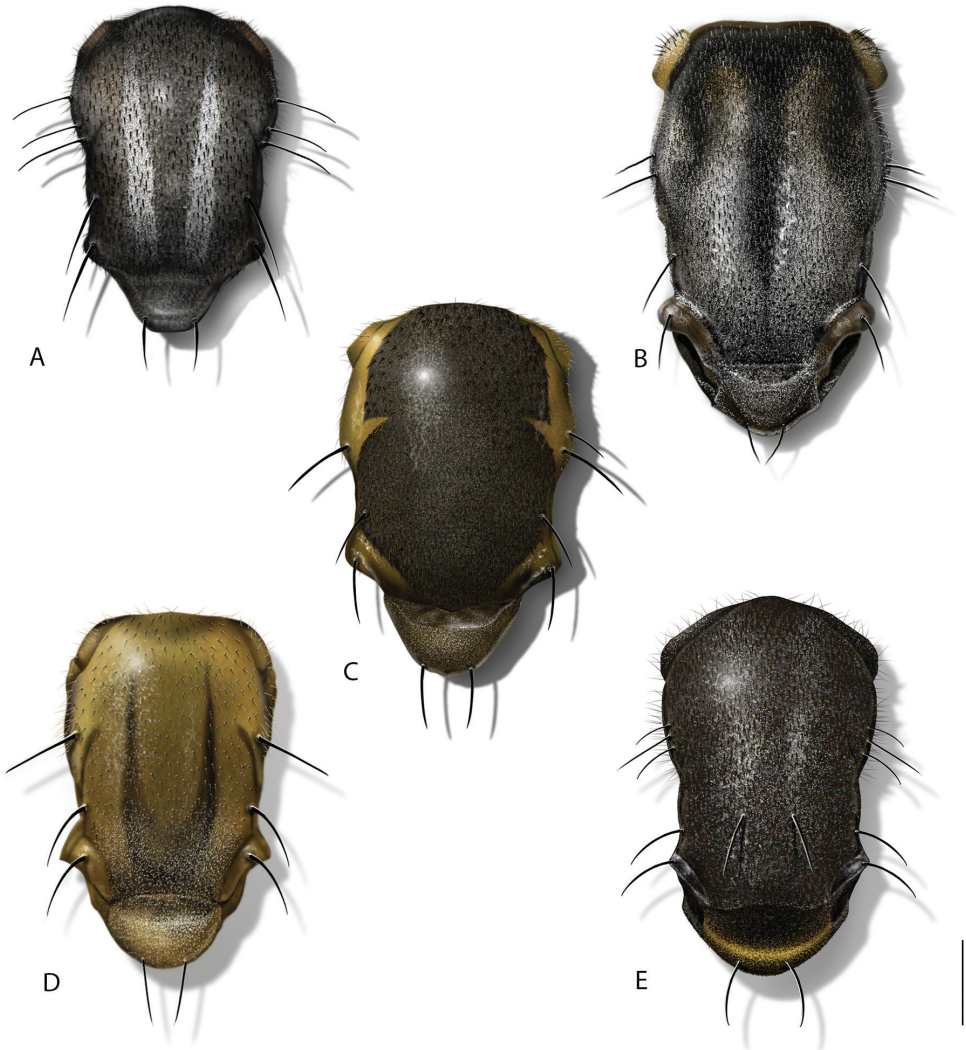


Figure 6. Scutum and scutellum of *Calophytus* gen. nov. and *Jeanchazeauia* gen. nov. **A** *C. schlingeri* sp. nov. **B** *C. grandiosus* sp. nov. **C** *C. matilei* sp. nov. **D** *C. webbi* sp. nov. **E** *J. nubilosus* sp. nov. (figures not to scale) (drawings by J. Marie Metz).

dorsolateral to antennal bases, eyes separated by width of ocellar tubercle in both sexes; parafacial black with silver pubescence. Occiput black, matte pubescent, more bronze coloured along postocular ridge, silver laterally and ventrally. Postocular macrosetae mostly black, in a single row in both sexes, multiple irregular rows laterally, replaced by white finer setae laterally and on gena. Scape $\frac{1}{2}\times$ head length; dark brown, sparsely silver pubescent; long, black, fine filiform setose except medial surface bare of setae. Basal flagellomere $\frac{1}{2}\times$ length of scape, elongate and gradually tapering to a blunt point apically; sparsely silver pubescent with short, fine, black setae around base. Second flag-

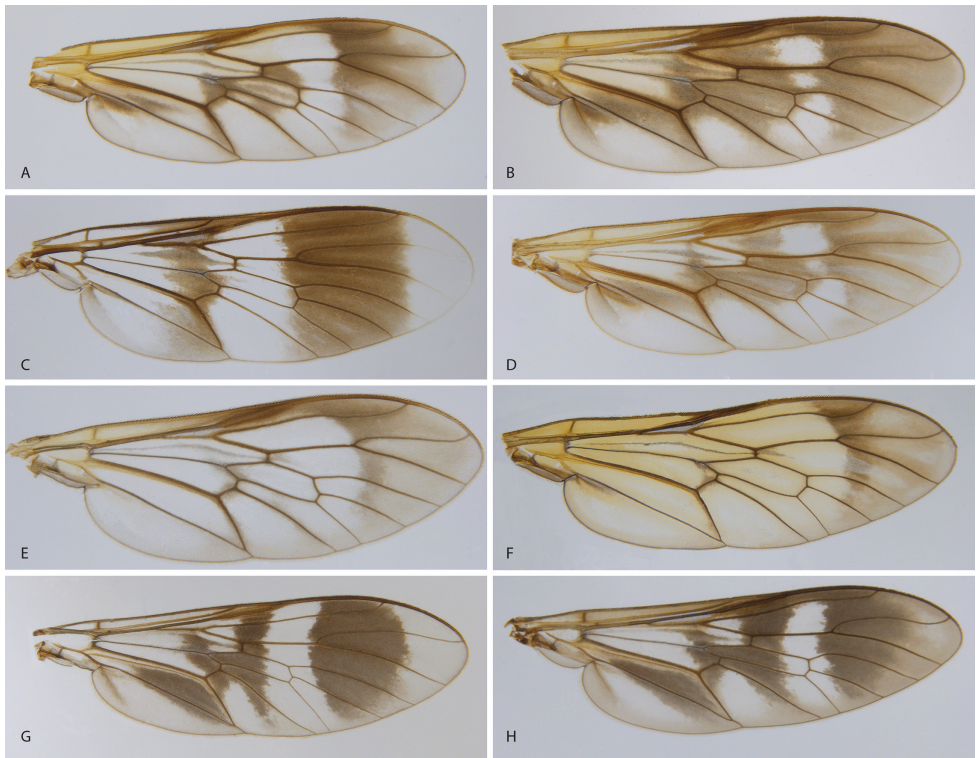


Figure 7. Wings of *Calophytus* gen. nov. and *Jeanchazeauia* gen. nov. **A** *C. chazeaui* sp. nov. **B** *C. schlingeri* sp. nov. **C** *C. grandiosus* sp. nov. **D** *C. matilei* sp. nov. **E** *C. webbi* sp. nov. **F** *C. monteithi* sp. nov. **G** *J. amoa* sp. nov. **H** *J. nubilosus* sp. nov. (female) (figures not to scale).

ellomere slightly conical, apex narrower than base; $< 1/10\times$ length of basal flagellomere. Third flagellomere subequal in length to second, conical. Style small, spiculate. Palpus one segmented, cylindrical, dark brown basally, light brown apically; silver pubescent admixed with white, setae basally, brown apically. Mouthparts brown with brown setae. *Thorax*. Dark brown-black with black and silver pubescence; scutum brown pubescent with anterior postpronotal lobe and notopleuron sparsely silver pubescent; scutellum with black matte pubescence anteriorly and medially, bronze pubescent along posterior margin; pleuron silver pubescent with two brown glabrous vertical bands passing from the notopleuron at the prothoracic spiracle posteroventrally through the anterior katepisternum, and from the wing base posteroventrally through the meron; macrosetae black (np: 3, sa: 1, pa: 1, dc: 1, sc: 1); scutum with short, black setae; postpronotal lobe, cervical sclerite, proepisternum, and lateral prosternum with white setae; katatergite with mostly white setae, both sides with one dark brown seta. *Legs*. Dark brown; coxae with dense silver pubescence, otherwise sparsely pubescent and admixed with short, black setae; macrosetae mostly black with a few light brown macrosetae on hind tibia. Coxae with white setae; forecoxa with two, midcoxa with three, and hind coxa with five black, anteroventral, marginal macrosetae; hind coxa lacking lateral seta. Posterior

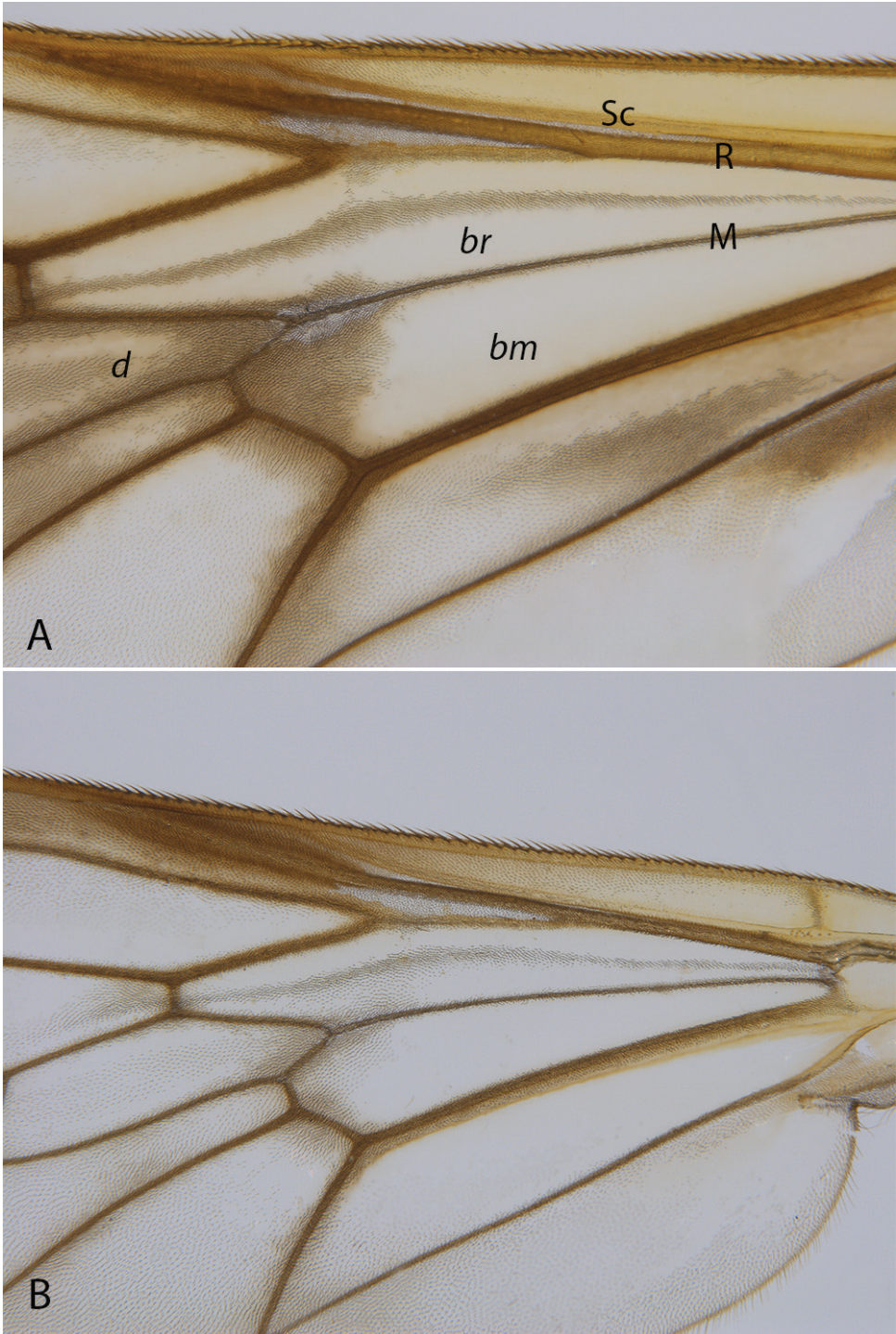


Figure 8. *Calophytus* spp. Wing detail showing cell *br* bisected with stripe of dark microtrichia along wing fold **A** *C. chazeau* sp. nov. **B** *C. webbi* sp. nov.



Figure 9. *Calophytus chazeaui* sp. nov. **A** adult male (MEI125624), lateral view **B** same, oblique view **C** adult female (MEI030131), oblique view **D** same, lateral view. Body length: male: 8.3 mm; female: 9.0 mm.

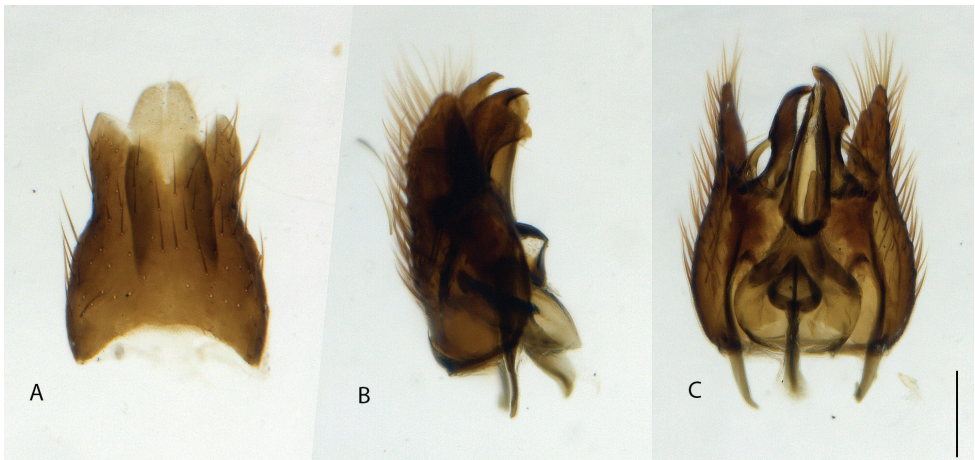


Figure 10. *Calophytus chazeaui* sp. nov., cleared male genitalia **A** epanthrium **B** gonocoxites with aedeagus, lateral view **C** same, dorsal view with epanthrium removed. Scale bar: 0.2 mm.

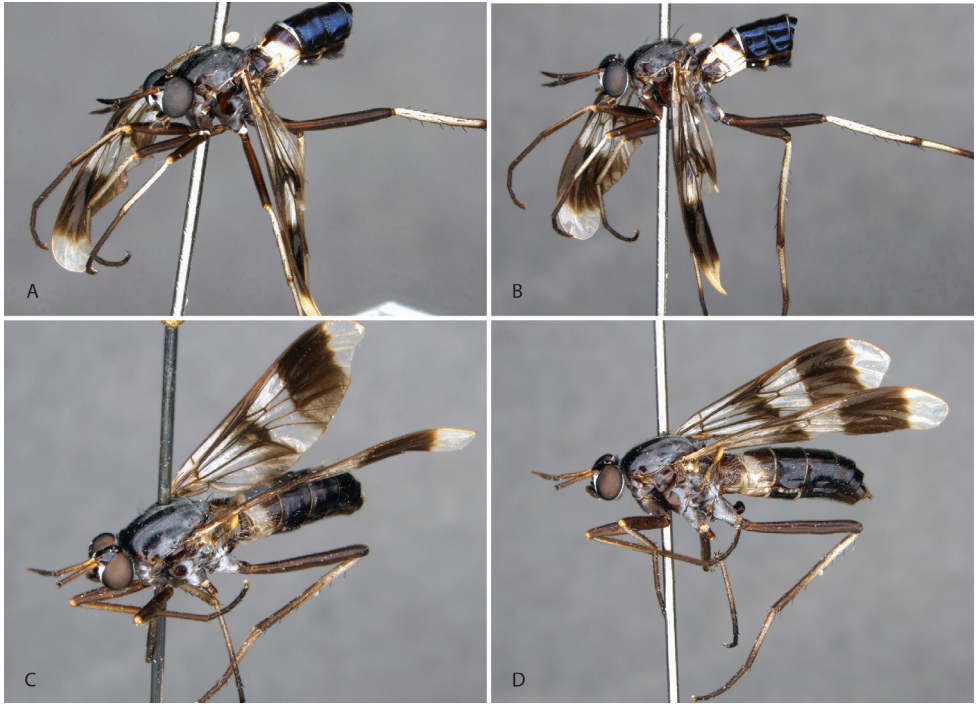


Figure 11. *Calophytus grandiosus* sp. nov. **A** adult male (MEI135021), oblique view **B** same, lateral view **C** adult female (MEI030208), oblique view **D** same, lateral view. Body length: male: 10.3 mm [intact length; male terminal segments and genitalia removed]; female: 11.8 mm.

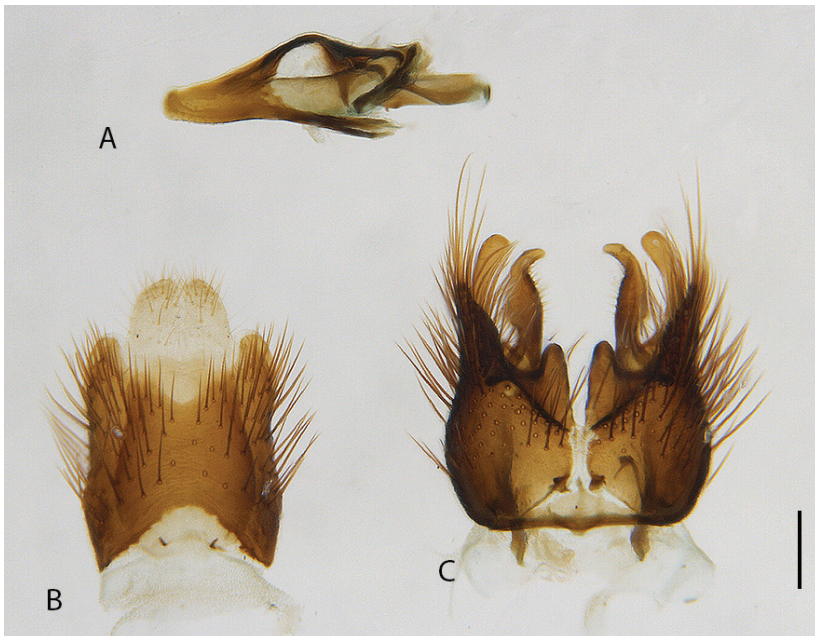


Figure 12. *Calophytus grandiosus* sp. nov., cleared male genitalia **A** aedeagus, lateral view **B** epandrium **C** gonocoxites, ventral view. Scale bar: 0.2 mm.



Figure 13. *Calophytus matilei* sp. nov. **A** adult male (MEI135018), oblique view **B** same, lateral view **C** adult female (MEI071892), oblique view **D** same, lateral view. Body length: male: 8.0 mm; female: 9.4 mm.

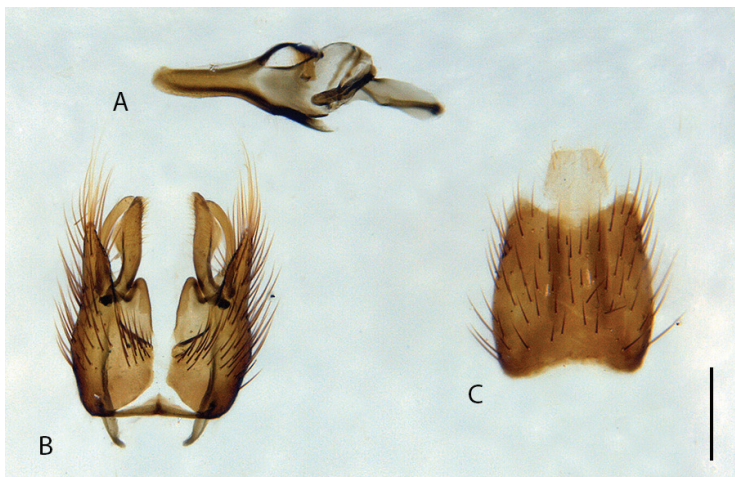


Figure 14. *Calophytus matilei* sp. nov., cleared male genitalia **A** aedeagus, lateral view **B** gonocoxites, ventral view **C** epandrium. Scale bar: 0.2 mm.



Figure 15. *Calophytus monteithi* sp. nov. **A** adult female (MEI138464), oblique view **B** same, lateral view. Body length: 10.3 mm.

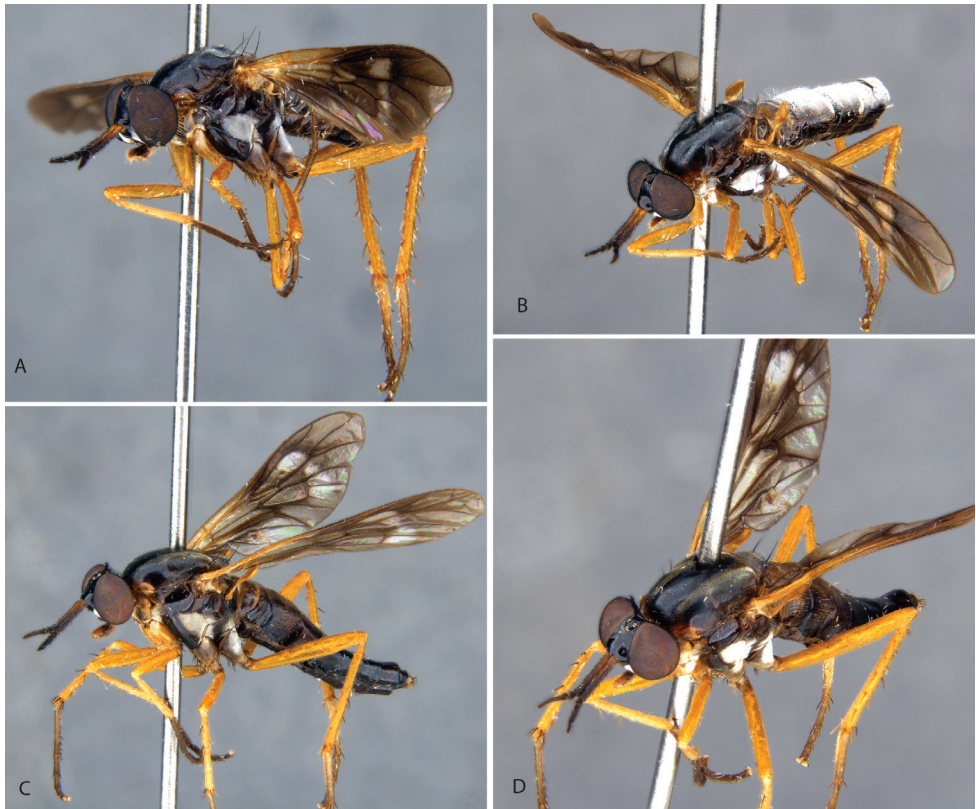


Figure 16. *Calophytus schlingeri* sp. nov. **A** adult male (MEI030158), anterolateral view **B** same, oblique view **C** adult female (MEI030172), lateral view **D** same, oblique view. Body length: male: 8.6 mm; female: 9.8 mm.

surface of femora with long, white setae admixed with short, black setae. Hind femur with one or two subapical anteroventral macrosetae; series of minute posteroventral macrosetae barely evident along middle of femur. *Wing*. Male wing membrane with entirely grey infuscation, darker subapically near anterior margin and apices of cells br and bm; membrane completely covered with microtrichia. Female wing strongly banded, with extensive hyaline areas; pterostigma brown; venation brown, cell m_3 widely open at wing margin. Haltere entirely dark brown, knob slightly lighter ventrally. *Abdomen*. Dark brown-black, short, black, setae on all segments, tergites I and II laterally and sternites I–V with long, white setae; male tergites II–IV and intersegmental membrane on sternites II and III covered with silver velutum pubescence. *Genitalia*. Male: tergite VIII emarginate medially; black setose laterally on posterior 1/2. Sternite VIII quadrate, slightly wider posteriorly, posterior margin black setose. Epandrium quadrate, emarginate anteriorly and posteriorly, lateral corners only slightly extended posteriorly; dark brown setae longer posterolaterally. Cerci bluntly pointed posteriorly, dark brown setae dorsally and apically. Subepandrial sclerite wide, 1/2 width of epandrium; partially sclerotised, lateral margins more strongly so. Gonocoxites rounded with subtriangular outer gonocoxal process; long, dark setae, densely spaced laterally and small patch ventromedially; inner gonocoxal process smoothly curving medially, acuminate, lacking setae

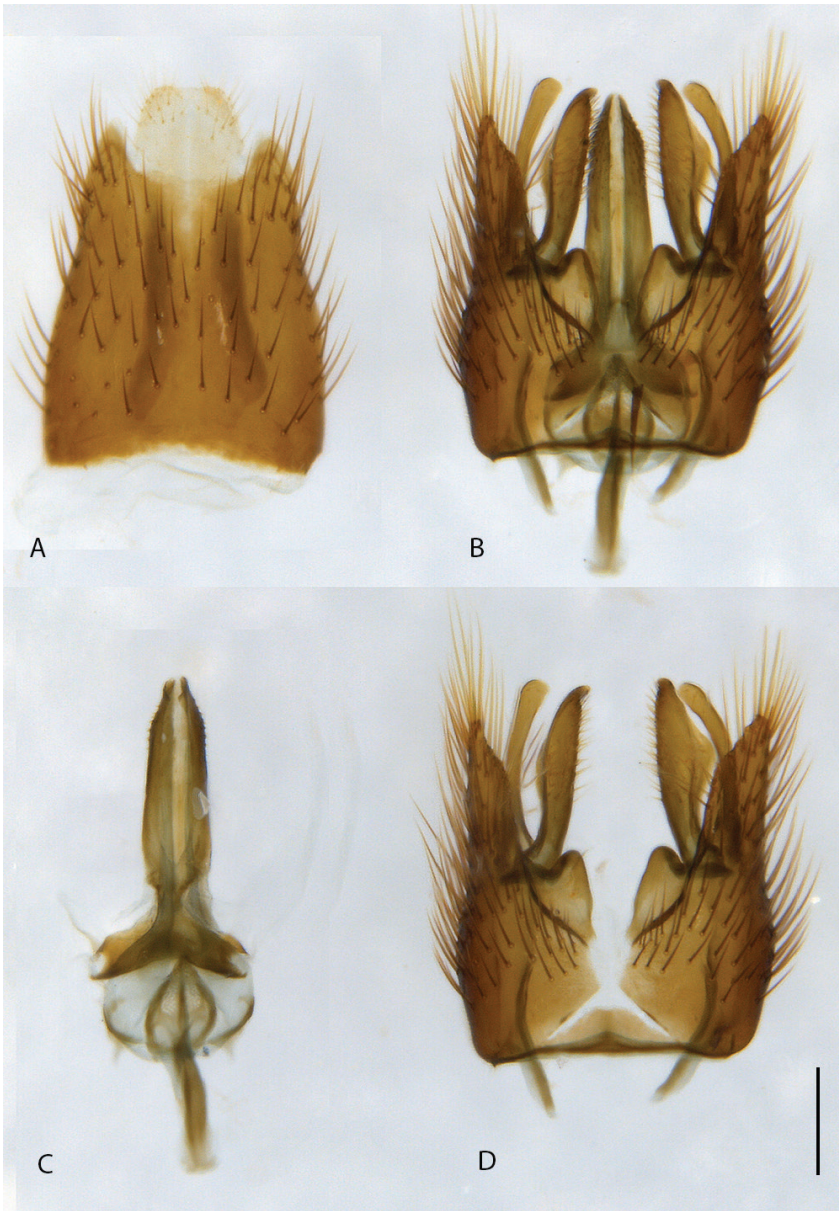


Figure 17. *Calophytus schlingeri* sp. nov., cleared male genitalia **A** epandrium **B** gonocoxites and aedeagus, ventral view **C** aedeagus, dorsal view **D** gonocoxites, ventral view. Scale bar: 0.2 mm.

apically; ventral lobe minutely setose ventrally, gonostylus curved dorsomedially with a broad, dorsal process at 2/3 of length with medial and lateral carinae basodorsally, dark brown setose ventrally and on medial face. Aedeagus with dorsal apodeme of parameral sheath 'T'-shaped, narrow posteriorly and widened anteriorly with anterolateral corners curving ventrally and laterally; distiphallus wide basally with lateral carinae, narrow apically, distiphallus spinose laterally; ventral apodeme dorsoventrally flattened, bifurca-



Figure 19. *Calophytus webbi* sp. nov. **A** adult male (MEI030179), lateral view **B** same, oblique view. Body length: 6.3 mm.

tions subparallel to ejaculatory apodeme; ejaculatory apodeme robust, roughly cylindrical; posterior end of ejaculatory apodeme broadened laterally and ventrally expanded to a point creating a basket-shaped posterior face, lateral ejaculatory apodeme short and subtriangular with lateral process; basiphallus membranous anteriorly. Female: tergites



Figure 20. *Calophytus webbi* sp. nov. adult female head, dorsolateral view.

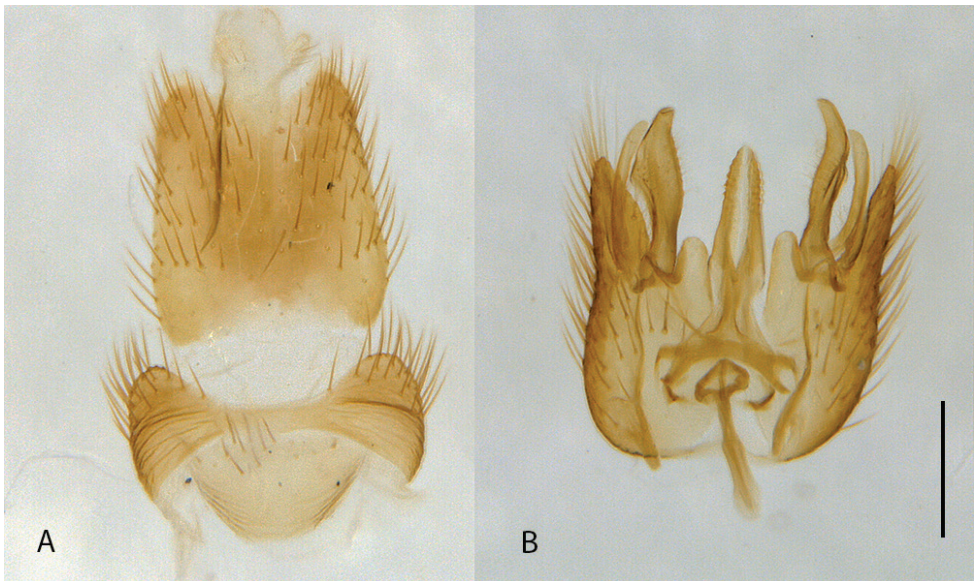


Figure 21. *Calophytus webbi* sp. nov., cleared male genitalia **A** epandrium and tergite VIII **B** gonocoxites and aedeagus, dorsal view with epandrium removed. Scale bar: 0.2 mm.

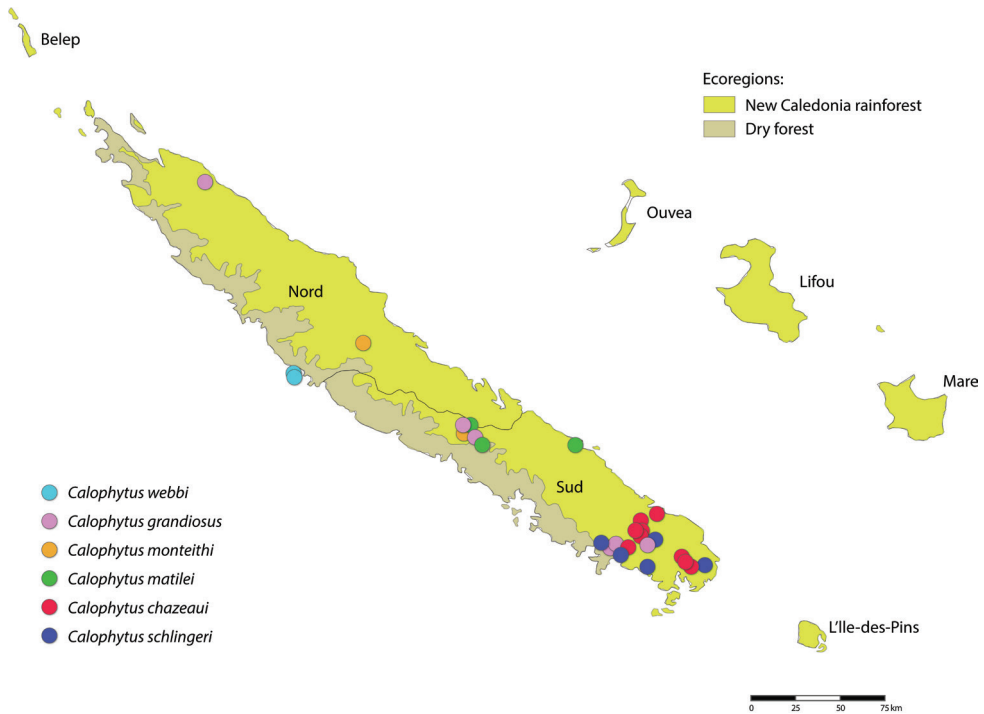


Figure 22. Distribution of *Calophytus* spp. collecting records throughout New Caledonia. Provinces are labelled and ecoregions delineated by colour.

VII and VIII highly modified, much wider than long, with a long and narrow anteromedial process; posterior margin slightly emarginate; with elongate dark setae. Sternite VIII slightly longer than wide, convex ventrally, posterior lobes tapering sharply posteriorly, separate, with a median aedeagal guide; extensive elongate, orange setae, bare at extreme lateral margin. Median lobe of tergite IX reduced, very short and not sclerotised. Acanthophorite with acanthophorite spines dark brown, A2 series spines indistinguishable from rest of acanthophorite setae. Sternite X quadrate. Cercus slightly laterally flattened, extended posteriorly, longer than wide, membranous, slightly sclerotised; furca longer than wide, semicircular anteriorly, tapered to a point posteriorly; origin of spermathecal ducts occurring immediately adjacent to furcal membrane; three spermathecae, much longer than wide, saclike, wider apically than basally; spermathecal duct thickened basally, extremely narrowed basal to spermathecae; bifurcation of spermathecal sac duct with spermathecal ducts very close to furcal membrane; spermathecal sac short, $2.5\times$ furcal length; sac ovoid, longer than wide; $\frac{3}{4}\times$ length of spermathecal sac duct.

Etymology. Derived from the Latin *nubilus*, cloudy, and *-osus*, full of; referring to the dark wing infuscation of the male.

Comments. *Jeanchazeauia nubilosus* sp. nov. exhibits remarkable sexual dimorphism in wing pattern, but little to no other differences in the body or head. The

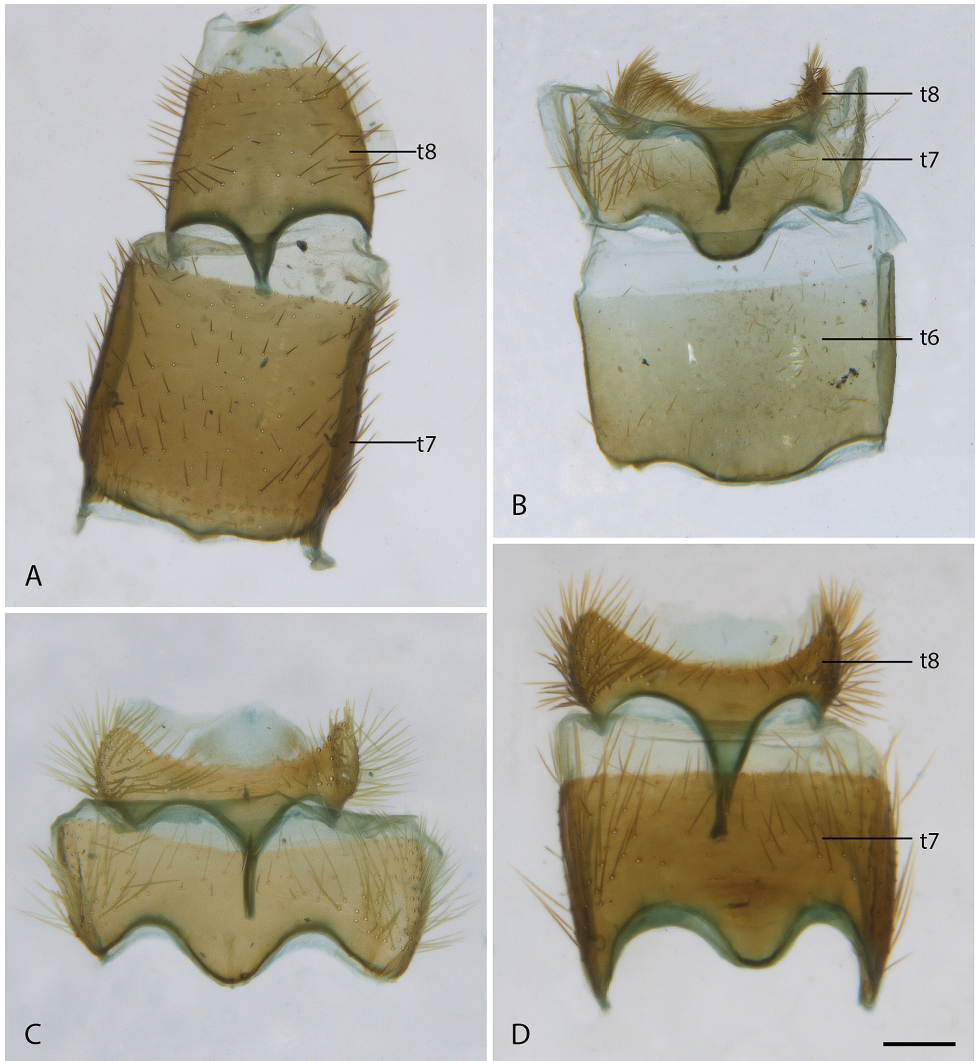


Figure 23. Female abdominal tergites VI–VIII **A** *Calophytus schlingeri* sp. nov. **B** *Jeanchazeauia amoa* sp. nov. **C** *Jeanchazeauia nubilosus* sp. nov. **D** *Jeanchazeauia rufinatus* sp. nov. Scale line: 0.2 mm.

male has largely uniform dark infuscate wings, while the wings of the female are strongly banded. It is not known if this condition extends to other species in the genus where the males are unknown, and such dramatic sexual dimorphism in wing patterning is rare in stiletto flies to this degree. *Jeanchazeauia nubilosus* sp. nov. has been collected in dry to humid tropical forest at higher elevations on several mountains in New Caledonia (e.g., Figs 31A, C, 32B). GenBank sequences for this species (see Winterton et al. 2016: table S1): KM885007 (28S rDNA), KM879119 (EF1a).

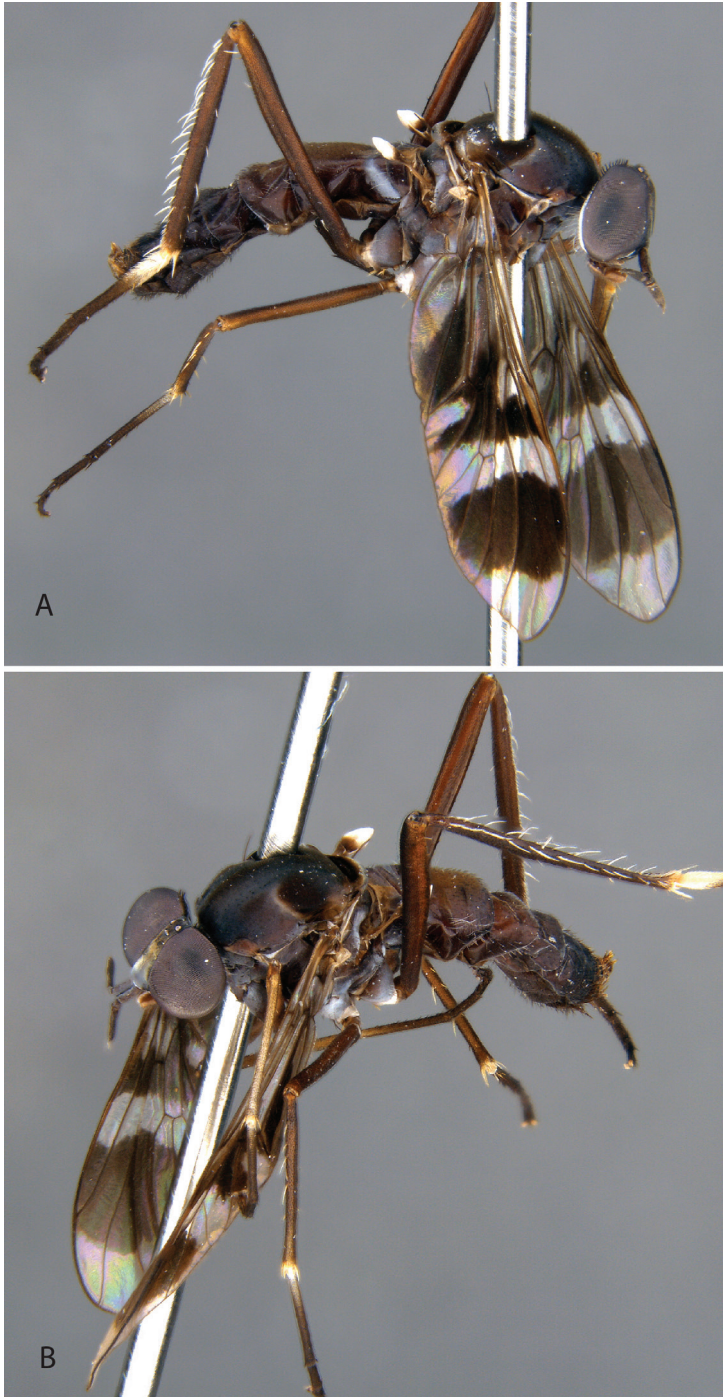


Figure 24. *Jeanchazeauia amoa* sp. nov. **A** adult female (MEI138463), lateral view **B** same, oblique view. Body length: 7.8 mm.

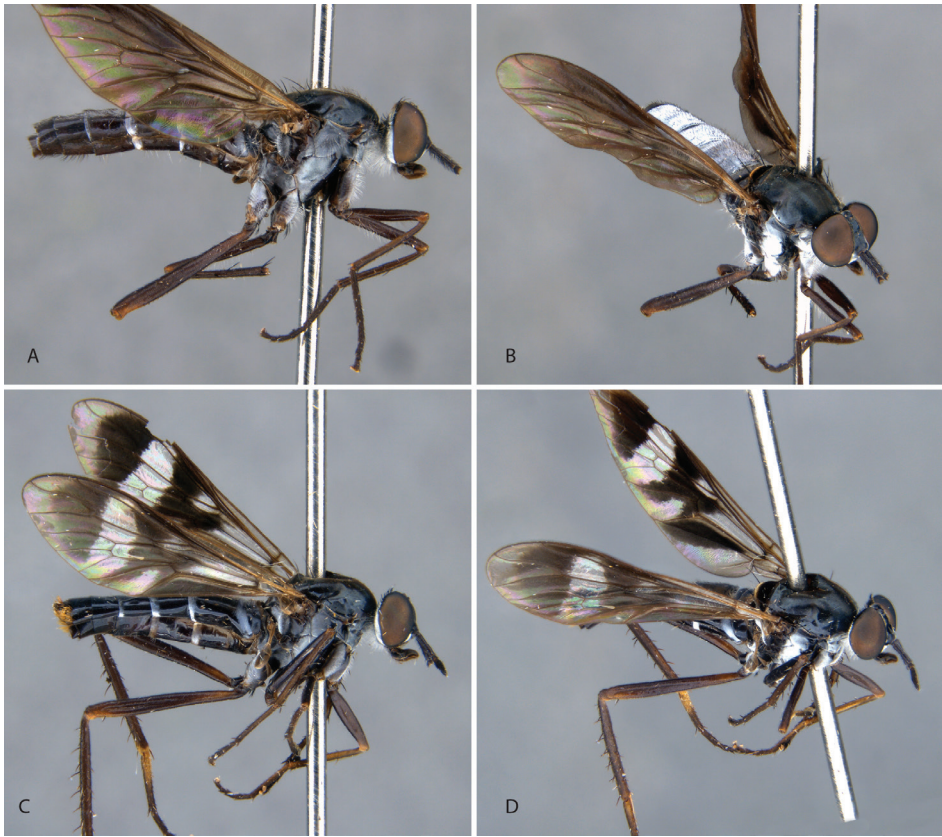


Figure 25. *Jeanchazeauia nubilosus* sp. nov. **A** adult male (MEI030207), lateral view **B** same, oblique view **C** adult female (MEI030203), lateral view **D** same, oblique view. Body length: male: 8.8 mm; female: 9.2 mm.

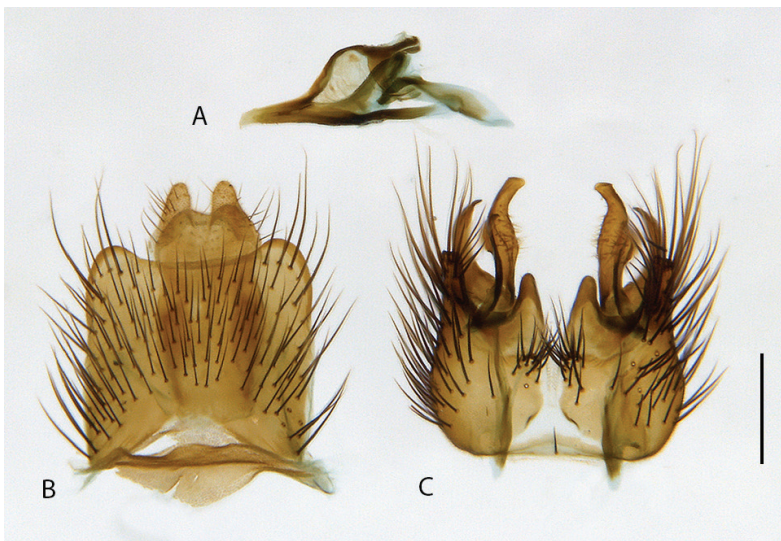


Figure 26. *Jeanchazeauia nubilosus* sp. nov. **A** cleared male genitalia **A** aedeagus, lateral view **B** epanandrium **C** gonocoxites, ventral view. Scale bar: 0.2 mm.

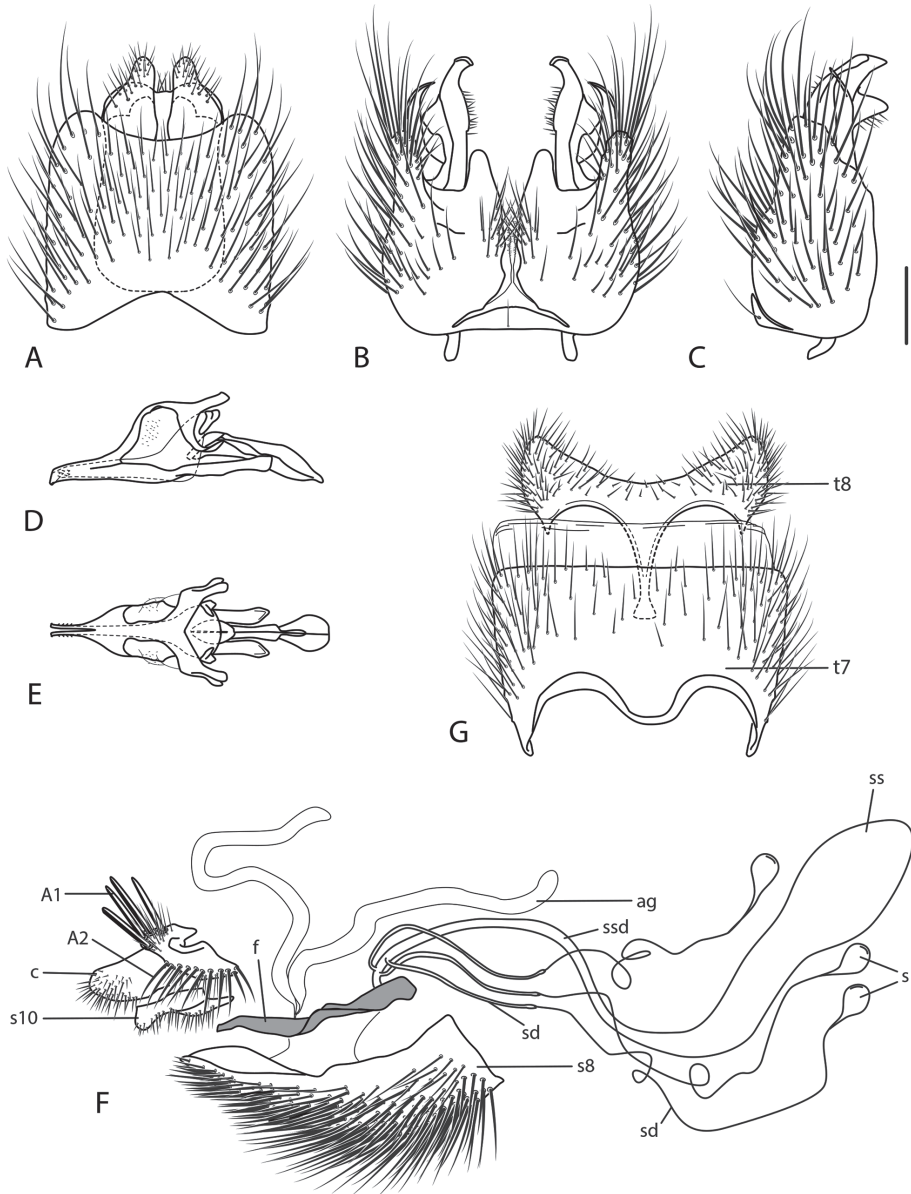


Figure 27. *Jeanchazeauia* spp. genitalia. *Jeanchazeauia nubilosus* sp. nov. **A** epandrium **B** gonocoxites, ventral view **C** same, lateral view **D** aedeagus, lateral view **E** same, dorsal view **F** female genitalia, lateral view, internal structures shown. *Jeanchazeauia rufinatus* sp. nov. **G** female tergites VII and VIII, dorsal view. Scale bar: 0.2 mm.

Specimens examined. *Holotype* male, NEW CALEDONIA: Province Nord: Mt. Dzumac [Dumbea, approximated as -22.106, 166.458], black light (UV), 27–28. II.1984, M. Pogue, M. Epstein (MEI030206, MNHN).

Paratypes. NEW CALEDONIA: Province Nord: 1 male, 13 km by road from Ouego[a] to Mont Mandjanié, Malaise trap along stream [-20.374, 164.482], 175 m, 26.XI.1992, D.W. Webb, E.I. & M. Schlinger, (MEI030207, CSCA). Province Sud: 1 male, Ré-

serve Spéciale de Botanique, Mount Ningua, Malaise trap [-21.735, 166.142], 1100 m, 12–21.XII.2000, L.J. Boutin, M.E. Irwin (MEI131365, CSCA); 3 females, Réserve Spéciale de Botanique, Mount Ningua, Malaise trap [-21.735, 166.142], 1100 m, various dates: 9–21.XII.2000, D.W. Webb, E.I. Schlinger, M.E. Irwin (MEI131362–4, CSCA); 2 females, Ningua Reserve Camp, Malaise trap, rainforest [-21.75, 166.15], 1100 m, 12–13.XI.2001, 27.XI–29.I.2002, Burwell, Monteith (MEI138461–2, QM); 2 females, 17 km NNE Nouméa, Mt. Koghis, Malaise trap in tropical forest [-22.167, 166.533], 500 m, 5–15.XI.1992, D.W. Webb (MEI030202–3, CSCA); 2 females, 17 km NNE Nouméa, Mt. Koghis, Malaise trap across forest stream [-22.167, 166.533], 500 m, 23–26.XII.1991, M.E. Irwin, D.W. Webb (MEI030195–6, MEI); 1 female, Nouméa, Mt. Koghis, Malaise trap [-22.167, 166.533], 500 m, 4.XII.1963, R. Straatman (MEI030197, BPBM); 1 female, 17 km NNE Nouméa, Mount Khogis, Malaise trap across path in rainforest [-22.176, 166.505], 425 m, 8.I.1996, M.E. Irwin, D.W. Webb, E.I. Schlinger, (MEI071888, CSCA); 3 females, 30 km NW Yate, Rivière Bleue, Malaise trap [-22.117, 166.658], 12–25.XI.1986, 11–27.X.1988, L.B. de Larbogne, J. Chazeau, A. & S. Tillier, (MEI030198–200, MNHN); 1 female, Rivière Bleue Provincial Park, 19.6 km Rivière Bleue Road, Malaise trap across forest path [-22.117, 166.658], 183 m, 18–20.XI.1992, D.W. Webb (MEI030201, CSCA).

***Jeanchazeauia rufinatus* sp. nov.**

<http://zoobank.org/75344FB2-15DD-402C-98CF-45DD58CFEF06>

Figs 23D, 27G, 28, 29, 30

Diagnosis. Female abdomen black with white band on tergite II, tergites IV and V with bright red suffusion; black macrosetae on all femora, posteroventral macrosetae on all femora; frons with silver pubescence; female wing with two regular bands.

Description. Length 10.0 mm. *Head.* Dark brown, overlain with dense silver pubescence. Frons with silver pubescence, dorsal area with faint bronze suffusion at some angles, several short, black, setae below ocellar tubercle, eyes separated by width of ocellar tubercle. Occiput and gena entirely bright silver pubescent, except matte black-bronze pubescence along post ocular ridge; postocular macrosetae mostly black, in a single row dorsally; white setal pile ventrolaterally onto gena. Scape 0.3× head length, dark brown, sparsely pubescent, short, black, setose except medial surface. Basal flagellomere 1.2× length of scape, gradually tapering to a blunt point apically, sparsely silver pubescent with short, black setae dorsally at base. Second flagellomere apical, slightly conical, apex narrower than base; < 1/10× length of basal flagellomere. Third flagellomere ½× length of second, conical. Style small, spiculate. Palpus one segmented, cylindrical, apex slightly capitate; dark brown; silver pubescent, admixed with brown setae. Mouthparts brown; brown setose. *Thorax.* Dark brown, overlain with black and silver pubescence; scutum brown pubescent with broad, silver pubescent dorsocentral stripes converging posteriorly; postpronotal lobes and posterior notopleuron silver pubescent; scutellum black, matte pubescent; pleuron silver pubescent with two brown pubescent vertical bands, first passing from the notum at the prothoracic spiracle pos-



Figure 28. *Jeanchazeauia rufinatus* sp. nov. adult female (MEI071891), lateral view. Body length: 10.0 mm.

terovertrally through the anterior katepisternum, second band from the wing base posteroventrally through the meron; macrosetae black (np: 2, sa: 1, pa: 1, dc: 0, sc: 1); scutum with short, black setae dorsally; postpronotum, postpronotal lobe, cervical sclerite, proepisternum, and lateral prosternum with at least some short, white setae; katatergite white setose. *Legs.* Dark brown; coxae densely silver pubescent, otherwise sparsely pubescent; short, black setose; all macrosetae black. Fore- and mid coxae admixed with long, black and white setae; hind coxa white setose. Forecoxa with two, midcoxa with four, and hind coxa with five black, anteroventral, marginal macrosetae. Hind femur with one subapical anteroventral macroseta; series of small dark posteroventral macrosetae along middle of all femora, larger on hind femur. *Wing.* Membrane mostly col-



Figure 29. *Jeanchazeauia rufinatus* sp. nov. adult female (MEI071891), oblique view. Body length: 10.0 mm.

ourless hyaline with two broad dark grey bands; basal band originating at pterostigma and covering membrane directly posterior to posterior wing margin; apical band covering wing tip except apical 1/6 of wing lighter grey; membrane with extensive areas bare of microtrichia. Pterostigma dark grey. Venation dark brown, cell m_3 wide open at wing margin. Haltere dark brown. *Abdomen.* Dark brown, sparsely silver pubescent, sparsely

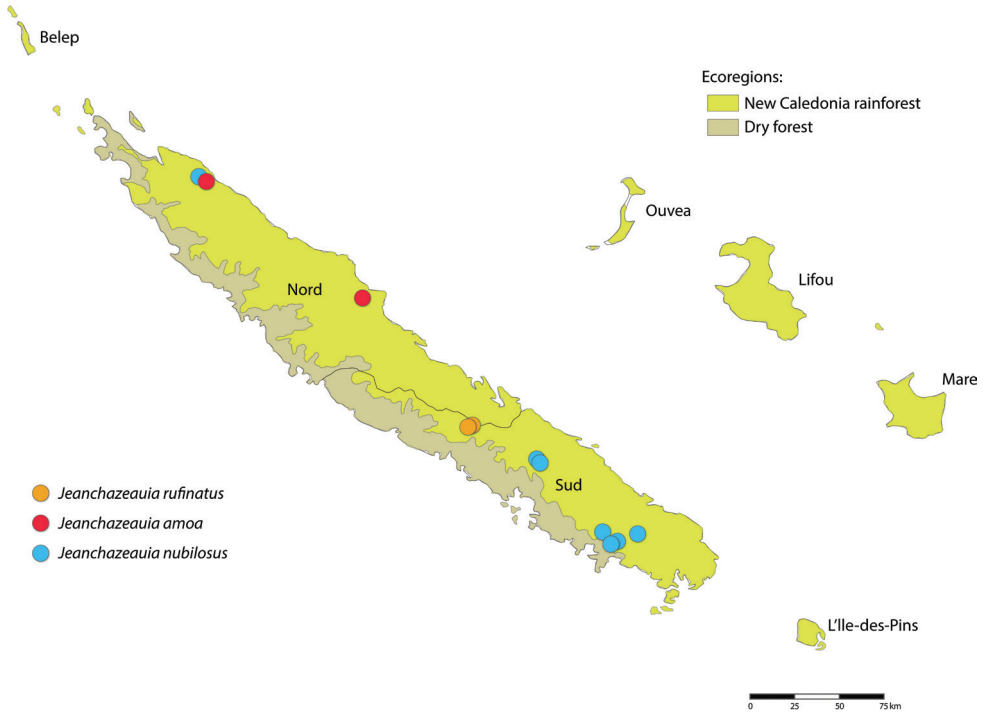


Figure 30. Distribution of *Jeanchazeauia* spp. collecting records throughout New Caledonia. Provinces are labelled and ecoregions delineated by colour.

brown pubescent medially on tergites I–III; tergite II with silver pubescent band on anterior 1/4; tergites IV and V and posterior margin of tergite III reddish orange, except extreme lateral margin dark brown; short, black, setose, apical segments with longer setae; tergites I and II with long, white and black setae laterally. *Genitalia*. Female: tergites VII and VIII highly modified, much wider than long, with an extremely long anteromedial, narrow projection; posterior margin slightly emarginated. Sternite VIII slightly longer than wide, slightly convex ventrally, posterior lobes tapering sharply posteriorly, separate, with a median aedeagal guide; dense, elongate, gold-brown setae present, bare at extreme lateral margin. Medial lobe of tergite IX reduced, very short and only slightly sclerotised, bare of setae. Acanthophorite dark brown; acanthophorite spines dark brown, A2 spines inseparable from rest of acanthophorite setae. Sternite X quadrate, slightly longer than wide, anterior margin truncate, posterior margin slightly emarginate; short, dark brown setose. Furca longer than wide, semicircular anteriorly, tapered to a point posteriorly, origin of spermathecal ducts occurring immediately adjacent to furcal membrane; three spermathecae, much longer than wide, sac-like, wider apically than basally; spermathecal duct thickened basally, extremely narrowed basal to spermathecae; bifurcation of spermathecal sac duct with spermathecal ducts very close to furcal membrane; spermathecal sac duct very long; sac ovoid, longer than wide. Spermathecal ducts and spermathecal sac duct uniting to form a common gonopore on furcal membrane; gonopore wide at orifice and narrowing to common duct.

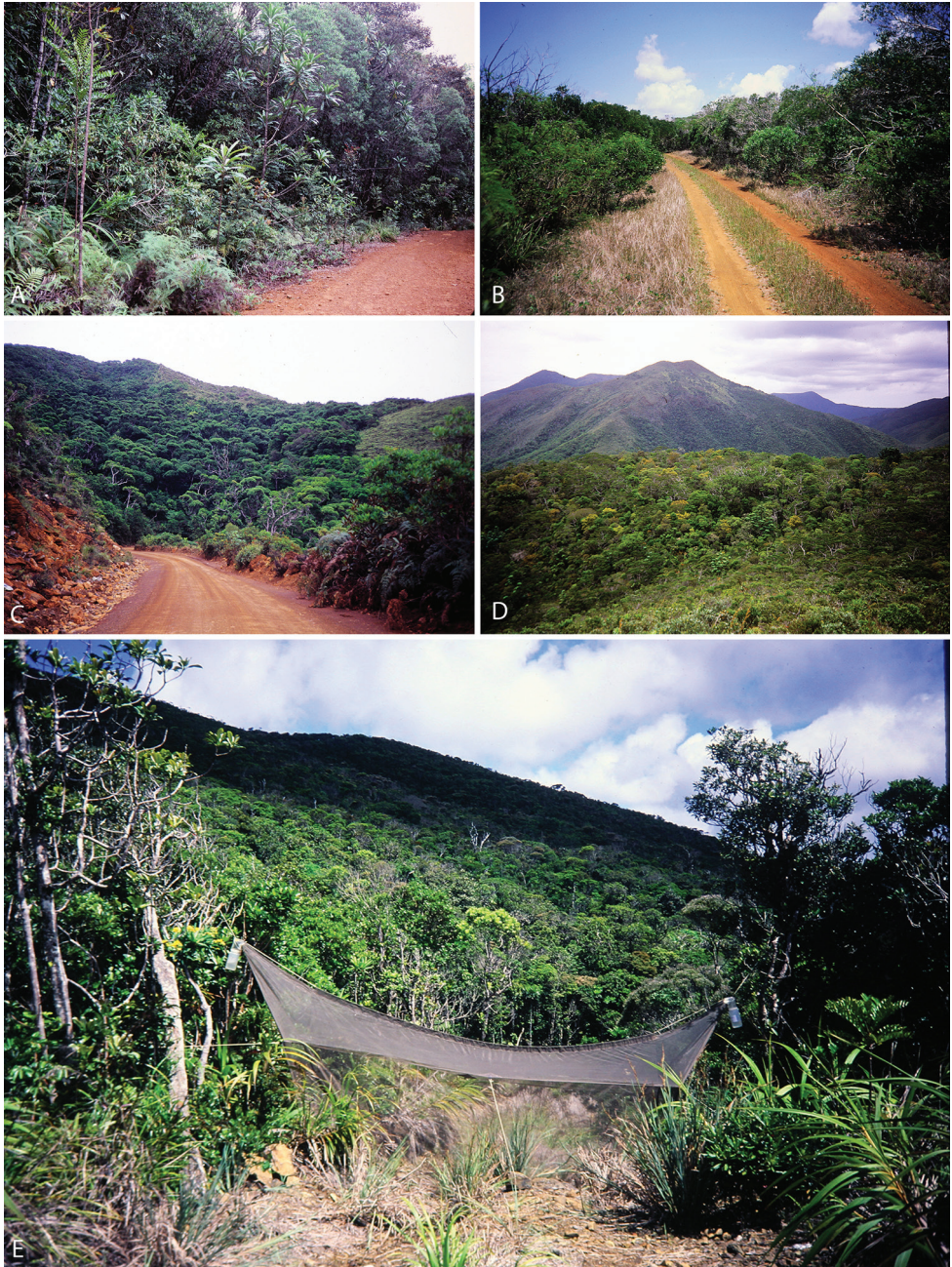


Figure 31. Natural habitats of New Caledonian agapophytine stiletto flies **A** Riviere Bleue Reserve, sclerophyll forest and maquis scrub, habitat of *C. chazeau* sp. nov., *C. grandiosus* sp. nov., *C. schlingeri* sp. nov., and *J. nubilosus* sp. nov. **B** Pindai Peninsula, tropical dry forest, habitat of *C. webbi* sp. nov. **C** Mount Dzumac, rainforest, habitat of *J. nubilosus* sp. nov. **D** Mount Dore, rainforest and dry sclerophyll forest **E** Mount Dore, Malaise trap in flyway (photographs by Michael E. Irwin).



Figure 32. Natural habitats of New Caledonian agapophytine stiletto flies **A** Mount Aoupinie, rainforest, habitat of *C. monteithi* sp. nov. **B** Mount Ningua, rainforest, habitat of *J. nubilosus* sp. nov. **C** Mount Mandjelia, habitat of *C. grandiosus* sp. nov. (photographs by Michael E. Irwin).

Etymology. Derived from the Latin *rufus*, red, reddish, and *-atus*, clothed; referring to the reddish area on the female abdomen. Gender is masculine.

Comments. *Jeanchazeauia rufinatus* sp. nov. can be readily identified by the intensely white pubescence over the entire frons area, and at least in the female by the reddish cuticle on tergites IV and V and on the posterior margin of tergite III. This species has been rarely collected and occurs in rainforest near Sarraméa in the southern province. No males are known.

Specimens examined. *Holotype* female, NEW CALEDONIA: Province Sud: Reserve Col d' Amieu, 7.5 km NW Sarraméa, Malaise, 21.585°S, 165.819°E [-21.585, 165.819], 4–9.XI.2000, D.W. Webb, E.I. Schlinger, M.E. Irwin, 300 m (MEI108229, MNHN).

Paratype. NEW CALEDONIA: 1 female Province Sud: 9 km NW Sarraméa, Malaise on forest hillside, 305 m, 9.I.1996, M.E. Irwin, D.W. Webb, E.I. Schlinger, 21°35'07"S, 165°48'55"E [-21.585, 165.815] (MEI071891, CSCA).

Acknowledgements

This paper is dedicated to the late Professor Emeritus Evert I. Schlinger and the late Dr Donald W. Webb. We are grateful to the various curators and collection managers who loaned out material for this study. We are also deeply grateful to the Schlinger Foundation for supporting expeditions to New Caledonia. While in New Caledonia, MEI and expedition members relied heavily on Dr Jean Chazeau and Lydia Bonnet de Larbogne for logistic support; this hospitality is immensely appreciated. We owe much gratitude to Ms Gail E. Kampmeier who developed the Mandala database used here. Thank you also to J. Marie Metz who produced some of the illustrations included here. The National Science Foundation (NSF) (DEB-0614213, DEB-9521925, and DEB-9977958) and the Schlinger Foundation provided funding for this study. Statements and viewpoints expressed herein do not necessarily reflect the views of NSF or the Schlinger Foundation. Thank you to David Ferguson, Christine Lambkin, Stephen Gaimari, and Martin Hauser for their helpful comments on the manuscript.

Mention of trade names or commercial products in this publication is solely for the purpose of providing specific information and does not imply recommendation or endorsement by the USDA; USDA is an equal opportunity provider and employer.

References

- Bigot JMF (1860) Diptères exotiques nouveaux. Annales de la Société Entomologique de France 8(1): 219–228.
- Cumming JM, Wood DM (2017) Adult morphology and terminology. In: Kirk-Spriggs AH, Sinclair BJ (Eds) Manual of Afrotropical Diptera, vol. 1. South African National Biodiversity Institute, Pretoria, 89–133.

- Hauser M, Irwin ME (2003) The Nearctic Genus *Ammonaios* Irwin and Lyneborg 1981 (Diptera: Therevidae). *Annals of the Entomological Society of America* 96: 738–765. [https://doi.org/10.1603/0013-8746\(2003\)096\[0738:TNGAIA\]2.0.CO;2](https://doi.org/10.1603/0013-8746(2003)096[0738:TNGAIA]2.0.CO;2)
- Irwin ME (1976) Morphology of the terminalia and known ovipositing behaviour of female Therevidae (Diptera: Asiloidea), with an account of correlated adaptations and comments on cladistic relationships. *Annals of the Natal Museum* 22: 913–935.
- Irwin ME, Winterton SL (2020) A new stiletto fly genus from South America (Diptera: Therevidae: Agapophytinae) *Zootaxa* 4751: 276–290. <https://doi.org/10.11646/zootaxa.4751.2.4>
- Kampmeier GE, Irwin ME (2009) Meeting the interrelated challenges of tracking specimen, nomenclature, and literature data in Mandala. In: Pape T, Meier R, Bickel D (Eds) *Diptera Diversity: Status, Challenges and Tools*. Brill Academic Publishers, Leiden, 407–438. <https://doi.org/10.1163/ej.9789004148970.I-459.65>
- Kröber O (1912) Die Thereviden der indo-australischen Region. (Dipt.). *Entomologische Mitteilungen* 1: 116–125. <https://doi.org/10.1002/mmnd.48019120102>
- Kröber O (1928) Neue Dipteren des Deutschen Entomolog. Museums in Dahlem (Conopidae, Omphralidae, Therevidae, Tabanidae). *Entomologische Mitteilungen* 17: 31–41.
- Lambkin LL, Turco F (2013) *Collessiama* (Diptera: Therevidae: Agapophytinae: *Taenogera* genus-group), a new genus from eastern Australia, with a key to the Australian genera of Therevidae. *Zootaxa* 3680: 96–117. <https://doi.org/10.11646/zootaxa.3680.1.7>
- Lyneborg L (2001) The Australian stiletto-flies of the *Anabarhynchus* genus-group (Diptera: Therevidae). *Entomonograph Volume 13*. Apollo Books: Stenstrup, 256 pp.
- Macquart JM (1848) Diptères exotiques nouveaux ou peu connus. Suite du 2^{me} supplément *Mémoires de la Société Royale des Sciences, de l'Agriculture et des Arts, de Lille* 1847(2): 161–237.
- Macquart JM (1850) Diptères exotiques nouveaux ou peu connus. 4^{me} supplément. *Mémoires de la Société Royale des Sciences, de l'Agriculture et des Arts, de Lille* 1849: 309–479.
- Malloch JR (1932) *Therevidae*. In: *British Museum (Natural History) (Ed.), Diptera of Patagonia and South Chile* 5 (3). The British Museum, London, 235–257.
- Mann JS (1928) Revisional notes on Australian Therevidae. Part 1. *Australian Zoologist* 5: 151–194.
- Pyle RL, Michel E (2008) ZooBank: Developing and nomenclatural tool for unifying 250 years of biological information. *Zootaxa* 1950: 39–50. <https://doi.org/10.11646/zootaxa.1950.1.6>
- Webb DW, Gaimari SD, Hauser M, Holston KC, Metz MA, Irwin ME, Kampmeier GE, Algmin K (2013) An annotated catalogue of the New World Therevidae (Insecta: Diptera: Asiloidea). *Zootaxa* 3600: 1–105. <https://doi.org/10.11646/zootaxa.3600.1.1>
- Winterton SL (2006) New species of *Eupsilocephala* Kröber from Australia (Diptera: Therevidae). *Zootaxa* 1372: 17–25. <https://doi.org/10.11646/zootaxa.1372.1.2>
- Winterton SL, Hardy NB, Gaimari SD, Hauser M, Hill HN, Holston KC, Irwin ME, Lambkin CL, Metz MA, Turco F, Webb D, Yang L, Yeates DK, Wiegmann BM (2016) The phylogeny of stiletto flies (Diptera: Therevidae). *Systematic Entomology* 41: 144–161. <https://doi.org/10.1111/syen.12147>
- Winterton SL, Irwin ME, Yeates DK (1999a) Systematics of *Nanexila* Winterton & Irwin, gen. nov. (Diptera: Therevidae) from Australia. *Invertebrate Taxonomy* 13: 237–308. <https://doi.org/10.1071/IT97029>

- Winterton SL, Irwin ME, Yeates DK (1999b) Phylogenetic revision of the *Taenogera* Kröber genus-group (Diptera: Therevidae), with descriptions of two new genera. Australian Journal of Entomology 38: 274–290. <https://doi.org/10.1046/j.1440-6055.1999.00126.x>
- Winterton SL, Merritt DJ, O’Toole A, Yeates DK, Irwin ME (1999c) Morphology and histology of the spermathecal sac, a novel structure in the female reproductive system of Therevidae (Diptera: Asiloidea). International Journal of Insect Morphology and Embryology 28: 273–279. [https://doi.org/10.1016/S0020-7322\(99\)00030-6](https://doi.org/10.1016/S0020-7322(99)00030-6)
- Winterton SL, Yang L, Wiegmann BM, Yeates DK (2001) Phylogenetic revision of Agapophytinae subf. n. (Diptera: Therevidae) based on molecular and morphological evidence. Systematic Entomology 26: 173–211. <https://doi.org/10.1046/j.1365-3113.2001.00142.x>

New data on *Garra makiensis* (Cyprinidae, Labeoinae) from the Awash River (Ethiopia) with remarks on its relationships to congeners on the Arabian Peninsula

Gernot K. Englmaier¹, Nuria Viñuela Rodríguez², Herwig Waidbacher³,
Anja Palandačić⁴, Genanaw Tesfaye⁵, Wolfgang Gessl¹, Paul Meulenbroek³

1 University of Graz, Institute of Biology, Universitätsplatz 2, A-8010 Graz, Austria **2** Department of Ecology, Faculty of Science, Charles University, Viničná 7, CZ-12844 Prague 2, Czech Republic **3** University of Natural Resources and Life Sciences, Institute of Hydrobiology and Aquatic Ecosystem Management (IHG), Vienna, Gregor-Mendel Straße 33, A-1180 Vienna, Austria **4** Natural History Museum Vienna, Burggring 7, A-1010 Vienna, Austria **5** National Fisheries and Aquatic Life Research Centre, P.O. Box: 64, Sebeta, Ethiopia

Corresponding author: Gernot K. Englmaier (gernotenglmaier@gmx.at)

Academic editor: M. E. Bichuette | Received 29 June 2020 | Accepted 14 September 2020 | Published 4 November 2020

<http://zoobank.org/735FE56F-6CBB-485F-8484-9CD8060A1E5B>

Citation: Englmaier GK, Viñuela Rodríguez N, Waidbacher H, Palandacic A, Tesfaye G, Gessl W, Meulenbroek P (2020) New data on *Garra makiensis* (Cyprinidae, Labeoinae) from the Awash River (Ethiopia) with remarks on its relationships to congeners on the Arabian Peninsula. ZooKeys 984: 133–163. <https://doi.org/10.3897/zookeys.984.55982>

Abstract

On the African continent, the genus *Garra* consists of several species often insufficiently separated from each other by diagnostic characters. Herein, a detailed morphological redescription of *Garra makiensis* from the Awash River drainage is presented, together with additional data on the type specimens of *G. makiensis* and *G. rothschildi*. Mitochondrial CO1 sequence data are also provided, including the historic paralectotype of *G. makiensis*, with a comparison to *Garra* species from Africa and the Middle East. Based on these sequences, *G. makiensis* clusters outside the group of African congeners and is a sister lineage to species from the south-east of the Arabian Peninsula. Although morphologically variable, *G. makiensis* is characterised by having a single unbranched pectoral-fin ray, a short distance between vent and anal-fin origin (7.3–19.7 % of pelvic – anal distance), chest and belly covered with scales, and a prominent axillary scale at base of pelvic fin (18.8–35.5 % of pelvic-fin length).

Keywords

Biogeography, biodiversity, CO1 sequence data, East Africa, freshwater fish, tubercles

Introduction

The endorheic Awash River drainage in the northern part of the Main Ethiopian Rift (MER) is subdivided into two freshwater ecoregions, the Ethiopian Highlands and the Northern Eastern Rift (Abell et al. 2008). It originates close to Ethiopia's capital city Addis Ababa at an altitude of > 3,000 m a.s.l. Along its course (1,250 km in length), it flows from the highlands into the MER, and drains into saline Lake Abbe at the Ethiopian-Djibouti border. Numerous smaller sub-drainage systems, among them the Gotta River, belong to the Awash catchment. Biogeographically, the region is classified as part of the Abyssinian Highlands ichthyofaunal province (Roberts 1975) (a sub-province of the Nilo-Sudanic province according to Snoeks and Getahun (2013)) or the Ethiopian Rift Valley province (Paugy 2010). Evidence for ichthyofaunal affinities with the Nile River system and the Central MER were recently provided by Beshera and Harris (2014) for the *Labeobarbus intermedius* complex and by Englmaier et al. (2020a) for small-sized smiliogastrin barbs (*Enteromius* Cope, 1867).

The fish fauna of the Awash is commonly described as “impoverished” (Roberts 1975: 291) with 10–13 species belonging to five families (Golubtsov et al. 2002; Englmaier et al. 2020a, 2020b). One of the poorly investigated groups of freshwater fishes in the region is the Afro-Asian genus *Garra* Hamilton, 1822. Menon (1964) and later Getahun (2000) and Stiassny and Getahun (2007) provided the first comprehensive morphological studies on African *Garra*. Twenty-four valid species of *Garra* are currently recognised in Africa (Moritz et al. 2019). They are distributed from North Africa (Nile River in Egypt) to drainage systems in West Africa (e.g., Senegal River) and central sub-Saharan Africa (Tanzania and Angola) (Daget et al. 1984; Getahun 2000; Stiassny and Getahun 2007; Habteselassie et al. 2010; Moritz et al. 2019). With 12 species, the genus was found to be particularly diverse in the Ethiopian Highlands and surrounding drainage systems (Stiassny and Getahun 2007). In the Awash River, recent surveys gave evidence for three well supported mitochondrial clades of *Garra*, identified as: *G. aethiopica* (Pellegrin, 1927), *G. dembeensis* (Rüppell, 1835) and *G. makiensis* (Boulenger, 1903) by Englmaier et al. (2020b).

Compared to *Garra* species in Asia and the Middle East (e.g., Krupp 1983; Yang et al. 2012; Sayyadzadeh et al. 2015; Esmaeili et al. 2016; Hashemzadeh Segherloo et al. 2016; Nebeshwar and Vishwanath 2017; Kirchner et al. 2020; Kottelat 2020), systematic relationships and diagnostic morphological characters of African taxa have not been well investigated (Stiassny and Getahun 2007). So far, no consistent opinion has been reached in assessing important diagnostic characters such as the presence/absence of a red or black blotch behind the upper edge of operculum, the scale pattern on ventral side, the size and shape of the gular disc (also referred to as “mental adhesive disc” in Zhang et al. (2002)) or the tuberculation on snout and head (Menon 1964; Getahun 2000; Golubtsov et al. 2002, 2012; Stiassny and Getahun 2007). Together with recent reports of considerable intraspecific morphological variability (Golubtsov et al. 2012; Englmaier 2018), this complicates species-level determination and has led to different taxonomic opinions and inconsistent distribution records of many African

species (see Getahun 2000; Golubtsov et al. 2002, 2012; Stiassny and Getahun 2007; Stiassny et al. 2007; Habteselassie 2009, 2012; Moritz et al. 2019).

One such problematic species, *G. makiensis*, was described from the Meki River (endorheic basin of Lake Ziway) in the Central MER (Boulenger 1903). In the first comprehensive revision of the genus, Menon (1964) provided a redescription of this species and included *G. rothschildi* (Pellegrin, 1905), described from the Gotta River in the Northern MER, as a synonym. This opinion was later corroborated by Getahun (2000) and Stiassny and Getahun (2007), who extended the distribution range of *G. makiensis* to the Southern MER, the Blue and White Nile, and the Omo River drainage. However, during recent surveys in the Awash River, preliminary observations showed that diagnostic characters described for *G. makiensis* in recent literature and identification keys (e.g., Stiassny and Getahun 2007; Habteselassie 2012) contain uncertainty and did not allow reliable species identification (Englmaier 2018).

Therefore, as a first step towards resolving taxonomic inconsistencies among African *Garra*, we present a detailed redescription of *G. makiensis* based on specimens from the Awash River drainage with new data on the type specimens of *G. makiensis* and *G. rothschildi*. Moreover, we provide mitochondrial CO1 sequence data for *Garra* species from the Awash River (*G. aethiopica*, *G. dembeensis*, *G. makiensis*), and the first CO1 sequence of the historic paralectotype of *G. makiensis* (BMNH 1905.7.25.88) in order to evaluate their phylogenetic relationships. These considerations are complemented with a morphological comparison of *G. makiensis* with closely related species and remarks on biogeographical implications.

Materials and methods

Specimens of *Garra* were collected in the Awash River, including its major tributaries (Fig. 1 and Table 1, Suppl. material 1: Table S1). Collections were made during the dry seasons between 2017 and 2019. Sampling methods are described in Englmaier et al. (2020a). After anaesthesia with etheric clove oil (*Eugenia caryophyllata*) diluted in water, fish specimens were fixed in 6 % pH neutral formalin (later stored in 75 % ethanol) or 96 % ethanol.

Garra species from the Awash River were identified as morphospecies based on external diagnostic characters (Englmaier et al. 2020b). In addition to comparison with type material (for *G. makiensis* and *G. aethiopica*) and original descriptions (Rüppell 1835; Boulenger 1903; Pellegrin 1927), the following available literature was used for identification: Getahun (2000), Golubtsov et al. (2002), Stiassny and Getahun (2007), Habteselassie et al. (2010), Habteselassie (2012), and Moritz et al. (2019).

Museum samples included specimens deposited in the collections of the Natural History Museum Vienna (NMW; Fig. 1: sampling sites S6–S16, T1, T3–T4); the British Museum of Natural History (BMNH; Fig. 1: sampling site M1); the American Museum of Natural History (AMNH; Fig. 1: sampling site G1); the Muséum national d'Histoire naturelle, Paris (MNHN); and the Musée royal de l'Afrique centrale, Tervuren (MRAC). Comparative material is listed in Table 1.

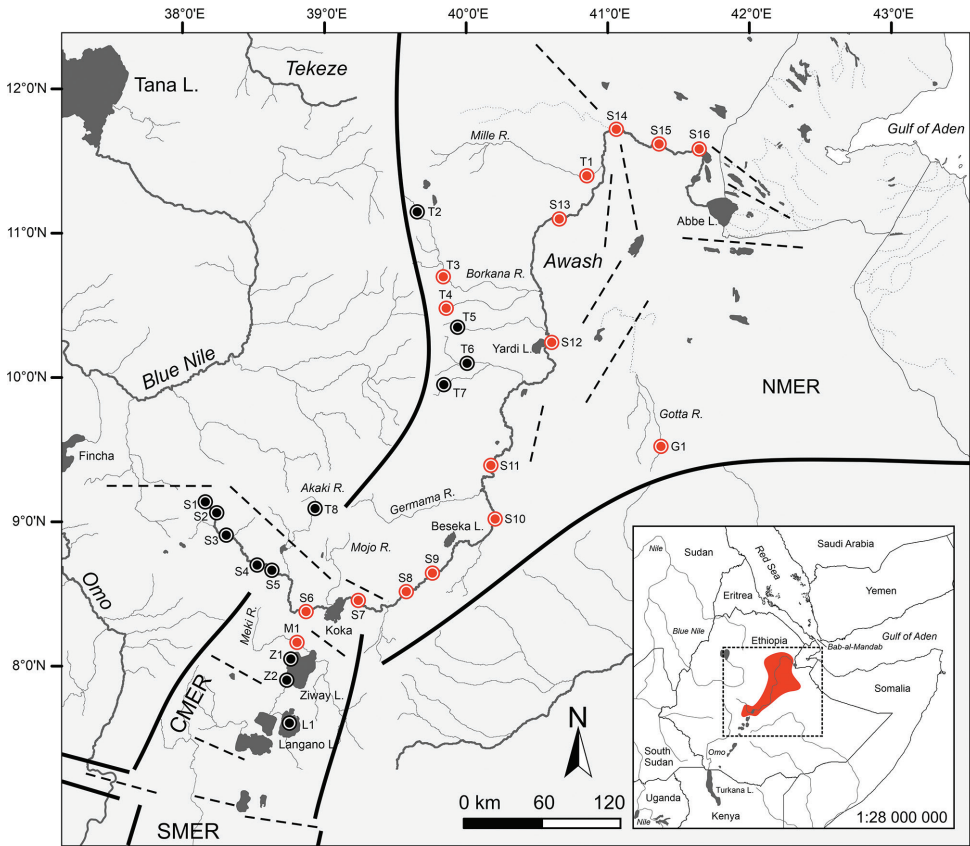


Figure 1. Map of the study area in the Northern and Central Main Ethiopian Rift (NMER, CMER) showing sampling sites and examined material; thick lines denoting Main Rift faults, dashed lines showing transversal faults (Bonini et al. 2005). Study sites: **S1–S6** and **T1–T8** Awash River drainage, **G1** Gotta River (type locality of *G. rothschildi*), **M1** Meki River (type locality of *G. makiensis*), **Z1–Z2** Lake Ziway, and **L1** Lake Langano. Sampling sites in red showing localities where *G. makiensis* is known from examined material or was recorded during recent surveys. The small inserted map showing known distribution range of *G. makiensis* in the Awash and Meki River drainages.

In the present study, we refer to the species names *Garra smarti* Krupp & Budd, 2009 and *Garra sindhi* Lyon, Geiger & Freyhof, 2016, although the specific epithet of both species was recently ‘corrected’ to *smartae* and *sindhae* by Kirchner et al. (2020). Krupp and Budd (2009) and Lyon et al. (2016) dedicated the species names to two different women, using the masculine genitive ending *-i*, instead of the common feminine genitive ending *-ae*. However, the names *smarti* and *sindhi* are not to be considered incorrect according to Art. 32.5 of the International Code of Zoological Nomenclature (1999) and are therefore not to be modified (see also Dubois (2007) and Nemésio and Dubois (2012) for species names derived from personal names).

Table 1. Comparative material used in the present study. Sampling sites referring to those given in Fig. 1.

Taxon name	Museum number	n	Types	SL, mm	Sampling site	Information
<i>Discognathus makiensis</i>	BMNH 1905.7.25.87	1	lectotype	67.1	M1	Maki [Meki] River, Ethiopia, coll. O. Neumann and C. v. Erlanger
<i>Discognathus makiensis</i>	BMNH 1905.7.25.88	1	paralectotype	47.6	M1	Maki [Meki] River, Ethiopia, coll. O. Neumann and C. v. Erlanger (voucher specimen for COI (MT946130))
<i>Discognathus rohschildi</i>	MNHN 1905-0246	1	syntype	135.3	G1	Gotta [Gota] River, Ethiopia (photographs and radiographs examined)
<i>Discognathus rohschildi</i>	MNHN 1905-0247	1	syntype	108.7	G1	Gotta [Gota] River, Ethiopia (photographs and radiographs examined)
<i>Garra makiensis</i>	MRAC 91-051-P-0044	21	non-types	68.9–44.4	G1	Gotta [Gotta] River, Harar province, Ethiopia (radiographs examined)
<i>Garra makiensis</i>	AMNH 227323	3	non-types	72.6–76.1	G1	Error Gota [Gotta] River, Eastern side of Erer town, pools near main road, Hararge, Ethiopia (09°30'N, 41°15'E) (radiographs examined)
<i>Garra makiensis</i>	NMW 99222	3	non-types	44.6–136.1	S9	Awash River at Nur Sada (8°33'9"N, 39°38'10"E; 1,214 m a.s.l.), Ethiopia, 31.01.2018, coll. G.K. Englmaier, G. Tesfaye, P. Meulenbroek and H. Wäidbacher (one voucher specimen for COI (MT946129))
<i>Garra makiensis</i>	NMW 99223	6	non-types	56.0–78.3	S7	Awash River at Woji (8°28'23"N, 39°12'43"E; 1,552 m a.s.l.), Ethiopia, 09.11.2017, coll. G.K. Englmaier, G. Tesfaye and P. Meulenbroek (one voucher specimen for COI (MT946124))
<i>Garra makiensis</i>	NMW 99224	9	non-types	43.3–90.6	S6	Awash River at Lafessa (8°23'16"N, 38°54'30"E; 1,608 m a.s.l.), Ethiopia, 08.11.2017, coll. G.K. Englmaier, G. Tesfaye and P. Meulenbroek (two voucher specimens for COI (MT946122, MT946123))
<i>Garra makiensis</i>	NMW 99225	3	non-types	70.6–71.4	S11	Awash River at Worer (9°20'6"N, 40°10'19"E; 743 m a.s.l.), Ethiopia, 29.01.2018, coll. G.K. Englmaier, G. Tesfaye, P. Meulenbroek and H. Wäidbacher.
<i>Garra makiensis</i>	NMW 99226	1	non-types	43.4	S8	Awash River at Koikada (8°30'2"N, 39°33'7"E; 1,260 m a.s.l.), Ethiopia, 09.12.2017, coll. G.K. Englmaier and G. Tesfaye.
<i>Garra makiensis</i>	NMW 99230	5	non-types	66.8–92.6	S12	Awash River at Kada Bada (10°13'53"N, 40°34'43"E; 570 m a.s.l.), Ethiopia, 28.01.2018, coll. G.K. Englmaier, G. Tesfaye, P. Meulenbroek and H. Wäidbacher (two voucher specimens for COI (MT946125, MT946126))
<i>Garra makiensis</i>	NMW 99231	16	non-types	49.1–119.9	S10	Awash River at Yimre (9°4'59"N, 40°10'3"E; 797 m a.s.l.), Ethiopia, 30.01.2018, coll. G.K. Englmaier, G. Tesfaye, P. Meulenbroek and H. Wäidbacher (two voucher specimens for COI (MT946127, MT946128))
<i>Garra makiensis</i>	NMW 99485	12	non-types	59.3–97.0	S13	Awash River at Adayitu (11°7'48"N, 40°46'3"E; 460 m a.s.l.), Ethiopia, 12.03.2019, coll. G.K. Englmaier, G. Tesfaye, P. Meulenbroek and H. Wäidbacher.
<i>Garra makiensis</i>	NMW 99489	4	non-types	53.5–82.2	T1	Lower Mille River (11°24'50"N, 40°45'37"E; 482 m a.s.l.), Ethiopia, 12.03.2019, coll. G.K. Englmaier, G. Tesfaye, P. Meulenbroek and H. Wäidbacher.
<i>Garra makiensis</i>	NMW 99491	7	non-types	42.2–106.1	S14	Awash River at Dubti (11°41'50"N, 41°7'23"E; 378 m a.s.l.), Ethiopia, 13.03.2019, coll. G.K. Englmaier, G. Tesfaye, P. Meulenbroek and H. Wäidbacher.
<i>Garra makiensis</i>	NMW 99504	2	non-types	141.3–147.9	T4	Jara River (10°31'14"N, 39°57'13"E; 1,434 m a.s.l.), Ethiopia, 17.03.2019, coll. G.K. Englmaier, G. Tesfaye, P. Meulenbroek and H. Wäidbacher.
<i>Garra makiensis</i>	NMW 99507	3	non-types	99.2–118.2	T3	Middle Borkana River (10°38'09"N, 39°55'54"E; 1,417 m a.s.l.), Ethiopia, 17.03.2019, coll. G.K. Englmaier, G. Tesfaye, P. Meulenbroek and H. Wäidbacher.

Morphological analyses

In total, 124 specimens were examined, including type specimens of *G. makiensis* and *G. rothschildi*. A maximum of 43 measurements (seven for the gular disc), 22 external body counts, and nine axial skeleton counts (from x-rays) were taken. Type specimens of *G. rothschildi* were examined from photographs and radiographs, and only meristic counts were taken. Measurements and counts are defined in Suppl. material 1: Table S2; and measurements illustrated in Fig. 2.

Most measurements follow Hubbs and Lagler (1958) and Holčík et al. (1989) and were made point to point using a digital calliper to the nearest 0.1 mm. Head length (HL) excludes the skin fold on the operculum. Length of the axillary scale was measured from the anteriormost to the posteriormost extremity. Length of the dorsal-fin rays was measured from the visible base of the ray to the end of the uppermost flexible part. We refer to the postpelvic region as an area on the ventral side between the insertion of the pelvic fins and the anterior margin of anus. Scales in the postpelvic region were counted along midline. The terminology used for the external oral and gular morphology, including the gular disc (referred to as “disc” or “mental adhesive disc” in Zhang et al. (2002) and Stiassny and Getahun (2007)) follows Kottelat (2020). Measurements of the gular disc were done as follows (Fig. 2 and Suppl. material 1: Table S2): 35, Disc length: Distance between the anteriormedian border of torus and the posteriormost point of labrum at midline. 36, Length of torus: Distance between the anterior- and posteriormedian borders at midline. 37, Length of pulvinus: Distance between the anterior and posterior extremities of pulvinus at midline. 38, Length of labrum: Distance between the anterior and posterior extremities of labrum at midline. 39, Disc width: Maximum width of labrum at intercept with labellum. 42, Width of torus: Distance between the lateral extremities of torus. 43, Width of pulvinus: Maximum width of pulvinus between lateral extremities. The terminology used for nuptial tubercles and grooves on the snout follows Nebeshwar and Vishwanath (2017) as described for *Garra*.

External meristic counts follow Skelton (1980) and those summarised in Englmaier et al. (2020a) (Suppl. material 1: Table S2). The posterior two branched rays in the dorsal and anal fins, located on the last complex proximal pterygiophore of the fin, were counted as two. As the anteriormost unbranched rays of the dorsal and anal fins are usually deeply embedded, ray counts for those fins were taken from radiographs. Total number of lateral-series scales were counted from the first scale behind the opercular opening to the last scale on the caudal fin (bearing the lateral-line canal or without the canal). Counts and terminology of the axial skeleton follow Naseka (1996). Vertebral counts and supraneural bones were examined from radiographs.

Multivariate analyses in the form of principal component analysis (PCA) and discriminant function analysis (DFA), were used to compare type specimens of *G. makiensis* (Meki River) with those species found in the adjacent Awash River. Data for *G. aethiopica* and *G. dembeensis* were taken from Englmaier (2018). Therefore, the dataset was reduced to the number of characters used in Englmaier (2018), following the number of

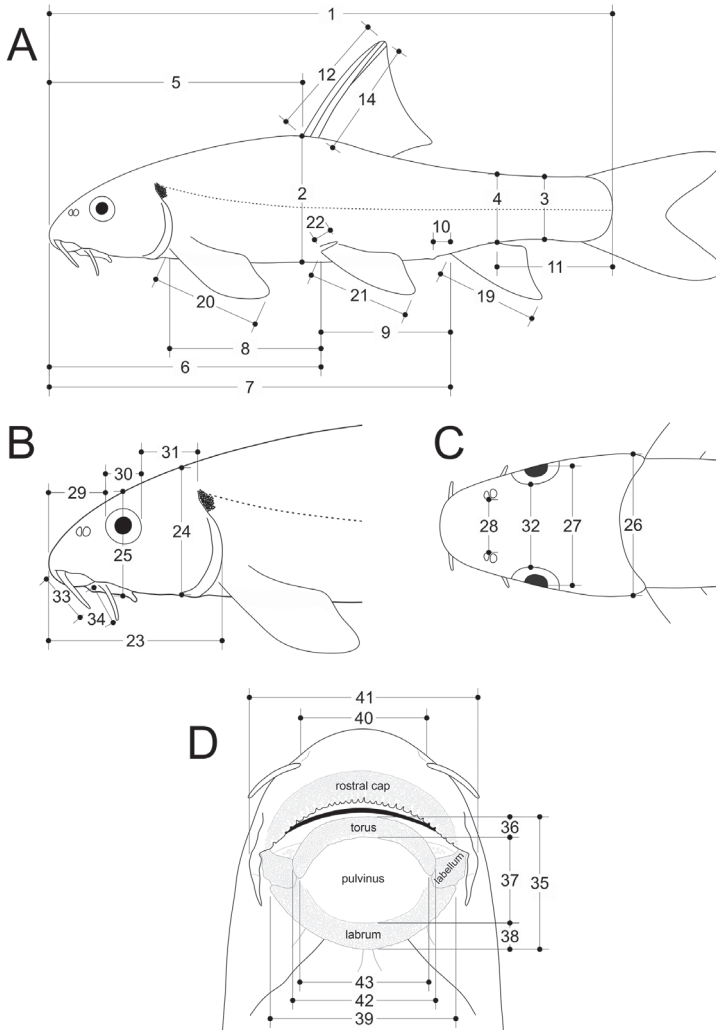


Figure 2. Schematic illustration of **A** body measurements **B** (lateral) and **C** (dorsal) head measurements, and **D** (ventral) head and gular disc (as defined in Kottelat (2020)) measurements. For a detailed description see Suppl. material 1: Table S2. 1, standard length (SL); 2, body depth at dorsal-fin origin; 3, minimum caudal-peduncle depth; 4, maximal caudal-peduncle depth; 5, predorsal length; 6, prepelvic length; 7, preanal length; 8, pectoral – pelvic distance; 9, pelvic – anal distance; 10, vent distance; 11, caudal-peduncle length; 12, dorsal-fin depth; 14, depth of 1st branched dorsal-fin ray; 19, anal-fin depth; 20, pectoral-fin length; 21, pelvic-fin length; 22, length of axillary scale; 23, head length; 24, head depth at nape; 25, head depth at eye; 26, head width at posterior end of operculum; 27, head width at eyes; 28, width between nostrils; 29, snout length; 30, eye horizontal diameter; 31, orbit – operculum distance; 32, interorbital width; 33, anterior barbel length; 34, posterior barbel length; 35, disc length; 36, length of torus; 37, length of pulvinus; 38, length of labrum; 39, disc width; 40, width between anterior barbels; 41, width of mouth; 42, width of torus; 43, width of pulvinus. Not illustrated are: 13, depth of last unbranched dorsal-fin ray; 15, depth of 2nd branched dorsal-fin ray; 16, depth of 3rd branched dorsal-fin ray; 17, depth of 4th branched dorsal-fin ray; 18, depth of 5th branched dorsal-fin ray.

morphometric and meristic characters introduced by Stiasny and Getahun (2007) for African *Garra*. Primary data and basic statistics are given in Suppl. material 1: Tables S3–S5. Statistical analyses were performed in Microsoft Excel and IBM SPSS Statistics v. 26.

Molecular analyses

Methods for DNA extraction, PCR amplification (using primers Fish-Co1-F and Fish-Co1-R according to Baldwin et al. (2009)) and sequencing of freshly sampled material (2017–2018) are described in Englmaier et al. (2020a).

For DNA extraction of historic museum material (BMNH 1905.7.25.88, *G. makiensis*, paralectotype) we used tissue from the branchial arches (right side of the specimen). DNA was extracted using the QIAamp DNA Mini and Blood Mini Kit (Qiagen) following the manufacturer's protocol. Final DNA concentration was 23.4 ng μl^{-1} . All lab work was performed in a DNA clean room with sterilised and UV radiated utensils. Because museum DNA is typically fragmented, we designed specific primers to amplify approximately 150 bp long fragments of the cytochrome *c* oxidase subunit 1 (CO1) (Table 2). Primers were designed based on the CO1 alignment of the extant *Garra* samples included in this study using Primer-BLAST (NCBI), and were arranged in a way that adjacent fragments extensively overlap. PCR reactions were done in 50 μl , with 5 μl buffer, 4 μl MgCl_2 (2.0 mM), 2 μl Enhancer, 1 μl dNTPs (500 μM), 0.50 μl of each primer (50 pmol μl^{-1} , for primer sequences see Table 2), 0.4 μl of AmpliTaq Gold 360 DNA Polymerase (1 unit) and 2–3 μl of DNA. The same touch-down PCR protocol was used for all primer pairs, with initial denaturation at 95 °C for 10 min, followed by five cycles at 95 °C for 30 s, 63 °C for 2 min and 72 °C for 45 s, and 40 cycles at 95 °C for 45 s, 61 °C for 45 s and 72 °C for 45 s. Final extension was performed at 72 °C for 7 min. PCR products were purified with a Qiagen PCR purification kit, and purified PCR products were sequenced (in both directions) by Microsynth with PCR primers. After amplification, fragments were aligned with MEGA6 (Tamura et al. 2011) and composed into a single sequence (451 bp total length).

The dataset used for phylogenetic analysis comprised 13 original CO1 sequences (611 bp) from freshly collected samples of *G. aethiopica*, *G. dembeensis* and *G. makiensis*, and the historic paralectotype sequence (451 bp). Obtained sequences were deposited on GenBank under accession numbers MT946118–MT946130. Additionally, we included 46 sequences retrieved from GenBank, corresponding to different *Garra* species from Africa and the Arabian Peninsula. An Asian *Garra* species was included as outgroup following Yang et al. (2012) (Suppl. material 1: Table S6).

Sequences were edited in MEGA7 (Kumar et al. 2016) and aligned with ClustalW. PartitionFinder2 (Lanfear et al. 2017) was used to estimate the best partition scheme and best fit substitution model. Phylogenetic reconstruction was conducted using Maximum Likelihood (ML) and Bayesian Inference (BI) methods. ML was performed using RAxML-HPC2 Workflow on XSEDE (v. 8.2.12) through CIPRES Science Gateway (Miller et al. 2011), with 1,000 bootstrap replicates. For BI, MrBayes v. 3.2.6 (Ronquist et al. 2012) was used. Two independent Markov Chain Monte Car-

Table 2. Sequences (5'–3') of primers used for the PCR reactions of the historic paralectotype of *Garra makiensis* (BMNH 1905.7.25.88).

Primer	Sequence (5'–3')	Product (incl. primers)
Garra_new_4_F	GTTACTGCCACGCTTTTGT	185 bp
Garra_new_4_R	CTTCGACTCCAGAGGAGGCT	
Garra_new_5_F	AGCCTCCTCGGAGTCGAAG	191 bp
Garra_new_5_R	GGGAAATGGCTGGGGGTTTT	
Garra_new_6_F	GGGGTTTTGGAACTGACTCG	195 bp
Garra_new_6_R	ATGCTCCTGCGTGAGCTAAG	
Garra_new_7_F	CTGCATCTAGCAGGGGTGTC	176 bp
Garra_new_7_R	ATCGTAATCCGGCAGCTAGT	
Garra_new_10_F	CCAGATATGGCATTCCACGG	155 bp
Garra_new_10_R	GCTCCTGCGTGAGCTAAGTT	

lo (MCMC) were run simultaneously for 5 million generations with sampling trees every 500 generations. The first 25 % of obtained trees was discarded as 'burn-in'. All computed trees were visualised and edited with FigTree v. 1.4.4 (Rambaut 2012) and Inkscape v. 0.92.3. MEGA7 (Kumar et al. 2015) was used to calculate between group mean distances (uncorrected p-distances).

Two different sequence alignments were used for calculating the p-distances: the first alignment did not include the paralectotype sequence of *G. makiensis* and each sequence had a length of 611 bp; the second dataset was trimmed to the length of the paralectotype sequence (451 bp) and was used to compare the paralectotype with the remaining studied species.

Results

Identification of the Awash samples as *G. makiensis* is based on 1) the morphological comparison to type specimens of *G. makiensis* and *G. rothschildi* (Tables 3, 4), including multivariate statistical analyses (PCA, DFA) of 17 morphometric and six meristic characters with a comparison to *G. aethiopica* and *G. dembeensis* from the Awash River (Fig. 3); and 2) CO1 sequence data with a p-distance of 0.08 % between the paralectotype and the samples of *G. makiensis* from the Awash River, and 9.53–11.31 % between the paralectotype and other African species (including *G. aethiopica* and *G. dembeensis* from the Awash).

Morphological analyses

Both PCA and DFA cluster type specimens of *G. makiensis* together with the Awash population identified as *G. makiensis*, while they are distinct from *G. aethiopica* and *G. dembeensis* (Fig. 3). Based on PCA the most distinguishing variables between the three species are dorsal-fin depth (% SL), number of unbranched and branched pectoral-fin rays, anal-fin depth (% SL), vent distance (% pelvic – anal distance), and pelvic-fin length (% SL) (Suppl. material 1: Table S4).

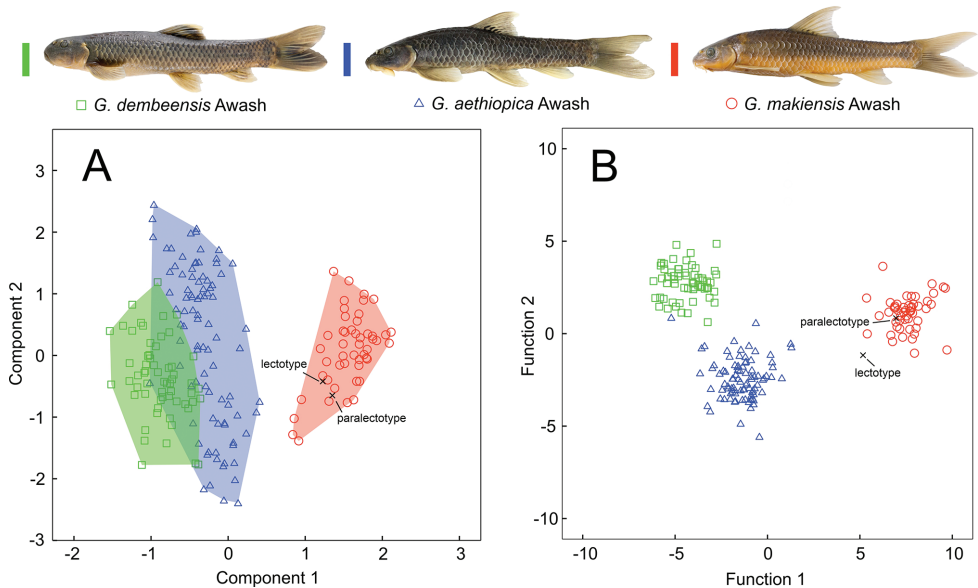


Figure 3. Results of **A** PCA and **B** DFA, comparing *Garra* species from the Awash River with type specimens of *G. makiensis* from the Meki River (lectotype: BMNH 1905.7.25.87, paralectotype: BMNH 1905.7.25.88). Analyses are based on 17 morphometric and six meristic characters as given in Suppl. material 1: Table S3.

A similar pattern of morphological differences is supported by DFA. Variables that contribute most for discrimination of the samples are vent distance (% pelvic – anal distance), dorsal-fin depth (% SL), total number of lateral-series scales, and number of branched pectoral-fin rays. Predicted classifications for the samples from the Awash (*G. aethiopica*, *G. dembeensis*, *G. makiensis*) and the type specimens of *G. makiensis* were 100 % correct, with the exception of one specimen identified as *G. aethiopica* falling within the group of *G. dembeensis* (Suppl. material 1: Table S5).

Taxonomy

Garra makiensis (Boulenger, 1903)

Figures 4–9

Discognathus makiensis Boulenger, 1903:330 (type locality: Maki [Meki] River, Ethiopia), Fig. 4A

Discognathus rothschildi Pellegrin, 1905:291 (type locality: Gotta [Gota] River, Ethiopia), Fig. 4B

Material examined. Comparative material from the Awash River drainage (including the Gotta River sub-drainage) is listed in Table 1.

Identification. See Figs 5–8 for general appearance of *G. makiensis* from the Awash River; Fig. 7 for tubercles on head; Fig. 8 for scales on chest and shape of gular

disc; and Fig. 9 for axial skeleton and shape of supraneural bones. Tubercles on scales and the pectoral fin, and scale pattern on ventral side are shown in Suppl. material 2: Figs S1, S2. Measurements and counts are given in Tables 3, 4.

Longest examined specimen 147.9 mm SL (female, NMW 99504). Body elongated, moderately compressed, more in the caudal region. Shape of body and head very variable. Dorsal head profile slightly convex, its transition to back usually smooth, in few specimens with a slight nuchal hump. In most specimens, predorsal back outline rises gently, slightly convex or straight, to dorsal-fin origin. Postdorsal profile slightly concave to caudal-fin origin. Caudal peduncle almost twice as long as its minimal depth. The vent is close to the anal-fin origin (7.3–19.7 % of pelvic – anal distance). Head usually as long as body depth at dorsal-fin origin. Head depth at nape shorter than head length. Snout blunt and longer than orbit – operculum distance. Transverse groove weakly developed (absent in some specimens); transverse lobe separated from lateral field by a shallow groove (or without groove). Two deep grooves originating above anterior barbel, posteriorly not connected; at posterior end of upper groove a patch of few tubercles in some specimens (Fig. 7).

Tubercles on snout and head in both males and females (smallest specimen with tubercles: 45.4 mm SL, Awash River, S14), but often completely absent or rudimentary developed (Figs 6, 7). Transverse lobe with large conical tubercles; tubercles extending to lateral surface and the area between anterior rim of eyes and nostrils. Depressed rostral margin usually without tubercles; in some specimens few and irregularly placed. Anterior extremity of the ethmoid field often elevated from depressed rostral surface and covered with large tubercles, especially in anterior region. Small tubercles are commonly spread on the frontal and occipital regions, sometimes extending to the operculum (Fig. 7 and Suppl. material 2: Fig. S1). In few specimens ($n = 7$), small circular tubercles on scales



Figure 4. General appearance of *Garra makiensis*. **A** BMNH 1905.7.25.87, lectotype of *G. makiensis*, female, 67.1 mm SL, Maki [Meki] River, Ethiopia, The Trustees of the Natural History Museum, London, **B** MNHN-1905-0246, syntype of *G. rothschildi*, 135.3 mm SL, Gotta [Gota] River, Ethiopia, The Muséum national d'Histoire naturelle, Paris.

Table 3. Morphometric data for examined *Garra makiensis* from the Meki River (type specimens) and the Awash River drainage. Information per specimen as in Table 1.

Character states	<i>G. makiensis</i> BMNH	<i>G. makiensis</i> BMNH	<i>G. makiensis</i> Awash River				
	1905.7.25.87 lectotype	1905.7.25.88 paralectotype	n	Min	Max	Mean	S.D.
Standard length (mm)	67.1	47.6	50	42.2	147.9	79.7	21.9
Percent of standard length							
Body depth at dorsal-fin origin	19.1	19.8	50	17.4	25.0	21.7	1.4
Minimum caudal-peduncle depth	11.1	11.5	50	9.1	12.6	10.7	0.7
Maximal caudal-peduncle depth	12.5	13.3	50	9.6	14.4	11.8	0.9
Predorsal length	45.7	46.9	50	43.1	49.7	45.1	1.4
Prepelvic length	51.0	53.0	50	46.2	53.1	48.8	1.1
Preanal length	74.7	75.8	50	70.7	75.0	72.6	1.0
Pectoral – pelvic distance	32.0	32.2	50	24.9	30.3	28.2	1.1
Pelvic – anal distance	25.1	23.6	50	22.8	27.5	24.9	1.1
Caudal-peduncle length	17.8	19.5	50	17.2	22.9	20.2	1.1
Dorsal-fin depth	24.4	26.9	50	25.1	29.9	27.9	1.1
Anal-fin depth	19.1	19.8	50	18.6	21.9	20.1	0.8
Pectoral-fin length	22.3	23.7	50	19.3	22.7	20.9	0.8
Pelvic-fin length	19.9	20.5	50	18.1	22.3	20.5	0.8
Head length	22.2	24.6	50	19.7	27.7	21.9	1.5
Head depth at nape	14.5	15.9	50	13.2	16.5	14.6	0.6
Head depth at eye	12.8	14.1	50	10.4	14.8	12.1	0.7
Head width at posterior end of operculum	15.0	16.3	50	13.6	17.1	14.8	0.8
Head width at eyes	12.9	13.6	50	12.3	17.3	13.7	1.1
Snout length	9.3	9.6	50	7.3	13.0	9.5	1.3
Eye horizontal diameter	4.8	5.6	50	3.8	6.1	4.6	0.5
Orbit – operculum distance	9.6	10.1	50	6.3	8.6	7.2	0.5
Interorbital width	9.6	10.4	50	10.0	12.5	10.7	0.5
Disc length	6.4	6.8	50	4.3	9.2	5.7	0.9
Disc width	6.6	7.1	50	5.4	11.9	7.1	1.5
Width between anterior barbels	5.5	5.8	50	4.7	9.6	5.9	1.1
Width of mouth	7.8	8.0	50	6.3	13.6	8.6	1.5
Percent of head length							
Head depth at nape	65.2	64.6	50	58.8	74.4	66.8	3.6
Head depth at eye	57.8	57.5	50	49.5	62.7	55.4	3.2
Head width at posterior end of operculum	67.5	66.1	50	59.5	73.9	67.8	3.1
Head width at eyes	58.3	55.3	50	55.3	68.9	62.7	3.1
Width between nostrils	29.1	27.8	50	25.4	36.0	31.8	2.3
Snout length	42.1	38.9	50	34.0	52.5	43.1	4.1
Eye horizontal diameter	21.9	22.6	50	17.0	24.6	21.1	1.9
Orbit – operculum distance	43.4	41.2	50	27.3	37.7	32.7	2.4
Interorbital width	43.1	42.3	50	44.3	53.4	49.0	2.2
Anterior barbel length	14.7	15.6	50	11.5	20.6	15.8	2.3
Posterior barbel length	18.8	21.3	50	8.6	23.3	15.5	3.7
Disc length	29.0	27.6	50	21.5	33.2	25.9	2.8
Disc width	29.6	28.9	50	25.6	44.7	32.3	5.5
Width between anterior barbels	24.7	23.5	50	21.6	36.7	27.0	3.7
Width of mouth	35.2	32.5	50	30.8	52.6	39.1	5.2
Percent of caudal peduncle length							
Minimum caudal-peduncle depth	62.7	58.8	50	42.2	62.4	52.9	4.8
Maximal caudal-peduncle depth	70.5	68.3	50	48.5	71.0	58.3	5.4
Percent of eye horizontal diameter							
Anterior barbel length	67.4	69.1	50	48.6	94.7	75.4	10.1
Posterior barbel length	85.8	94.3	50	37.7	105.6	73.7	15.6
Percent of pelvic – anal distance							
Vent distance	9.4	9.0	50	7.3	19.7	13.7	2.2
Percent of pelvic-fin length							
Length of axillary scale	21.5	33.1	50	18.8	35.5	27.2	3.8

Character states	<i>G. makiensis</i> BMNH 1905.7.25.87 lectotype	<i>G. makiensis</i> BMNH 1905.7.25.88 paralectotype	<i>G. makiensis</i> Awash River				
			n	Min	Max	Mean	S.D.
Percent of dorsal-fin depth							
Depth of last unbranched dorsal-fin ray			49	83.3	93.8	89.0	2.3
Depth of first branched dorsal-fin ray			50	80.7	90.7	86.4	2.4
Depth of second branched dorsal-fin ray	84.5	80.6	50	69.4	97.6	76.9	4.1
Depth of third branched dorsal-fin ray	66.2	65.1	50	52.8	70.8	62.3	3.5
Depth of fourth branched dorsal-fin ray	54.5	52.5	50	40.8	57.6	49.4	3.1
Depth of fifth branched dorsal-fin ray	49.9	45.4	50	34.3	46.9	40.9	3.0
Percent of disk length							
Length of torus	22.5	22.0	50	11.2	24.3	16.6	2.7
Length of pulvinus	57.1	53.3	50	37.0	65.9	52.8	7.3
Length of labrum	20.4	24.8	50	13.1	47.9	30.5	8.9
Disc width	102.1	104.6	50	95.2	156.8	124.7	15.3
Width of mouth	121.3	118.0	50	111.7	183.4	151.1	16.1
Width of torus	71.5	70.6	50	68.6	97.6	84.1	6.9
Width of pulvinus	60.6	62.5	50	59.6	88.6	73.2	6.0

in the predorsal region and the lateral side of the abdominal region (above lateral line). A single specimen (NMW 99231, male, 91.2 mm SL, Awash River, S10) with tubercles on dorsal side of the pectoral fins (at fin membranes) (Suppl. material 2: Fig. S1).

Gular disc well-developed but often variable in size and shape (Fig. 8). Its width greater than its length. Width of torus less than disc length. Pulvinus wider than long and with few papillae. Labrum well-developed and longer than torus. Width of mouth usually less than snout length. Abundant papillae on rostral cap, torus, labellum and labrum. Rostral cap with invected ventral margin. Two pairs of barbels, their length usually shorter than eye diameter; anterior barbel slightly longer or about equal to posterior barbel.

Dorsal fin with 3 or 4, commonly 4, unbranched and 8 branched rays, its last unbranched ray is the longest (89.0 % of dorsal-fin depth); length of first branched ray 86.4 % of dorsal-fin depth; second branched ray much shorter (76.9 % of dorsal-fin depth). Pelvic fin with a single unbranched ray and 7–9, commonly 8, branched rays; pelvic splint present. Long axillary scale at base of pelvic fin, its length 18.8–35.5 % of pelvic-fin length. Pectoral fin with a single unbranched ray and 13–17, commonly 16, branched rays. Caudal fin forked with 2+17 principal rays. Upper procurrent rays 7 (9), 8 (49) or 9 (3), lower procurrent rays 6 (14), 7 (42) or 8 (6).

Lateral line complete and going along midline. Total lateral-series with 37–40, commonly 38, scales. Lateral-series scales to posterior margin of hypurals 35–39, commonly 36. Transversal scale rows between lateral line and dorsal-fin origin 4 or 5, commonly 5; and 4–6, commonly 5 between lateral line and anal-fin origin. Chest, belly, postpelvic and predorsal regions fully scaled. Scales on chest usually deeply embedded (Fig. 8 and Suppl. material 2: Fig. S2); predorsal scales irregularly arranged. Between anal-fin origin and anus 0 (1) 1 (16) or 2 (42) scales; and 6 (6), 7 (24), 8 (22) or 9 (3) scales in postpelvic region. Circumpeduncular scale rows 16.

Total vertebrae 35–39, commonly 37; with abdominal vertebrae 20–22; predorsal abdominal vertebrae 9–12; caudal vertebrae 14–17; and 11–14 vertebrae between first pterygiophores of dorsal and anal fins. Most frequent vertebral formulae 21+16 (19,

Table 4. Meristic character states in type specimens of *Garra makiensis* and *G. rothschildi* as well as additional specimens of *G. makiensis* from the Gotta River (AMNH 227323, MRAC 91-051-P-0044) and the Awash River drainage (deposited at NMW). Numbers in squared brackets referring to mean±SD. Information per specimen as in Table 1.

Character states	<i>G. makiensis</i> BMNH 1905.7.25.87 lectotype	<i>G. makiensis</i> BMNH 1905.7.25.88 paralectotype	<i>G. rothschildi</i> MNHN 1905-0246 syntype	<i>G. rothschildi</i> MNHN 1905-0247 syntype	<i>G. makiensis</i> Gotta River	<i>G. makiensis</i> Awash River
Unbranched dorsal-fin rays	4	4	4	4	3(5), 4(19) [3.8±0.4]	3(9), 4(30) [3.8±0.4]
Branched dorsal-fin rays	8	8	8	8	8(24) [8.0±0.0]	8(96) [8.0±0.0]
Unbranched anal-fin rays	3	3	3	3	3(24) [3.0±0.0]	3(46) [3.0±0.0]
Branched anal-fin rays	6	6	6	6	6(24) [6.0±0.0]	6(96) [6.0±0.0]
Unbranched pelvic-fin rays	1	1	1	1	1(24) [1.0±0.0]	1(81) [1.0±0.0]
Branched pelvic-fin rays	8	8	8	9	7(1) 8(12) [7.9±0.3]	8(81) [8.0±0.0]
Unbranched pectoral-fin rays	1	1	1	1	1(8) [1.0±0.0]	1(81) [1.0±0.0]
Branched pectoral-fin rays	15	16	15	15	14(1), 15(2), 16(2) [15.2±0.8]	13(1), 14(5), 15(20), 16(47), 17(8) [15.7±0.8]
Principal caudal-fin rays	17	17	17	17	17(24) [17.0±0.0]	17(46) [17.0±0.0]
Upper caudal-fin procurrent rays	8	9	8	8	7(2), 8(20), 9(1), 11(1) [8.1±0.7]	7(7), 8(27), 9(2) [7.9±0.5]
Lower caudal-fin procurrent rays	7	7	7	7	7(20), 8(4) [7.2±0.4]	6(14), 7(20), 8(2) [6.7±0.6]
Total number of lateral-series scales	37	38	39	38	38(4), 39(1) [38.2±0.5]	37(7), 38(31), 39(33), 40(10) [38.6±0.8]
Lateral-series scales to posterior margin of hypurals	34	36	36	36	36(4), 37(1) [36.2±0.5]	35(10), 36(32), 37(29), 38(9), 39(1) [36.5±0.9]
Total number of later-line scales	37	38	39	38	36(1), 38(4) [37.6±0.9]	36(3), 37(19), 38(27), 39(24), 40(8) [38.2±1.0]
Scale rows between lateral line – dorsal-fin origin	5	5	5	4	5(5) [5.0±0.0]	4(1), 5(80) [5.0±0.1]
Scale rows between lateral line – pelvic-fin origin	4	4	4	4	4(5) [4.0±0.0]	4(80), 5(1) [4.0±0.1]
Scale rows between lateral-line – anal-fin origin	4	4	4	4	4(3), 5(2) [4.4±0.6]	4(8), 5(42) [4.2±0.4]
Scale rows between lateral line – anus	5	5	5	5	5(1)	4(1), 5(48), 6(1) [5.0±0.2]
Circumpeduncular scales	16	16			16(5) [16.0±0.0]	16(81) [16.0±0.0]
Post-pelvic scales	9	9			6(3), 7(1), 9(1) [6.8±1.3]	6(3), 7(23), 8(22), 9(2) [7.5±0.7]
Anal scales	2	2	2	2	2(5) [2.0±0.0]	0(1), 1(16), 2(33) [1.6±0.5]
Total number of vertebrae	36	36	37	37	35(2), 36(19), 37(3) [36.0±0.5]	35(1), 36(4), 37(22), 38(18), 39(1) [37.3±0.8]
Abdominal vertebrae	20	20	21	20	20(8), 21(14), 22(2) [20.8±0.6]	20(4), 21(31), 22(11) [21.2±0.6]
Caudal vertebrae	16	16	16	17	14(2), 15(13), 16(9) [15.3±0.6]	14(1), 15(6), 16(24), 17(15) [16.2±0.7]
Predorsal abdominal vertebrae	10	10	10	10	9(1), 10(20), 11(1), 12(2) [10.2±0.6]	9(2), 10(23), 11(21) [10.4±0.6]

Character states	<i>G. makiensis</i> BMNH 1905.7.25.87 lectotype	<i>G. makiensis</i> BMNH 1905.7.25.88 paralectotype	<i>G. rothschildi</i> MNHN 1905-0246 syntype	<i>G. rothschildi</i> MNHN 1905-0247 syntype	<i>G. makiensis</i> Gotta River	<i>G. makiensis</i> Awash River
Preanal caudal vertebrae	3	3	2	3	1(9), 2(10), 3(5) [1.8±0.8]	1(4), 2(29), 3(13) [2.2±0.6]
Postanal vertebrae	13	13	14	14	12(1), 13(11), 14(12) [13.5±0.6]	12(1), 13(9), 14(28), 15(7), 16(1) [13.8±0.6]
Vertebrae between first pterygiophores of dorsal and anal fins	13	13	13	13	11(2), 12(11), 13(10), 14(1) [12.4±0.7]	12(13), 13(23), 14(10) [12.9±0.7]
Intermediate vertebrae	4	4	5	5	4(7), 5(12), 6(5) [4.9±0.7]	4(13), 5(28), 6(4) [4.8±0.6]
Supraneural bones	4	4	4	4	4(4) [4.0±0.0]	3(1), 4(10), 5(10) [4.4±0.6]

n = 74). Supraneural bones 3–5 (commonly 4 (16) or 5 (10), n = 27), first two square shaped and last two to three in front of dorsal fin elongated and largest (Fig. 8).

Morphological variability. Similar to other *Garra* species in Africa and the Arabian Peninsula (Krupp 1983; Golubtsov et al. 2012; Englmaier 2018), we found considerable morphological variability in *G. makiensis* (Fig. 6). Based on our data, we cannot confirm the presence of a sexual dimorphism, but the largest specimens were females (> 140 mm SL), and more males with prominent tuberculation on snout and head were found. Though few specimens were examined, and samples were collected during dry season only, our data suggest that body shape and tuberculation in *G. makiensis* might be (directly or indirectly) related to abiotic habitat characteristics. Specimens with a more slender body shape and without (or reduced) tubercles on snout and head (Fig. 6B) were caught in low flow velocity habitats, whereas deep bodied specimens with large conical tubercles on snout and head (Fig. 6C) exclusively occurred in high flow velocity habitats over coarse substrate. Intermediate morphs (Fig. 6A) and large growing specimens with reduced tubercles (Fig. 6D) were occasionally found.

Colouration. In life (Fig. 5): Body colour usually light grey, above lateral line often pale-brown or blueish iridescent and darker than below. Head yellowish brown, mouth and ventral side cream. Iris white and yellow. Some individuals show an indistinct, roundish, dark blotch at posteriormost caudal peduncle. At anteriormost lateral line (behind upper edge of operculum) a small dark (rarely blueish iridescent, never red) blotch, not extending on gill cover. Fin membranes usually hyaline, sometimes light grey or yellowish; on caudal fin often light orange. Fin rays hyaline or pale. Dorsal fin with four to six indistinct black blotches at base of branched rays (strongest between 3rd and 6th branched rays).

In formalin (initial fixation) and later transferred to 75 % ethanol (Figs 6–8): Specimens usually light to dark grey, sometimes cream or brownish; darker above lateral line; ventral side cream to yellowish or orange. Back usually dark greyish; head brownish grey. Dark mid-lateral stripe usually of increasing intensity at caudal peduncle, often forming an indistinct blotch at posteriormost caudal peduncle. Fins pale, anterior part of caudal-fin base brownish. Indistinct black blotches at base of branched dorsal-fin rays (strongest between 3rd and 6th branched rays).



Figure 5. *Garra makiensis*, alive, NMW 99224, 52.0 mm SL, Awash River at Lafessa (S6). Photograph by W. Graf.

Habitat. *Garra makiensis* was sampled from the mainstem Awash River and its tributaries (Mille River (T1), Borkana River (T3) and Jara River (T4)) (Figs 1, 10 and Suppl. material 1: Table S1). The altitude ranged from 1,608 m a.s.l. (8°23'16"N, 38°54'30"E, S6) to 338 m a.s.l. (11°30'50"N, 41°38'51"E, S16). Specimens were collected from shoreline habitats, deeper stretches of the main channel, side channels, stagnant water bodies of the floodplains and lacustrine habitats (e.g., lakes Yardi and Gamari, Koka Reservoir); both low-flow and high-flow velocity habitats were inhabited. Substrate composition ranged from silt and sand to coarse stony substrate. The water was usually turbid (suspended solids); water temperature ranged from 21.1 °C to 31.9 °C; conductivity was between 286.7–1,710.3 $\mu\text{S cm}^{-1}$; and dissolved oxygen was close to saturation (65.1–124.1 %) (Englmaier et al. 2020b).

Distribution. *Garra makiensis* is endemic to Ethiopia where it is found in endorheic drainages (Awash (including the Gotta River sub-drainage) and Meki) of the Northern and Central MER (Fig. 1) (Golubtsov et al. 2002). It is absent from the headwaters and was found characteristic for the middle and lower sections of the Awash River (Englmaier et al. 2020b). In the current study, we cannot confirm the presence of *G. makiensis* in the Meki River, its type locality. The Meki drainage is highly altered by human impacts (e.g., water abstraction, sand mining) and the last records of *G. makiensis* in this drainage date back to 1984 (Golubtsov et al. 2002). The extended distribution range reported by Stiassny and Getahun (2007), including the southern part of the MER, the Blue and White Nile drainages and the Omo River drainage, contains uncertainty and needs clarification (Wakjira and Getahun 2017).

Molecular analyses

The alignment used for BI and ML phylogenetic reconstructions comprised 59 CO1 sequences of a length of 611 bp, and one sequence (BMNH 1905.7.25.88, *G. makiensis*, paralectotype) with a length of 451 bp. The alignment included nine individuals of *G. makiensis*, two individuals of *G. dembeensis* and two individuals of *G. aethiopica*, all from the Awash River. Forty-six other sequences of *Garra* species from Africa and the Middle East were included to resolve the phylogenetic relationships of the Awash species (Fig. 11).

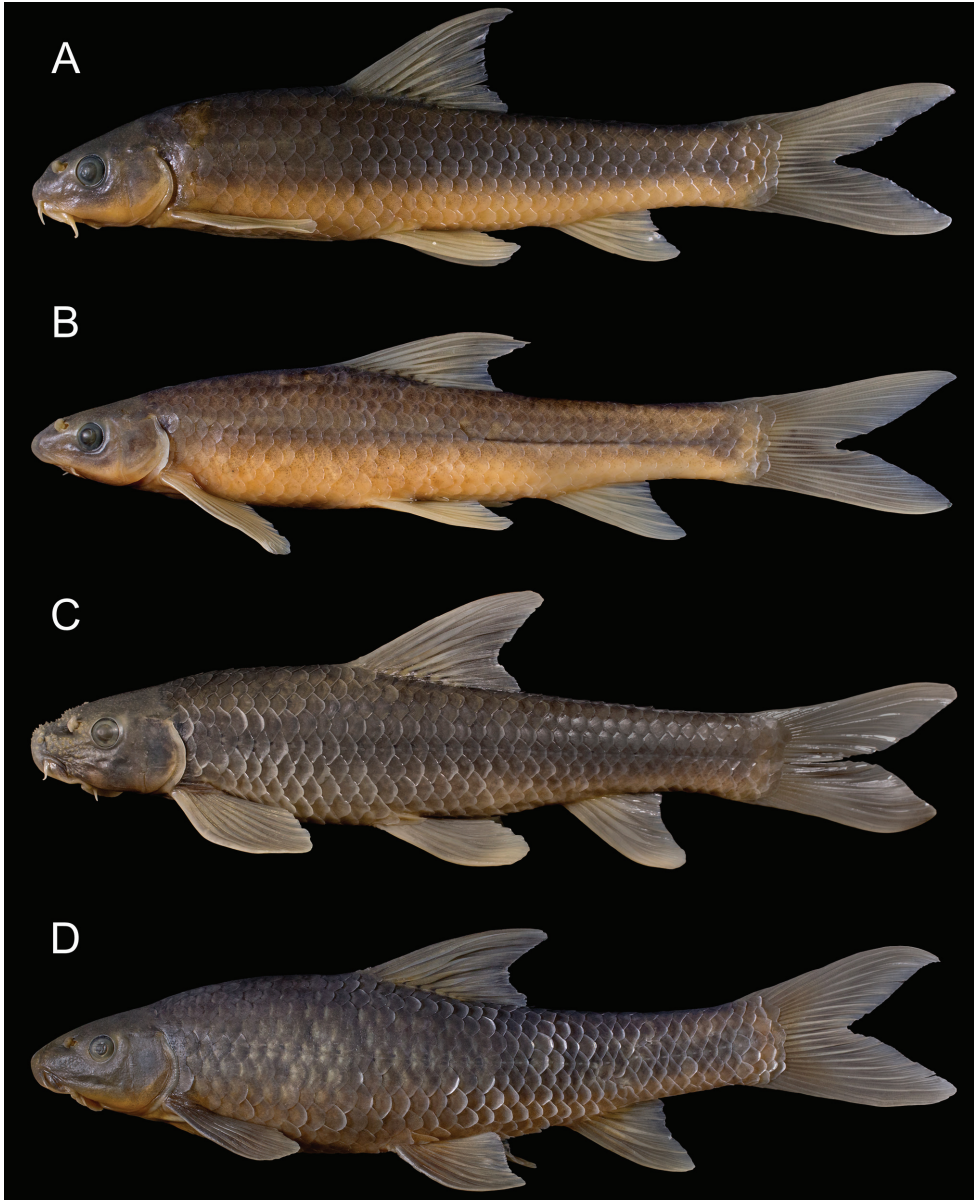


Figure 6. General appearance and morphological variability of *Garra makiensis* from the Awash River. **A** NMW 99485, female, 85.8 mm SL, Adayitu (S13), **B** NMW 99485, female, 82.2 mm SL, Adayitu (S13), **C** NMW 99491, male, 106.1 mm SL, Dubti (S14), **D** NMW 99504, female, 147.9 mm SL, Jara River (T3).

Garra makiensis clusters together with species from the south-western Arabian Peninsula (*G. tibanica* Trewavas, 1941, *G. buettikeri* Krupp, 1983, *G. dunsirei* Banister, 1987, *G. smarti* and *G. sindhi*) forming a monophyletic group (Bayesian posterior probability, BPP 0.96; bootstrap value, bs 86; Clade A, Fig. 11). The lineage of *G.*



Figure 7. Lateral and dorsal view of head, in *Garra makiensis* from the Awash River. **A** and **D** same specimen as in Fig. 6B, **B** and **E** same specimen as in Fig. 6C, **C** and **F** same specimen as in Fig. 6D.

makiensis appears as a strongly supported sister lineage to all remaining species within Clade A (BPP 1; bs 100). Pairwise distances between *G. makiensis* and Arabian Peninsula species range from 9.51 % to 10.23 % (Suppl. material 1: Table S7). *Garra makiensis* is clearly distinct from congeners in the Awash River. Pairwise distance between *G. makiensis* and *G. aethiopica* is 9.90 % and 9.78 % between *G. makiensis* and *G. dembeensis*. The paralectotype of *G. makiensis* clusters together with our samples of *G. makiensis* from the Awash River (p-distance 0.08 %, Suppl. material 1: Table S7), corroborating the identification of the Awash population as *G. makiensis*.

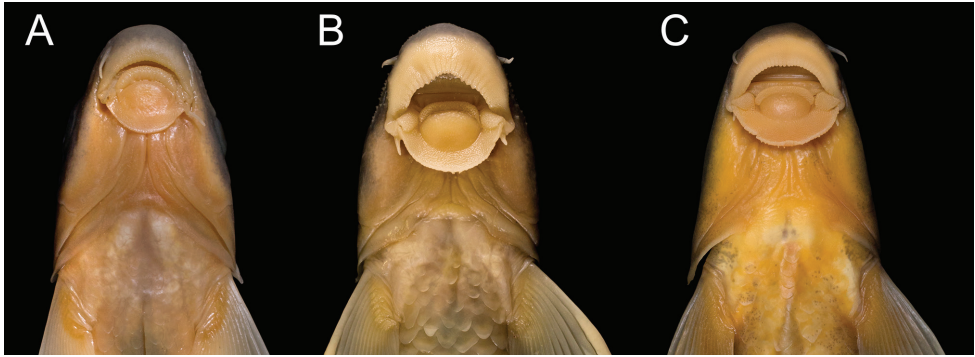


Figure 8. Ventral view of head, in *Garra makiensis* from the Awash River. **A** same specimen as in Fig. 6B, **B** same specimen as in Fig. 6C, **C** same specimen as in Fig. 6D.

Garra aethiopica forms a distinct, monophyletic lineage within a cluster of other African *Garra* (BPP 1; bs 100). Pairwise distance between *G. aethiopica* and all other African congeners range from 6.46 % to 8.27 %. Individuals of *G. dembeensis* from the Awash River appear as a sister clade to *G. tana* Getahun & Stiassny, 2007 (BPP 1; bs 100) (Lake Tana, Upper Blue Nile drainage) and do not cluster together with other sequences named as *G. dembeensis* from the Congo (KT193003, KT193004, KT192819, KT192820) and the Nile River (KF929909, LC506574, LC506575) drainages. Pairwise distance between *G. dembeensis* from Awash River and *G. tana* is 1.06 % (Suppl. material 1: Table S7).

In summary, mitochondrial CO1 data provide support that *G. makiensis* is more closely related to *Garra* species in the south-west of the Arabian Peninsula than to congeners from Africa, as all of them belong to a different, well-supported, monophyletic clade (BPP 0.96; bs 77). Below we provide a morphological comparison of *G. makiensis* with closely related species of Clade A (Fig. 11).

Comparison of *G. makiensis* with congeners of Clade A.

Garra species of Clade A (Fig. 11) are currently known only from the north-east of Ethiopia (*G. makiensis*) and the south-west of the Arabian Peninsula (Trewavas 1941; Balletto and Spanò 1977; Krupp 1983; Banister 1987; Golubtsov et al. 2002; Krupp and Budd 2009; Lyon et al. 2016). For morphological comparison we combined all specimens of *G. makiensis* from Ethiopia, including the type specimens of *G. makiensis* and *G. rothschildi*, into one sample. No original material of *G. buettikeri*, *G. dunsirei*, *G. smarti*, and *G. sindhi* was examined and we refer to published data (original descriptions: Trewavas (1941), Krupp (1983), Banister (1987), Krupp and Budd (2009), and Lyon et al. (2016)) for comparison. *Garra tibanica* includes several subspecies (Balletto and Spanò 1977) of unknown systematic relationship and taxonomic status. We, therefore, refer to *G. tibanica* as described by Trewavas (1941) and present new data on axial skeleton elements for the type specimens (Suppl. material 1: Table S8).

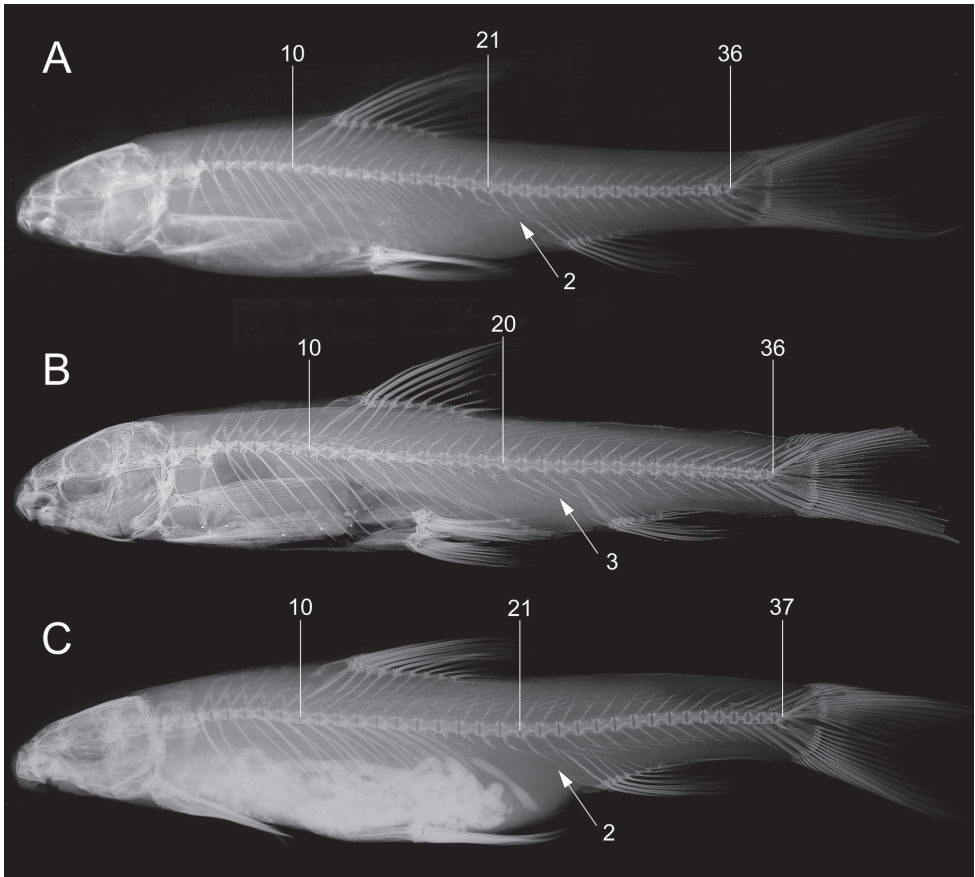


Figure 9. Axial skeletons and supraneural bones in *Garra makiensis*. **A** NMW 99223, 56.0 mm SL, Awash River at Wonji (S7), 10 showing last predorsal abdominal vertebra and 21 last abdominal vertebra, total vertebrae 36:21+15, **B** lectotype of *G. makiensis*, same specimen as in Fig. 4A, 10 showing last predorsal abdominal vertebra and 20 last abdominal vertebra, total vertebrae 36:20+16, The Trustees of the Natural History Museum, London, **C** syntype of *G. rothschildi*, same specimens as in Fig. 4B, 10 showing last predorsal abdominal vertebra and 21 last abdominal vertebra, total vertebrae 37:21+16, The Muséum national d'Histoire naturelle, Paris. Arrows showing position and numbers of preanal caudal vertebrae.

Garra makiensis can be distinguished from *G. buettikeri* (eastern side of the Asir mountains, draining to the Wadi ad-Dawasir, Saudi Arabia) by 4–5 scales between the lateral line and the dorsal-fin origin (vs. 6.5–8.5); 16 circumpeduncular scales (vs. 18–20); and caudal peduncle length 17–23 % SL (vs. 15–19 % SL). The number of lateral-series scales largely overlap (37–40, mode 38 vs. 36–39, mode 37), but the lowest count, 36 ($n = 10$), recorded in *G. buettikeri* was not found in *G. makiensis*. Analysis of mitochondrial CO1 place *G. buettikeri* closest to *G. tibanica* (p-distance 0.57 %; Suppl. material 1: Table S7) (Hamidan et al. 2014).

Garra makiensis differs from *G. tibanica* (coastal Wadi Tiban drainage, Yemen) by 37–40, commonly 38, scales in the lateral series (vs. 32–34); 35–39, commonly 37, to-

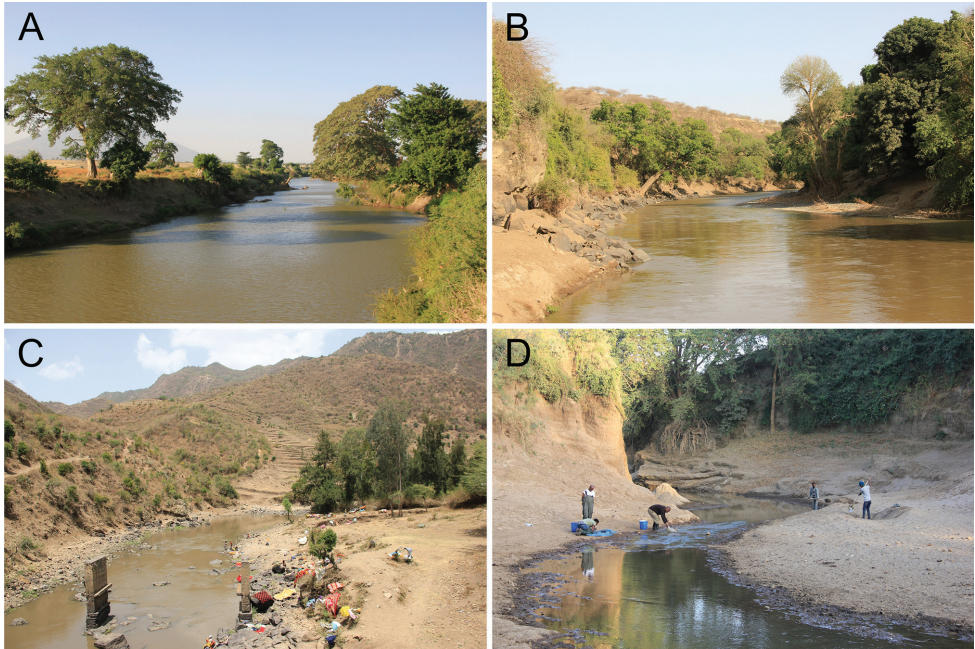


Figure 10. Habitat of *Garra makiensis* in the Awash River drainage and sampling site in the Lower Meki River where *G. makiensis* was absent. **A** Awash River at Lafessa (S6, 1,608 m a.s.l.), **B** Awash River at Yimre (S10, 797 m a.s.l.), **C** Middle Borkana River (T3, 1,417 m a.s.l.), **D** Lower Meki River, upstream of Meki town (1,663 m a.s.l.).

tal vertebrae (vs. 32–33); 20–22 abdominal vertebrae (vs. 19); 14–17 caudal vertebrae (vs. 13–14); and 11–14 vertebrae between first pterygiophores of dorsal and anal fins (vs. 10–12). *Garra makiensis* shares with *G. tibanica* such characters as a completely scaled chest and belly (Trewavas 1941: 12); the pattern of nuptial tubercles on snout (Krupp 1983: fig. 38); and a short distance between anus and anal-fin origin (7.3–19.7 vs. 16.7–20.0 % of pelvic – anal distance) (Trewavas 1941).

Garra makiensis clearly differs from *G. dunsirei* (sinkhole at Tawi Atair, Dhofar Region, Oman) by the presence of scales on chest and belly (vs. reduced scales on ventral side), 16 circumpeduncular scales (vs. 12); 35–39, commonly 37, total vertebrae (vs. 36 or 37); width of gular disc wider than its length (vs. width of gular disc slightly smaller than its length); and eye diameter 4–6 % SL (vs. 3–4 % SL). Mitochondrial CO1 data place *G. dunsirei* close to *G. smarti* and *G. sindhi* (p-distances 1.47 % and 1.96 % respectively; Suppl. material 1: Table S7) from the same geographic area (Lyon et al. 2016).

Garra makiensis is distinct from *G. smarti* (Wadi Hasik, Dhofar Region, Oman) by 37–40, commonly 38, scales in the lateral series (vs. 34–35, commonly 34); 35–39, commonly 37 total vertebrae (vs. 32–34, mode 33); 20–22 abdominal vertebrae (vs. 19–20); 14–17 caudal vertebrae (vs. 13–15); width of gular disc wider than its length (vs. width of gular disc usually longer than its width); and anal fin depth 19–22 % SL (vs. 16–17 % SL).

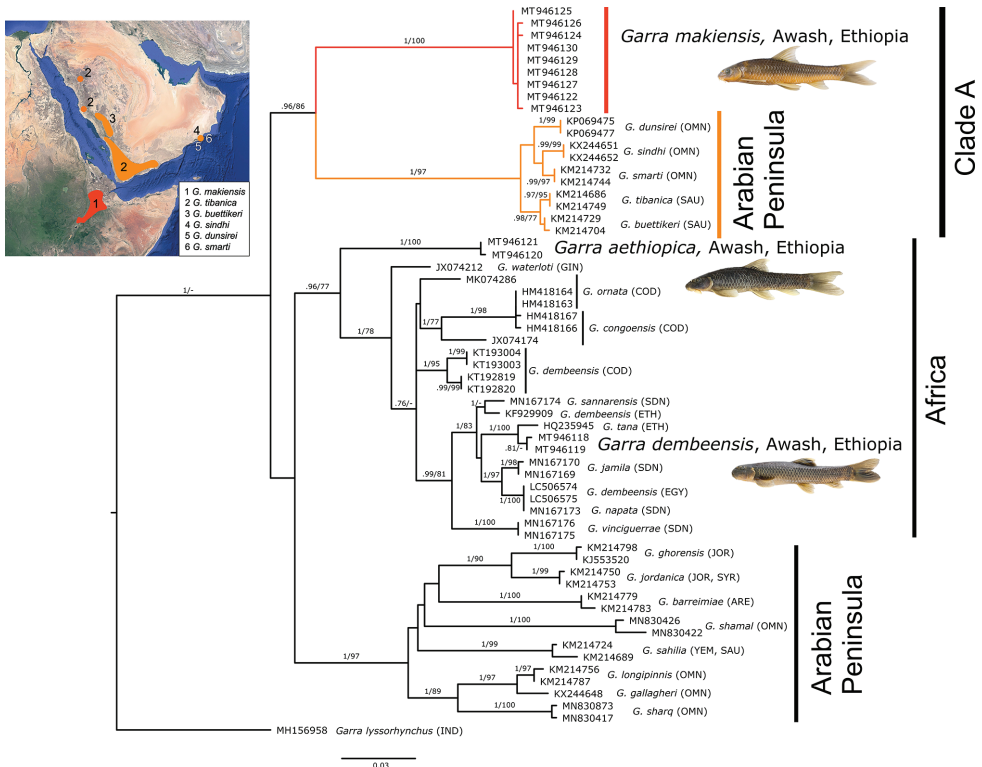


Figure 11. ML tree based on CO1 sequences (611 bp; MT946130 paralectotype of *G. makiensis*, 451 bp), showing phylogenetic relationships of *Garra* species from Awash with congeneric lineages from Africa and the Middle East. Numbers above branches represent Bayesian posterior probability (BPP) of BI/ bootstrap values (bs) of ML. Only values above .70/70 are shown. On the top left, small map showing the distribution of Clade A in Ethiopia and the Arabian Peninsula; distribution of species on the Arabian Peninsula according to Krupp (1983) (source of map: Google Earth Pro v. 7.3). Colours of branches in Clade A correspond to those in the map. Countries of origin of the sequences are represented with ISO codes. The topology of the BI analysis is given in Suppl. material 2: Fig. S4.

Garra makiensis is further distinguished from *G. sindhi* (Lower Wadi Andhur, Dofar Region, Oman) by 13–17, commonly 16, branched pectoral fin rays (vs. 12); 37–40, commonly 38, scales in the lateral series (vs. 36); 34–39 scales in the lateral-line series to posterior margin of hypurals (vs. 34); and anal-fin depth 19–22 % SL (vs. 14–20 % SL). Both species are similar by their prominent axillary scale; deeply embedded scales on chest; and commonly 2 scales between anus and anal-fin origin.

Biogeographical aspects

The distribution ranges and systematic relationships of African *Garra* species are still poorly investigated. Our morphological and mtDNA data suggest 1) a palaeohydrolog-

ical connection between the Awash River drainage and the lakes of the Central MER as *G. makiensis* is known from both drainage systems (see also Englmaier et al. 2020a and references therein); 2) the distinctiveness of *G. makiensis* in comparison to *G. aethiopica* and *G. dembeensis* from the Awash, suggesting a different evolutionary or colonisation history of *Garra* species in the region; and 3) a closer relationship between *G. makiensis* and *Garra* species in the south-west of the Arabian Peninsula than to African congeners.

Biogeographical similarities between the Horn of Africa and the Arabian Peninsula are evident for different animal groups (e.g., Pook et al. 2009; Zinner et al. 2009; Portik and Papenfuss 2012; 2015; Šmíd et al. 2013; Gilbert et al. 2014; Garcia-Alix et al. 2016; Yanai et al. 2020). Though dispersal routes across the Bab-al-Mandab Strait have been proposed by several studies (Šmíd et al. 2013; Stewart and Murray 2017), the exact timing is still controversial (Fernandes et al. 2006). Geological data provide evidence that the formation of the southern Red Sea rift section began in the early Oligocene with a first culmination from the upper Oligocene to the lower Miocene (30–23 Ma), followed by a geologically well-established reconnection period of Africa and Arabia at the Bab-al-Mandab-strait in the uppermost Miocene and Pliocene (10–5 Ma) (Bosworth et al. 2005; Autin et al. 2010). Postulated land bridge periods in younger times are not supported (Fernandes et al. 2006).

The restricted distribution of *G. makiensis* in the Northern and Central MER, and its close relationship to *Garra* species in the south-west of the Arabian Peninsula (based on CO1 sequence data) may support the hypotheses of dispersal events and vicariance around the southern Red Sea area. However, based on our mtDNA data, *G. makiensis* is currently the only known African species of Clade A (Fig. 11) and further investigations of the coastal drainages in the Horn of Africa are needed to clarify ichthyofaunal similarities across the Red Sea. Several examples can be found in literature: 1) a close affinity of *G. tibanica* with *G. blanfordii* (Boulenger, 1901) from coastal drainages in Eritrea was suggested by Trewavas (1941); 2) Menon (1958, 1964) placed *G. ethelwynnae* Menon, 1958 from Salamona (Eritrea) close to *G. tibanica*; and 3) Stiassny and Getahun (2007) synonymised *G. tibanica* and *G. brittoni* Trewavas, 1941 with *G. quadrimaculata* (Rüppell, 1835) from the Ethiopian Highlands. Furthermore, the Somalian cavefish *G. andruzzi* (Viciguerra, 1924) might reflect early dispersal events among *Garra* species in Africa (Yang et al. 2012).

The high genetic diversity and tree topology observed, not only within Clade A but in the whole studied dataset, suggest a complex evolutionary history and different evolutionary rates within the focal taxa. A more thorough sampling and deeper genome-level sequencing are needed to clarify the phylogenetic relationships and taxonomic status of several African *Garra* species.

In summary, we provide new data on morphology, mtDNA, and distribution of *G. makiensis* in Ethiopia. By introducing a wide set of morphological characters, we hope to support further morphological comparisons among *Garra* species in African and beyond. The CO1 sequence of the historic paralectotype of *G. makiensis* demonstrates that the use of historic museum material in phylogenetic analyses and species identification provides an invaluable potential for taxonomic studies, in

particular in phenotypically variable groups. In the future, further research on African *Garra* is needed to clarify phylogenetic relationships, evolutionary history, and intraspecific morphological plasticity, including the variability of tubercles observed in the present study.

Acknowledgements

Fieldwork of GKE, HW, GT and PM was conducted under the auspices of the LARIMA – Sustainable High LAnd Rivers MAnagement in Ethiopia – project (Project Number 106) funded by the Austrian Partnership Programme in Higher Education and Research for Development (APPEAR) of the Austrian Development Cooperation (ADC) and the Austrian Agency for International Cooperation in Education and Research (OeAD). GKE was supported by a grant from the Doctoral Academy Graz, Ecology and Evolution in Changing Environments (EECE), University Graz. Steven Weiss (University of Graz), Nina Bogutskaya and Sandra Kirchner (NMW), Wolfram Graf, Susanne Krumböck (BOKU-Vienna) and Gerold Winkler (IPGL, BOKU-Vienna) provided valuable comments and support to the study. We thank Simon Loader, James MacLaine, and Oliver Crimmen (BMNH) for assistance with the historic paralectotype of *G. makiensis*. Ernst Mikschi (NMW), Jos Snoeks (MRAC), and Radford Arrindell (AMNH) allowed access to collection material under their care. We are grateful to Abebe Getahun and Maarten Van Steenberge for constructive comments on an earlier version of the manuscript. Finally, we thank the local communities along the Awash River and its tributaries for providing access to the sampling localities.

Data availability

Data and alignments are available from the supplementary material and from the corresponding author upon reasonable request. Newly obtained sequences are deposited in GenBank under accession numbers MT946118–MT946130.

References

- Abell R, Thieme ML, Revenga C, Bryer M, Kottelat M, Bogutskaya N, Coad B, Mandrak N, Balderas SC, Bussing W, Stiassny MLJ, Skelton P, Allen GR, Unmack P, Naseka A, Ng R, Sindorf N, Robertson J, Armijo E, Higgins JV, Heibel TJ, Wikramanayake E, Olson D, López HL, Reis RE, Lundberg JG, Sabaj Pérez MH, Petry P (2008) Freshwater Ecoregions of the World: A New Map of Biogeographic Units for Freshwater Biodiversity Conservation. *BioScience* 58(5): 403–414. <https://doi.org/10.1641/B580507>

- Autin J, Leroy S, Beslier M, d'Acremont E, Razin P, Ribodetti A, Bellahsen N, Robin C, Al Toubi K (2010) Continental break-up history of a deep magma-poor margin based on seismic reflection data (northeastern Gulf of Aden margin, offshore Oman). *Geophysical Journal International* 180: 501–519. <https://doi.org/10.1111/j.1365-246X.2009.04424.x>
- Baldwin CC, Mounts JH, Smith DG, Weigt LA (2009) Genetic identification and color descriptions of early life-history stages of Belizean *Phaeoptyx* and *Astrapogon* (Teleostei: Apogonidae) with comments on identification of adult *Phaeoptyx*. *Zootaxa* 2008: 1–22.
- Balletto E, Spanò S (1977) Ciprinidi del genere *Garra* Hamilton 1822, raccolti nello Yemen dal Prof. Giuseppe Scortecci. *Annali del Museo Civico di Storia Naturale 'Giacomo Doria'* 81: 246–287.
- Banister KE (1987) Two new species of *Garra* (Teleostei-Cyprinidae) from the Arabian Peninsula. *Bulletin of the British Museum of Natural History (Zoology)* 52: 59–70. <https://doi.org/10.5962/bhl.part.18301>
- Beshera KA, Harris PM (2014) Mitochondrial DNA phylogeography of the *Labeobarbus intermedius* complex (Pisces, Cyprinidae) from Ethiopia. *Journal of Fish Biology* 85(2): 228–245. <https://doi.org/10.1111/jfb.12408>
- Bonini M, Corti G, Innocenti F, Manetti P, Mazzarini F, Abebe T, Pecskey T (2005) Evolution of the Main Ethiopian Rift in the frame of Afar and Kenya rifts propagation. *Tectonics* 24(1): 1–21. <https://doi.org/10.1029/2004TC001680>
- Bosworth W, Huchon P, McClay K (2005) The Red Sea and Gulf of Aden Basins. *Journal of African Earth Sciences* 43(1–3): 334–378. <https://doi.org/10.1016/j.jafrearsci.2005.07.020>
- Boulenger GA (1901) On a small collection of fishes from Lake Victoria made by order of Sir H. H. Johnston, K.C.B. *Proceedings of the Zoological Society of London* 2 (3) (art. 2): 158–162. <https://doi.org/10.1111/j.1469-7998.1901.tb08172.x>
- Boulenger GA (1903) Report on the fishes collected by Mr. Oscar Neumann and Baron Carlo von Erlanger in Gallaland and southern Ethiopia. *Proceedings of the Zoological Society of London* 2(2) (art. 3): 328–334.
- Cope ED (1867) Synopsis of the Cyprinidae of Pennsylvania. With supplement on some new species of American and African fishes. *Transactions of the American Philosophical Society* 13: 351–410. <https://doi.org/10.2307/1005371>
- Daget J, Gosse JP, Thys van den Audenaerde DFE (1984) CLOFFA 1. Check-list of the freshwater fishes of Africa, Vol. 1. Tervuren, Mrac, Paris, Orstom, 410 pp.
- Dubois A (2007) Genitives of species and subspecies nomina derived from personal names should not be emended. *Zootaxa* 1550: 49–68. <https://doi.org/10.11646/zootaxa.1550.1.2>
- Englmaier GK (2018) Longitudinal zonation of fish assemblages in a tropical river: Awash river basin, central Ethiopia, With taxonomic and ecological considerations on the genus *Garra* (Teleostei: Cyprinidae). Master thesis, University of Natural Resources and Life Sciences, Vienna, 119 pp.
- Englmaier GK, Tesfaye G, Bogutskaya NG (2020a) A new species of *Enteromius* (Actinopterygii, Cyprinidae, Smiliogastrinae) from the Awash River, Ethiopia, and the re-establishment of *E. akakianus*. *ZooKeys* 902: 107–150. <https://doi.org/10.3897/zookeys.902.39606>

- Englmaier GK, Hayes DS, Meulenbroek P, Terefe Y, Lakew A, Tesfaye G, Waidbacher H, Malicky H, Wubie A, Leitner P, Graf W (2020b) Longitudinal river zonation in the tropics: Examples of fish and caddisflies from the endorheic Awash River, Ethiopia. *Hydrobiologia* 847(19): 4063–4090. <https://doi.org/10.1007/s10750-020-04400-0>
- Esmaili HR, Sayyadzadeh G, Coad BW, Eagderi S (2016) Review of the genus *Garra* Hamilton, 1822 in Iran with description of a new species: a morpho-molecular approach (Teleostei: Cyprinidae). *Iranian Journal of Ichthyology* 3(2): 82–121.
- Fernandes CA, Rohling EJ, Siddall M (2006) Absence of post-Miocene Red Sea land bridges: biogeographic implications. *Journal of Biogeography* 33: 961–966. <https://doi.org/10.1111/j.1365-2699.2006.01478.x>
- Garcia-Alix A, Minwer-Barakat R, Suarez EM, Freudenthal M, Aguirre J, Kaya F (2016) Updating the Europe-Africa small mammal exchange during the late Messinian. *Journal of Biogeography* 43: 1336–1348. <https://doi.org/10.1111/jbi.12732>
- Getahun A (2000) Systematic Studies of the African Species of the Genus *Garra* (Pisces: Cyprinidae). Doctoral thesis, The City University of New York, USA, 477 pp.
- Gilbert CC, Bibi F, Hill A, Beech MJ (2014) Early guenon from the late Baynunah Formation, Abu Dhabi, with implications for cercopithecoid biogeography and evolution. *Proceedings of the Academy of Natural Sciences of the United States of America* 111: 10119–10124. <https://doi.org/10.1073/pnas.1323888111>
- Golubtsov AS, Dgebuadze YuYu, Mina MV (2002) Fishes of the Ethiopian Rift Valley, Chapter 10. In: Tudorancea C, Taylor WD Baele G and Suchard MA (Eds) *Ethiopian Rift Valley Lakes. Biology of Inland Waters Series*. Backhuys Publishers, Leiden, 167–258.
- Golubtsov AS, Cherenkov SE, Tefera F (2012) High Morphological Diversity of the Genus *Garra* in the Sore River (the White Nile Basin, Ethiopia): One More Cyprinid Species Flock? *Journal of Ichthyology* 52(11): 817–820. <https://doi.org/10.1134/S0032945212110057>
- Habteselassie R (2009). Fish diversity and habitat characterisation in selected catchment areas of Ethiopia with the description of the new fish species *Garra cheberera*. Doctoral Thesis, University of Natural Resources and Life Sciences, Vienna, 143 pp.
- Habteselassie R (2012). *Fishes of Ethiopia, Annotated Checklist with Pictorial Identification Guide*. Ethiopian Fisheries and Aquatic Science Association, Addis Ababa, 250 pp.
- Habteselassie R, Mikschi E, Ahnelt H, Waidbacher H (2010) *Garra chebera*, a new species of cyprinid fish from an isolated basin in Ethiopia (Teleostei: Cyprinidae). *Annalen des Naturhistorischen Museums in Wien* 111: 43–53.
- Hamidan NA, Geiger MF, Freyhof J (2014) *Garra jordanica*, a new species from the Dead Sea basin with remarks on the relationship of *G. ghorensis*, *G. tibanica* and *G. rufa* (Teleostei: Cyprinidae). *Ichthyological Exploration of Freshwaters* 25(3): 223–236.
- Hamilton F (1822) *An account of the fishes found in the river Ganges and its branches*. Edinburgh & London. <https://doi.org/10.5962/bhl.title.59540>
- Hashemzadeh Segherloo I, Abdoli A, Eagderi S, Esmaili HR, Sayyadzadeh G, Bernatchez L, Hallerman E, Geiger MF, Özulug M, Laroche J, Freyhof J (2016) Dressing down: convergent reduction of the mental disc in *Garra* (Teleostei: Cyprinidae) in the Middle East. *Hydrobiologia* 785: 47–59. <https://doi.org/10.1007/s10750-016-2902-8>

- Holčík J, Banarescu P, Evans D (1989) A General Introduction to Fishes. In: Holčík J (Ed.) The Freshwater Fishes of Europe, Vol. 1, Part II, AULA-Verlag, Wiesbaden, 18–147.
- Hubbs CL, Lagler KF (1958) Fishes of the Great Lakes region. University of Michigan Press. Ann Arbor, Michigan, 213 pp.
- International Commission on Zoological Nomenclature (1999) International Code of Zoological Nomenclature, Fourth edition: adopted by the International Union of Biological Sciences. The International Trust for Zoological Nomenclature, London, 106 pp.
- Kirchner S, Kruckenhauser L, Pichler A, Borkenhagen K, Freyhof J (2020) Revision of the *Garra* species of the Hajar Mountains in Oman and the United Arab Emirates with the description of two new species (Teleostei: Cyprinidae). *Zootaxa* 4751(3): 521–545.
- Kottelat M (2020) *Ceratogarra*, a genus name for *Garra cambodgiensis* and *G. fasciacauda* and comments on the oral and gular soft anatomy in labeonine fishes (Teleostei: Cyprinidae). *The Raffles Bulletin of Zoology Supplement* 35: 156–178.
- Krupp F (1983) Fishes of Saudi Arabia: Freshwater fishes of Saudi Arabia and adjacent regions of the Arabian Peninsula. *Fauna of Saudi Arabia* 5: 568–636.
- Krupp F, Budd K (2009) A new species of the genus *Garra* (Teleostei: Cyprinidae) from Oman. *aqua, International Journal of Ichthyology* 15(2): 117–120.
- Kumar S, Stecher G, Tamura K (2016) MEGA7: molecular evolutionary genetics analysis version 7.0 for bigger datasets. *Molecular Biology and Evolution* 33(7): 1870–1874. <https://doi.org/10.1093/molbev/msw054>
- Lanfear R, Frandsen PB, Wright AM, Senfeld T, Calcott B (2017) PartitionFinder 2: new methods for selecting partitioned models of evolution for molecular and morphological phylogenetic analyses. *Molecular Biology and Evolution* 34(3): 772–773. <https://doi.org/10.1093/molbev/msw260>
- Lyon RG, Geiger MF, Freyhof J (2016) *Garra sindhi*, a new species from the Jebel Samhan Nature Reserve in Oman (Teleostei: Cyprinidae). *Zootaxa* 4154(1): 79–88. <https://doi.org/10.11646/zootaxa.4154.1.5>
- Menon AGK (1958) *Garra ethelwynnae*, a new cyprinid fish from Eritrea (Africa). *Current Science* 27(11): 450–451.
- Menon AGK (1964) Monograph of the cyprinid fishes of the genus *Garra*, Hamilton. *Memoirs of the Indian Museum* 14: 173–260.
- Miller MA, Pfeiffer W, Schwartz T (2011) The CIPRES Science Gateway: A community resource for phylogenetic analysis. In: Proceedings of the 2011 TeraGrid Conference: Extreme Digital Discovery-TG'11 11 41: 1–8. <https://doi.org/10.1145/2016741.2016785>
- Moritz T, Straube N, Neumann D (2019) The *Garra* species (Cyprinidae) of the Main Nile basin with description of three new species. *Cybium* 43: 311–329.
- Naseka AM (1996) Comparative study on the vertebral column in the Gobioninae (Cyprinidae, Pisces) with special reference to its systematics. *Publicaciones Especiales Instituto Espanol de Oceanografia* 21: 149–167.
- Nebeshwar K, Vishwanath W (2017) On the snout and oromandibular morphology of genus *Garra*, description of two new species from the Koladyne River basin in Mizoram, India, and redescription of *G. manipurensis* (Teleostei: Cyprinidae). *Ichthyological Exploration of Freshwaters* 28(1): 17–53.

- Nemésio A, Dubois A (2012) The endings of specific nomina dedicated to persons should not be emended: nomenclatural issues in Phalangopsidae (Hexapoda: Grylloidea). *Zootaxa* 3270: 67–68. <https://doi.org/10.11646/zootaxa.3270.1.7>
- Paugy D (2010) The Ethiopian subregion fish fauna: an original patchwork with various origins. *Hydrobiologia* 649: 301–315. <https://doi.org/10.1007/s10750-010-0273-0>
- Pellegrin J (1905) Poissons d'Abyssinie et du lac Rodolphe (collection Maurice de Rothschild). *Bulletin du Muséum d'histoire naturelle, Paris*, 11: 290–294.
- Pellegrin J (1927) Description d'un Cyprinidé nouveau d'Abyssinie appartenant au genre *Discognathus*. *Bulletin de la Société Zoologique de France* 52: 231–233.
- Pook CE, Joger, Stümpel N, Wüster W (2009) When continents collide: phylogeny, historical biogeography and systematics of the medically important viper *Echis* (Squamata: Serpentes: Viperidae). *Molecular Phylogenetics and Evolution* 53(3): 792–807. <https://doi.org/10.1016/j.ympev.2009.08.002>
- Portik DM, Papenfuss TJ (2012) Monitors cross the Red Sea: the biogeographic history of *Varanus yemenensis*. *Molecular Phylogenetics and Evolution* 62(1): 561–565. <https://doi.org/10.1016/j.ympev.2011.09.024>
- Portik DM, Papenfuss TJ (2015) Historical biogeography resolves the origins of endemic Arabian toad lineages (Anura: Bufonidae): Evidence for ancient vicariance and dispersal events with the Horn of Africa and South Asia. *BMC Evolutionary Biology* 15: 152. <https://doi.org/10.1016/j.ympev.2011.09.024>
- Rambaut A (2018) FigTree v. 2.4.4. <https://github.com/rambaut/figtree/releases> [downloaded January 2019]
- Ronquist F, Teslenko M, van der Mark P, Ayres DL, Darling A, Höhna S, Larget B, Liu L, Suchard MA, Huelsenbeck JP (2012) MrBayes 3.2: efficient Bayesian phylogenetic inference and model choice across a large model space. *Systematic Biology* 61(3): 539–542. <https://doi.org/10.1093/sysbio/sys029>
- Reid GM (1985) A revision of African species of *Labeo* (Pisces: Cyprinidae) and a re-definition of the genus. *Cramer, Braunschweig*, 322 pp.
- Roberts TR (1975) Geographical distribution of African freshwater fishes. *Zoological Journal of the Linnean Society* 57(4): 249–319. <https://doi.org/10.1111/j.1096-3642.1975.tb01893.x>
- Rüppell E (1835) Neuer Nachtrag von Beschreibungen und Abbildungen neuer Fische, im Nil entdeckt. *Museum Senckenbergianum: Abhandlungen aus dem Gebiete der beschreibenden Naturgeschichte, von Mitgliedern der Senckenbergischen Naturforschenden Gesellschaft in Frankfurt am Main* 2(1): 1–28.
- Sayyadzadeh G, Esmaili HR, Freyhof J (2015) *Garra mondica*, a new species from the Mond River drainage with remarks on the genus *Garra* from the Persian Gulf basin in Iran (Teleostei: Cyprinidae). *Zootaxa* 4048(1): 75–89. <https://doi.org/10.11646/zootaxa.4048.1.4>
- Skelton PH (1980) Systematics and Biogeography of the Redfin *Barbus* Species (Pisces: Cyprinidae) from Southern Africa. PhD thesis, Rhodes University, Grahamstown, South Africa, 416 pp.

- Šmíd J, Carranza S, Kratochvíl L, Gvoždík V, Nasher AK, Moravec J (2013) Out of Arabia: A Complex Biogeographic History of Multiple Vicariance and Dispersal Events in the Gecko Genus *Hemidactylus* (Reptilia: Gekkonidae). *PLOS ONE* 8(5): e64018. <https://doi.org/10.1371/journal.pone.0064018>
- Snoeks J, Getahun A (2013) African fresh and brackish water fish biodiversity and their distribution: more unknowns than knowns. In: Snoeks J, Getahun A (Eds) Proceedings of the 4th international conference on African fish and fisheries. Royal Museum for Central Africa, Tervuren, 69–76.
- Stewart KM, Murray AM (2017) Biogeographic implications of fossil fishes from the Awash River, Ethiopia. *Journal of Vertebrate Paleontology* 37(1): e1269115. <https://doi.org/10.1080/02724634.2017.1269115>
- Stiassny MLJ, Getahun A (2007) An overview of labeonin relationships and the phylogenetic placement of the Afro-Asian genus *Garra* Hamilton, 1922 (Teleostei: Cyprinidae), with the description of five new species of *Garra* from Ethiopia, and a key to all African species. *Zoological Journal of the Linnean Society* 150(1): 41–83. <https://doi.org/10.1111/j.1096-3642.2007.00281.x>
- Stiassny MLJ, Teugels GG, Hopkins CD (2007) Poissons d’eaux douces et saumâtres de basse Guinée, ouest de l’Afrique centrale. The fresh and brackish water fishes of lower Guinea, west-central Africa, Volume 1. IRD Éditions, Paris, 800 pp.
- Tamura K, Stecher G, Peterson D, Filipski A, Kumar S (2011) MEGA6: Molecular Evolutionary Genetics Analysis Version 6.0. *Molecular Biology and Evolution* 30(12): 2725–2729. <https://doi.org/10.1093/molbev/mst197>
- Trewavas E (1941) British Museum (Natural History) expedition to southwest Arabia 1937–8. 3. Freshwater fishes. *British Museum (Natural History)* 1(3): 7–15.
- Vinciguerra D (1924) Descrizione di un ciprinide cieco proveniente dalla Somalia Italiana. *Annali del Museo Civico di Storia Naturale ‘Giacomo Doria’* 51: 239–243.
- Wakjira M, Getahun A (2017) Ichthyofaunal diversity of the Omo-Turkana basin, East Africa, with specific reference to fish diversity within the limits of Ethiopian waters. *Check List* 13(2): 2059. <https://doi.org/10.15560/13.2.2059>
- Yanai Z, Graf W, Terefe Y, Sartori M, Gattolliat J-L (2020) Re-description and range extension of the Afrotropical mayfly *Cloeon perkinsi* (Ephemeroptera, Baetidae). *European Journal of Taxonomy* 617: 1–23. <https://doi.org/10.5852/ejt.2020.617>
- Yang L, Arunachalam M, Sado T, Levin BA, Golubtsov AS, Freyhof J, Friel, JP, Chen WJ, Hirt MV, Manickam R, Agnew MK, Simons AM, Saitoh K, Miya M, Mayden RL, He S (2012) Molecular phylogeny of the cyprinid tribe Labeonini (Teleostei: Cypriniformes). *Molecular Phylogenetics and Evolution* 65(2): 362–379. <https://doi.org/10.1016/j.ympev.2012.06.007>
- Zhang E, He SP, Chen YY (2002) Revision of the cyprinid genus *Placocheilus* Wu, 1977 in China, with description of a new species from Yunnan. *Hydrobiologia* 487: 207–217. <https://doi.org/10.1023/A:1022938132599>
- Zinner D, Groeneveld LF, Keller C, Roos C (2009) Mitochondrial phylogeography of baboons (*Papio* spp.) – Indication for introgressive hybridization? *BMC Evolutionary Biology* 9: 83. <https://doi.org/10.1186/1471-2148-9-83>

Supplementary material I

Supplementary tables

Authors: Gernot K. Englmaier, Nuria Viñuela Rodríguez, Herwig Waidbacher, Anja Palandačić, Genanaw Tesfaye, Wolfgang Gessl, Paul Meulenbroek

Data type: species data

Explanation note: **Table S1.** Sampling sites in the Northern and Central Main Ethiopian Rift. *Garra makiensis* was found only at sites S6–S16, T1 and T3–T4 in the Awash River drainage. **Table S2.** List of character states (morphometric characters (point to point measurements), and meristic characters) for the genus *Garra* used in the present study. **Table S3.** Primary data (morphometric and meristic) used in DFA (Fig. 3). Data for *Garra dembeensis* and *G. aethiopica* were taken from Englmaier (2018). Measurements and counts refer to those defined in Suppl. material 1: Table S2. **Table S4.** PCA statistics, **A** Communalities, **B** Total Variance Explained, **C** Component Matrix. **Table S5.** DFA statistics, **A** Tests of equality of group means, **B** Structure matrix, **C** Canonical Discriminant Function Coefficients, **D** Classification Function Coefficients, **E** Classification results. **Table S6.** Voucher specimens included in the present study. **Table S7.** Mean genetic distances based on CO1 sequences (uncorrected p-distances), in %. The comparison of the paralectotype to all other samples (in yellow) is based on a sequence length of 451 bp; comparisons among other samples do not include the paralectotype and are based on a sequence length of 611 bp. **Table S8.** Counts of axial skeleton elements in type specimens of *Garra tibanica*.

Copyright notice: This dataset is made available under the Open Database License (<http://opendatacommons.org/licenses/odbl/1.0/>). The Open Database License (ODbL) is a license agreement intended to allow users to freely share, modify, and use this Dataset while maintaining this same freedom for others, provided that the original source and author(s) are credited.

Link: <https://doi.org/10.3897/zookeys.984.55982.suppl1>

Supplementary material 2

Supplementary figures

Authors: Gernot K. Englmaier, Nuria Viñuela Rodríguez, Herwig Waidbacher, Anja Palandačić, Genanaw Tesfaye, Wolfgang Gessl, Paul Meulenbroek

Data type: species data

Explanation note: **Figure S1.** Examples of tubercles and position of axillary scale in *Garra makiensis*, NMW 99231, 91.2 mm SL, male, Awash River at Yimre (S10). **A** tubercles on snout, head, and scales (above lateral line), **1** showing roundish tubercles extending from frontal region to operculum, **2** showing long axillary scale at base of pelvic fin; **B** conical tubercles on pectoral fin, **3** and **4** showing position of conical tubercles on fin membranes between fin rays. The presence of tubercles on the pectoral fin among African *Garra* species was only reported for *G. ornata* (Nichols & Griscom, 1917) so far (Getahun 2000). However, in this species tubercles were reported from the “underside of the pectoral fins” (Getahun 2000: 121). **Figure S2.** Ventral side of *Garra makiensis* from the Awash River with a completely scaled chest, belly, and postpelvic region (scales on chest usually deeply embedded). **A** NMW 99504, 147.9 mm SL, Jara River (T3) **B** NMW 99491, 106.1 mm SL, Dubti (S14); **1** showing scales on chest, **2** showing presence of a single unbranched pectoral-fin ray in *G. makiensis*. **Figure S3.** Ventral side of *Garra makiensis* from the Gotta River. **A** MNHN-1905-0247, syntype of *G. rothschildi*, 108.7 mm SL, The Muséum national d’Histoire naturelle, Paris; **B** AMNH 227323, Errer Gota [Gotta] River, Eastern side of Errer town, pools near main road, Hararge, Ethiopia (09°30’N, 41°15’E), The American Museum of Natural History. Arrows showing embedded scales on chest. **Figure S4.** BI tree based on CO1 sequences.

Copyright notice: This dataset is made available under the Open Database License (<http://opendatacommons.org/licenses/odbl/1.0/>). The Open Database License (ODbL) is a license agreement intended to allow users to freely share, modify, and use this Dataset while maintaining this same freedom for others, provided that the original source and author(s) are credited.

Link: <https://doi.org/10.3897/zookeys.984.55982.suppl2>

